School on Reference Systems, Crustal Deformation and Ionosphere Monitoring

Instituto Geográfico Nacional Tommy Guardia
Panama City, Panama
October 21 - 23, 2013

Hermann Drewes
International Association of Geodesy
Munich
Germany

SIRGAS Scientific Council

Claudio Brunini
Universidad Nacional de La Plata,
Consejo Nacional de Investigaciones Científicas y Técnicas
La Plata
Argentina

SIRGAS President

Laura Sánchez
Deutsches Geodätisches Forschungsinstitut
München
Germany

SIRGAS Vice-President

	Sunday 2013-10-20	Monday 2013-10-20	Tuesday 2013-10-20	Wednesday 2013-10-20
07:00-08:30		Registration		
08:30-09:30		**Aperture**	Terrestrial Reference System and Frame	Modern vertical reference systems
09:30-10:30		Types of coordinates Modern geodetic reference systems and frames		
10:30-11:00		**Coffee break**		
11:00-12:30		Celestial Reference System and Frame Rotation and tides of the Earth	Regional Reference Frames SIRGAS: definition, realisation, maintenance	Crustal deformation observation and modelling
12:30-14:30		**Lunch**		
14:30-16:00	Registration	GPS positioning: observables and observation equations	Adjustment of GPS networks	Ionosphere modelling and analysis
16:00-16:30		**Coffee break**		
16:30-17:15		GPS processing	Classical vertical reference systems	Scientific objectives of SIRGAS Availability and applicability of SIRGAS
17:15-18:00				**Open questions and discussion**
		Hermann Drewes	Claudio Brunini	Laura Sánchez

School on Reference Systems, Crustal Deformation and Ionosphere Monitoring

Contents

1. Coordinate systems, types of coordinates

A coordinate system provides the basis for unique determination of the position of points in lines, surfaces or spaces (1D, 2D, 3D).

To define a coordinate system one has to specify

0. the type of coordinates (rectilinear, curved, plane, spatial);
1. the location of the origin;
2. the orientation of the axes;
3. the unit of measure.

Coordinates cannot be determined directly but only w.r.t. a system!

We shall discuss the following types of coordinate systems:

- Global three-dimensional Cartesian coordinates [X, Y, Z]
- Ellipsoidal coordinates [φ, λ, h]
- Local topocentric Cartesian coordinates [x, y, z], [n, e, u]
- Plane coordinates (Mercator, Lambert, azimuthal) [N, E]
- Coordinates referring to irregular surfaces [H] (see chapter 4)

1.1 Global Cartesian 3D coordinates

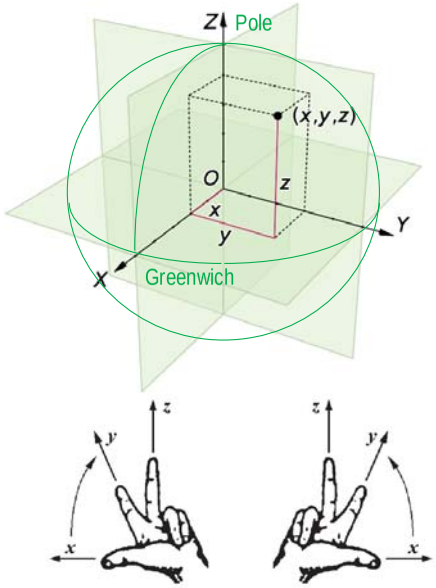

- Cartesian systems have rectilinear orthogonal axes.
- We distinguish right-hand and left-hand systems. In geodesy we use the right-hand system.
- In global systems, the *origin* is the centre of mass of the Earth; the *direction* of the Z-axis is towards the conventional pole of rotation, the *direction* of the X-axis is close to the Greenwich meridian; the *unit of measure* is the metre.
- These parameters are called *datum*.

Transformation of Cartesian coordinates (1)

- A coordinate transformation is the change of coordinates from one coordinate system to another one with a different datum.
- A coordinate transformation applies parameters which can be derived empirically from a set of identical points in both systems.
- For undeformed coordinate sets in three-dimensional Cartesian systems it is common to use the 7-parameters similarity transformation (after Helmert 1893):

$$\begin{bmatrix} X \\ Y \\ Z \end{bmatrix}_{(D)} = \begin{bmatrix} X \\ Y \\ Z \end{bmatrix}_{(P)} + \begin{bmatrix} T_1 \\ T_2 \\ T_3 \end{bmatrix} + \begin{bmatrix} 0 & -R_3 & +R_2 \\ +R_3 & 0 & -R_1 \\ -R_2 & +R_1 & 0 \end{bmatrix} * \begin{bmatrix} X \\ Y \\ Z \end{bmatrix}_{(P)} + M * \begin{bmatrix} X \\ Y \\ Z \end{bmatrix}_{(P)}$$

$$= \begin{bmatrix} T_1 \\ T_2 \\ T_3 \end{bmatrix} + \begin{bmatrix} 1+M' & -R_3 & +R_2 \\ +R_3 & 1+M' & -R_1 \\ -R_2 & +R_1 & 1+M' \end{bmatrix} * \begin{bmatrix} X \\ Y \\ Z \end{bmatrix}_{(P)}$$

T_1, T_2, T_3: Translations in X, Y, Z
R_i: Rotations around X-,Y-,Z-axes
M: Factor of unit measures (scale)

Transformation of Cartesian coordinates (2)

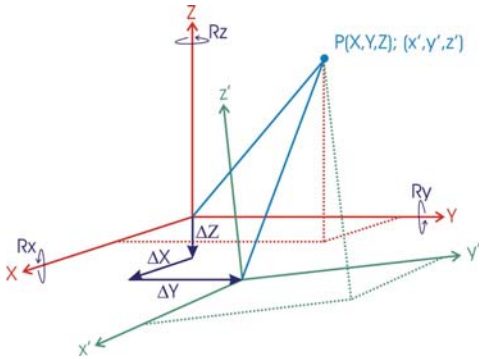

X', Y', Z' = initial system
X, Y, Z = new system

$$\begin{bmatrix} X \\ Y \\ Z \end{bmatrix} = M \cdot \begin{bmatrix} 1 & +R_Z & -R_Y \\ -R_Z & 1 & +R_X \\ +R_Y & -R_X & 1 \end{bmatrix} \cdot \begin{bmatrix} X'-X'_p \\ Y'-Y'_p \\ Z'-Z'_p \end{bmatrix} + \begin{bmatrix} \Delta X \\ \Delta Y \\ \Delta Z \end{bmatrix}$$

- The Helmert transformation produces correlations of T, R, M parameters if the centre of points (i.e. the average of coordinates) differs from the origin.
- To avoid this correlation, the transformation of Molodensky-Badekas is used:
- ΔX, ΔY, ΔZ: origin coordinates of the initial in the new system.
- R_X, R_Y, R_Z : Rotations of axes.
- X'_p, Y'_p, Z'_p: Average of point coordinates in the initial system.
- M: Factor of measures (scale).

1.2 Global spherical coordinates

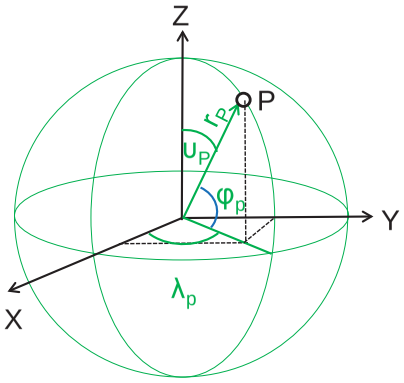

- A global spherical system is preferred (and sufficient) for many representations, e.g. the gravity field, global geography, kinematics of tectonic plates, etc.
- r_p: radial geocentric distance,
  φ_p: latitude,
  υ_p: polar distance (co-latitude 90-φ_p),
  λ_p: geocentric longitude.

$$\begin{bmatrix} X \\ Y \\ Z \end{bmatrix} = r \begin{bmatrix} \sin\upsilon\cos\lambda \\ \sin\upsilon\sin\lambda \\ \cos\upsilon \end{bmatrix} = r \begin{bmatrix} \cos\varphi\cos\lambda \\ \cos\varphi\sin\lambda \\ \sin\varphi \end{bmatrix}$$

Global spherical coordinates can easily be converted to Cartesian coordinates X,Y, Z.

Ellipsoidal coordinates (1)

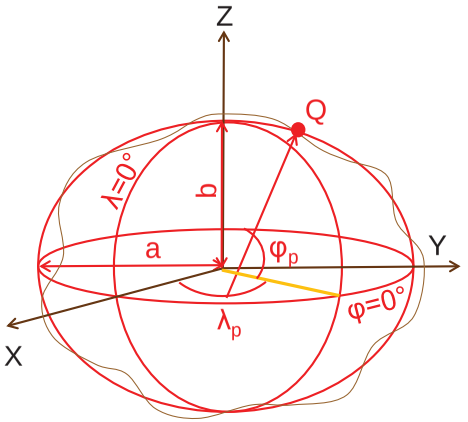

- The figure of the Earth is better approximated by an ellipsoid than by a sphere, because the Earth's rotation produces a flattening with semi-minor axis (b) about 21 km shorter than semi-mayor axis (a).
- In geodesy we use an ellipsoid that optimally fits the geoid according to the Gauss-Listing definition, i.e. coinciding with the mean sea level in static equilibrium.

Polar flattening: $f = \dfrac{a-b}{a}$

Eccentricity: $e = \dfrac{\sqrt{a^2-b^2}}{a}$

- The shape of the ellipsoid is given by semi-mayor axis (a) and polar flattening (f) or eccentricity (e).

Ellipsoidal coordinates (2)

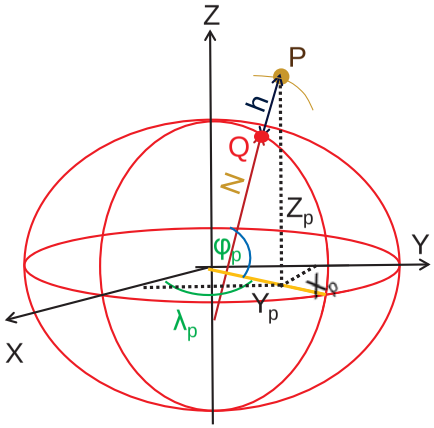

- The ellipsoidal surface system is extended into space by inclusion of the (ellipsoidal, geometric) height h of point P above the ellipsoid, measured along the normal vector. The projection of P upon the ellipsoid corresponds to point Q.
- The coordinates triad (φ, λ, h) is called curvilinear coordinates.

$$\vec{r} = \begin{bmatrix} X \\ Y \\ Z \end{bmatrix} = \begin{bmatrix} (N+h)\cos\varphi\cos\lambda \\ (N+h)\cos\varphi\sin\lambda \\ ((1-e^2)N+h)\sin\varphi \end{bmatrix}$$

- The ellipsoidal coordinates can be converted to Cartesian coordinates X,Y,Z using the meridian radius N:

$N = a / (1 - e^2 \sin^2 \varphi)^{0.5}$

Conversion of Cartesian to ellipsoidal coordinates

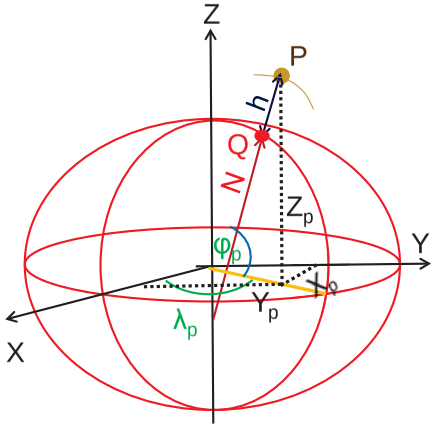

- A conversion is the change between two types of coordinates referring to the same datum.
- Conversion of Cartesian coordinates to ellipsoidal coordinates is done by an iteration process:

$\varphi = \text{atan}\,(Z + e^2\, N \sin\varphi)/(X^2+Y^2)^{0.5}$

$\lambda = \text{atan}\, Y/X$

$h = X \sec\lambda \sec\varphi - N$

$\varepsilon = e^2 / (1 - e^2)$

$b = a(1 - f)$

$p = (X^2 + Y^2)^{0.5}$

$q = \text{atan}[(Z\, a) / (p\, b)]$

To avoid the iteration, one computes φ by

$\varphi = \text{atan}[(Z + \varepsilon\, b \sin^3 q) / (p - e^2\, a \cos^3 q)]$

Transformation of ellipsoidal coordinates

The change of ellipsoidal coordinates from a source system to a transformed system can directly be handled like a displacement (offset) using the formulae of Molodensky:

$$\varphi_t = \varphi_s + d\varphi; \quad \lambda_t = \lambda_s + d\lambda, \quad h_t = h_s + dh$$

with:

$d\varphi'' = (-dX \sin\varphi_s \cos\lambda_s - dY \sin\varphi_s \sin\lambda_s + dZ \cos\varphi_s + (a\,df + f\,da) \sin^2\varphi_s) / (r_s \sin 1'')$
$d\lambda'' = (-dX \sin\lambda_s + dY \cos\lambda_s) / (n_s \cos\varphi_s \sin 1'')$
$dh = dX \cos\varphi_s \cos\lambda_s + dY \cos\varphi_s \sin\lambda_s + dZ \sin\varphi_s + (a\,df + f\,da) \sin^2\varphi_s - da$

where:

dX, dY, dZ = parameters of geocentric translation.
da = difference of semi-mayor axes of the transformed and the source ellipsoid.
df = difference of the flattening of the ellipsoids.
$da = a_t - a_s, \qquad df = f_t - f_s = 1/(1/f_t) - 1/(1/f_s).$
r_s and n_s = curvature radius of the meridian sections and the first vertical, respectively, in a given latitude φ_s on the initial ellipsoid:
$r_s = a_s (1 - e_s^2) / (1 - e_s^2 \sin^2\varphi_s)^{3/2}, \quad n_s = a_s / (1 - e_s^2 \sin^2\varphi_s)^{1/2}$

The formulae for dφ and dλ provide the changes in φ and λ in seconds of arc.

1.3 Local (topocentric) coordinates (1)

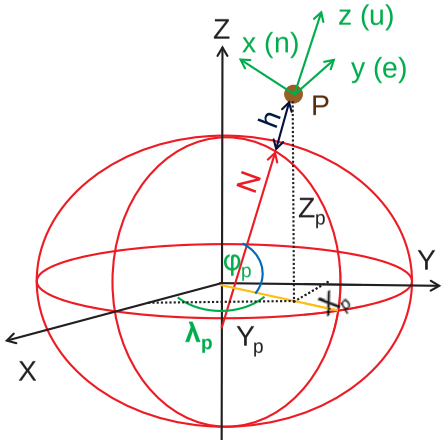

Topocentric coordinate systems are typically used in astronomy (horizontal coordinates, heights and azimuths).

- Local topocentric coordinates refer to a local reference system related to the Earth's gravity field: The origin is the observer ("topocentre" P), the orientation is given with respect to the local vertical (zenith, plumb line):
- The z-axis points to the zenith, rectangular to the plane x, y;
- The x-axis points to the north of the meridian;
- The y-axis points to the east, thus forming a left-hand system.
- x, y, z are equivalent to denotations north (n), east (e) and up (u).

Local (topocentric) coordinates (2)

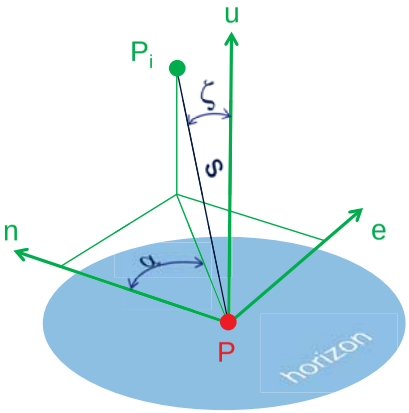

The topocentric systems are fundamental for connecting measurements of different techniques (local ties).

- Point P_i is described w.r.t. the origin P by the geodetic azimuth α, the zenith angle ζ and the distance s.
- The geodetic azimuth α is defined as the angle in the horizon plane between the meridian plane of P and the plane formed by the normals in P and P_i.
- The zenith angle ζ is measured in the vertical plane between the ellipsoidal vertical and the connecting line P- P_i, counted positive from the zenith.
- The distance s is only used in local geodetic systems (not in astronomic systems).

Conversion of topocentric to geocentric coordinates

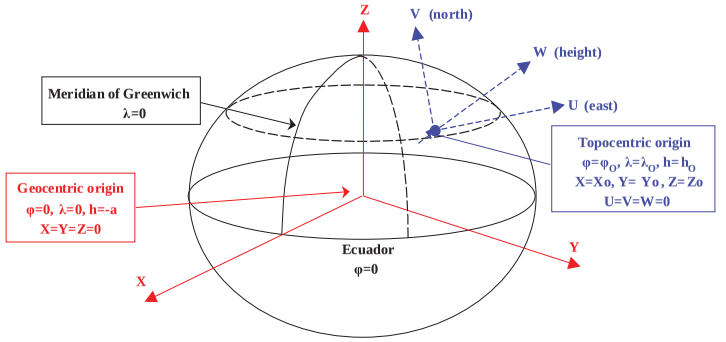

$$\begin{bmatrix} X \\ Y \\ Z \end{bmatrix} = R^{-1} * \begin{bmatrix} E \\ N \\ U \end{bmatrix} - \begin{bmatrix} X_0 \\ Y_0 \\ Z_0 \end{bmatrix}$$

with:

$$R^{-1} = R^T = \begin{bmatrix} -\sin\lambda_0 & -\sin\varphi_0 \cos\lambda_0 & \cos\varphi_0 \cos\lambda_0 \\ \cos\lambda_0 & -\sin\varphi_0 \sin\lambda_0 & \cos\varphi_0 \sin\lambda_0 \\ 0 & \cos\varphi_0 & \sin\varphi_0 \end{bmatrix}$$

$$X = X_O - E \sin\lambda_O - N \sin\varphi_O \cos\lambda_O + U \cos\varphi_O \cos\lambda_O$$
$$Y = Y_O + E \cos\lambda_O - N \sin\varphi_O \sin\lambda_O + U \cos\varphi_O \sin\lambda_O$$
$$Z = Z_O + N \cos\varphi_O + U \sin\varphi_O$$

1.4 Plane coordinates

- Plane coordinate systems enable representing the ellipsoidal (or spherical) surface in a plane through mathematical or geometrical specifications, e.g. by projections.
- As the representation of a curved surface in a plane is not possible without distortion, one has to decide on a representation distorting less the angles, the distances or the areas, respectively.

In principle there are three types of projections:
- Projections onto a cone,
- Projections onto a cylinder,
- Projections onto a plane.

The orientation of the surfaces can be
- normal (axis of the surface parallel to the Earth's rotation axis),
- transversal (axis parallel to the equator),
- oblique (axis in an arbitrary direction).

Projections

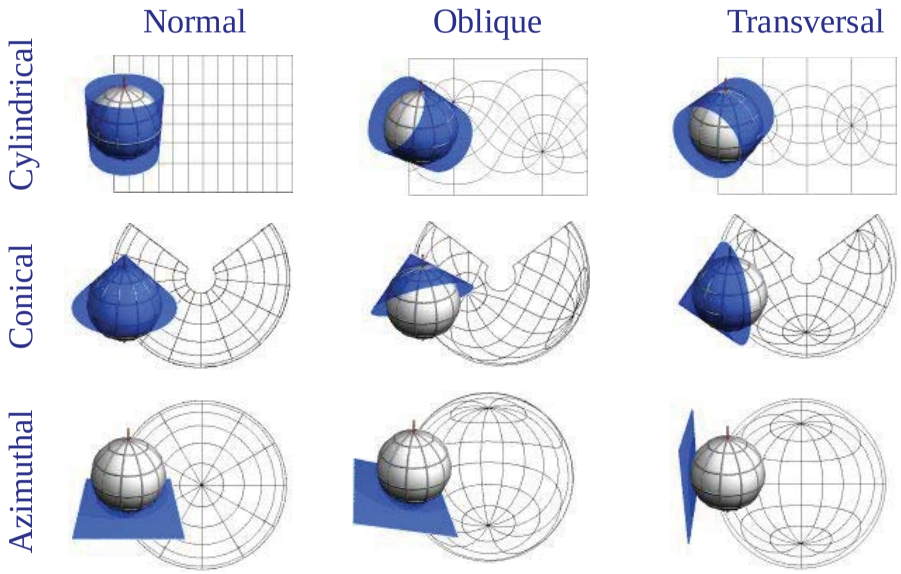

Special types of projections and distortions

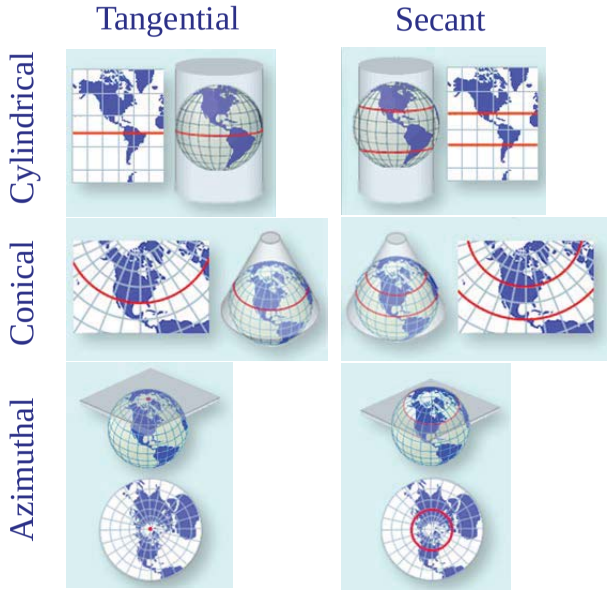

The metric distortions may be grouped into:
- Conformity: does not present (diferencial) angular distortion.
- Equivalence: presents coextensive (equal) areas.
- Equidistance: (some) meridian(s) and parallel(s) represent the true (relations of) length.

Gauss-Krüger plane conform coordinate system

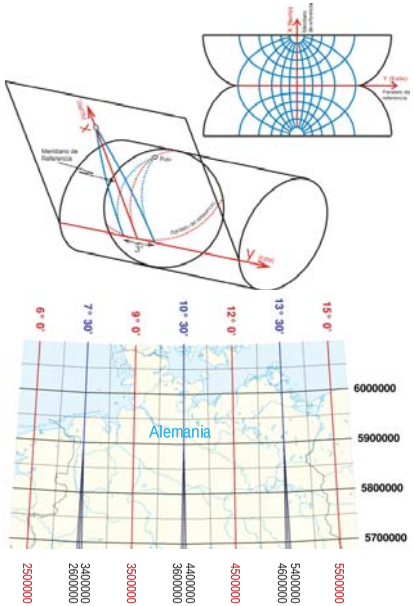

- The Gauss-Krüger system is based on a transversal cylindrical projection. It is not a geometrical projection but a mathematical conform transformation without differential angular distortion.
- It is regionally applied and divided in zones of 3° longitude extension.
- The central meridian and the equator are straight lines. The other meridians and parallels are complex curves.
- The scale is true along the central meridian and constant along the lines parallel to the meridian. It increases with the distance from the meridian.

Universal Transversal Mercator (UTM) System

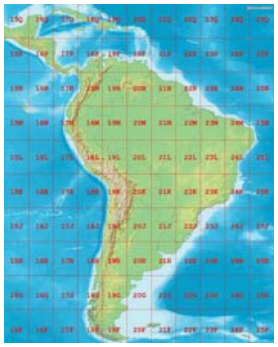

- The UTM system is similar to Gauss-Krüger.
- It is globally applied and divided in zones of 6° longitude extension.
- To reduce the distortion at the zone limits, a scale factor of 0,9996 is applied in the central meridian, so that the lines in 1°37' east and west distance present the true scale (1,0000).
- The Earth from 84ºN to 80ºS is divided into 20 stripes of 60 zones of 6º longitude extension.
- The border meridians are divisible by 6 and the zones are numbered from 1 to 60.
- The stripes of 8° (12° in the northernmost) are designated from south to north by letters (C to X without I and O) beginning with C in 80ºS.

Conical conform Lambert system

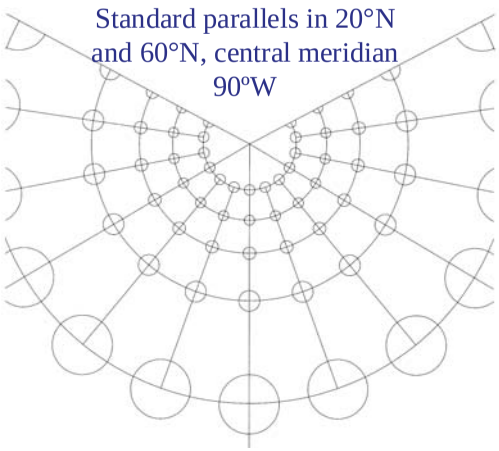

The distortion is constant along each parallel. There is no distortion along the standard parallels.

- The meridians are straight lines convergent to the pole.
- The angles between the meridians are true.
- The parallels are unequally separated; they are concentric circles around the poles.
- Two standard parallels are length-preserving (true scale).
- There is symmetry around each standard parallel.
- The pole closest to a standard parallel is a point, the other pole is not shown.

Polar stereographic system

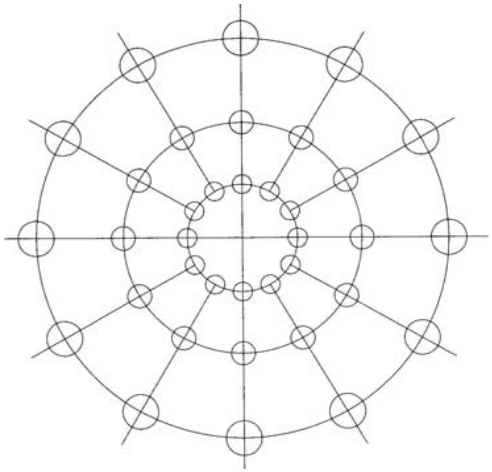

The distortion is constant along each parallel. There is no distortion along the standard parallel.

- The meridians are straight lines convergent to the pole.
- The angles between the meridians are true.
- The parallels are unequally separated; they are concentric circles around the poles.
- One standard parallel is length-preserving (true scale).
- There is symmetry around each standard parallel.
- The pole closest to a standard parallel is a point, the other pole is not shown.

2 Geodetic reference systems and frames
2.1 Definition of reference systems and frames

Reference System: *Definition* of standards, parameters, models, etc. serving as the basis for the representation of the geometry of the Earth surface and its temporal variation (e.g., speed of light c_0, standard gravitational parameter GM, models of special and general relativity, models of the atmosphere (ionosphere and troposphere), three-dimensional orthogonal Cartesian coordinate system with its temporal variation consistent with the Earth's rotation).

Reference Frame: *Realisation* (materialisation) of a reference system by a set of physical and mathematical quantities (e.g., a number of physically marked points at the Earth surface with given three-dimensional Cartesian coordinates X, Y, Z for a fixed epoch and its linear variations with time (dX/dt, dY/dt, dZ/dt), i.e. constant velocities (v_X, v_Y, v_Z).

Geodetic datum

Geodetic datum: Parameters fixing the origin, orientation and scale of a coordinate system w.r.t. the Earth (e.g., in a ***global 3D Cartesian system***: the *origin* is realised in the geo-centre, the *orientation* is realised by the position of the Earth rotation pole and the direction of one conventional reference longitude at a defined epoch, the *scale* is realised by the metre unit based on the speed of light in vacuum).

Important:

1. **Reference systems** cannot be determined by measurements, but they are defined conventionally; i.e., the geodetic coordinates and directions are not estimable but need a defined coordinate system.
2. **Reference frames** must realise the reference system strictly according to its definition (e.g. geocentric and not crust fixed).
3. **The geodetic datum** must be given unambiguously. 3D-systems require 7 parameters. There must not be fixed more coordinates.

Hierarchy of reference systems

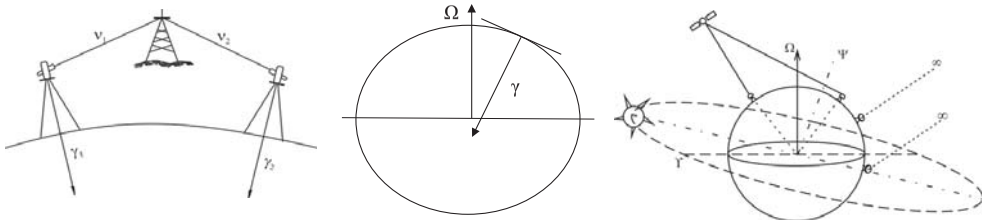

Denomination	Principal vectors	Application example
Observation system (local)	line-of-sight ν gravity γ	measurement of directions & distances
Horizon system (regional)	gravity γ Earth rotation Ω	terrestrial networks
Equator system (global)	Earth rotation Ω celestial origin ϒ	satellite geodesy
Celestial system (extragalactic)	celestial origin ϒ celestial reference pole	radio astronomy

Examples of global reference systems

Terrestrial reference systems (TRS)

World Geodetic System 1984 (WGS84): Global terrestrial reference system, originally established for orbit determination of TRANSIT Doppler satellites (WGS72), later adopted for the orbit determination of NAVSTAR GPS satellites (WGS84).

WGS84 adopted the ITRF (see next slide) for its realisation in 2002.

International Terrestrial Reference System (ITRS): Reference system of the International Earth Rotation and Reference Systems' Service (IERS) established for determining the celestial (ICRS) and terrestrial (ITRS) reference systems and their interrelation, i.e. the orientation and rotation of the Earth in space (EOP, ERP).

Examples of reference frames

Global and regional reference frames

International Terrestrial Reference Frame (ITRF):
Materialisation of the ITRS by stations at the Earth surface and given coordinates for a fixed epoch and its variations with time (velocities).
ITRF2008: more than 900 points in more than 500 sites.

The ITRF serves also for the precise orbit determination of the GPS satellites by the International GNSS Service (IGS).

Sistema de Referencia Geocéntrico para las Américas (SIRGAS):
Densification of the ITRF, initially established for South America by a GPS campaign with 58 stations in 1995 and extended to the Caribbean, Central and North America in 2000 with 184 stations. At present there are more than 250 permanent stations.

Examples of geodetic datums

Preliminary South American Datum 1956 (PSAD56):
Established by astronomically observed coordinates in La Canoa, Venezuela, referring to the international ellipsoid 1924 (Hayford).
Deviation from geo-centre: ΔX= -288 m, ΔY= 175 m, ΔZ= -376 m.

South American Datum 1969 (SAD69):
Established in Chúa, Brazil, referring to the GRS67 ellipsoid.
Deviation from geo-centre: ΔX = -57 m, ΔY = 1 m, ΔZ = -41 m.

North American Datum 1983 (NAD83):
Adjustment of astronomical, Doppler and VLBI measurements referring to the GRS80 ellipsoid.
Deviation from geo-centre: ΔX = 1,0 m, ΔY = -1,9 m; ΔZ = 0,5 m.

International Terrestrial Reference Frame (ITRF2008):
Use of Earth gravity field parameters $C_{11}=S_{11}=C_{10}=0$ in computing the orbits of Laser satellites for station positioning; orientation according to a defined meridian; metric scale unit.

Traditional and modern reference systems

Why do we need new reference systems? Why can't we continue using the traditional systems (PSAD56, SAD69, NAD83)?

→ Because we are using satellite techniques. We have to guarantee identical reference systems for terrestrial points and satellites.

Modern reference systems must be defined by a **global** datum:

The **origin** is the Earth's centre of mass (geo-centre $X_0=Y_0=Z_0=0$), because satellites are orbiting around the geo-centre (Kepler's law).

The **orientation** is given by the earth rotation axis (Z-axis) and the convention of a zero-longitude (X-axis in the Greenwich meridian).

The metric **scale** is given by the speed of light and (in case of use of satellite techniques) by the standard gravitational parameter GM.

Modern reference systems are always three-dimensional:
X, Y, Z, or transformed to North, East, Height w.r.t. an ellipsoid.

Traditional and modern reference systems

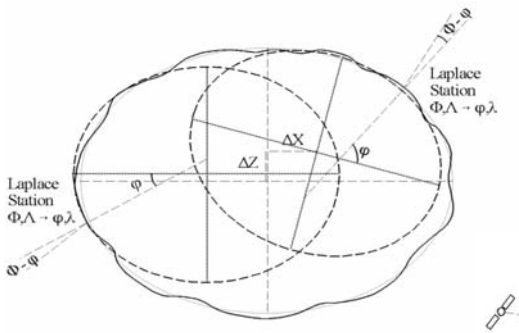

Traditional reference systems:

- regional definition
- national realisation
- local datum

Many systems around the globe

Modern reference systems:

- global definition
- global and regional realisation
- geocentric datum

One system all over the world

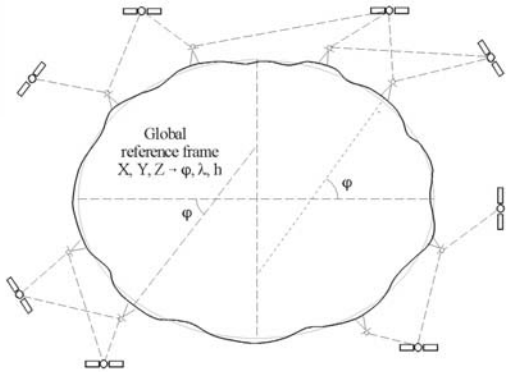

Organisation of modern reference frames

The modern reference systems are installed and maintained by the services of the International Association of Geodesy (**IAG**).

There is one service for each of the geodetic observation techniques:

- International GNSS (Global Navigation Satellite Systems) Service (**IGS**),
- International Laser Ranging Service (**ILRS**),
- International VLBI (Very Long Baseline Interferometry) Service for Geodesy and Astrometry (**IVS**),
- International DORIS (Doppler Orbitography and Radio-positioning Integrated by Satellite) Service (**IDS**).

The International Earth Rotation and Reference Systems' Service (**IERS**) coordinates the activities for establishing and maintaining the International Terrestrial Reference Frame (**ITRF**).

International Earth Rotation and Reference Systems Service

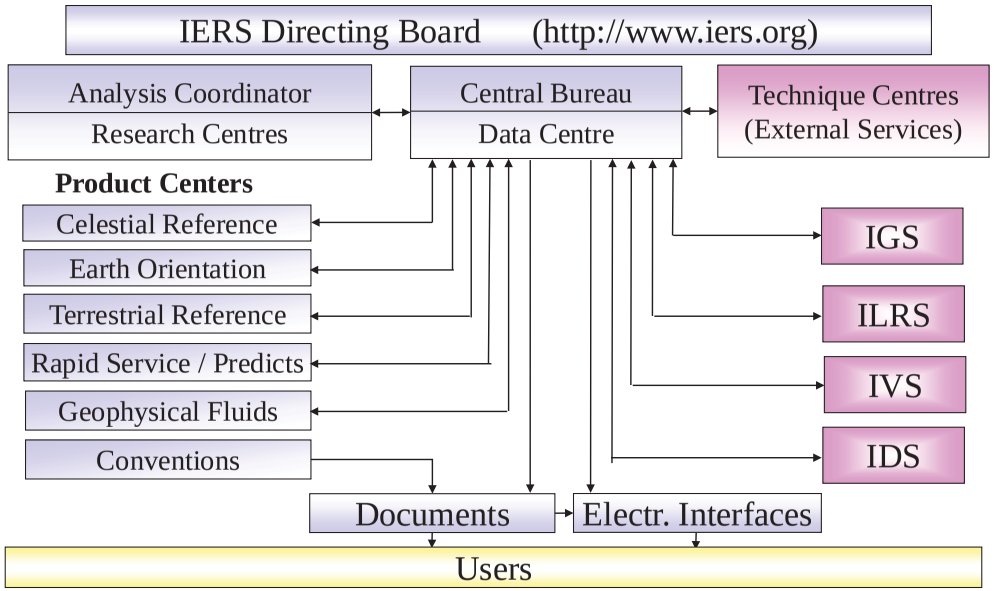

General structure of IAG Services

- *President* and elected *Directing* (or *Governing*) Board.
- *Central Bureau (Coordinating Office*).
- *Station network* for observations maintained by individual institutions at their own costs with *Operation Centre(s)*.
- *Satellites* operated by space agencies at their own costs (in case of satellite observation services).
- *Correlation Centres* of the observation data (in case of VLBI).
- *Data Centres* collecting the observation data and the results of the analysis and combination.
- *Analysis Centres* for processing the data and generating products for scientific and practical use.
- *Combination Centres* for evaluating and combining the products generated by the different analysis centres.

→ All the activities are voluntary and at the costs of the institutions.

International GNSS Service (IGS)

IGS Tracking Network (http://igs.org)

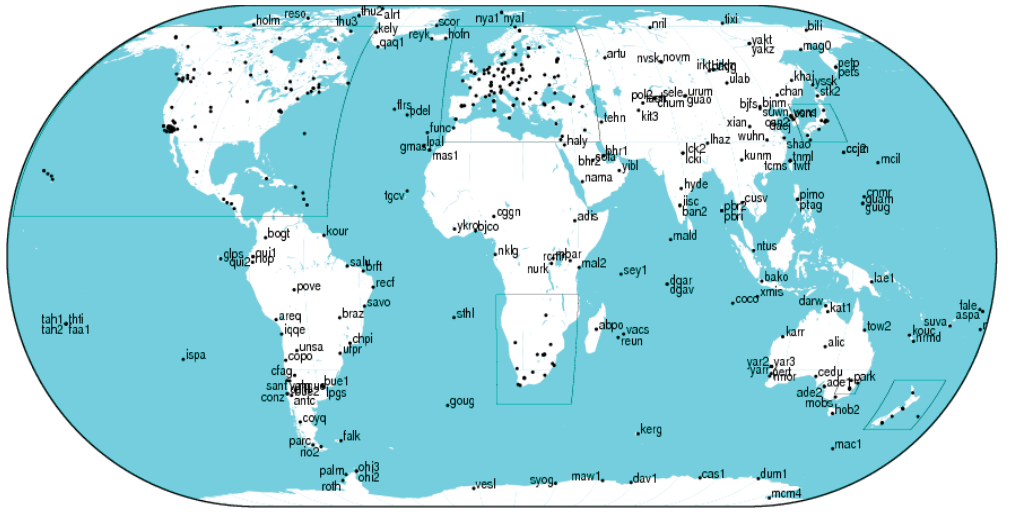

427 stations in total, 360 in operation (2013-09-15)

Int. Satellite Laser Ranging Service (ILRS)

ILRS Tracking Network (http://ilrs.gsfc.nasa.gov)

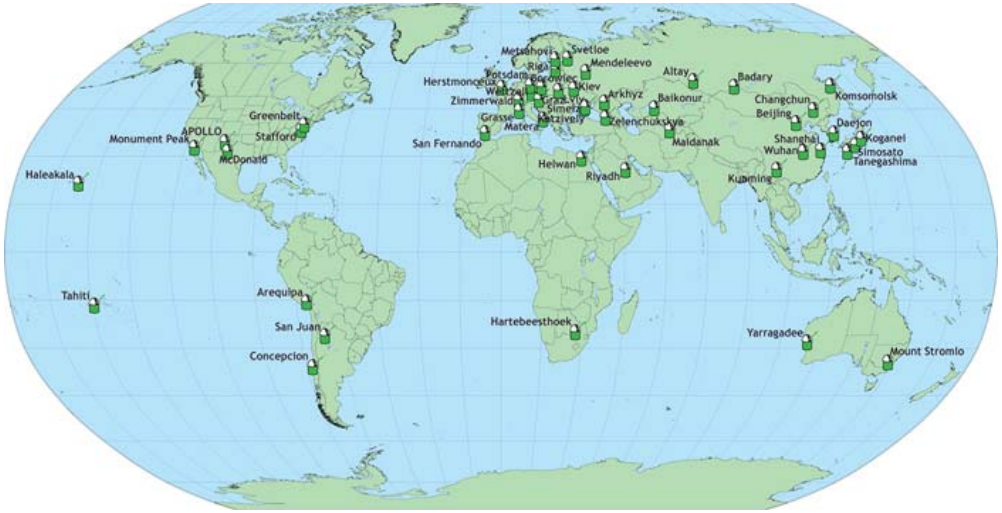

50 stations in operation (2013-01-09)

International VLBI Service (IVS)

IVS Tracking Network (http://ivscc.gsfc.nasa.gov)

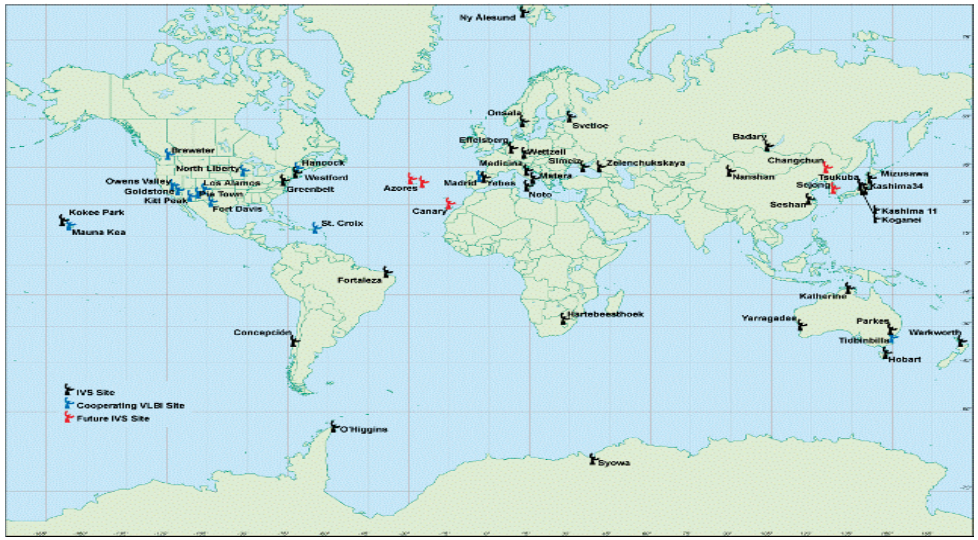

31 stations in operation (2013-08-16)

International DORIS Service (IDS)

IDS Tracking Network (http://ids.cls.fr)

75 stations in total, 59 in operation (2010-07-21)

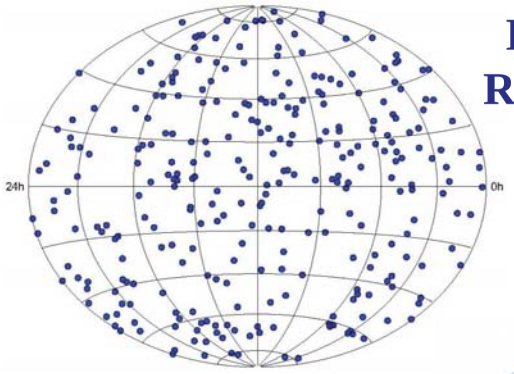

International Celestial Reference Frame (ICRF)

realised by the coordinates of Quasi Stellar Radio Sources (Quasars) observed by VLBI

Internat. Terrestrial Refer. Frame (ITRF)

realised by the coordinates of marked stations at the Earth's crust with 3-D coordinates

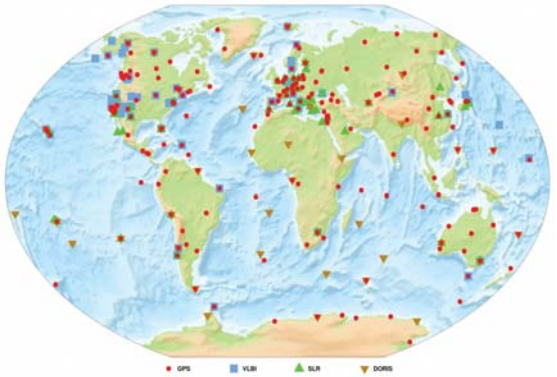

2.2 Celestial (inertial) reference system and frame

Celestial reference system = Conventional inertial system

- Inertial systems are non-accelerated systems without external force.
- The original laws of physics (Newton's laws, celestial mechanics, relativity theory, ...) refer to inertial systems.

↕

Earth orientation parameters (EOP)

- Rotation of the terrestrial with respect to the celestial system

↕

Terrestrial reference system = Conventional global system

- Terrestrial reference systems are associated with the solid Earth.
- They participate in all the motions of the solid earth and all the deformations of the Earth's crust.

Celestial (inertial) reference system

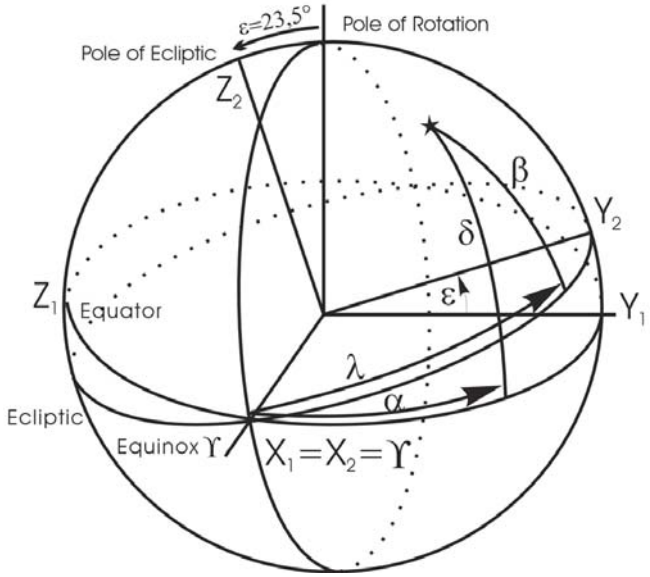

Ecliptic and equatorial systems

Coordinates of an object in space (star, radio source):

- equatorial system: right ascension α declination δ
- ecliptic system: ecliptic longitude λ ecliptic latitude β (hardly ever used)

Realisation of the celestial reference system by the International Celestial Reference Frame (ICRF)

The International Celestial Reference System (ICRS) is realised by the astronomic coordinates (right ascension and declination) of quasi-stellar astronomic radio sources (Quasars) observed by the Very Long Baseline Interferometry (VLBI). This realisation is called "International Celestial Reference Frame" (ICRF).

The current ICRF (ICRF2 of 2009) contains the coordinates of extragalactic radio sources for epoch 2000.0 in three categories:

- 295 datum defining sources,
- 3080 additional global sources,
- 39 instable sources with special treatment,

- 3414 sources in total.

Realisation of the ICRF by VLBI

Station O'Higgins, Antarctica, of BKG/DLR, Germany

Very Long Baseline Interferometry (VLBI)

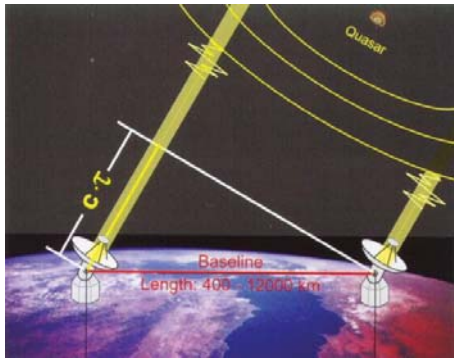

Two telescopes receive signals of the same radio source (Quasar) at different times.

Principle of VLBI analysis (1)

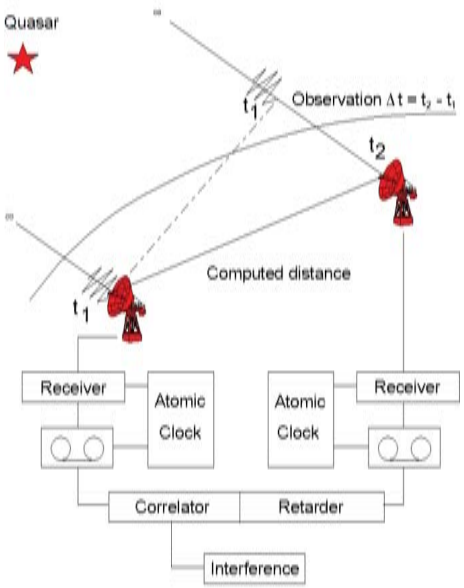

1. **Observation**

   Simultaneous recording of the signals from the same Quasars.

2. **Correlation**

   Calculation of the maximum correlation by delaying the signal of one receiver: → Δt.

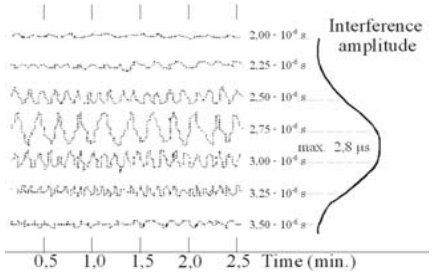

Principle of VLBI analysis (2)

Correlators (IGG Bonn, Germany)

One correlator is needed for each baseline. Today we have broadband data transmission (e-VLBI) and near real-time computer correlation.

3. **Corrections of VLBI observations**

- Ionospheric refraction
- Tropospheric refraction (dry and wet)
- Time (clock) correction
- Telescope calibration (deformations, eccentricities, signal travel time within the telescope to electronic centre)

The corrections are similar to GPS because the frequencies are similar.

Principle of VLBI analysis (3)

4. Analysis

Computation of the terrestrial baseline length and the direction to the Quasar.

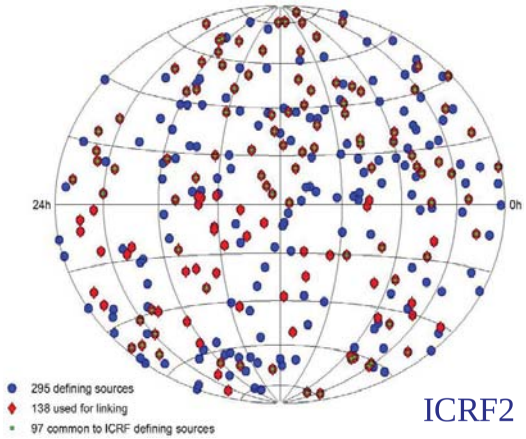

ICRF2

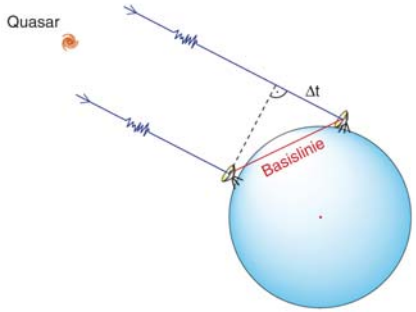

5. Adjustment

Computation of the Quasar coordinates (α, δ) relative to the terrestrial reference frame by simultaneous adjustment of all observations.

Example of ICRF2 coordinates

Designation	Source	α	δ	$\sigma_0(\alpha)$	$\sigma_0(\delta)$	$C_{\alpha\text{-}\delta}$	mean	first	last	N_{exp}	N_{obs}
ICRF J000435.6−473619	0002−478	00 04 35.65550384	−47 36 19.6037899	0.00001359	0.0002139	0.383	52501.0	49330.5	54670.7	28	129
ICRF J001031.0+105829	0007+106	00 10 31.00590186	10 58 29.5043827	0.00000491	0.0000930	−0.187	53063.9	47288.7	54803.7	29	559
ICRF J001101.2−261233	0008−264	00 11 01.24673846	−26 12 33.3770171	0.00000660	0.0000936	−0.183	52407.5	47686.1	54768.6	45	592
ICRF J001331.1+405137	0010+405	00 13 31.13020334	40 51 37.1441040	0.00000482	0.0000683	−0.139	51619.2	48434.7	54713.7	22	1083
ICRF J001611.0−001512	0013−005	00 16 11.08855479	−00 15 12.4453413	0.00000435	0.0001005	−0.235	52403.0	47394.1	54492.8	67	716
ICRF J001945.7+732730	0016+731	00 19 45.78641940	73 27 30.0174396	0.00000989	0.0000424	−0.050	49249.8	44343.6	54865.7	458	25038
ICRF J002232.4+060804	0019+058	00 22 32.44120914	06 08 04.2690807	0.00000439	0.0000956	−0.237	52705.8	47394.1	54880.7	42	800
ICRF J003824.8+413706	0035+413	00 38 24.84359231	41 37 06.0003032	0.00000499	0.0000613	−0.035	52262.4	49422.9	54887.7	18	1024
ICRF J005041.3−092905	0048−097	00 50 41.31738756	−09 29 05.2102688	0.00000278	0.0000428	−0.030	51323.1	44773.8	54816.7	1802	41482
ICRF J005109.5−422633	0048−427	00 51 09.50182012	−42 26 33.2932480	0.00000932	0.0001177	0.013	53857.8	52306.7	54907.7	31	315
ICRF J010245.7+582411	0059+581	01 02 45.76238248	58 24 11.1366009	0.00000523	0.0000414	0.009	52030.9	48720.9	54880.7	1864	236989
ICRF J010645.1−403419	0104−408	01 06 45.10796851	−40 34 19.9602291	0.00000376	0.0000455	0.016	52201.3	47640.2	54903.8	1175	11531
ICRF J010915.4−604948	0107−610	01 09 15.47520598	−60 49 48.4599686	0.00001744	0.0001750	0.108	53933.9	52780.7	54726.7	24	102
ICRF J011205.8+224438	0109+224	01 12 05.82471754	22 44 38.7863909	0.00000379	0.0000653	−0.007	51836.0	48434.7	54872.7	37	1851
ICRF J011327.0+494824	0110+495	01 13 27.00680344	49 48 24.0431742	0.00000597	0.0000727	−0.135	52989.4	49422.9	54781.7	20	759
ICRF J011857.2−214130	0116−219	01 18 57.26216666	−21 41 30.1399986	0.00000683	0.0001138	−0.058	52128.2	50632.3	54768.6	19	289
ICRF J012141.5+114950	0119+115	01 21 41.59504339	11 49 50.4131012	0.00000279	0.0000429	−0.018	52622.1	47394.1	54901.7	1151	36167
ICRF J013305.7−520003	0131−522	01 33 05.76255607	−52 00 03.9457209	0.00001218	0.0001605	0.251	52621.9	48162.4	54901.7	28	126
ICRF J013658.5+475129	0133+476	01 36 58.59480585	47 51 29.1000445	0.00000407	0.0000414	0.014	52890.7	44343.6	54907.7	1307	117353
ICRF J013708.7+312235	0134+311	01 37 08.73362970	31 22 35.8553611	0.00000553	0.0001012	0.044	53105.6	50219.8	54901.7	13	550
ICRF J014125.8−092843	0138−097	01 41 25.83215547	−09 28 43.6741894	0.00000455	0.0000878	−0.020	52777.3	46875.8	54768.6	34	1008
ICRF J015456.2+474326	0151+474	01 54 56.29988783	47 43 26.5395732	0.00000530	0.0000654	−0.014	53123.2	49750.8	54657.8	21	1395
ICRF J020333.3+723353	0159+723	02 03 33.38496841	72 32 53.6672938	0.00001231	0.0000546	0.052	52872.5	47011.4	54907.7	35	1482
ICRF J020504.9+321230	0202+319	02 05 04.92536007	32 12 30.0954538	0.00000367	0.0000520	−0.038	52311.3	45466.3	54852.7	62	2357
ICRF J021748.9+014449	0215+015	02 17 48.95475182	01 44 49.6990704	0.00000348	0.0000673	−0.120	51978.4	48919.9	54837.7	37	1200
ICRF J022428.4+065923	0221+067	02 24 28.42819659	06 59 23.3415393	0.00000382	0.0000683	−0.214	52153.5	47394.1	54662.7	68	1173
ICRF J022934.9−784745	0230−790	02 29 34.94659358	−78 47 45.6017972	0.00003546	0.0001073	0.032	52873.3	47626.5	54726.7	49	247
ICRF J023145.8+132254	0229+131	02 31 45.89405431	13 22 54.7162668	0.00000281	0.0000422	−0.006	49841.4	44773.8	54844.7	2537	66911
ICRF J023631.1−295355	0234−301	02 36 31.16942057	−29 53 55.5402759	0.00000978	0.0001544	−0.032	53761.6	53126.1	54741.8	16	135
ICRF J023653.2−613615	0235−618	02 36 53.24574589	−61 36 15.1834250	0.00002197	0.0001688	0.249	53734.9	52861.2	54670.7	17	106
ICRF J023752.4+284808	0234+285	02 37 52.40567732	28 48 08.9900231	0.00000313	0.0000421	−0.023	49361.6	44447.0	54664.7	1199	53070
ICRF J023945.4−023440	0237−027	02 39 45.47226775	−02 34 40.9144020	0.00000359	0.0000672	−0.090	52760.9	49253.8	54901.7	36	1437
ICRF J030335.2+471616	0300+470	03 03 35.24222254	47 16 16.2754406	0.00000417	0.0000433	−0.048	48470.0	44343.6	54844.7	757	25008
ICRF J030350.6−621125	0302−623	03 03 50.63134799	−62 11 25.5498711	0.00001499	0.0001135	0.150	51436.6	48162.4	54726.7	44	248
ICRF J030642.6+624302	0302+625	03 06 42.65954796	62 43 02.0241642	0.00000833	0.0000613	−0.047	52280.3	48614.0	54662.7	37	1334

(continued on next page)

Interrelation of CRF and TRF

The celestial bodies (stars, radio sources) and artificial satellites used for space measurements in the Terrestrial Reference System (TRS) do not participate in the Earth rotation. Therefore we have to know the Earth Orientation Parameters (EOP) with respect to the Celestial Reference System (CRS) at any instantaneous time of measurements at the Earth surface.

The EOP provide the connection between the CRF and the TRF. They are derived from the continuous observation of the Earth's rotation.

We distinguish between the orientation of the Earth in space (precession and nutation), the orientation with respect to the body of the Earth (polar motion), and the variation of the rotational velocity (variation of Universal Time UT or Length of Day LOD, respectively).

Connection between CRF and TRF via EOP

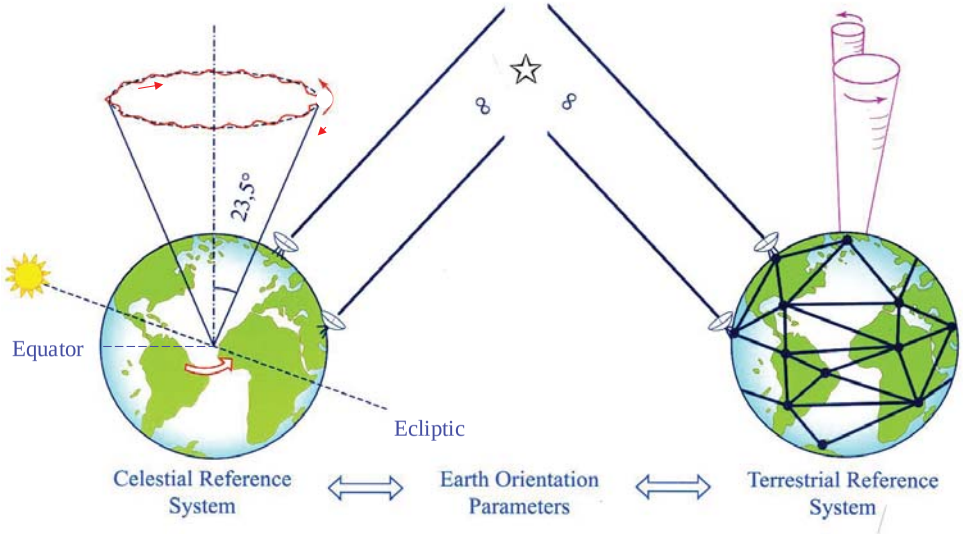

The reference systems must be consistent: CRF-EOP-TRF

Variation of orientation in space

The cause of the variation of Earth orientation in space (precession and nutation) is the asymmetric effect of the lunisolar gravitational forces on the equatorial bulge.

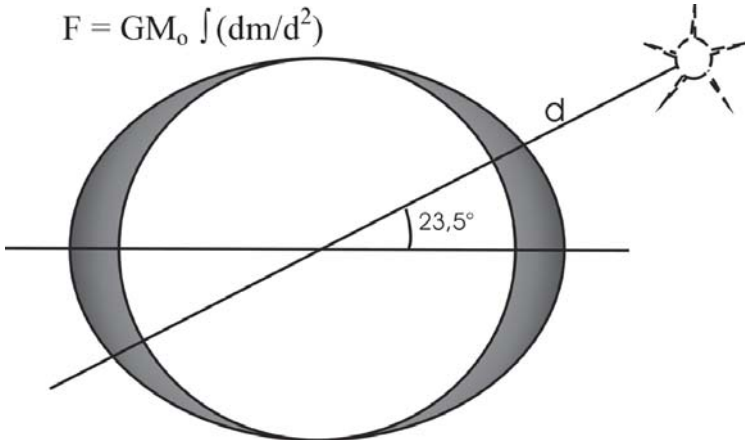

Precession and nutation

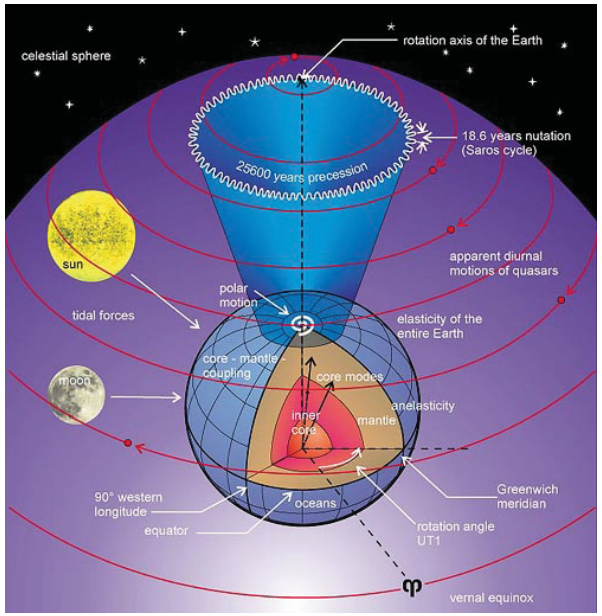

The lunisolar forces produce a wobble of the rotation axis of the Earth in space.

Traditionally it was distinguished between the frequencies of precession (lower frequency) and nutation (higher frequencies).

This differentiation was terminated with the IAU 2000 and IUGG 2003 resolutions.

Precession and nutation in the inertial space

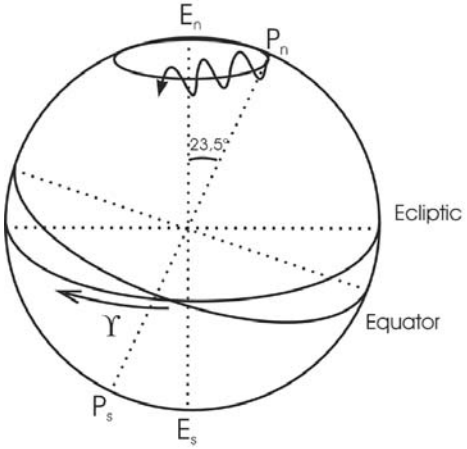

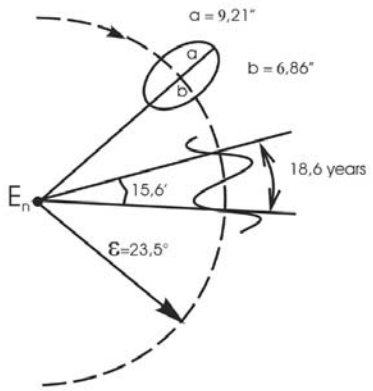

$P = R_3(-z)\, R_2(\theta)\, R_3(-\zeta)$ $N = R_1(-\varepsilon-\Delta\varepsilon)\, R_3(-\Delta\psi)\, R_1(\varepsilon)$

The system 2000 of the International Astronomical Union (IAU2000) fixes the origin of right ascension at epoch 2000.0 ("non rotating"). The new precession-nutation model ($\Delta\psi$, $\Delta\varepsilon$) includes all the effects.

Reduction of precession and nutation in geodetic and astronomical observations

Conventional Inertial System (CIS) Realised as ICRF by Quasar coordinates		Celestial Intermediate System
Equatorial system at a fixed epoch (e.g. t_0 = 2000.0)	Precession-Nutation →	Instantaneous (true) equatorial system
Z-axis = celestial pole at a fixed epoch (e.g. t_0 = 2000.0)		Z-axis = Celestial Intermediate Pole (CIP)

2.3 Rotation and tides of the Earth

Variation of Earth rotation relative to the Earth's body

1. The Earth rotation axis does not coincide with the symmetry axis (principal axis of inertia)

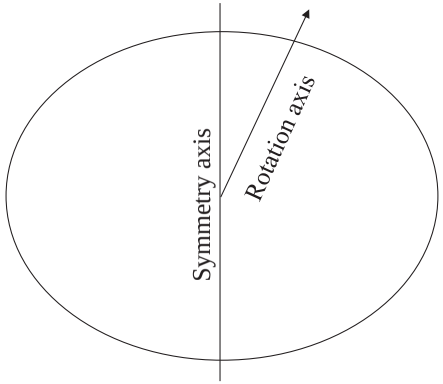

2. The angular momentum varies due to displacements and motions of masses.

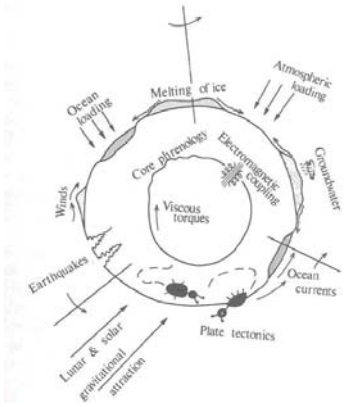

Polar motion (X_P, Y_P) and variation of the rotational velocity UT1-UTC

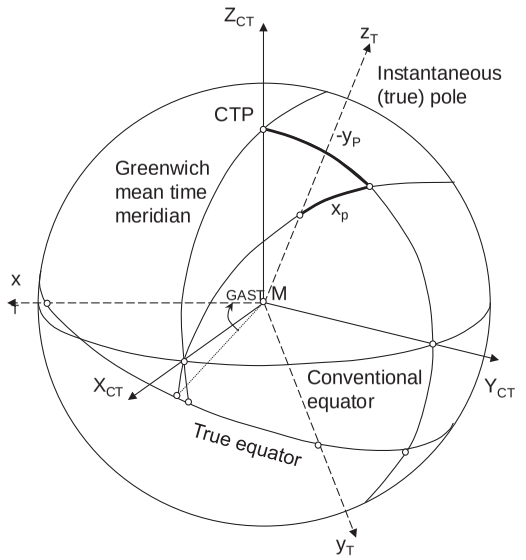

Earth Rotation Parameters (**ERP**: X_P, Y_P, DUT)

CTP = Conventional Terrestrial Pole

GAST = Greenwich Apparent Sidereal Time

UT1 = Universal Time

UTC = Universal Time Coordinated (TAI)

DUT = UT1 - UTC
= Variation of GAST

dDUT = Variation of LOD (Length of Day)

Reduction of ERP variations

Celestial intermediate system		Conventional Terrestrial System (CTS)
Instantaneous (true) equatorial system	Polar motion (X_p, Y_p), and variation of angular velocity (DUT = UT1 – UTC) →	Global system at a fixed epoch (e.g. t = 2000.0)
Z-axis = Celestial Intermediate Pole (CIP)		Z-axis = axis of the coordinate system for the points in the conventional system

Rotation of the Earth as a rigid body

Law of conservation of the angular momentum in an inertial system:

$d\mathbf{H}/dt = \mathbf{0}$ (**H** = angular momentum)

$\mathbf{H} = \mathbf{I} \cdot \boldsymbol{\omega}$ (**I** = moment of inertia, **ω** = rotational velocity)

In an inertial celestial system (Euler equation):

$d\mathbf{H}/dt = \mathbf{L}$ (**L** = lunisolar torque → precession, nutation)

In a terrestrial system (→ polar motion):

$d\mathbf{H}/dt + \boldsymbol{\omega} \times \mathbf{H} = 0$ (if axis **H** ≡ axis **ω** there is no motion!)

With principal moments of inertia of the body of the Earth A, B, C:

$$\mathbf{H} = \mathbf{I} \cdot \boldsymbol{\omega} = \begin{vmatrix} A & & \\ & B & \\ & & C \end{vmatrix} \cdot \begin{vmatrix} \omega_1 \\ \omega_2 \\ \omega_3 \end{vmatrix}$$

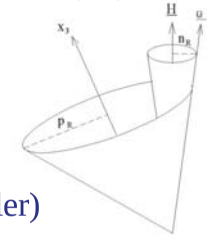

The solution is a circular motion with the radius

$p_R = \sqrt{\omega_1^2 + \omega_2^2} = 0{,}2''$ and period $1/\sigma = 305$ days (Euler)

Rotation of the Earth as a non rigid body

$\mathbf{I}(t) = \mathbf{I} + \Delta\mathbf{I}(t)$ time variable moment of inertia due to mass displacements in the terrestrial system

$\mathbf{H}(t) = \mathbf{I}(t) \cdot \boldsymbol{\omega}$ time variable angular momentum

$d\mathbf{H}/dt + \boldsymbol{\omega} \times \mathbf{H} = \mathbf{L}$ Liouville equation (instead of Euler equation)

The solution of the Liouville equation results (in the same way as the Euler equation) in the period and the amplitude of the circular motion of the Earth rotation pole. This is for an elastic Earth:

$1/\sigma = 435$ days (Chandler period)

In addition to the variation of the moment of inertia by the displaced masses there is an effect by the motion (velocity v) of the masses:

$\mathbf{h}(t) = \int (\mathbf{x} \times \mathbf{v})\, dM$ angular momentum due to the motion of masses

$\mathbf{H}(t) = \mathbf{I}(t) \cdot \boldsymbol{\omega} + \mathbf{h}(t)$ "forced" angular momentum

Angular momentum caused by moving masses

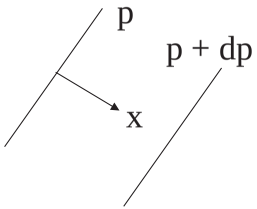

Strongest mass movements in the Earth system are those of the atmosphere and the oceans. Temperature variations (dT) change the mass density. The volume (dv) varies opposing to the pressure (p) and produces thermodynamic energy

$$dQ = c \cdot dT + p \cdot dv$$

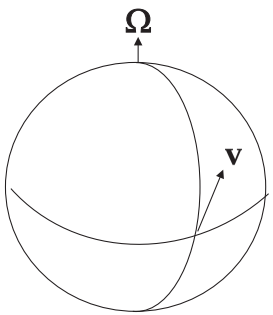

The thermodynamic energy generates an acceleration of masses in the atmospheric and oceanic **pressure** field

$$d^2x / dt^2 = dv / dt = -1/\rho\, dp/dx$$

The motion of masses interferes with the Earth rotation and causes the **Coríolis** acceleration

$$d^2x / dt^2 = dv / dt = -2\, \boldsymbol{\Omega} \times \mathbf{v}$$

Variation of Earth rotation by moving masses

In case of equilibrium between the accelerations caused by pressure and by the Coriolis force there is a “geostrophic” motion (Greek: strephein = to turn)

$$1/\rho \, dp/dx - 2\,\boldsymbol{\Omega} \times \mathbf{v} = 0$$

This motion has no acceleration and results different in the northern and southern hemispheres:

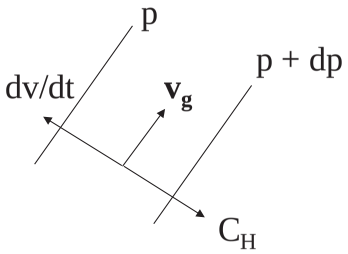

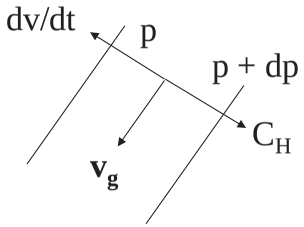

The high pressure of the atmosphere is on the right of currents in the northern hemisphere and on the left in the southern hemisphere.

Circulation of the atmosphere (principal winds)

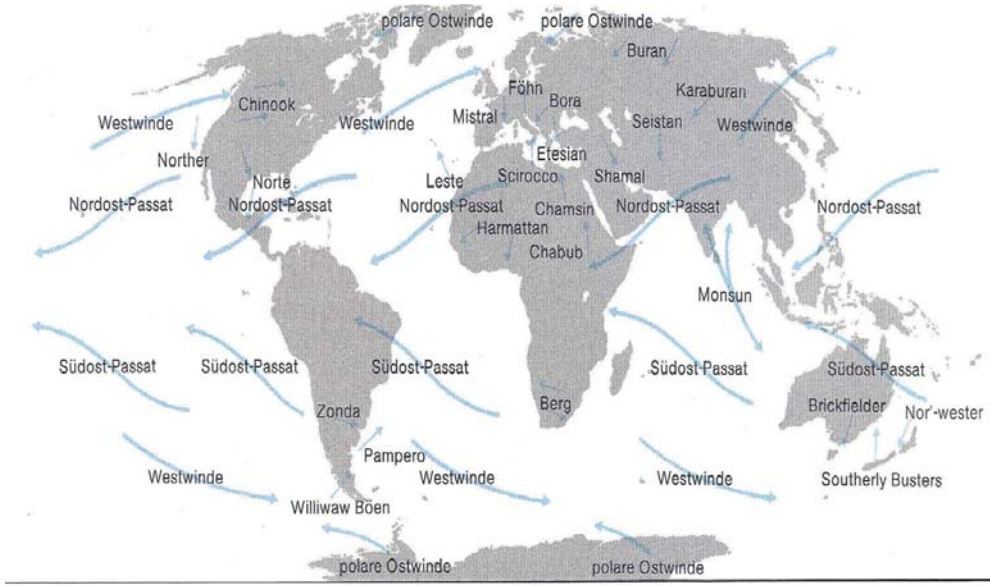

Circulation of the oceans (principal currents)

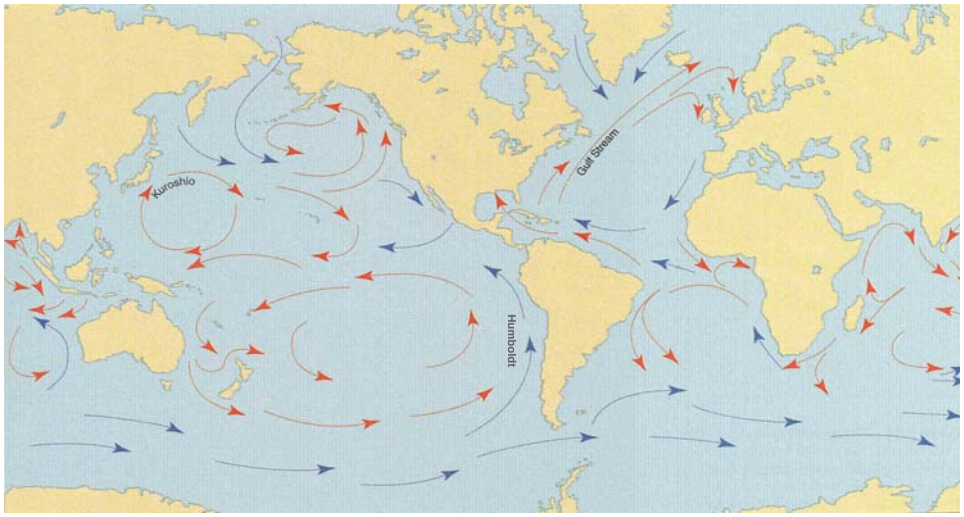

The deviations of on-going atmospheric and oceanic currents from the geostrophic currents generate the variations of Earth rotation.

Observation of variations of Earth rotation by space geodetic techniques (VLBI, SLR, GPS)

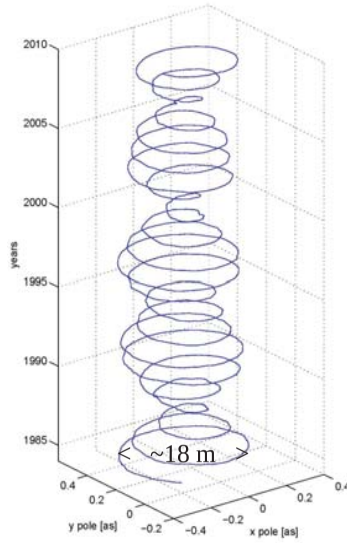

Polar motion [″] = [arcsec]
1″ ≈ 31 m in latitude and equatorial longitude

Variation of rotational velocity (LOD [sec])

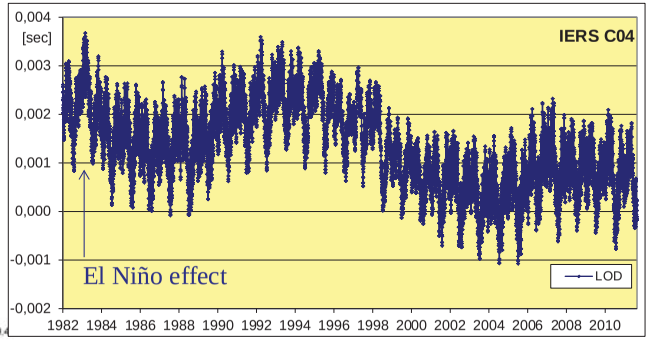

1 ms ≈ 46 cm linear motion at the equator

Partitioning of polar motion

Motion with Chandler period (435 days) [″]

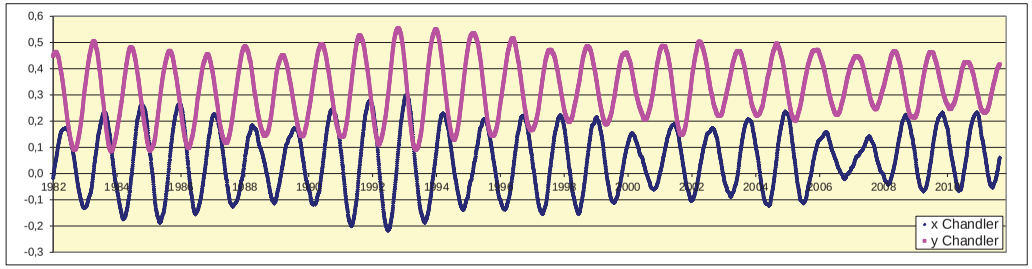

Motion with annual period (365,25 days) [″]

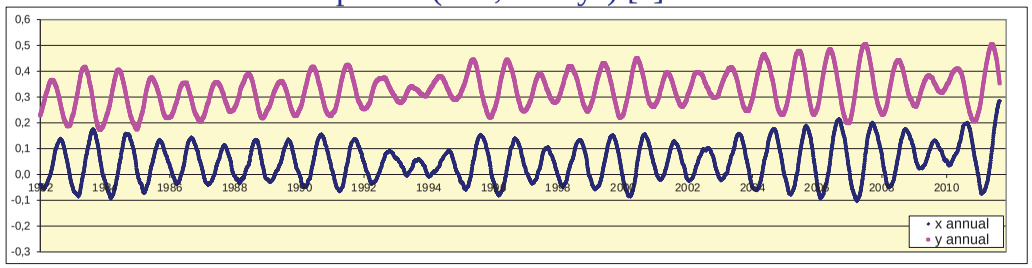

Causes of variations of Earth rotation

Y_P component and atmospheric angular momentum [“]

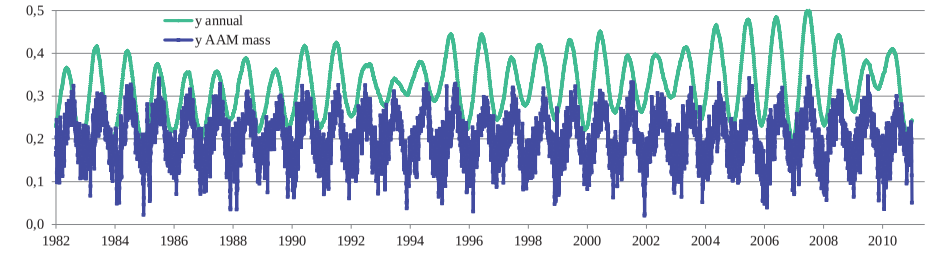

LOD and angular momentum of atmospheric mass motions [s]

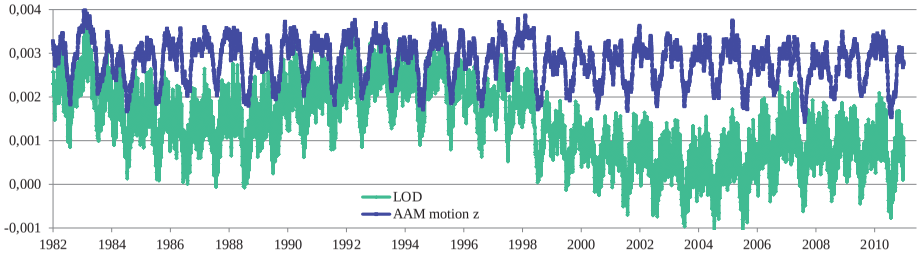

Importance of variations of Earth rotation for reference systems

The variations of Earth rotation with respect to the **inertial space** (precession and nutation) affect the coordinates of celestial bodies (right ascencion and declination). They must be reduced from the positions in the celestial reference system (Quasars, satellite orbits).

The variations of Earth rotation with respect to the Earth’s body (polar motion and UT1/LOD) affect the terrestrial coordinates (latitude and longitude). They must be reduced from the positions in the terrestrial reference system (reference frame).

If the variations of Earth rotation are not reduced, they produce errors in the precise positioning using space techniques (e.g. GPS) coming up to several metres.

Lunisolar tidal acceleration (1)

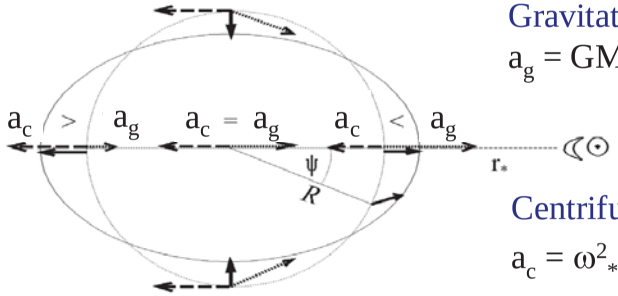

Gravitational acceleration

$a_g = GM_* / (R^2 + r^2_* - 2Rr_* \cos\psi)$

Centrifugal acceleration

$a_c = \omega^2_* (r_* - R \cos\psi)$

Total acceleration: (Doodson’s constant $D_* = 0{,}75\ GM_* R^2 / r^3_*$)

- radial: $a_r = 2/R\ D_* (\cos 2\psi_* + 1/3)$ - tangential: $a_\psi = 2/R\ D_* \sin 2\psi$

Effects of Moon and Sun

Celestial body *	$M_* : M_{Earth}$	$R : r_*$	D_*
Moon	1 : 81,3	1 : 60	2,628 m²/s²
Sun	332946 : 1	1 : 23481	1,208 m²/s²

Lunisolar tidal acceleration (2)

Most important partial tides (Torge 1989)

Symbol	Period [h]	Amplitude [μms^{-2}]	Origin (Lunar/Solar)
Long period components			
M_0	∞	102,9	L constant flattening
S_0	∞	47,7	S constant flattening
Diurnal periods			
K_1	23,93	436,9	L, S inclination of the ecliptic
O_1	25,82	310,6	L principal wave
P_1	24,07	144,6	S principal wave
Semidiurnal components			
M_2	12,42	375,6	L principal wave
S_2	12,00	174,8	S principal wave
N_2	12,66	71,9	L ecliptic orbit

Lunisolar tidal acceleration (3)

Variation of amplitudes as a function of latitude

Acceleration [μgal = 10 nms^{-2}] Inclination [10^{-3} "]

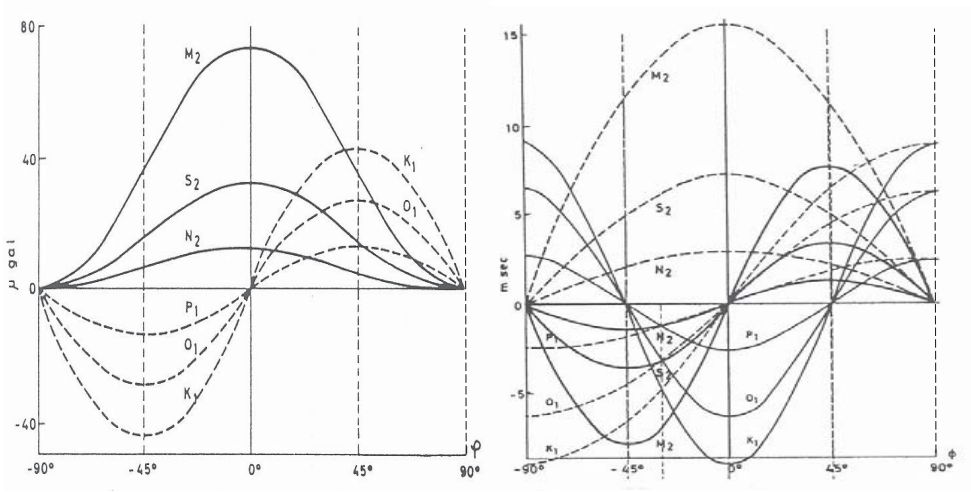

Deformation caused by Earth tides (1)

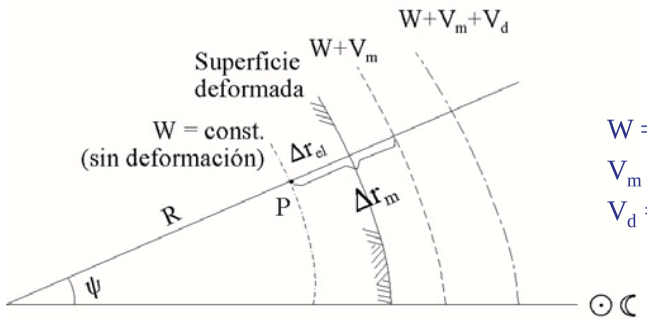

W = gravitational potential
V_m = tidal potential
V_d = deformation potential

Deformation of the elastic Earth generated by the potential V_m:

$\Delta r_{el} = h \cdot \Delta r_m = h \cdot V_m/g$ (h = Love number)

Deformation of the level surface ($W + V_m$) generated by the mass displacements:

$V_d = k \cdot V_m$ (k = Love number)

Deformation caused by Earth tides (2)

Horizontal surface deformation (l = Shida number):

$\Delta x_{el} = l\,(1/g)\,(\partial V/\partial \varphi)$ $\Delta y_{el} = l\,(1/g)\,(\partial V/\cos\varphi\,\partial \lambda)$

Gravimetric amplitude factor: $\delta = 1 - 1{,}5\,k + h$

Inclination amplitude factor: $\gamma = 1 + k - h$

h(f), k(f), l(f), δ(f), γ(f) are frequency dependent parameters reflecting the elastic behaviour of the body of the Earth.

Magnitudes	**Lunar effect**	**Solar effect**
Equipotential surface deformation	~36 cm	~16 cm
h ≈ 0,64 (topography deformation)	~23 cm	~10 cm
k ≈ 0,32 (subsequent level deformation)	~12 cm	~ 5 cm
l ≈ 0,16 (horizontal deformation)	~10^{-8} = 1 μm /100 m	
δ ≈ 1,164 (gravimetric amplitude)	-1,1 ... +0,5	-0,5 ... +0,3 μms^{-2}
γ ≈ 0,674 (inclination amplitude)	± 0,017"	± 0,008"

Observation of Earth tides

Horizontal pendulum

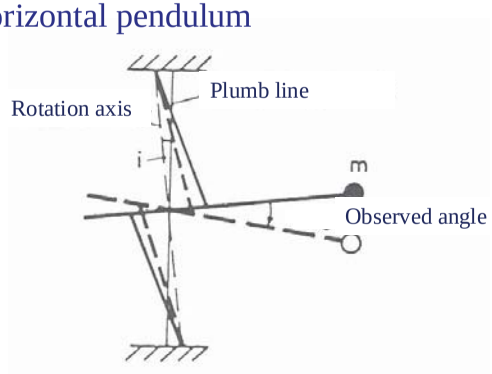

Zöllner principle

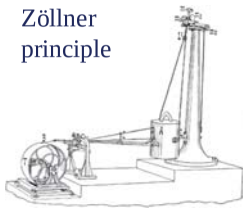

Superconducting Gravimeter

Observation of ocean tides

Principle of a tide gauge

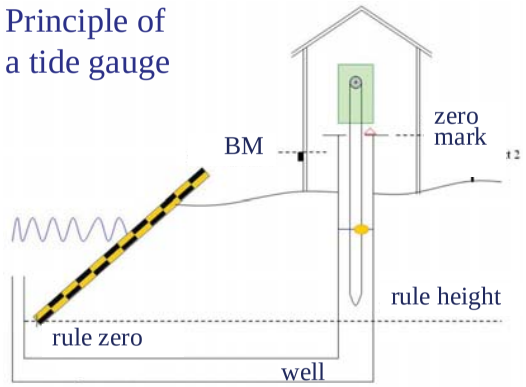

Principle of satellite altimetry

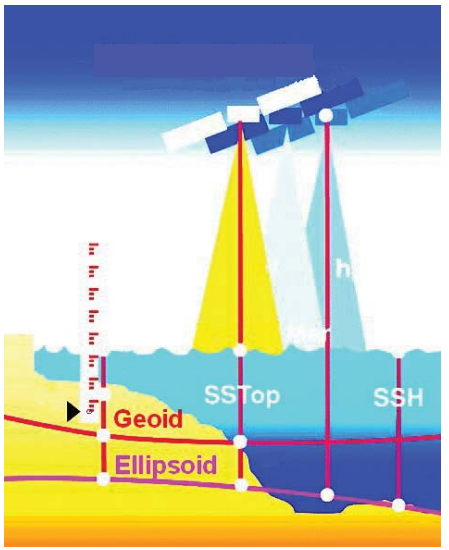

Ocean tide model

Example M_2-model: Amplitude (dashed lines [cm]) and phase ([h])

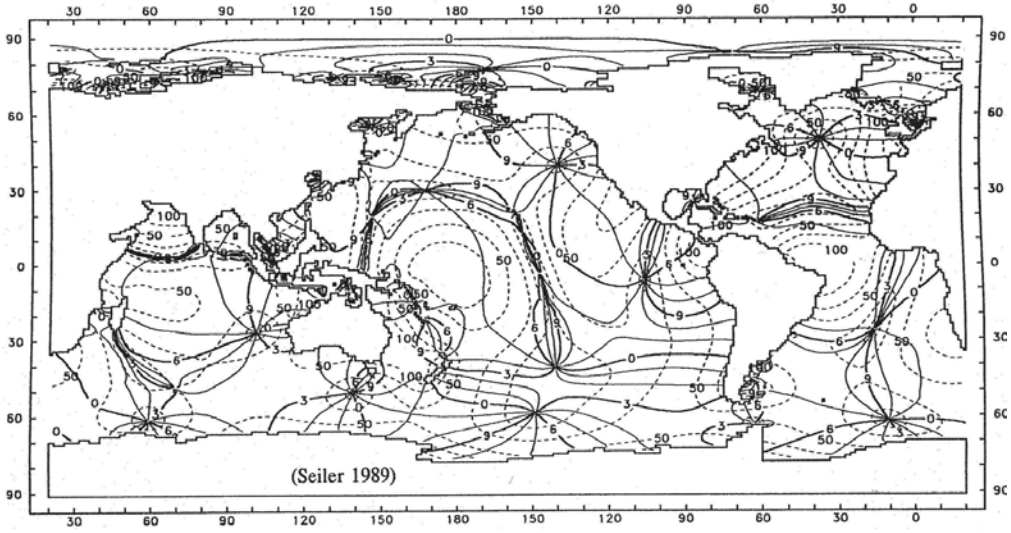

Importance of Earth and ocean tides for terrestrial reference systems

Tides affect the Earth surface in two ways:

- Deformation caused by gravitational forces of Moon and Sun;
- Deformation caused by variable ocean and atmosphere loading.

The effects on the terrestrial reference frame must be reduced (e.g. by the terrestrial model FES2004 and the ocean model Scherneck).

In the (geometric) terrestrial reference system we reduce the entire effect including the deformation caused by the permanent potential of Moon and Sun. The result is a system completely free of tidal effects (“tide free system”).

In the measurement of terrestrial gravity the effect of the permanent potential is not reduced but only the temporal effects. The result is a system of the average tides (“mean tide system”).

As a consequence positions and gravity values are not consistent.

2.4 Terrestrial reference system and frame

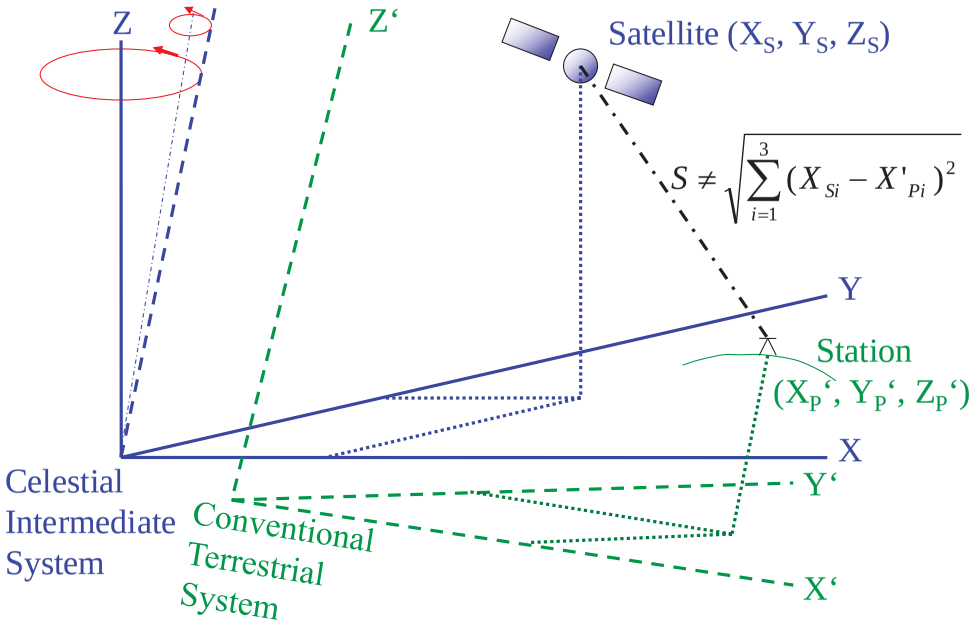

Required consistency of reference systems

Consequences of non-consistent systems

1. Single (precise) point positioning (PPP)

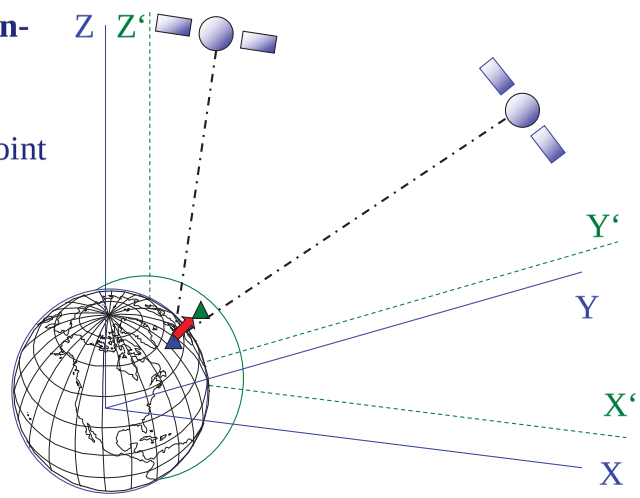

The difference between the reference systems (origin and orientation) enters completely into the coordinates (e.g. polar motion up to 18 m)

Required consistency of reference systems

Consequences of non-consistent systems

2. Relative (differential) positioning by GPS

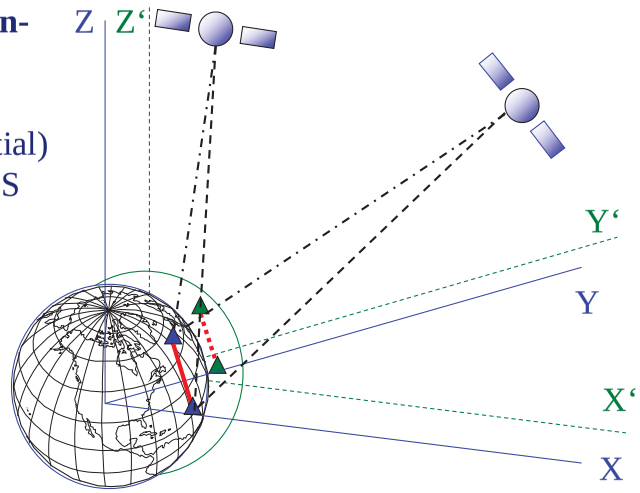

A scale factor of ~ 2 ... 3 · 10^{-7} per metre difference in the reference systems enters into the baselines (18 m polar motion: ~ 5 mm/km)

Consistency of CRS and TRS by transformation

Conventional Inertial System (CIS)

Precession-Nutation

Celestial Intermediate Pole (CIP)

Polar motion, DUT variation

Conventional Terrestrial System (CTS)

Coordinates (angles) of the Quasars (ICRF)

↓

N ($\Delta\psi$, $\Delta\varepsilon$)

X_{Pole}, Y_{Pole}, UT1 - UTC

↓

Point coordinates (3-D) at the Earth surface

International Terrestrial Reference System (ITRS)

The terrestrial reference system must be consistent with the celestial reference system used for satellite orbits. ITRS is a **3-D Cartesian** system.

- **The origin** of the ITRS is defined by the Earth's centre of mass (including atmosphere and oceans), because satellites are orbiting around the geo-centre according to Kepler's laws.
- **The orientation** of the axes is defined conventionally by fixing the Z-axis close to the Earth rotation axis and the X-axis close to the Greenwich meridian in its positions at a given epoch. The time evolution must be given by station motion parameters (velocities) not generating a global rotation with respect to the Earth rotation.
- **The scale unit** is metric as defined by the speed of light in vacuum according to the International System of Units (SI) and by the standard gravitational parameter GM (for satellite techniques).
- **Standards and models** are defined by the IERS Conventions.

Realisation of the datum of the ITRS

The datum is realised by combination of geodetic space techniques:

- SLR provides the relation to the geo-centre by determining the orbit in the Earth gravity field with corresponding parameters:

The centre of mass is the integral over all the masses of the Earth:

$X_0 = \iiint X\, dm / M$

$Y_0 = \iiint Y\, dm / M$

$Z_0 = \iiint Z\, dm / M$

The spherical harmonics of the Earth gravity field are:

$C_{11} = \iiint X\, dm / a\, M$

$S_{11} = \iiint Y\, dm / a\, M$

$C_{10} = \iiint Z\, dm / a\, M$

A gravity model with $C_{11}=S_{11}=C_{10}$ provides geocentric coordinates!

- VLBI provides the orientation by the EOP ($\Delta\psi$, $\Delta\varepsilon$, X_p, Y_p, UT1);
- SLR and VLBI provide the scale unit by measuring distances based on the metre definition (speed of light reduced to the atmosphere).

(GPS does not measure distances but differences of distances)

Principle of Satellite Laser Ranging (SLR)

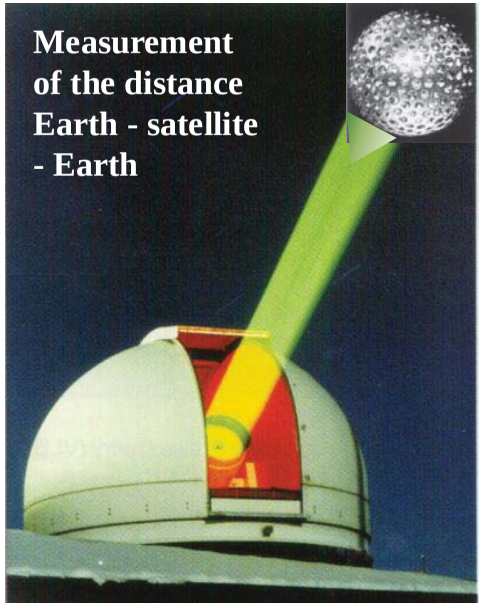

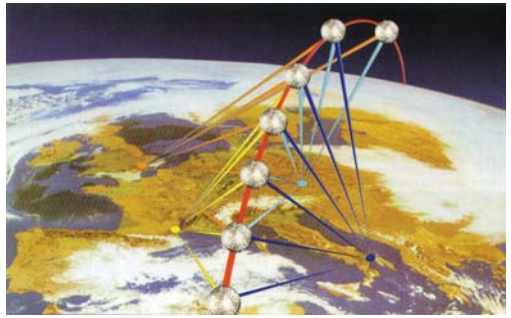

- Laser-ranging is always global.
- The distances from the telescopes to satellites are measured by the signal's travel time as round trip.
- There is only one clock, therefore there is no need of estimating clock corrections (like in GPS).

Realisation of the origin in the geo-centre by SLR

Laser ranging processing includes the computation of global orbits.

Employing an Earth gravity field model with spherical harmonic coefficients $C_{11}= S_{11}= C_{10}= 0$ provides ephemerides referring to the centre of mass (geo-centre).

Subtracting the measured distance from the geocentric radius vector provides geocentric coordinates of the telescope.

This is different in GPS, where we get only baselines because clock errors have to be estimated.

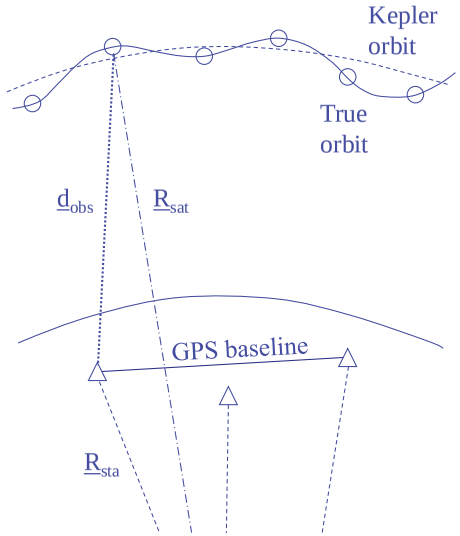

$\underline{R}_{sat}^{geoc} - \underline{d}_{obs} = \underline{R}_{sta} \Rightarrow$ geocentric

Realisation of the orientation by convention

One could realise the orientation also by the degree-two spherical harmonics of the gravity field which provide the symmetry axes (axes of maximum moment of inertia) of the masses of the Earth:

$C_{21} = \iiint X \cdot Z \, dm / a^2M$, $\quad S_{21} = \iiint Y \cdot Z \, dm / a^2M$

$S_{22} = \iiint X \cdot Y \, dm / 2a^2M$

However, these coefficients cannot be determined with the required precision. Therefore the orientation is realised by convention, fixing the Z-axis close to the Earth rotation axis and the X-axis close to the Greenwich meridian as given by the Bureau International de l'Heure (BIH, a predecessor of the IERS) for the epoch 1984,0.

These parameters have to be extrapolated in time in a way that no global rotation of the Earth crust (realised by the observation stations) remains in the coordinates time series (see later slides).

Realisation of the metric scale

- The scale unit of the terrestrial reference system is the metre as defined in the Internacional System of Units (SI) by the speed of light in vacuum. To reduce the speed for atmospheric effects, an atmosphere model is introduced and its parameters are corrected by estimation in the common data adjustment.
- The estimated parameters are depended on the signal frequency and correlated with instrumental properties (e.g. electronic delay of the signal, phase centres, deformations), station heights and others. Therefore we get different "metric" scales for different techniques.
- In order to avoid distorsions between the techniques, the scale is defined by one or two techniques (SLR and VLBI in ITRF2008) and the scales of the others are estimated w.r.t. these.

(The best would be to eliminate all the instrumental effects by an external calibration resulting in identical scales for all techniques.)

Evolution of the ITRS in time (1)

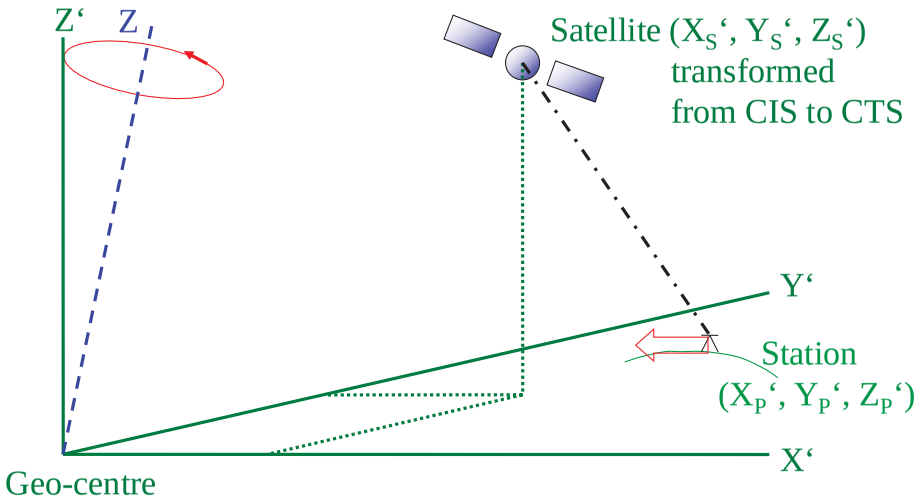

The terrestrial stations are moving because of crustal deformations. Satellites do not participate in this movement.

Evolution of the ITRS in time (2)

- Besides the varying Earth rotation we have to correct the reference frame coordinates by its motions w.r.t. the CTS in order to conserve the consistency with the CIS, i.e. the satellite ephemerides.
- Principal terrestrial station motions are caused by plate tectonics which is a long-time process. Therefore they are modelled by linear coordinate changes, i.e. by constant velocities d**X**/dt, d**Y**/dt, d**Z**/dt.
- This modelling requires a kinematic reference system to which the velocities refer and which is consistent with the Earth rotation, i.e. it must not generate a global rotation of the Earth crust.
- The kinematic reference system is defined by geologic/geophysical models of tectonic plate motion generating no net rotations (NNR);
  - until ITRF91: AM0-2 (*Minster and Jordan 1974, 1978)*;
  - until ITRF94: NNR NUVEL-1 (*Argus and Gordon 1991*);
  - until present : NNR NUVEL-1A (*De Mets et al. 1994).*

Geologic-geophysical plate model NNR NUVEL-1A

12 mayor plates with given motion by rotation vectors (see chapter 6)

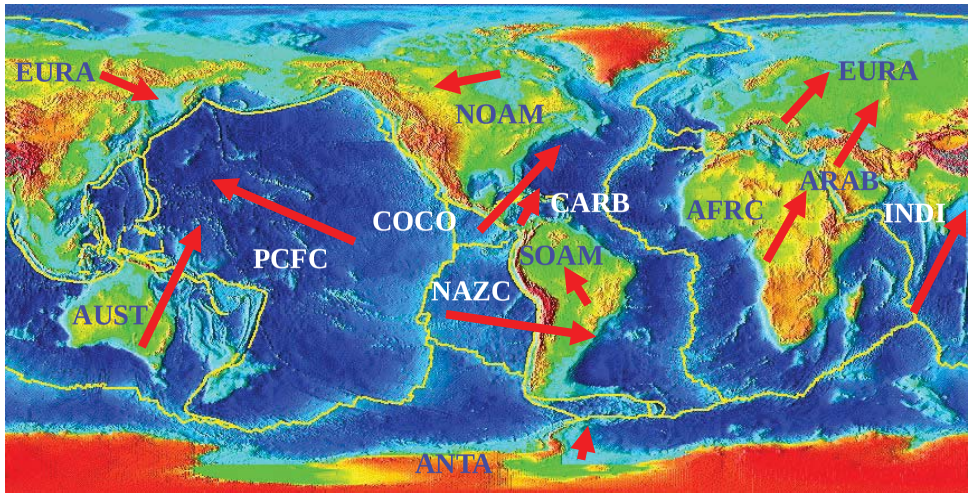

Geodetic station motions (velocities) shall refer to this model.

Realisation of the ITRS by the ITRF

- The International Terrestrial Reference System (ITRS) is realised by the International Terrestrial Reference Frame (ITRF).
- According to resolutions of the International Union of Geodesy and Geophysics (IUGG) the ITRF is the only terrestrial reference frame to be used in science and practice. (WGS84 adopted ITRF in 2002.)

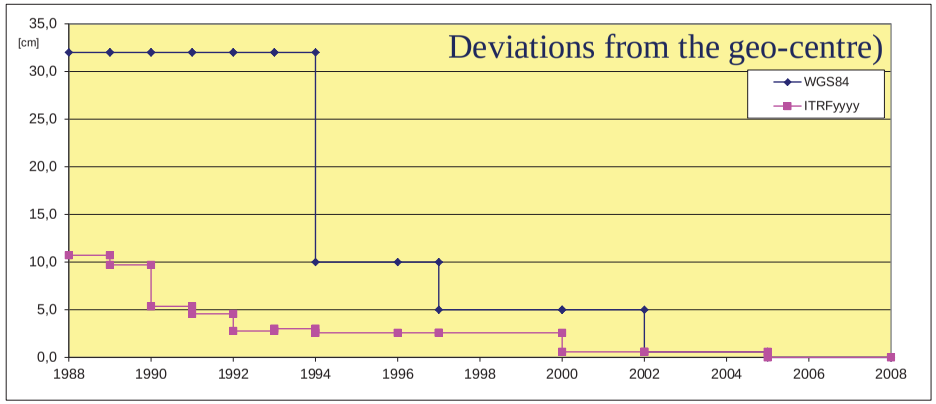

Realisations of the ITRF

The ITRF is realised by combining individual solutions of positions (and velocities) provided by analysis centres of different techniques.
until 2000: international call for individual solutions by IGN Paris;
since 2005: combination of solutions of IAG services (IGN, DGFI).

No. of	stations	sol's: VLBI	SLR	GPS	DORIS	Total	
ITRF 88	120	5	6	-	-	11	
ITRF 89	113	6	8	-	-	14	
ITRF 90	120	4	7	-	-	11	
ITRF 91	131	5	7	1	-	13	
ITRF 92	155	5	6	6	-	17	
ITRF 93	160	6	4	5	-	15	
ITRF 94	209	6	1	5	3	15	
ITRF 96	290	4	2	7	3	16	
ITRF 97	309	4	5	6	3	18	regional densifications
ITRF 2000	477	3	9	6 + 8*	3	21 + 8*	
ITRF 2005	338	1	1	1	1	4	
ITRF 2008	578	1	1	1	1	4	

Organisation of the ITRF since 2001

- The IERS Product Centre for the ITRF (IGN Paris) releases a call to the IAG Services (IVS, ILRS, IGS, IDS) to provide weekly (in case of VLBI session-wise) solutions of their analysis centres including 3D station position coordinates (X, Y, Z) and daily Earth Orientation Parameters (EOP) combined by their combination centres to one technique solution preferably in terms of datum-free (alternatively loosely constrained, i.e. $\sigma = \pm 1$ m) normal equations.
- The (presently two) ITRF combination centres (IGN, DGFI Munich)
  - analyse the weekly time series to identify the degree of freedom of the datum (e.g. eventual constraints by introducing conditions on station coordinates), gross errors, jumps in coordinates, etc.;
  - combine the weekly solutions of each observation technique into one solution of coordinates for a defined reference epoch and its linear variations (velocities) → **intra-technique combination**.

Examples of weekly coordinates analysis

Earthquake Arequipa, Peru 2001

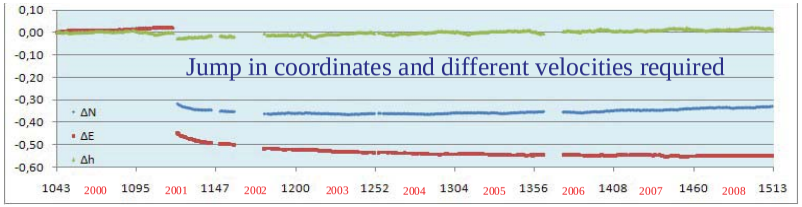

Antenna change Høfn 2001 Iceland

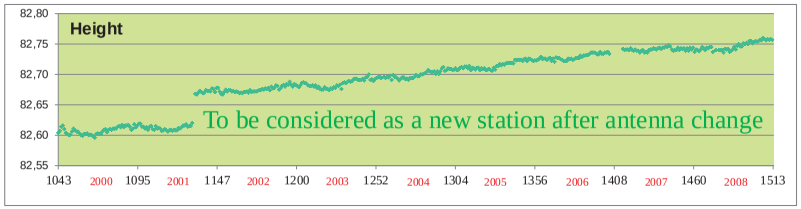

Seasonal variation, Brasilia, Brasil

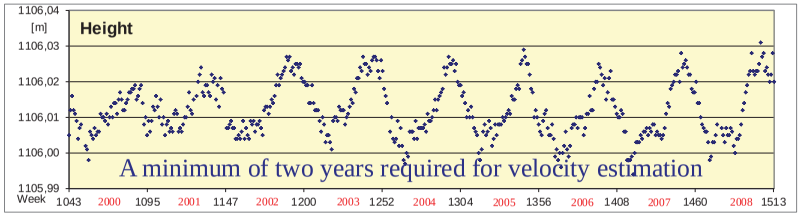

Analysis of the normal equations (DGFI)

- The normal equations must not have any constraints on the datum ("datum free" normal equations) i.e. the datum defect must be 7.
- A fixed datum in different weeks refers the coordinates to different origins, orientations and scales, which then cannot be combined.
- All the input data were analysed for the datum defect. The result is:
  - GPS (IGS): no defect at all (all parameters are fixed), ☹
  - SLR (ILRS): defect 3 (3 translations and scale are fixed), ☺
  - VLBI (IVS) defect 6 (scale fixed), ☺
  - DORIS (IDS) no defect at all (all parameters are fixed). ☹
- If the defect is not appropriate, one has to "liberate" the datum, i.e. one has to introduce columns and rows into the normal equations for those datum parameters which should be free.

(IGN did not use normal equations but solutions + covariance matrices)

Input data for ITRF 2008: X, Y, Z, X_P, Y_P, UT1

Technique	Service Analysis Centre	Data: epochs, weekly series	Interval
GPS	IGS AC NRC Ottawa	Weekly solutions (LOD)	1997 - 2008
SLR	ILRS CC ASI Matera	Weekly solutions (LOD)	1983 - 2008
VLBI	IVS CC GIUB Bonn	24 h sessions, free normal equations	1980 - 2008
DORIS	IDS CC CLS Toulouse	Weekly solutions (LOD)	1993 - 2008
Total	~1500 occupations ~ 920 points 578 stations	~4500 solutions with daily EOPs (UT1 only by VLBI)	1980 - 2008

Combination procedure (DGFI)

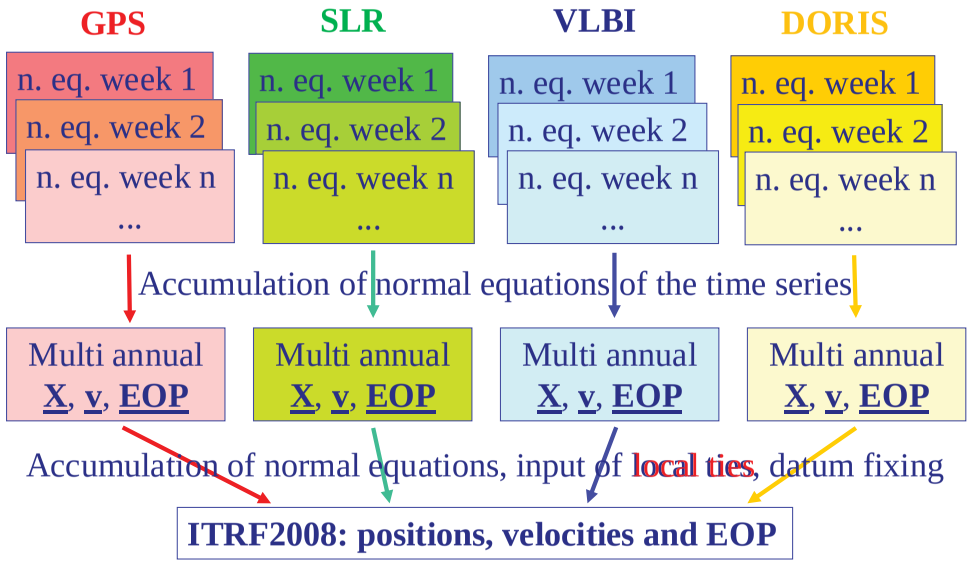

(IGN did not use normal equations but combined by Helmert transformation)

Local ties at co-location stations

- To combine the normal equations of the different techniques we need connections (coordinate differences) between their reference points.
- The definition and realisation of the reference points (phase centres) is complicated and the ties must be transformed to the global frame.

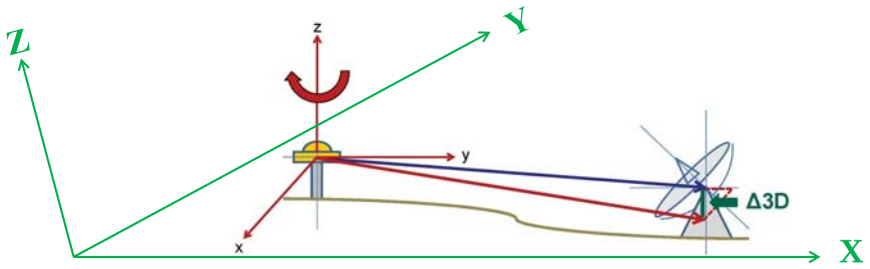

- The reliability of the local measurements may be evaluated by
  - comparing them with the estimated 3-D coordinate differences,
  - comparing the velocities obtained from the different techniques,
  - comparing EOPs obtained from the different techniques (DGFI only)

Co-location sites of space techniques

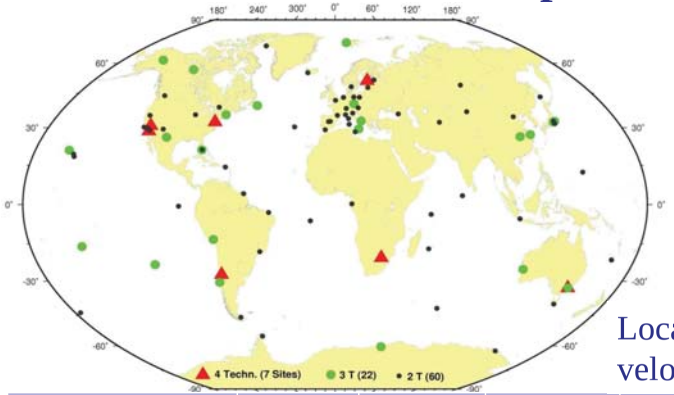

No. of co-locations

4 techniques: 7

3 techniques: 22

2 techniques: 60

Local ties and identical velocities selected (DGFI)

	no. ties	σ [mm]	limit [mm]	no. select	no. vel.	no. select
GPS-VLBI	97	0.5 ... 1.0	32	33	54	24
GPS-SLR	117	0.5 ... 1.0	30	30	51	23
GPS-DORIS	137	0.5 ... 1.0	30	34	42	14
VLBI/SLR-DORIS	93	0.5 ... 1.0	30	28	30	6
VLBI-SLR					17	11

Introduction of the datum parameters

- DGFI: The input data are (made to) datum free normal equations.
- IGN: The individual solutions are stacked by Helmert-transformation
- The datum parameters are introduced in the final combination:
- The ITRF2008 datum refers to the **epoch 2005.0** by
  - 3 translations given by SLR: coordinates' origin = geo-centre,
  - 3 rotations by the ITRF2005: orientation according to BIH1984,
  - 1 scale by SLR and VLBI: speed of light corrected by atmosphere,
  - 3 velocities of translations by SLR: velocity origin = geo-centre,
  - 3 velocities of rotation (with EOP): by NNR condition:
    IGN: geophysical model NNR NUVEL-1A;
    DGFI: geodetic model APKIM (see chapter 6);
  - 1 drift of the scale by SLR and VLBI (only IGN).

Station velocities of the ITRF2008

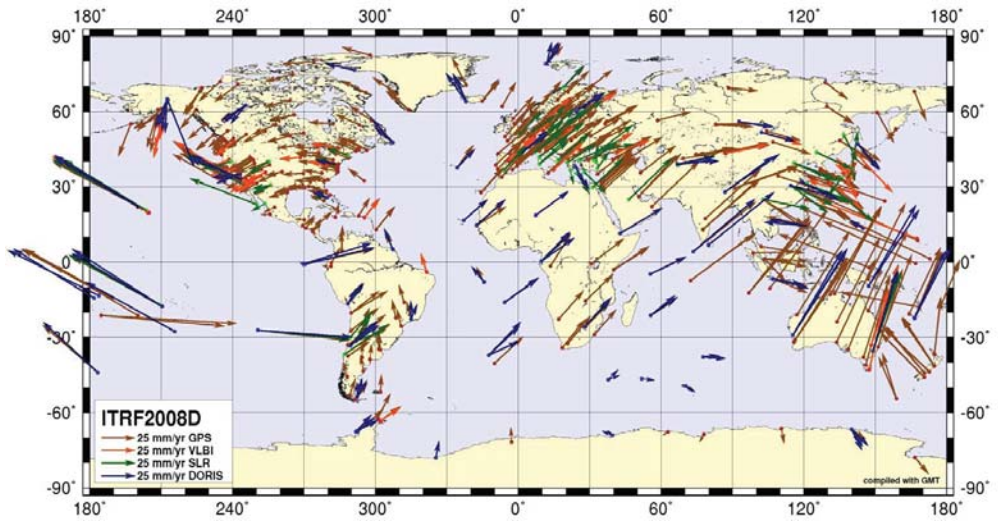

Different velocities in a site refer to different periods either due to seismic events or instrumental changes (e.g. antenna change).

Precision of the ITRF2008

Statistics of formal errors in IGN and DGFI computations

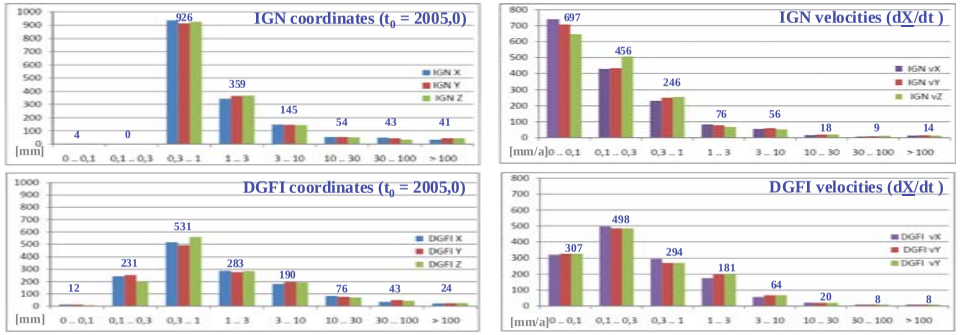

Comparison of ITRF2008 by IGN and DGFI ([mm] / [mm/a])

	ΔT(X)	ΔT(Y)	ΔT(Z)	ΔR(X)	ΔR(Y)	ΔR(Z)	ΔScale	RMS
SLR	-0,1/-0,2	0,0/-0,5	-0,3/ 0,1	0,5/ 0,3	-1,0/0,4	1,8/ 0,4	-2,0/ 0,1	2,0/ 0,8
VLBI	-1,8/ 0,4	1,3/ 0,4	-0,9/-0,1	0,1/ 0,0	-1,3/0,0	5,3/-0,1	2,1/-0,1	0,4/ 0,1
GPS	-1,1/ 0,1	0,1/-0,1	-4,9/ 0,0	0,4/ 0,0	-1,3/0,1	0,1/ 0,0	2,9/ 0,0	1,3/ 0,2
DORIS	1,3/ -0,1	0,1/ 0,4	-3,0/ 0,8	0,0/ 0,0	-2,7/0,0	-3,3/ 0,0	3,2/-0,1	3,2/ 1,0

WGS84 in ITRF2008

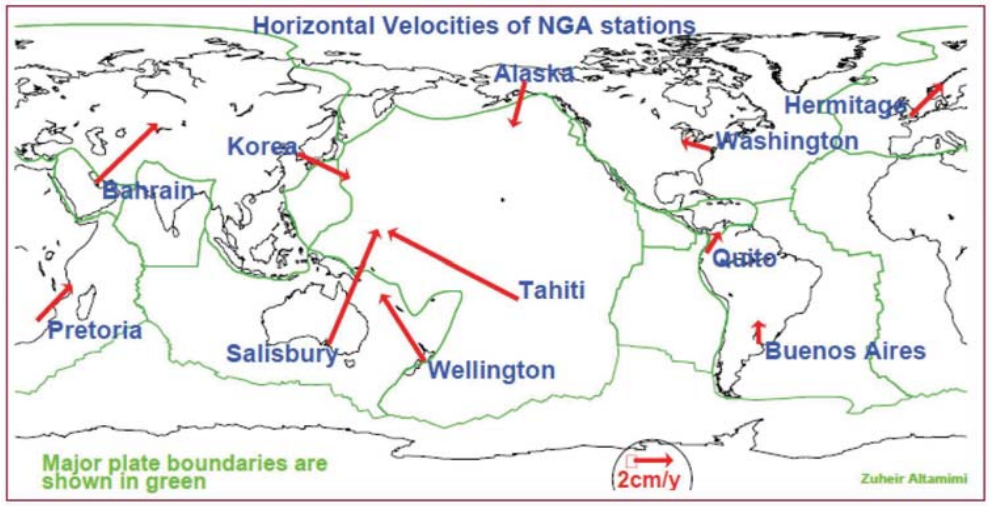

WGS84 was designed for satellite orbit determination and single point positioning (PPP). 11 stations are not sufficient for a reference frame.

2.5 Regional and national reference frames

The global ITRF is densified by regional reference frames observed by GPS in connection with global IGS stations included in the ITRF. The first network of this type was observed in Europe in 1988.

1988	EUNAV-88 (pre-campaign)
1989	EUREF-89 (densific.)/Turkey
1990	EUREF-NW (Iceld./Greenld.)
1991	EUREF-EAST/Hun/Slov/Czech
1992	EUREF-Poland/Baltic/Bulgaria
1993	EUREF-Cyprus/Iceland/D/NL
1994	EUREF-Lux/Slov/Croa/Roman.
1995	EUREF-Ukraine/Slovenia
1996	EUREF-FYROM/Bosnia
1998	EUREF-Serbia/Monte./Albania
1999	EUREF-Moldavia

South American Reference Frame

Sistema de Referencia Geocéntrico para América del Sur (SIRGAS)

58 stations observed for 10 days in May 1995 (see chapter 5)

The Americas Reference Frame

Sistema de Referencia Geocéntrico para las Américas (SIRGAS)

184 stations observed for 10 days in May 2000 extending the reference frame to all Americas.

The continental frames are further densified by national reference frames

National densifications by GPS campaigns

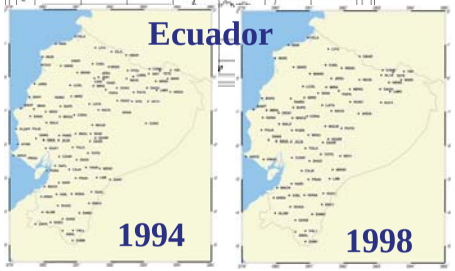

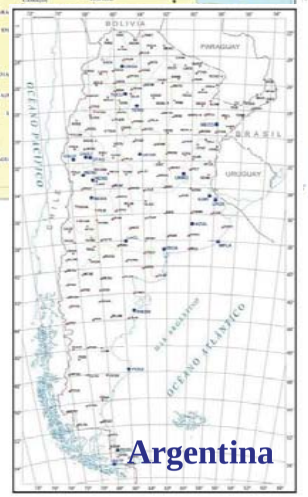

Disadvantages of reference frames by campaigns

- When using the reference frame for practical positioning one has to occupy simultaneously the reference stations in addition to the new stations by other receivers (more GPS receivers required).
- The reference frame coordinates (positions at a defined reference epoch) serve as reliable values for connecting the new points, but: The points are moving with the Earth's crust
  - continuously with the tectonic plates,
  - irregularly in deformation zones,
  - sporadically by earthquakes.
- The coordinates have to be transformed from the definition epoch to the observation epoch of new (connected) stations. This is problematic if these motions are not known (observed).
- It is much better to establish reference frames by continuously observing stations. This is done in all continents.

European Permanent Tracking Network (EPN)

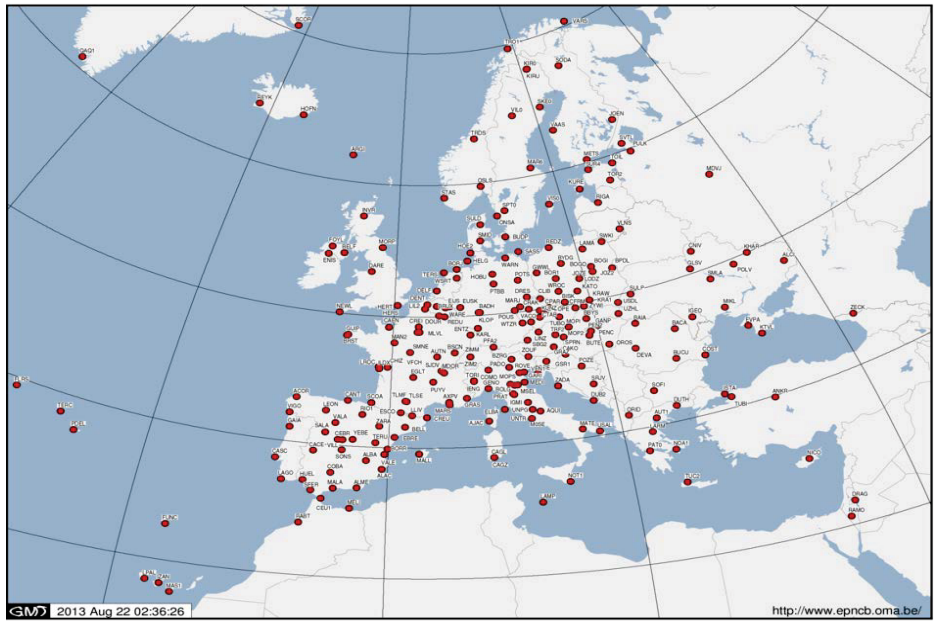

African Reference Frame (AFREF)

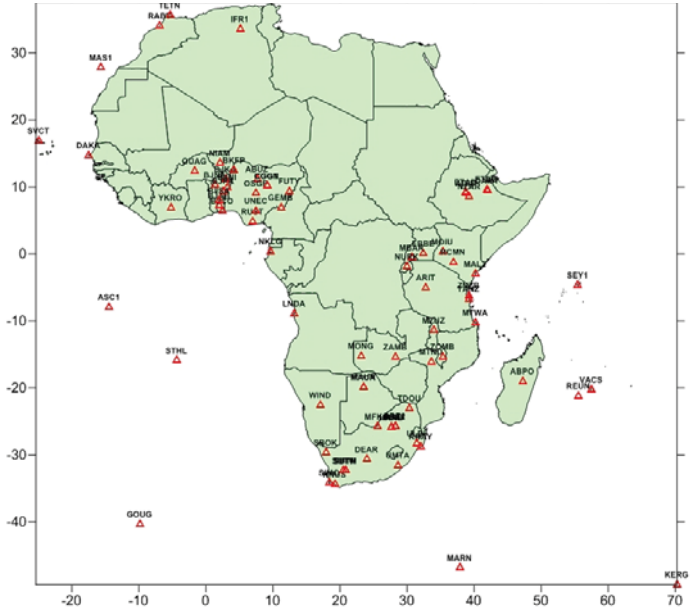

Asia-Pacific Reference Frame

North American Reference Frame (NAREF)

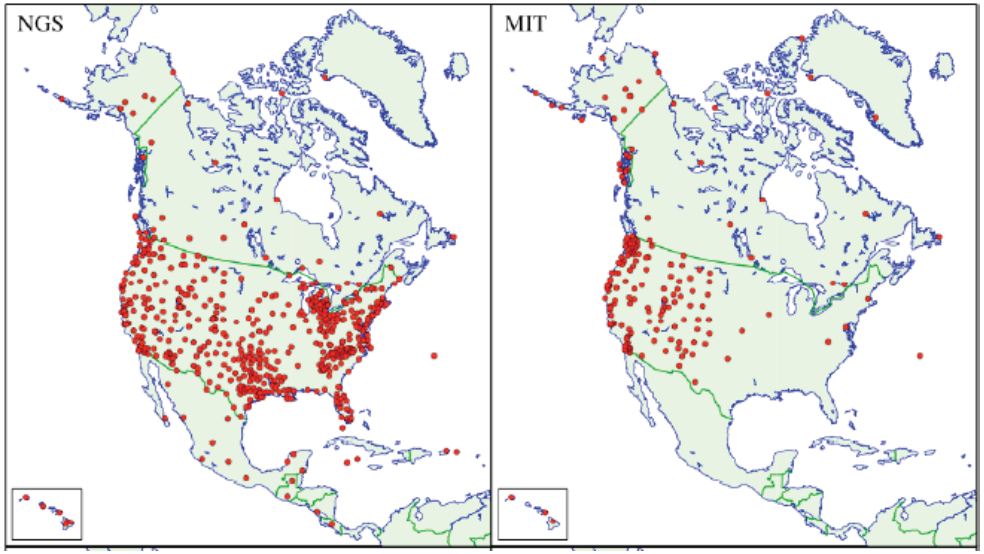

(6 different reference frames of different institutions)

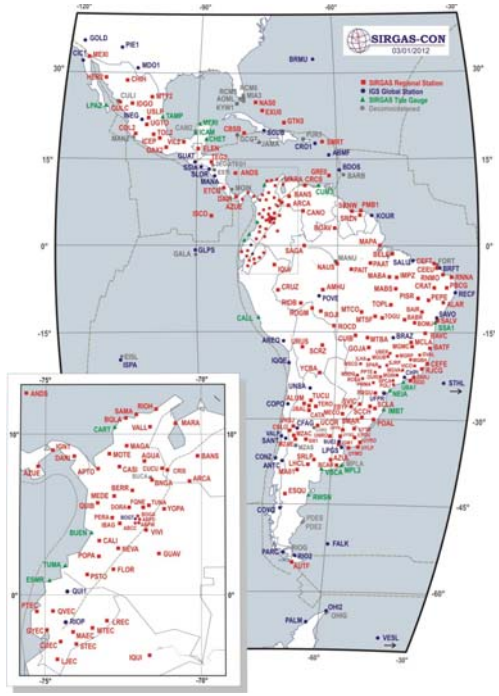

SIRGAS network of continuously observing stations (SIRGAS-CON)

(> 300 stations)

Covering the area of Mexico, Central America, The Caribbean, South America and some parts of Antarctica (see chapter 5)

National densifications by continuously observing stations (examples)

Brazil (RBMC)

Colombia (MAGNA-ECO)

Realisation of the regional reference frames (1)

The regional reference frames are densifications of the ITRF. As the ITRF contains also SLR, VLBI and DORIS stations, and to facilitate the easy access, the IGS provides an ITRF extract for GNSS users.

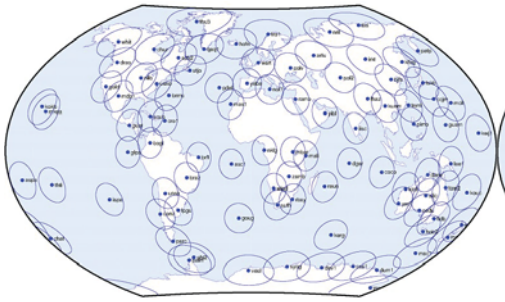

The **IGS08 core network** consists of 91 stations and forms the basis for the orbit determinations.

The **IGS08 full network** consists of 232 stations and is the basis for the regional densifications.

Realisation of the regional reference frames (2)

The IGS updates the reference frames by reprocessing and considering changes in the station occupations. These new frames are called IGb.

State map of the IGS08 core network on GPS week 1701

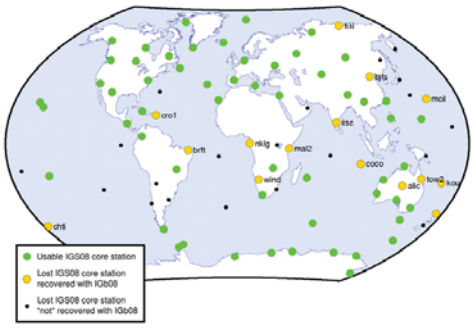

State map of the IGS08 network on GPS week 1701

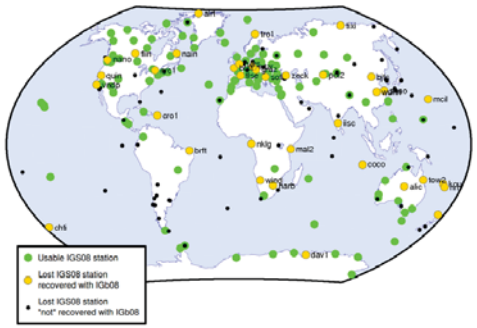

The analysis centres for the continental networks compute weekly solutions of station coordinates referring to the actually valid IGb frame. Users should apply these frames (SIRGAS) for positioning.

Realisation of the regional reference frames (3)

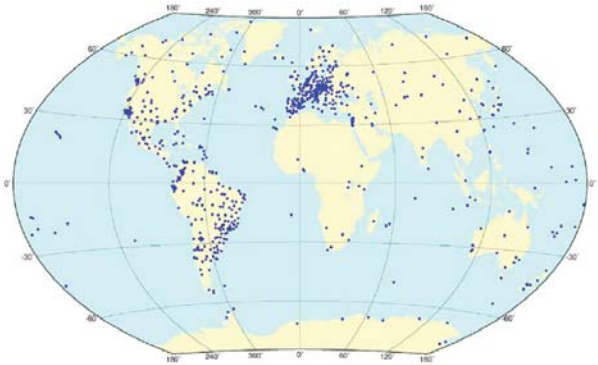

All IGS Regional Network Associate Analysis Centres (RNAAC) deliver weekly solutions to the Global Network Associate Analysis Centres (GNAAC), where they are combined to the global polyhedron (1008 stations at (2013-09-18).

The RNAAC also compute multi-annual solutions including precise station coordinates at a defined epoch (t_0) and its linear variations in time (constant velocities v). These shall be used to extrapolate the coordinates from the definition epoch to the observation epoch t_i:
$X(t) = X(t_0) + v\,(t_i - t_0)$.

NAREF velocities

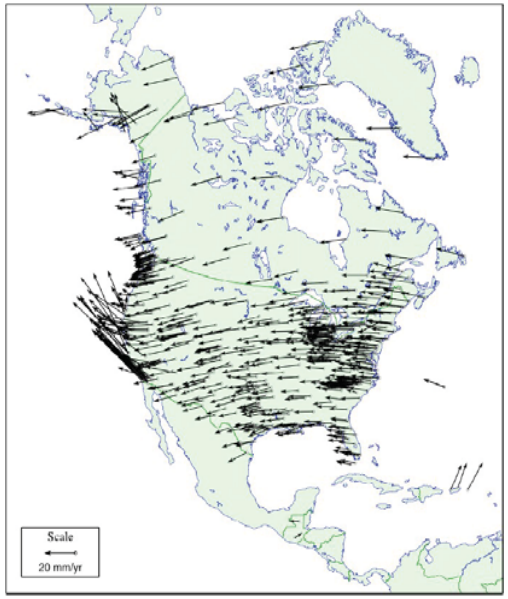

SIRGAS velocities

Precise use of the terrestrial reference frame

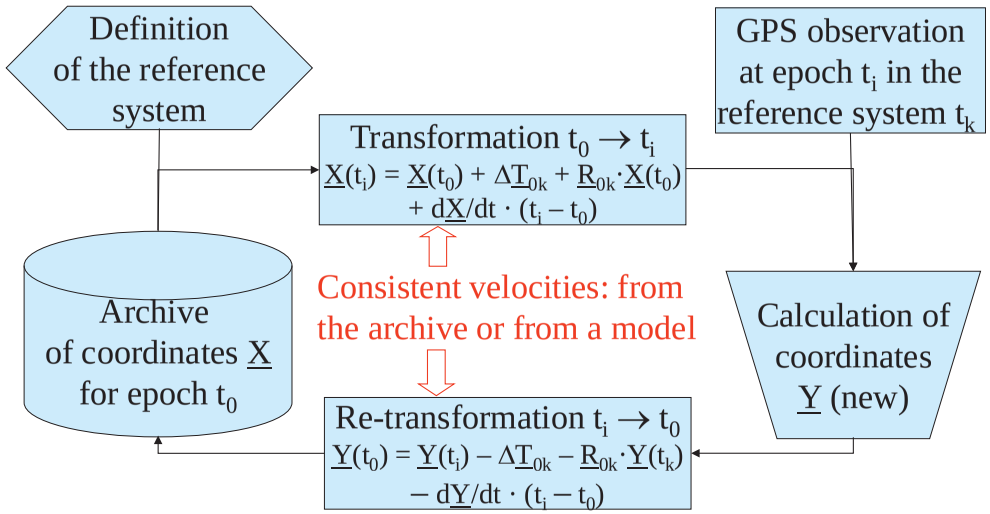

Rem.: A difference of 1 m between reference frames causes relative errors of ~2…3 · 10^{-7} baseline errors (40 cm → 1 mm/10km)

Velocity model for South America and Caribbean

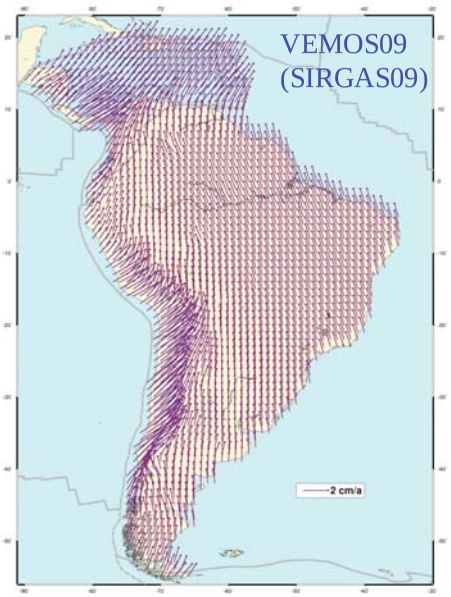

How to use the ITRF/IGS stations in detail?

- For GNSS positioning one should use the IGS coordinates or its densifications (e.g. SIRGAS) which are given in SINEX format.
- The points have a detailed identification: SC PC DO OC SD SN

  SC = site code (4 characters), e.g. AZUE
  PC = point code within the site, e.g. A
  DO = monument identification (domes no.): iiinsrjjj (e.g. 41301M001)
  iii = country no., e.g. Panama = 413, ns = number of site,
  r = reference (Monument, interSection), jjj = no. of occupation
  OC = observation technique : D = DORIS, L = SLR, P = GPS, R = VLBI
  SD = station description (21 characters), e.g. Ciudad de Chitre, Panama
  SN = number of coordinate solution for this point, e.g. 0001,
  Occupation **periods** are defined in another section of the SINEX file.
- Coordinates (STAX, STAY, STAZ) and velocities (VELX, VELY, VELZ) are given with this identification. Observe carefully the period!
- If the SIRGAS weekly solutions are used, one has to realize that they refer to the epoch of the particular week!

3. GNSS Positioning

- *Began on October 4, 1957 with the launch of the Soviet satellite Sputnik.*
- *Soon after (1958) William Guier and George Weiffenbach, at the Applied Physics Lab of the Johns Hopkins University, computed the satellite orbit using the Doppler shift measured on the signal from a point of known position.*

- *Quickly was recognized that the problem could be reversed: calculate the position of the measuring point from a satellite of known orbit.*
- *That initiated the 'Navy Navigation Satellite System' (NNSS) program of the US Army, which spawned the first GNSS known as TRNASIT.*
- *The TRANSIT constellation was composed by 5 satellites and operated from 1960 to 1996, being opened to civil users in 1967.*

The TRANSIT successor

- *From 1964 to 1966 higher requirements for a new GNSS were establish by the USA AF: determine the instantaneous position of a point at rest or moving, at any time and place, by simultaneously measuring the ranges to 4 satellites of known positions.*

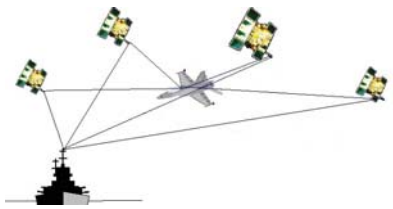

- *That requirement was fulfilled by the GPS whit a 24-satellites constellation.*
- *Satellites have been launched from 1978.*
- *Opened to civil users in 1983.*
- *Initial Operational Capability achieved in December 1993.*
- *Complete 24-satellite constellation in March 1994.*
- *A total of 64 satellites have been launched to date.*
- *Presently there are 31 operational satellites.*

Present and planed GPS status

- *All the satellites carry redundant atomic clocks.*
- *Broadcast two carriers named L1 and L2.*
- *Carriers are modulated with different civil and military codes.*
- *Military codes are encrypted.*
- *7 Block II-RM satellites modulate new civil (CA on L2) and military (M) codes.*
- *4 Block II-F satellites broadcast a new carrier (L5) to provide safety-of-life services.*
- *A new generation of satellites (Block III-A) will be launched from 2014.*

Present and planed GNSS status

- *Presently, only the USA GPS and the Russian GLONASS are fully operational at global scale.*
- *China is expanding its regional Beidou into the global Compass .*
- *The EU is deploying its Galileo (presently, only 4 satellites).*
- *India and Japan are developing regional navigation systems.*
- *There are many augmentation systems for improving navigation integrity and accuracy at local or regional scale (e.g.: the USA WAAS or the EU EGNOS).*

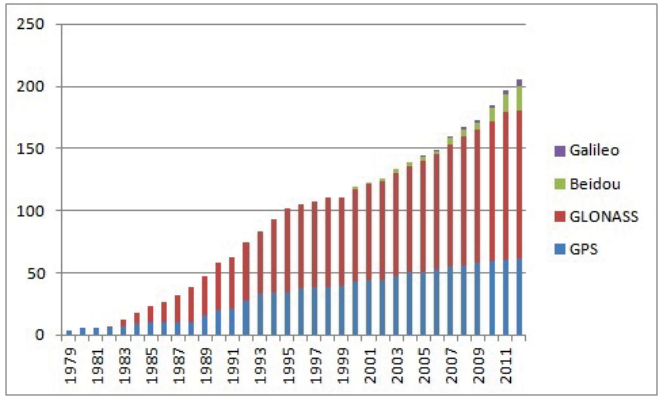

GPS constelation

- 6 orbital planes, 55° inclination, 60° in longitude;
- 31 satellite, 4+ satellites per plane;
- ~circular orbits, ~26.000 km radii (~20.000 km above the Earth surface);
- 12^h sidereal (11^h 58^m UT) revolution period, orbital speed: 3.9 km/s.

- 4+ satellites over the horizon at any place and time.
- Same ground track every day ~4^m after.

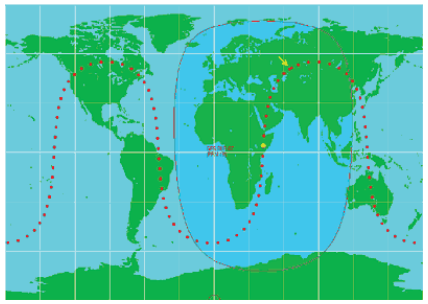

Navigation principle

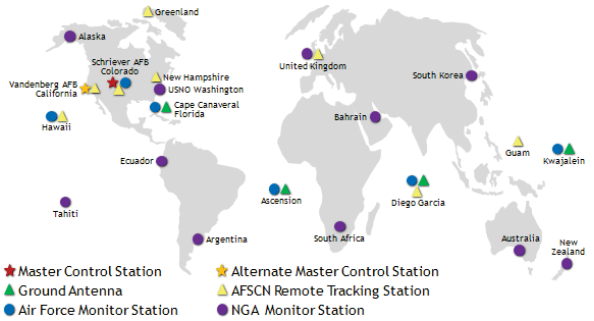

- A world-wide infrastructure composed by tracking stations, terrestrial and ground-to-satellites data links and operational centres, monitor and control the constellation.

- Based on recent measurements, satellites orbits are computed and extrapolated to the near future.
- Extrapolated orbits are broadcasted to users (the 'broadcasted ephemerides') by the satellites.
- Measuring simultaneously the ranges to 4 satellites the receiver corrects its clocks and compute its positioning using the trilateration principle.

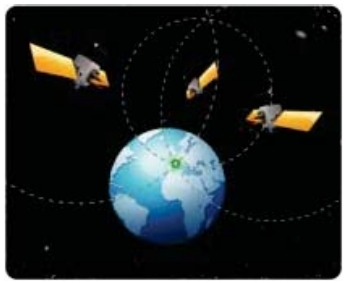

3.1 mathematical foundation

The equation of observation

The receiver position (unknown) is computed based on the satellite position (known) and the satellite-to-receiver range (measured).

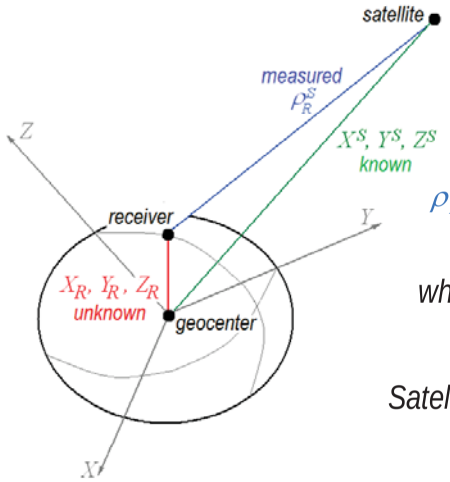

The equation of observation results from the Pythagoras's Theorem.

$$\rho_R^S = \sqrt{\left(X^S - X_R\right)^2 + \left(Y^S - Y_R\right)^2 + \left(Z^S - Z_R\right)^2} + \upsilon_R^S$$

where υ_R^S stands for all the unaccounted errors.

Satellite and receiver coordinates must be in the same reference system.

The system of equations of observation

The equation of observation contains 3 unknowns:

$$\rho_R^S = \sqrt{\left(X^S - X_R\right)^2 + \left(Y^S - Y_R\right)^2 + \left(Z^S - Z_R\right)^2} + \upsilon_R^S$$

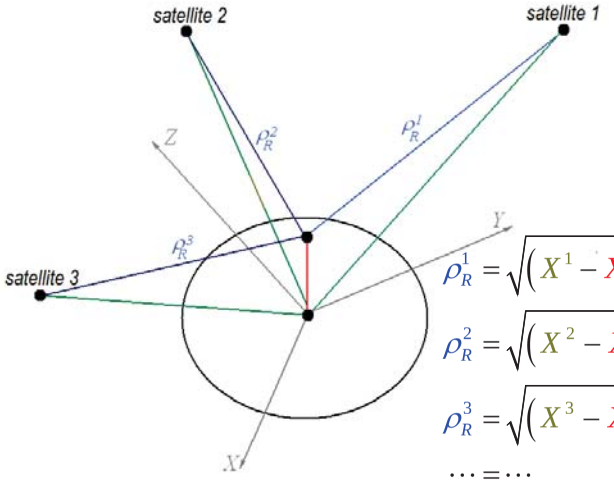

Solving the problem requires simultaneous measurements to, at least, 3 satellites:

$$\rho_R^1 = \sqrt{\left(X^1 - X_R\right)^2 + \left(Y^1 - Y_R\right)^2 + \left(Z^1 - Z_R\right)^2} + \upsilon_R^1$$

$$\rho_R^2 = \sqrt{\left(X^2 - X_R\right)^2 + \left(Y^2 - Y_R\right)^2 + \left(Z^2 - Z_R\right)^2} + \upsilon_R^2$$

$$\rho_R^3 = \sqrt{\left(X^3 - X_R\right)^2 + \left(Y^3 - Y_R\right)^2 + \left(Z^3 - Z_R\right)^2} + \upsilon_R^3$$

$$\cdots = \cdots$$

Linearization of the equation of observation

Receiver approximate position

Direction cosine of the measured satellite

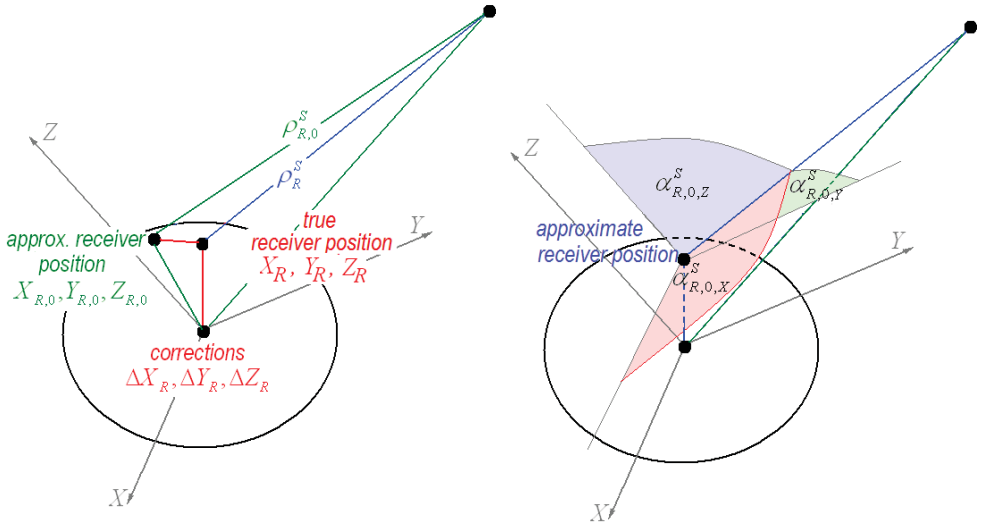

Linearization of the equation of observation

$$\rho_R^S = \sqrt{\left(X^S - X_R\right)^2 + \left(Y^S - Y_R\right)^2 + \left(Z^S - Z_R\right)^2} + \upsilon_R^S$$

$$\cong \rho_{R,0}^S + \cos\left(\alpha_{R,0,X}^S\right)\cdot\Delta X_R + \cos\left(a_{R,0,Y}^S\right)\cdot\Delta Y_R + \cos\left(a_{R,0,Z}^S\right)\cdot\Delta Z_R + \upsilon_R^S$$

approximate receiver-satellite range

receiver approximate coordinates

$$\rho_{R,0}^S = \sqrt{\left(X^S - X_{R,0}\right)^2 + \left(Y^S - Y_{R,0}\right)^2 + \left(Z^S - Z_{R,0}\right)^2}$$

$$\cos\left(\alpha_{R,0,X}^S\right) = \frac{X^S - X_{R,0}}{\rho_{R,0}^S}$$

direction cosines of the measured satellite

$$\Delta X_R = X_R - X_{R,0}$$

corrections to the receiver approximate coordinates.

$$\vdots$$

From the geocentric to the local system

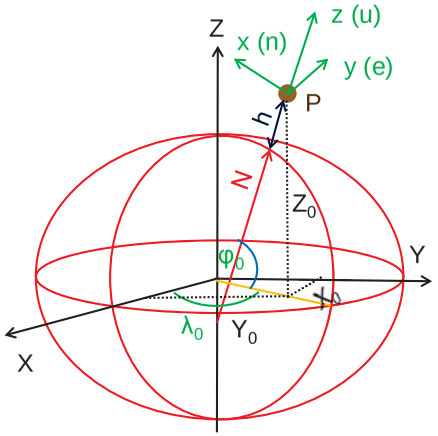

Geocentric coordinates (X, Y, Z) can be transformed to local (e, n, u) coordinates by means of:

- translation of the origin from the geocenter to the approximate receiver position;
- rotation of the axes by the latitude and longitude (φ_0, λ_0) of the new origin.

The equation of observation in the local system

After applying the transformation the equation of observation reads:

$$\rho_R^S = \rho_{R,0}^S + \cos\left(a_{R,0,e}^S\right)\cdot\Delta e_R + \cos\left(\alpha_{R,0,n}^S\right)\cdot\Delta n_R + \cos\left(a_{R,0,v}^S\right)\cdot\Delta v_R + \upsilon_R^S$$

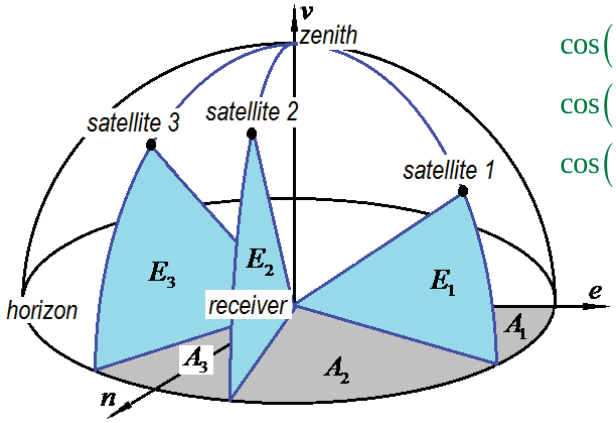

$$\cos\left(a_{R,0,e}^S\right) = \sin\left(E_{R,0}^S\right)\cdot\cos\left(A_{R,0}^S\right)$$

$$\cos\left(\alpha_{R,0,n}^S\right) = \cos\left(E_{R,0}^S\right)\cdot\cos\left(A_{R,0}^S\right)$$

$$\cos\left(a_{R,0,v}^S\right) = \sin\left(E_{R,0}^S\right)$$

E = satellite elevation

A = satellite azimuth

The system of equations of observation

$$\rho_R^1 = \rho_{R,0}^1 + \cos\left(a_{R,0,e}^1\right)\cdot\Delta e_R + \cos\left(\alpha_{R,0,n}^1\right)\cdot\Delta n_R + \cos\left(a_{R,0,v}^1\right)\cdot\Delta v_R + \upsilon_R^1$$
$$\rho_R^2 = \rho_{R,0}^2 + \cos\left(a_{R,0,e}^2\right)\cdot\Delta e_R + \cos\left(\alpha_{R,0,n}^2\right)\cdot\Delta n_R + \cos\left(a_{R,0,v}^2\right)\cdot\Delta v_R + \upsilon_R^2$$
$$\vdots$$
$$\rho_R^n = \rho_{R,0}^n + \cos\left(a_{R,0,e}^n\right)\cdot\Delta e_R + \cos\left(\alpha_{R,0,n}^n\right)\cdot\Delta n_R + \cos\left(a_{R,0,v}^n\right)\cdot\Delta v_R + \upsilon_R^n$$

Using matrix notation

$$\begin{vmatrix}\rho_R^1-\rho_{R,0}^1\\ \rho_R^2-\rho_{R,0}^2\\ \vdots\\ \rho_R^n-\rho_{R,0}^n\end{vmatrix} = \begin{vmatrix}\cos\left(a_{R,0,e}^1\right) & \cos\left(\alpha_{R,0,n}^1\right) & \cos\left(a_{R,0,v}^1\right)\\ \cos\left(a_{R,0,e}^2\right) & \cos\left(\alpha_{R,0,n}^2\right) & \cos\left(a_{R,0,v}^2\right)\\ \vdots & \vdots & \vdots\\ \cos\left(a_{R,0,e}^n\right) & \cos\left(\alpha_{R,0,n}^n\right) & \cos\left(a_{R,0,v}^n\right)\end{vmatrix}\cdot\begin{vmatrix}\Delta e_R\\ \Delta n_R\\ \Delta v_R\end{vmatrix} + \begin{vmatrix}\upsilon_R^1\\ \upsilon_R^2\\ \vdots\\ \upsilon_R^n\end{vmatrix}$$

$\mathbf{L}(n\times 1)$ $\mathbf{A}(n\times 3)$ $\mathbf{x}(3\times 1)$ $\mathbf{v}(n\times 1)$

Least Squares solution

$$\mathbf{L} = \mathbf{A}\cdot\mathbf{x} + \mathbf{v} \quad \text{and} \quad \mathbf{v}^T\cdot\mathbf{v} = \min \quad \Rightarrow \quad \hat{\mathbf{x}} = \left(\mathbf{A}^T\cdot\mathbf{A}\right)^{-1}\cdot\mathbf{A}^T\cdot\mathbf{L}$$

supra-index T stands for transposed matrix

$\hat{\mathbf{x}} = \left(\Delta\hat{n}_R, \Delta\hat{e}_R, \Delta\hat{v}_R\right)^T$ *are the unknown estimates;*

$\hat{\mathbf{v}} = \mathbf{L} - \mathbf{A}\cdot\hat{\mathbf{x}}$ *are the error estimates;*

$$\hat{\sigma} = \pm\sqrt{\frac{\sum_{i=1}^{n}\hat{\upsilon}_i^2}{n-1}}$$ *is the unity of weight standard deviation;*

The variance-covariance of the unknowns

$$\hat{\mathbf{C}}_{\mathbf{x}} = \hat{\sigma}^2\cdot\left(\mathbf{A}^T\cdot\mathbf{A}\right)^{-1} = \hat{\sigma}^2\begin{pmatrix}q_{nn}^2 & q_{ne} & q_{nv}\\ q_{en} & q_{ee}^2 & q_{ev}\\ q_{vn} & q_{ve} & q_{vv}^2\end{pmatrix}$$

measurement errors

cofactor matrix of the unknowns geometrical configuration of the measured satellites

Dilution of the precision factors

The receiver position and its error can be computed from:

$$\hat{n}_R = n_{R,0} + \Delta\hat{n}_R \qquad \hat{\sigma}_n = \hat{\sigma}\cdot q_{nn}$$
$$\hat{e}_R = e_{R,0} + \Delta\hat{e}_R \qquad \hat{\sigma}_e = \hat{\sigma}\cdot q_{ee}$$
$$\hat{v}_R = v_{R,0} + \Delta\hat{v}_R \qquad \hat{\sigma}_v = \hat{\sigma}\cdot q_{vv}$$

The q factors (co-factors) depends only on the geometrical configuration of the measured satellites and defined the Dilution of the Precision (DOP) factors:

$$\hat{\sigma}_P = \hat{\sigma}\cdot\sqrt{q_{nn}^2 + q_{ee}^2 + q_{vv}^2} = \hat{\sigma}\cdot PDOP \qquad \text{3-D}$$
$$\hat{\sigma}_H = \hat{\sigma}\cdot\sqrt{q_{nn}^2 + q_{ee}^2} = \hat{\sigma}\cdot HDOP \qquad \text{horizontal}$$
$$\hat{\sigma}_V = \hat{\sigma}\cdot q_{vv} = \hat{\sigma}\cdot VDOP \qquad \text{vertical}$$

Error sources

Measurement errors: will be discussed later on.

Errors in the satellite position:

- *Broadcasted ephemerids: ±1 m*
- *RT IGS orbits: ±5 cm*
- *Final IGS orbits: ±2.5 cm*

Approximate receiver position (can be improved iteratively).

These errors apply on the approximate receiver-satellite range and, with much less importance, on the direction cosines:

$$\rho_{R,0}^S = \sqrt{\left(X^S - X_{R,0}\right)^2 + \left(Y^S - Y_{R,0}\right)^2 + \left(Z^S - Z_{R,0}\right)^2}$$
$$\cos\left(\alpha_{R,0,n}^S\right) = \cos\left(E_{R,0}^S\right)\cdot\cos\left(A_{R,0}^S\right)$$
$$\cos\left(a_{R,0,e}^S\right) = \sin\left(E_{R,0}^S\right)\cdot\cos\left(A_{R,0}^S\right)$$
$$\cos\left(a_{R,0,v}^S\right) = \sin\left(E_{R,0}^S\right)$$

3.2 pseudo-range measurement

3.2 pseudo-range measurement

GPS carriers

GPS signals result from the superposition of different modulations on different carriers.

Carriers are pure sinusoidal waves mathematically described by 3 parameters:

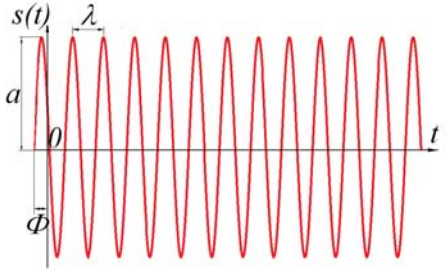

$$s(t) = a \cdot \sin(2 \cdot \pi \cdot f \cdot t + \phi)$$

a = amplitude

f = frequency

ϕ = phase

$$f = \frac{c}{\lambda}$$

c: speed of light in vacuum, 299792,458 km/s

λ: wavelength

GPS satellites broadcast 2 carriers: L1 and L2 (Block II-F also L5), whose frequencies and wavelength are:

L1: $f_1 = f_0 \times 154 = 1575.42$ MHz; $\lambda_1 = 19.05$ cm

L2: $f_2 = f_0 \times 120 = 1227.60$ MHz; $\lambda_2 = 24.45$ cm

$f_0 = 10.23$ MHz

GPS codes

GPS carriers are modulated with civil and military codes and with the broadcasted ephemerides.

Codes are a pseudo-random binary sequence (only two values: 0 or 1) modulated on the phase of the carrier (code transitions change 180° the phase of the carrier).

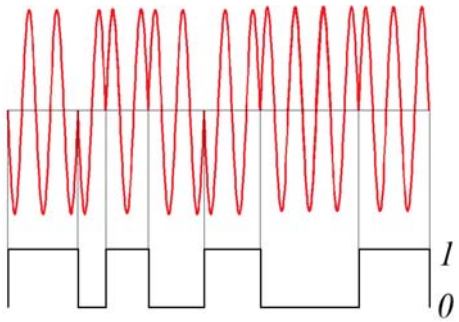

	CA (coarse acquisition)	P (precise)
Chip length	~300 m	~30 m
Repetition interval	1 ms	1 week
Modulate on	L1 (and L2 in the II-RM)	L1 and L2
Encrypted	no	anti spoofing (partially used by GPS receivers)

Measurement of the satellite to receiver range

Assuming satellite and receiver clocks synchronized to GPS time:

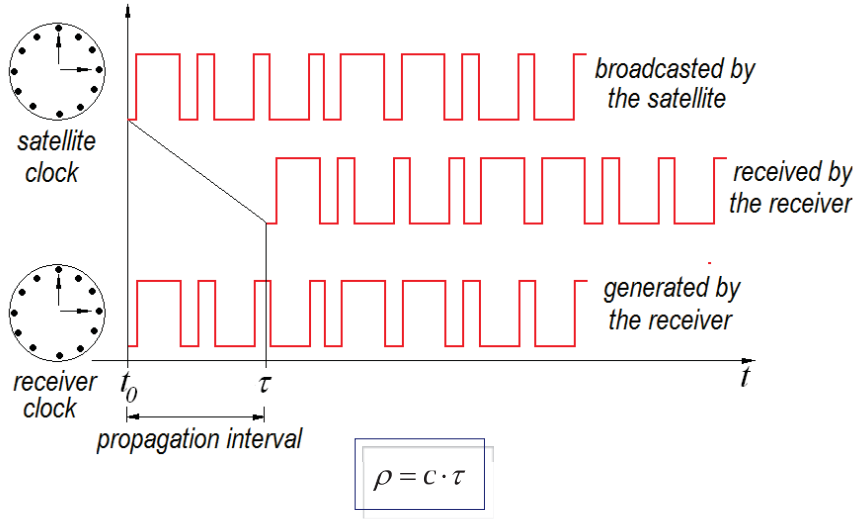

$$\rho = c \cdot \tau$$

Measurement of the satellite to receiver pseudo-range

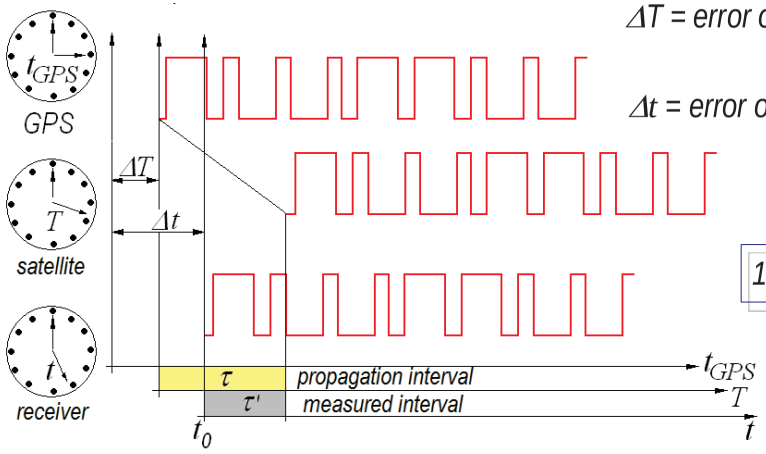

ΔT = error of the satellite clock w.r.t. GPS time;

Δt = error of the receiver clock w.r.t. GPS time.

1 ns ←→ 30 cm!

$$\tau = \tau' + \Delta t - \Delta T$$

$$\rho = c \cdot \tau = c \cdot (\tau' + \Delta t - \Delta T) = \underbrace{c \cdot \tau'}_{P} + c \cdot (\Delta t - \Delta T)$$

Equation of observation for pseudo-range

unknown: the receiver clock offset

$$P_R^S - c \cdot \Delta T^S - \rho_{R,0}^S = \cos\left(a_{R,0,e}^S\right) \cdot \Delta e_R + \cos\left(\alpha_{R,0,n}^S\right) \cdot \Delta n_R + \cos\left(a_{R,0,v}^S\right) \cdot \Delta v_R + c \cdot \Delta t_R + \upsilon_R^S$$

correction: the satellite clock offset

The system of equation of observations for n satellites reads

$$\underbrace{\begin{vmatrix} P_R^1 \\ P_R^2 \\ \vdots \\ P_R^n \end{vmatrix} - c \cdot \begin{vmatrix} \Delta T^1 \\ \Delta T^2 \\ \vdots \\ \Delta T^n \end{vmatrix} - \begin{vmatrix} \rho_{R,0}^1 \\ \rho_{R,0}^2 \\ \vdots \\ \rho_{R,0}^n \end{vmatrix}}_{\mathbf{L}(n \times 1)} = \underbrace{\begin{vmatrix} \cos\left(a_{R,0,e}^1\right) & \cos\left(\alpha_{R,0,n}^1\right) & \cos\left(a_{R,0,v}^1\right) & -c \\ \cos\left(a_{R,0,e}^2\right) & \cos\left(\alpha_{R,0,n}^2\right) & \cos\left(a_{R,0,v}^2\right) & -c \\ \vdots & \vdots & \vdots & \vdots \\ \cos\left(\alpha_{R,0,e}^n\right) & \cos\left(a_{R,0,n}^n\right) & \cos\left(a_{R,0,v}^n\right) & -c \end{vmatrix}}_{\mathbf{A}(n \times 4)} \cdot \underbrace{\begin{vmatrix} \Delta e_R \\ \Delta n_R \\ \Delta v_R \\ \Delta t_R \end{vmatrix}}_{\mathbf{x}(4 \times 1)} + \underbrace{\begin{vmatrix} \upsilon_R^1 \\ \upsilon_R^2 \\ \vdots \\ \upsilon_R^n \end{vmatrix}}_{\mathbf{v}(n \times 1)}$$

Error sources

Error source	CA	P	Behaviour
Measurement	±1 m	± 30 cm	random, increases at low elevation.
Multipath	±3 m	± 1 m	quasi-random, 12[h] sidereal time repetition pattern; increases at low elevation.

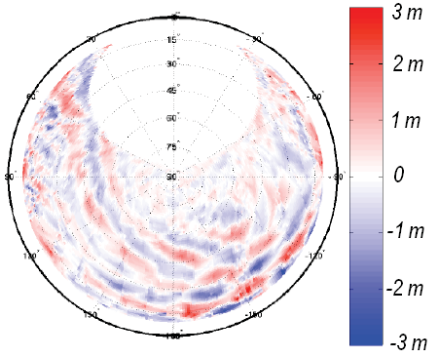

Error sources

Errors in the satellite clock correction:

- *Broadcast ephemerid: ±5 ns (±1.5 m)*
- *RT IGS orbits: ±150 ps (±4.5 cm)*
- *Final IGS orbits: ±7.5 ps (±2.2 cm)*

Carrier phase measurement

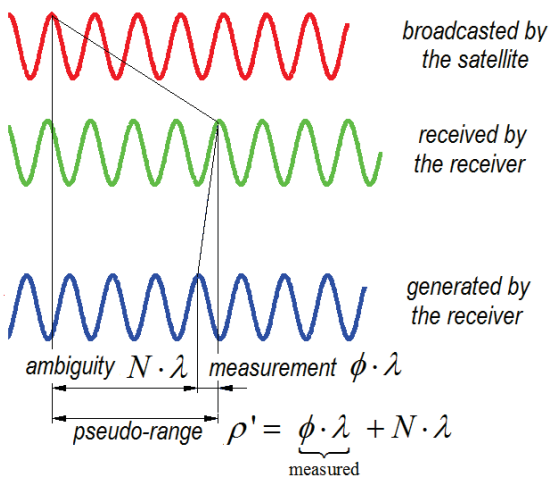

$$\rho = \rho' + c\cdot(\Delta t - \Delta T)$$

$$\rho = \underbrace{\phi\cdot\lambda}_{l} + N\cdot\lambda + c\cdot(\Delta t - \Delta T)$$

an integer number

Equations of observation for carrier phase measurements

$$l_R^1 - \rho_{R,0}^1 - c\cdot\Delta T^1 = \cos(a_{R,0,e}^1)\cdot\Delta e_R + \cos(\alpha_{R,0,n}^1)\cdot\Delta n_R + \cos(a_{R,0,v}^1)\cdot\Delta v_R - c\cdot\Delta t_R - \lambda\cdot N_R^1 + \upsilon_R^1$$
$$l_R^2 - \rho_{R,0}^2 - c\cdot\Delta T^2 = \cos(a_{R,0,e}^2)\cdot\Delta e_R + \cos(\alpha_{R,0,n}^2)\cdot\Delta n_R + \cos(a_{R,0,v}^2)\cdot\Delta v_R - c\cdot\Delta t_R - \lambda\cdot N_R^2 + \upsilon_R^2$$
$$\vdots$$
$$l_R^n - \rho_{R,0}^n - c\cdot\Delta T^n = \cos(a_{R,0,e}^n)\cdot\Delta e_R + \cos(\alpha_{R,0,n}^n)\cdot\Delta n_R + \cos(a_{R,0,v}^n)\cdot\Delta v_R - c\cdot\Delta t_R - \lambda\cdot N_R^n + \upsilon_R^n$$

In matrix form:

$$\mathbf{L} = \mathbf{A}\cdot\mathbf{x} + \mathbf{v}$$

ambiguities an integer number

$$\mathbf{A} = \begin{pmatrix} \cos(\alpha_{R,0,e}^1) & \cos(\alpha_{R,0,n}^1) & \cos(\alpha_{R,0,v}^1) & -c & -\lambda & 0 & \cdots & 0 \\ \cos(\alpha_{R,0,e}^2) & \cos(\alpha_{R,0,n}^2) & \cos(\alpha_{R,0,v}^2) & -c & 0 & -\lambda & \cdots & 0 \\ \vdots & \vdots & \vdots & \vdots & \vdots & \vdots & \ddots & \vdots \\ \cos(\alpha_{R,0,e}^n) & \cos(\alpha_{R,0,n}^n) & \cos(\alpha_{R,0,v}^n) & -c & 0 & 0 & \cdots & -\lambda \end{pmatrix}$$

(Δn_R, Δe_R, Δv_R, Δt_R, N_R^1, N_R^2, N_R^n above the columns; *n measurements* to the right; *3+1+n unknowns* below)

Solution of the equation of observation system

Accurate solutions are obtained with the 'geometrical' method:

- *accumulate measurements until the number of equations gets greater than the number of unknowns; and*
- *the condition number of the matrix* $\mathbf{A}$ *gets smaller enough to ensure a good de-correlation of the different unknowns.*

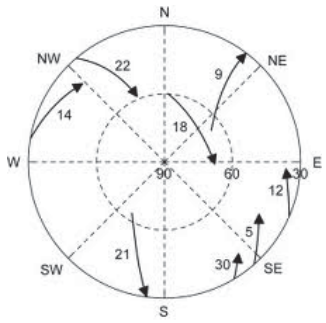

direction cosines change slowly

← 1.5 hours

Error sources

Error source	CA	P	L1 or L2	Behaviour
Measurement	*±1 m*	*± 30 cm*	*±2 mm*	carrier phase measurements are ultra-precise but ambiguous
Multipath	*±3 m*	*± 1 m*	*±10 mm*	

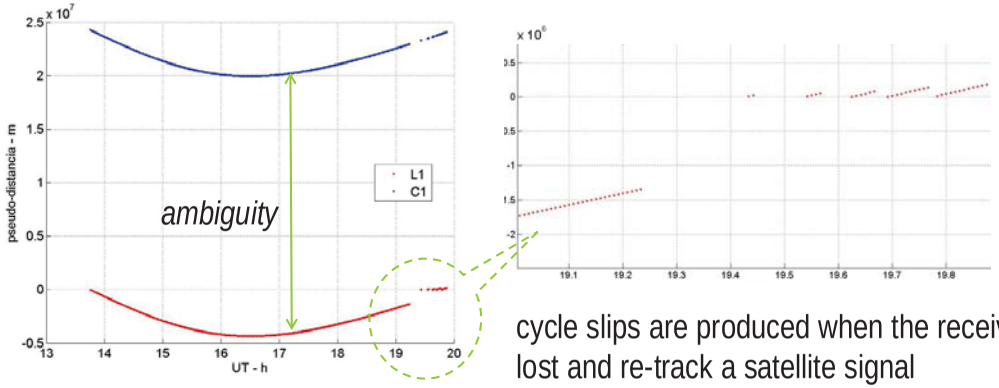

cycle slips are produced when the receiver lost and re-track a satellite signal

3.3 models to reduce error sources

3.3 models to reduce error sources

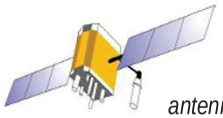

orbit
clock
relativity
antenna phase centers
wind up
instrumental biases
multipath

ionized atmosphere
(~50-1000 km)

neutral atmosphere
(~0-50 km)

clock
antenna phase center
instrumental biases
multipath
measurement errors

Effects that must be accounted for precise positioning

continental drift
crustal deformation
seismic and volcano activity
Earth tides
Earth orientation and irregular rotation
post-glacial rebound
ocean, hydrological and atmospheric loading

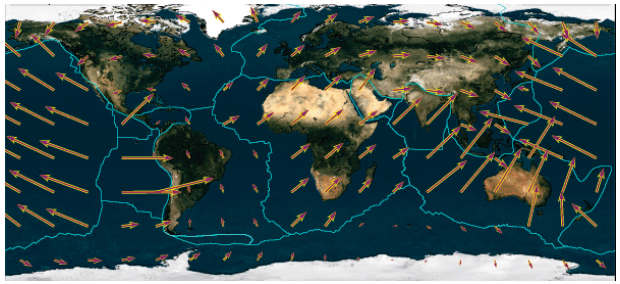

Posicionamiento preciso

Error budget (if not corrected)

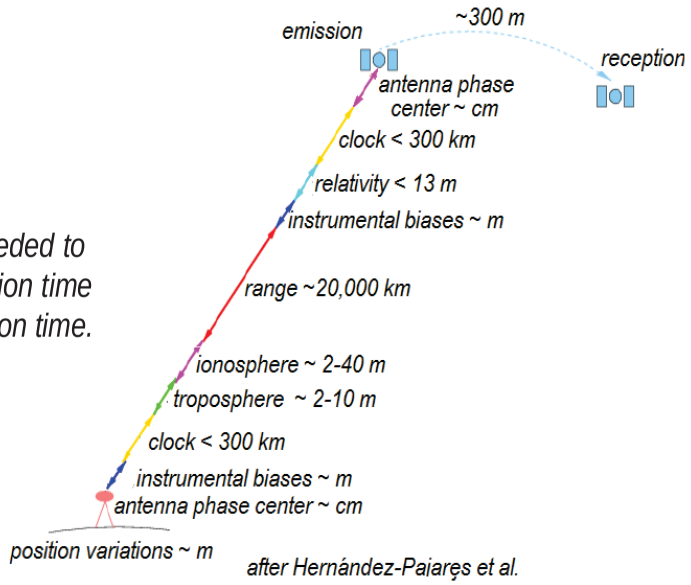

Note: an algorithm is needed to compute the GPS emission time from the receiver reception time.

Relativistic correction

Satellite clock is moving with respect to the receiver clock; in addition, satellite and receiver clocks are under different gravity potentials.

$$\frac{t_S - t_R}{t_R} = -\frac{1}{2}\cdot\left(\frac{V_r}{c}\right)^2 \qquad \frac{t_S - t_R}{t_R} = \frac{U_R - U_S}{c^2}$$

V_r = relative velocity
U_S = satellite potential; U_R = receiver potential
t_S = satellite time; t_R = receiver time

The major part of these errors is corrected by changing the frequency of the satellite oscillator from 10.23 to 10.2299999954 MHz (~38 μs/day).

The variable part of these errors can be computed as:

$$\Delta\rho_{REL} = -\frac{2}{c}\cdot\sqrt{\mu_E}\cdot e\cdot\sqrt{a}\cdot\sin(E)$$

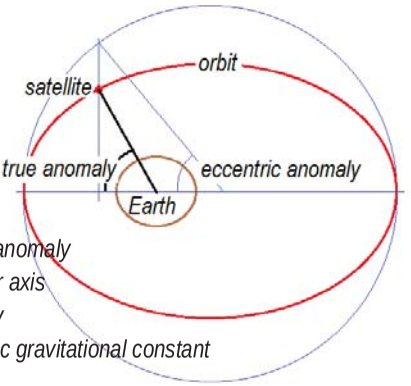

E = eccentric anomaly
a = semi-major axis
e = eccentricity
μ_E = geocentric gravitational constant

Antenna phase centers

The measured pseudo-range is between antenna phase centers.

- *Satellite coordinates correspond to the center of mass →*

  must be translated to antenna phase center with an eccentricity vector.

- *Geodetic coordinates must be referred to a geodetic mark →*

  the antenna phase center of the receiver must be related to the geodetic mark with an eccentricity vector.

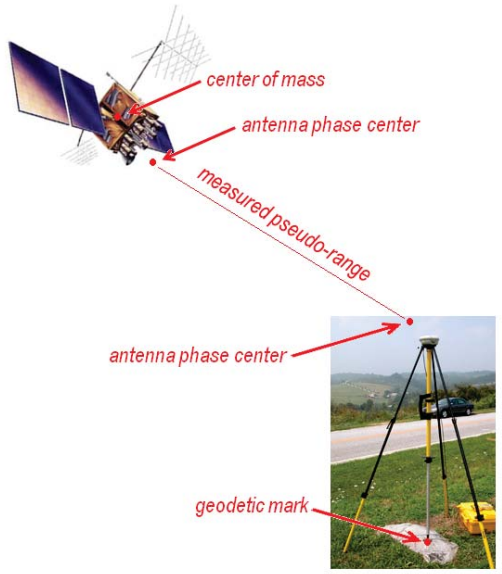

Antenna phase center of the receiver

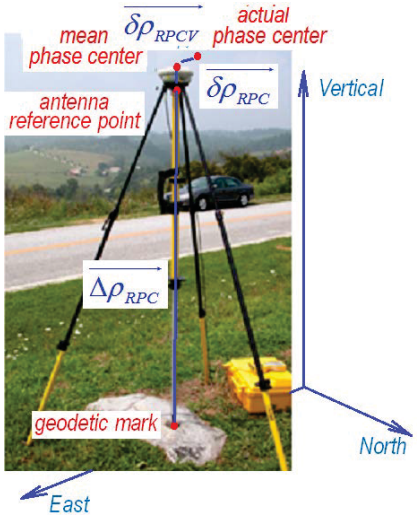

Constant parts

$$\overrightarrow{\Delta\rho_{RECC}} = \overrightarrow{\Delta\rho_{RPC}} + \overrightarrow{\delta\rho_{RPC}} + \overrightarrow{\delta\rho_{RPCV}}$$

Variable part (Phase Center Variation)

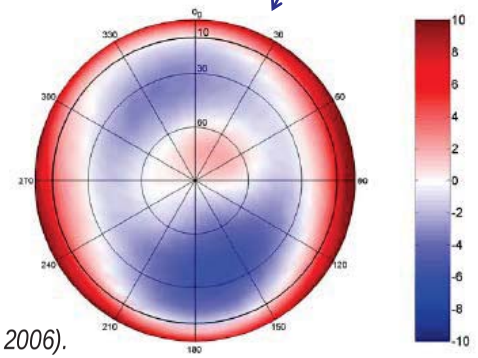

PCV in mm (after Steigenberger et al., 2006).

Values are different for L1 and L2 and change if a radome is on the antenna.

Antenna phase center of the satellites

The orientation of the x-y-z system changes w.r.t. the observer as long as satellite moves

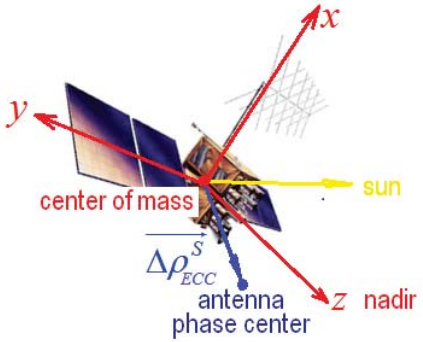

constant part

$$\overrightarrow{\Delta\rho^S_{ECC}} = \overrightarrow{\Delta\rho^S_{PCM}} + \overrightarrow{\delta\rho^S_{PCV}}$$

variable part (Phase Center Variation)

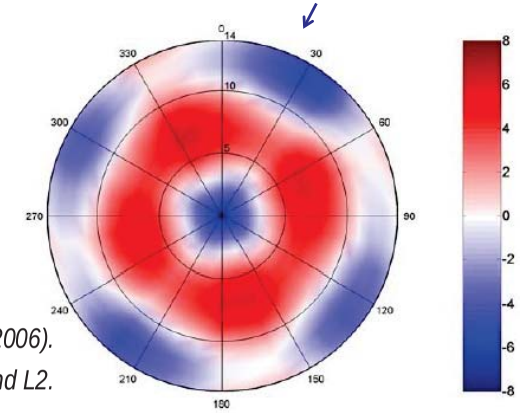

PCV in mm (after Steigenberger et al., 2006).

Values are different for L1 and L2.

Carrier phase wind-up

It is due to the circular polarization of the GPS signals.

Values are different for L1 and L2.

Depends on the relative orientation of satellite and receiver antennas.

Changes in the relative orientation cause a phase variation that the receiver misunderstands as a range variation.

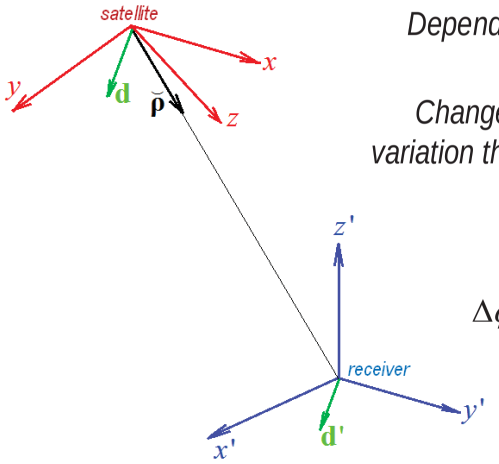

$$\Delta\phi = sign\left[\breve{\boldsymbol{\rho}}\cdot\left(\mathbf{d}'\times\mathbf{d}\right)\right]\cdot\arccos\left[\frac{\mathbf{d}'\cdot\mathbf{d}}{\|\mathbf{d}'\|\cdot\|\mathbf{d}\|}\right]$$

$$\mathbf{d} = \breve{\mathbf{x}} - \breve{\boldsymbol{\rho}}\cdot\left(\breve{\boldsymbol{\rho}}\cdot\breve{\mathbf{x}}\right) + \breve{\boldsymbol{\rho}}\times\breve{\mathbf{y}}$$

$$\mathbf{d}' = \breve{\mathbf{x}}' - \breve{\boldsymbol{\rho}}\cdot\left(\breve{\boldsymbol{\rho}}\cdot\breve{\mathbf{x}}'\right) + \breve{\boldsymbol{\rho}}\times\breve{\mathbf{y}}'$$

Instrumental biases

The satellite and the receiver electronics produce delays (a few nanoseconds) in the time of emission and reception of the signals.

If not corrected, these delays are misinterpreted as an increase of the propagation time and hence of the measured pseudo-range (a few meters).

Delays are different for code and carrier measurements.

Delays are frequency dependent.

Errors caused by the atmosphere

Speed of light in the atmosphere, v, differs from the vacuum, c:

$n = \frac{c}{v}$ refraction index; $n=1$ in vacuum.

The propagation intervals in the atmosphere and in vacuum are:

$$\tau = \int_0^{\rho} \frac{dr}{v} = \frac{1}{c} \cdot \int_0^{\rho} n \cdot dr \qquad \tau' = \frac{1}{c} \cdot \int_0^{\rho} 1 \cdot dr$$

(neglecting the bending)

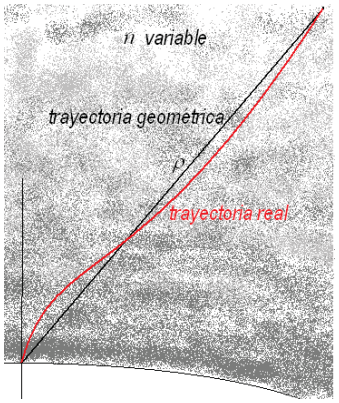

and the difference:

$$\Delta\tau = \tau - \tau' = \frac{1}{c} \cdot \int_0^{\rho} (n-1) \cdot dr$$

which is equivalent to a range error: refractivity

$$\Delta\rho = c \cdot \Delta\tau = \int_0^{\rho} (n-1) \cdot dr = 10^{-6} \int_0^{\rho} N \cdot dr$$

Ionospheric error

The ionosphere extends from ~50 km above the Erath surface and is characterized by the presence of free electrons (electrons dissociated from atoms and molecules).

Its mass is lower than 0.1% of the total atmospheric mass, but free electrons interact with electromagnetic waves changing its speed of propagation.

$$N_I = \pm \frac{40.3 \times 10^6}{f^2} \cdot ED$$

f = frequency (Hz);
ED = electron density (electrons/m^3)
- for carrier / + for code

$$\Delta\rho_I = \pm \frac{40.3}{f^2} \cdot \int_0^{\rho} ED \cdot dr = \pm \frac{40.3 \times 10^{16}}{f^2} \cdot TEC$$

TEC Total Electron Content
(TECu 1 TECu = 10^{16} electrons/m^3)

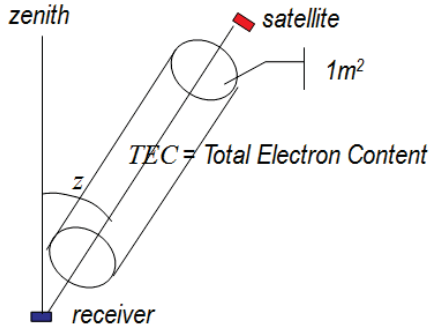

frequency	error (1 TECu)
L1: 1,57542E+09	0,162 m
L2: 1,22760E+09	0,267 m

TEC maps computed by SIRGAS

TEC varies with local time, season, solar activity, latitude and geomagnetic perturbation.

Ionospheric delay may reach 40 m for a low elevation satellite.

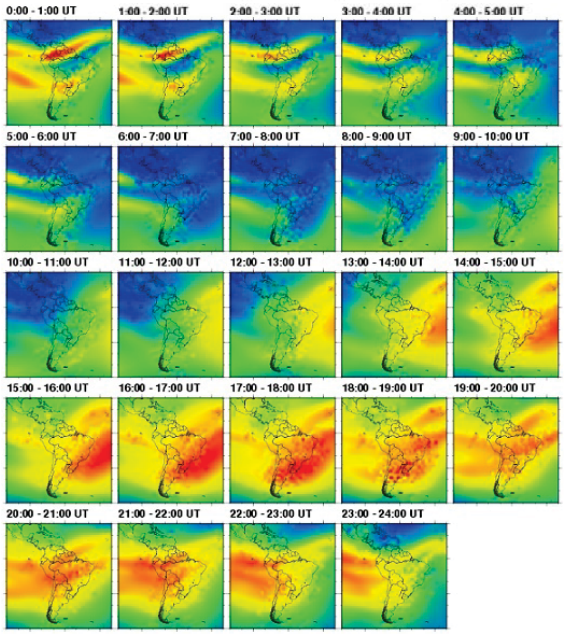

Ionosphere free combination of carrier phase measurements

Eliminates the ionospheric error:

$$l_1 = \rho + \underbrace{\Delta\rho_{I,1}}_{-\frac{40.3}{f_1^2}\cdot TEC} + \lambda_1 \cdot N_1 + \upsilon_1 \qquad l_2 = \rho + \underbrace{\Delta\rho_{I,2}}_{-\frac{40.3}{f_2^2}\cdot TEC} + \lambda_2 \cdot N_2 + \upsilon_2$$

$$l_3 = \underbrace{\frac{f_1^2}{f_1^2 - f_2^2}}_{2.5457} \cdot l_1 - \underbrace{\frac{f_2^2}{f_1^2 - f_2^2}}_{1.5457} \cdot l_2$$

$$\upsilon_3 = 2.5457 \cdot \upsilon_1 - 1.5457 \cdot \upsilon_2 \Rightarrow \sigma_3 = \sqrt{2.5457^2 \cdot \sigma_1^2 + 1.5457^2 \cdot \sigma_2^2} \cong 3 \cdot \sigma_1 \cong 3 \cdot \sigma_2$$

~ 3 times greater than the errors in L1 or L2 measurements

$$b_3 = 2.5457 \cdot N_1 \cdot \lambda_1 - 1.5457 \cdot N_2 \cdot \lambda_2$$

the ambiguity is not an integer anymore

Tropospheric error

The neutral atmosphere (troposphere + stratosphere) extends ~ 50 km above the earth surface; according to the Hopfield model:

$N_T = N_D + N_W$ *Dry (~90%) + Wet (~20%) components*

$$N_D(h) = \underbrace{77.64 \cdot \frac{p}{T}}_{N_{D,h=0}} \cdot \underbrace{\left(\frac{h_S - h}{h_D}\right)^4}_{\text{height variability}} \qquad h_D = 40136 + 148.72 \cdot (T - 273.16)$$

$$N_W(h) = \underbrace{\left(-12.96 \cdot \frac{e}{T} + 3.718 \cdot 10^5 \cdot \frac{e}{T^2}\right)}_{N_{W,h=0}} \cdot \underbrace{\left(\frac{h_H - h}{h_W}\right)^4}_{\text{height variability}} \qquad h_W = 11000$$

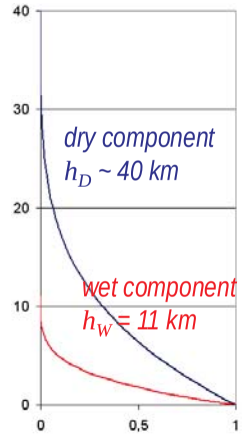

h_D *and* h_W *= scale height (m)*
p *= atmospheric pressure (mb)*
T *= temperature (K)*
e *= partial water vapor pressure (mb)*
all reduced to h=0.

$$\Delta\rho_{D,z=0} = 10^{-6} \int_0^{h_D} N_D(h) \cdot dh = \frac{10^{-6}}{5} \cdot N_{D,h=0} \cdot h_D$$

$$\Delta\rho_{W,z=0} = 10^{-6} \int_0^{h_W} N_W(h) \cdot dh = \frac{10^{-6}}{5} \cdot N_{W,h=0} \cdot h_W$$

Tropospheric correction

The total tropospheric delay (dry + wet) for a zenith distance z, is given by:

$$\Delta\rho_T(z) = \Delta\rho_{D,z=0} \cdot m_D(z) + \Delta\rho_{W,z=0} \cdot m_W(z)$$

$$m_{D/W}(z) = \frac{1 + \dfrac{a_{D/W}}{1 + \dfrac{b_{D/W}}{1 + c_{D/W}}}}{\cos(z) + \dfrac{a_{D/W}}{\cos(z) + \dfrac{b_{D/W}}{\cos(z) + c_{D/W}}}}$$

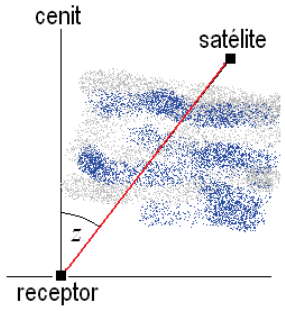

$m_{D/W}(z)$ *= Dry/Wet mapping functions (e.g.: 'Vienna' mapping function);*

$a_{D/W}$, $b_{D/W}$, $c_{D/W}$ *= empirically determined functions dependent on latitude, day of year and height.*

Estimation of the tropospheirc correction

Models are not accurate enough to correct the tropospheric error (specially the wet component.

Errors affects mostly the estimation of the height.

An empirical correction is added to account for the unmodeled correction:

$$\Delta\rho_{T,z=0} = \overline{\Delta\rho}_{T,z=0} + \delta\rho_{T,z=0}$$

Zenith delay — *Modeled value* — *Empirical correction*

An empirical correction is estimated together with the station coordinates, the receiver clock and the ambiguities.

Typically one correction per hour is estimated.

3.4 point and differential positioning

Equation of observation for point positioning

Ionosphere-free combination of carrier phase measurements

Receiver-satellite range computed from satellite ephemerides and approximate receiver coordinates

Receiver-satellite direction cosines

Corrections to the approximate receiver coordinates

$$l_{3R}^{S} - \rho_{R,0}^{S} - \Delta\rho_{R}^{S} = \cos\left(a_{R,0,e}^{S}\right)\cdot\Delta e_{R} + \cos\left(\alpha_{R,0,n}^{S}\right)\cdot\Delta n_{R} + \cos\left(a_{R,0,v}^{S}\right)\cdot\Delta v_{R} - c\cdot\Delta t_{R}$$

$$-b_{3R}^{S} + m_{W}\left(z_{R}^{S}\right)\cdot\delta\rho_{TR} + \upsilon_{3R}^{S}$$

Correction to receiver clock

Corrections:
- satellite clock
- relativity
- satellite and receiver antennas phase centers and wind-up
- troposphere (dry + wet)
- coordinate variations (solid tides, ocean loading, EOP, etc.)

Troposphere wet mapping function

Measurement + multipath errors on the ionosphere free combination

Ionosphere-free bias (including satellite and receiver instrumental biases.

Unmodeled tropospheric correction

Receiver clock and tropospheric corrections

time dependence	unknown	updating interval	type of constraint
constant	receiver coordinates (assuming that geophysical variations are modeled)	none	none
	Ambiguities (assuming that cycle slips have not occurred)	None	none
varying	receiver clock	one per epoch	relative
	tropospheric correction	one per hour	abs. and rel.

σ_a is the standard deviation for the absolute value

σ_r is the standard deviation for the temporal variation

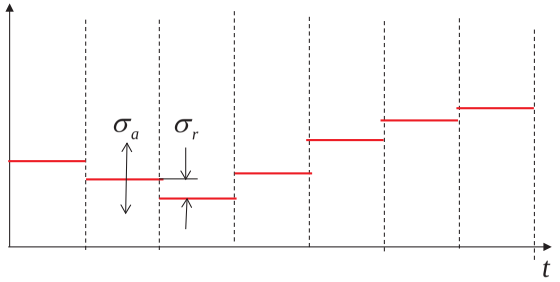

Equation of observation for differential positioning

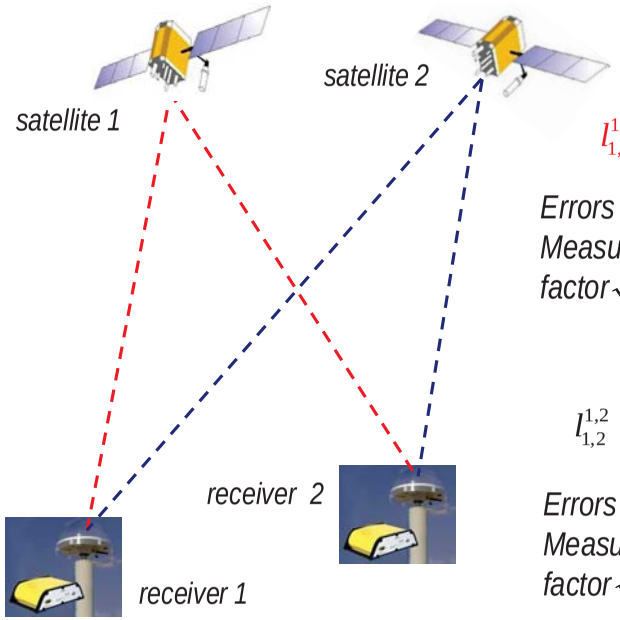

Single differences

$$l_{1,2}^{1} = l_{1}^{1} - l_{2}^{1} \qquad l_{1,2}^{2} = l_{1}^{2} - l_{2}^{2}$$

Errors in the satellite clocks cancel out; Measurements errors increase by a factor $\sqrt{2}$.

Double difference

$$l_{1,2}^{1,2} = l_{1,2}^{1} - l_{1,2}^{2} = \left(l_{1}^{1} - l_{2}^{1}\right) - \left(l_{1}^{2} - l_{2}^{2}\right)$$

Errors in the receiver clocks cancel out; Measurements errors increase by a factor $\sqrt{5}$.

Effect on receiver coordinates

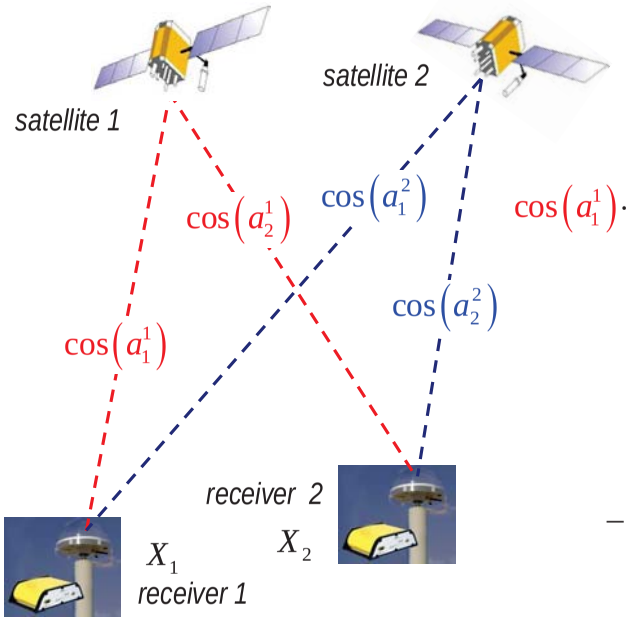

$$l_{1,2}^{1,2} = \left(l_{1}^{1} - l_{2}^{1}\right) - \left(l_{1}^{2} - l_{2}^{2}\right)$$

$$\cos\left(a_1^1\right)\cdot X_1 - \cos\left(a_2^1\right)\cdot X_2$$

$$\cos\left(a_1^2\right)\cdot X_1 - \cos\left(a_2^2\right)\cdot X_2$$

$$\left[\cos\left(a_1^1\right) - \cos\left(a_1^2\right)\right]\cdot X_1$$

$$-\left[\cos\left(a_2^1\right) - \cos\left(a_2^2\right)\right]\cdot X_2$$

Effect on bias and troposphere

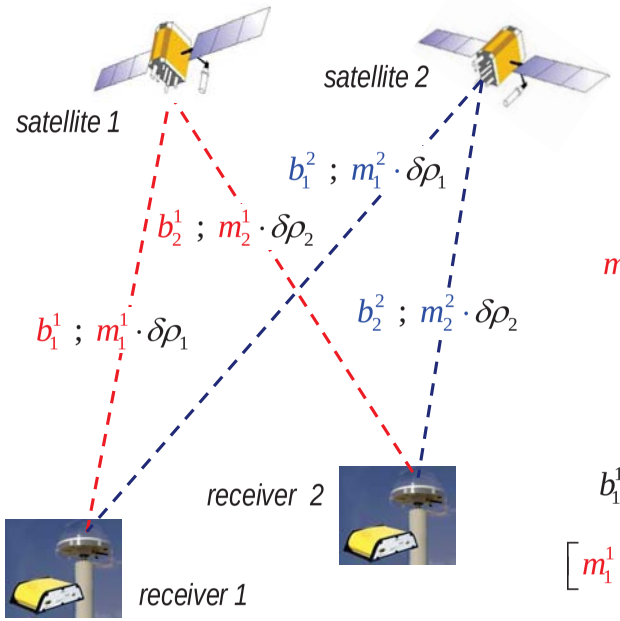

$$l_{1,2}^{1,2} = \left(l_1^1 - l_2^1\right) - \left(l_1^2 - l_2^2\right)$$

$$b_1^1 - b_2^1 \qquad b_1^2 - b_2^2$$

$$m_1^1 \cdot \delta\rho_1 - m_2^1 \cdot \delta\rho_2 \qquad m_1^2 \cdot \delta\rho_1 - m_2^2 \cdot \delta\rho_2$$

$$b_{1,2}^{1,2} = \left[b_1^1 - b_1^2\right] - \left[b_2^1 - b_2^2\right]$$

$$\left[m_1^1 - m_1^2\right] \cdot \delta\rho_1 - \left[m_2^1 - m_2^2\right] \cdot \delta\rho_2$$

Correlations between baselines

Let 's assume 3 receivers and 2 satellites which leads to 6 single differenced combinations possible

$$\begin{vmatrix} l_{1,2}^1 = l_1^1 - l_2^1 \\ l_{1,2}^2 = l_1^2 - l_2^2 \\ l_{2,3}^1 = l_2^1 - l_3^1 \\ l_{2,3}^2 = l_2^2 - l_3^2 \\ l_{3,1}^1 = l_3^1 - l_1^1 \\ l_{3,1}^2 = l_3^2 - l_1^2 \end{vmatrix} = \underbrace{\begin{vmatrix} 1 & 0 & -1 & 0 & 0 & 0 \\ 0 & 1 & 0 & -1 & 0 & 0 \\ 0 & 0 & 1 & 0 & -1 & 0 \\ 0 & 0 & 0 & 1 & 0 & -1 \\ -1 & 0 & 0 & 0 & 1 & 0 \\ 0 & -1 & 0 & 0 & 0 & 1 \end{vmatrix}}_{\mathbf{A}_{0/S}} \cdot \begin{vmatrix} l_1^1 \\ l_1^2 \\ l_2^1 \\ l_2^2 \\ l_3^1 \\ l_3^2 \end{vmatrix}$$

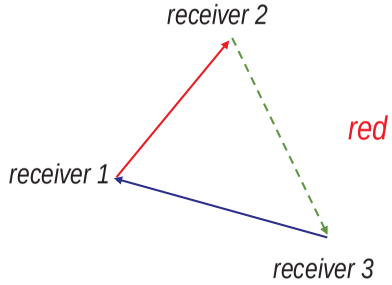

red + green = - blue

The variance-covariance matrix is singular

$$\mathbf{C}_{SD} = \mathbf{A}_{0/S} \cdot \mathbf{A}_{0/S}^T = \begin{vmatrix} 2 & 0 & -1 & 0 & -1 & 0 \\ 0 & 2 & 0 & -1 & 0 & -1 \\ -1 & 0 & 2 & 0 & -1 & 0 \\ 0 & -1 & 0 & 2 & 0 & -1 \\ -1 & 0 & -1 & 0 & 2 & 0 \\ 0 & -1 & 0 & -1 & 0 & 2 \end{vmatrix}$$

Correlation between single and double differences

Let's assume that the red and green independent baselines are chosen (more measurements, short lengths, other criteria):

$$\begin{vmatrix} l_{1,2}^1 = l_1^1 - l_2^1 \\ l_{1,2}^2 = l_1^2 - l_2^2 \\ l_{2,3}^1 = l_2^1 - l_3^1 \\ l_{2,3}^2 = l_2^2 - l_3^2 \end{vmatrix} = \underbrace{\begin{vmatrix} 1 & 0 & -1 & 0 & 0 & 0 \\ 0 & 1 & 0 & -1 & 0 & 0 \\ 0 & 0 & 1 & 0 & -1 & 0 \\ 0 & 0 & 0 & 1 & 0 & -1 \end{vmatrix}}_{\mathbf{A}_{0/S}} \cdot \begin{vmatrix} l_1^1 \\ l_1^2 \\ l_2^1 \\ l_2^2 \\ l_3^1 \\ l_3^2 \end{vmatrix} \qquad \begin{vmatrix} l_{1,2}^{1,2} = l_{1,2}^1 - l_{1,2}^2 \\ l_{2,3}^{1,2} = l_{2,3}^1 - l_{2,3}^2 \end{vmatrix} = \underbrace{\begin{vmatrix} 1 & -1 & 0 & 0 \\ 0 & 0 & 1 & -1 \end{vmatrix}}_{\mathbf{A}_{S/D}} \cdot \begin{vmatrix} l_{1,2}^1 \\ l_{1,2}^2 \\ l_{2,3}^1 \\ l_{2,3}^2 \end{vmatrix}$$

$$\begin{vmatrix} l_{1,2}^{1,2} \\ l_{2,3}^{1,2} \end{vmatrix} = \mathbf{A}_{S/D} \cdot \mathbf{A}_{0/S} \cdot \begin{vmatrix} l_1^1 \\ l_1^2 \\ l_2^1 \\ l_2^2 \\ l_3^1 \\ l_3^2 \end{vmatrix} = \underbrace{\begin{vmatrix} 1 & -1 & -1 & 1 & 0 & 0 \\ 0 & 0 & 1 & -1 & -1 & 1 \end{vmatrix}}_{\mathbf{A}_{0/D}} \cdot \begin{vmatrix} l_1^1 \\ l_1^2 \\ l_2^1 \\ l_2^2 \\ l_3^1 \\ l_3^2 \end{vmatrix} \qquad \mathbf{C}_{DD} = \mathbf{A}_{0/D} \cdot \mathbf{A}_{0/D}^T = \begin{vmatrix} 5 & 0 & -4 & 0 \\ 0 & 5 & 0 & -4 \\ -4 & 0 & 5 & 0 \\ 0 & -4 & 0 & 5 \end{vmatrix}$$

3.5 network computation

Just an example

Observations	
Receivers	50
Sampling rate	1/15^s
Average satellites per epoch	6
Observation period	24 h (86400^s)
Equations of observation	50 x 1/15 x 86400 x 6 = 1728000

unknowns		
Receivers coordinates	3 x 50 = 150	
Receiver clocks	50 x 1/15 x 86400 = 288000	*One per epoch; constrained.*
Tropospheric corrections	50 x 24 = 1200	*One per hour; constrained.*
Biases	50 x 31 x 2 = 3100	*Assuming 2 continuous satellites arcs per day (no cycle slips).*
Total	292450	

The system of equations of observation

$\mathbf{L} = \mathbf{A} \cdot \mathbf{x} + \mathbf{v}$ $\quad\quad$ Σ_L = variance-covariance matrix of the measurements

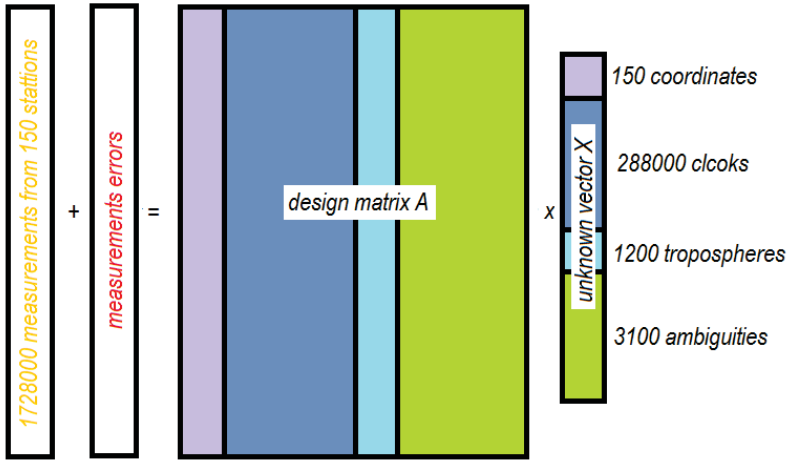

Normal system

$\mathbf{N} \cdot \mathbf{x} = \mathbf{b}$ $\quad\quad$ $\mathbf{N} = \mathbf{A}^T \cdot \Sigma_L^{-1} \cdot \mathbf{A}$ $\quad\quad$ $\mathbf{b} = \mathbf{A}^T \cdot \Sigma_L^{-1} \cdot \mathbf{L}$

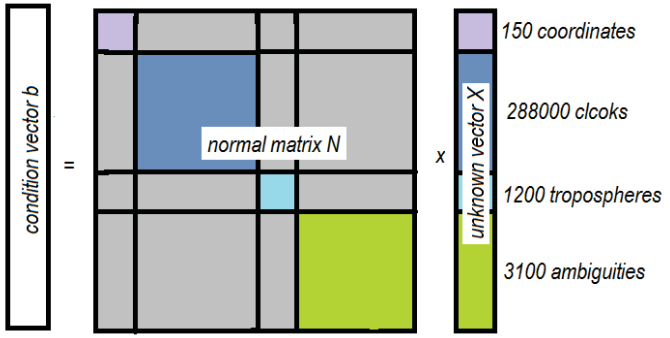

The solution provides the unknowns, $\mathbf{x} = \mathbf{N}^{-1} \cdot \mathbf{b}$, *the residuals,* $\mathbf{v} = \mathbf{L} - \mathbf{A} \cdot \mathbf{x}$, *the standard deviation of the unity of weight,* $\sigma_0 = \sqrt{\dfrac{\mathbf{v}^t \cdot \Sigma_L^{-1} \cdot \mathbf{v}}{n-m}}$ *,and the variance-covariance matrix of the unknowns,* $\Sigma_X = N^{-1}$.

Combination of solutions

The SIRGAS processing centers compute weekly 'loosely constrained' normal equations (the reference frame is defined by only the $_{\text{stations}}$ *coordinates).*

The SIRGAS combination centers compute the final solution by stacking the individual normal equations and imposing the datum to the network.

Fixed solution $\quad$ *Weighted solution* $\quad$ *No net rotation & no net translation solution*

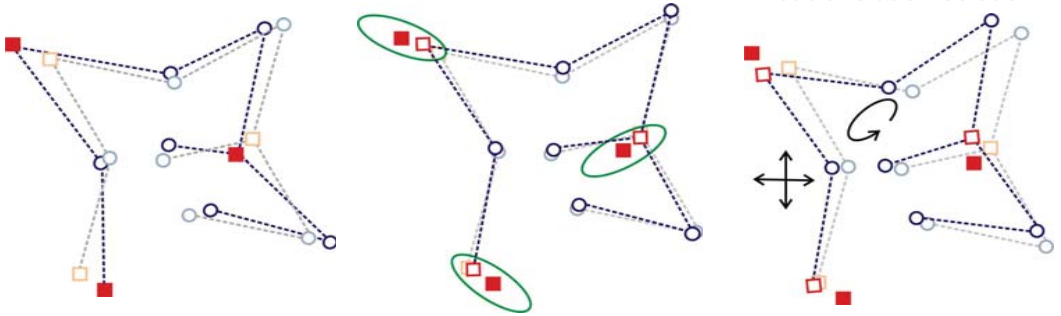

After L. Sánchez

4. Vertical reference systems

Any vertical reference system is basically composed by

1) **a reference surface**, i.e. the zero-height level (**vertical datum**)
2) **a vertical coordinate**, i.e. a type of height

Its realisation is given by a vertical network, i.e. a set of points, whose heights are of the same type considered in (2) and refer to the datum specified in (1).

If the reference surface and height type depend on the Earth's gravity field, we talk about a **physical height system** (e.g. orthometric heights and geoid, or normal heights and quasi-geoid) if not, it is a **geometrical height system** (e.g. ellipsoidal heights and reference level ellipsoid).

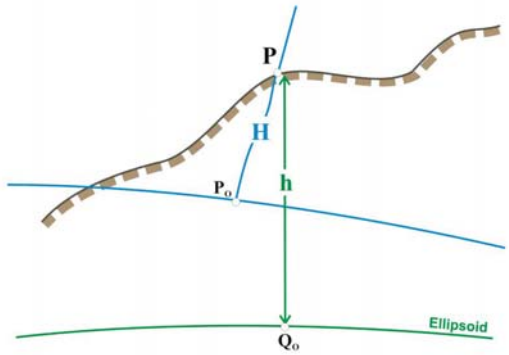

4.1 Geometrical height system

Vertical coordinate: Ellipsoidal height (h): length, along the ellipsoid normal, from the ellipsoid to the point $P(\mathbf{X})$.

- today, h is derived from geocentric coordinates $[X,Y,Z]$
- earlier (for the adjustment of triangulation networks), $h = H + N$

Reference surface: a level (or equipotential) ellipsoid.

$$U_0 = U(\mathbf{X}) = const.$$

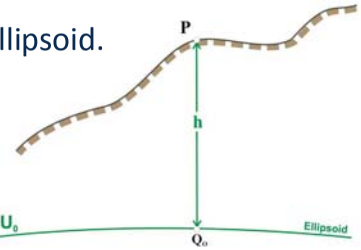

U_0 can be univocally determined as a function of the ellipsoid parameters:

$$U_0 = \frac{GM}{\sqrt{a^2-b^2}} \arctan\left(\frac{\sqrt{a^2-b^2}}{b}\right) + \frac{1}{3}\omega^2 a^2$$

$$= \frac{GM}{b}\left(1 + \sum_{n=1}^{\infty}(-1)\frac{e'^{2n}}{2n+1} + \frac{1}{3}m\right)$$

GM → geocentric gravitational constant
a → semi-major axis
b → semi-minor axis
ω → (nominal mean Earth's) angular velocity

$$e'^2 = \frac{a^2-b^2}{b^2}, \quad m = \frac{\omega^2 a^2 b}{GM}$$

Geometrical height system

The **realisation** of a geometrical reference system **depends on**

- the **orientation and position** of the ellipsoid whit respect to the ITRS (reference system for $[X,Y,Z]$).
- the **ellipsoid parameters**: if any of those changes, reference surface and vertical coordinate change.
- the **primary geocentric coordinates** $[X,Y,Z]$: if they change, the vertical coordinate changes.

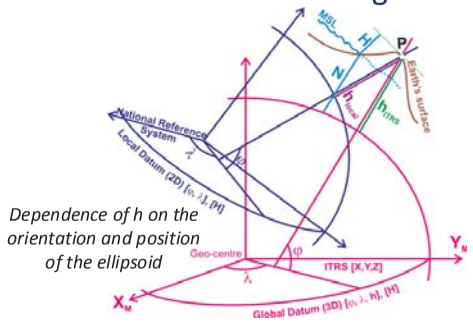

Dependence of h on the orientation and position of the ellipsoid

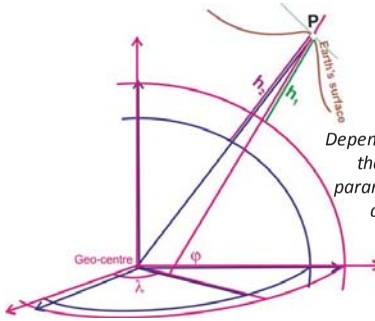

Dependence of h on the ellipsoid parameters (form and size)

Geometrical height system

Dependence of h on the changes of [X,Y,Z]

Source: www.sirgas.org

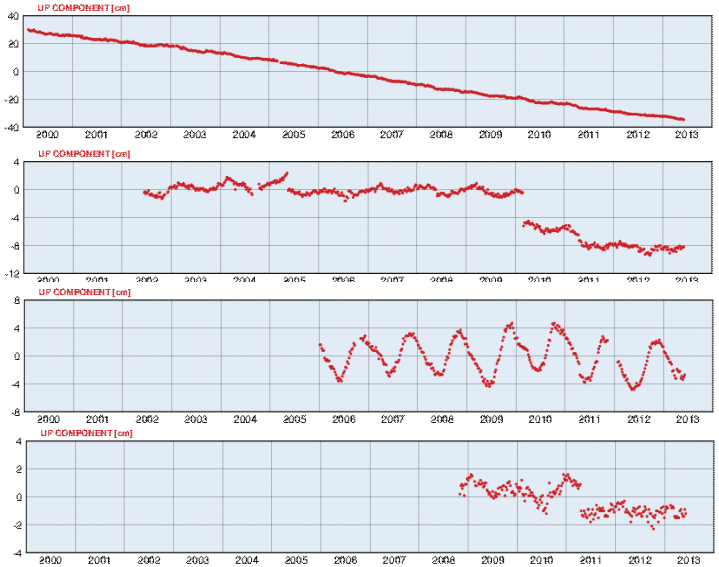

BOGA: Bogotá, Colombia
Subsidence

CONZ: Concepción, Chile
Earthquake

NAUS: Manaus, Brazil
Hydrological loading

UYTA: Tacuarembo, Uruguay
Introduction of ITRF2008

Components of a geometrical vertical reference system

Vertical coordinate: Ellipsoidal height h referred to a **certain epoch** t and its **variations with time**:

$$h(\mathbf{X}, t) \quad ; \quad \frac{dh(\mathbf{X})}{dt}$$

Reference surface: stationary in time and space for a better modelling of height changes:

$$U_0 = U(\mathbf{X}) = const.$$

For that, one has to be familiarized with **standards, conventions, and procedures** applied for the realisation of the ITRS, i.e. the **International Terrestrial Reference Frame (ITRF)** and its regional densifications like **SIRGAS** (Latin America and Caribbean), **EPN**: EUREF Permanent Network (Europe), etc.

Remarks on the geometrical height system

- Ellipsoidal heights are not measurable directly; they must be derived from other geodetic parameters.
- The primary coordinates $[X,Y,Z]$ must be computed in the same reference frame in which the GNSS satellite orbits are given, i.e. ITRF or its regional densifications must be used as reference frame in GNSS processing.
- For global compatibility, the same ellipsoid must be used for the conversion $[X,Y,Z] \rightarrow [\varphi,\lambda,h]$, at present the GRS80.
- Ellipsoidal heights in local geodetic datums (e.g. PSDA56, NAD27, etc.) can only be obtained by means of transformations.
- The vertical position in GNSS is 2 … 3 times less accurate than the horizontal position, because most of the error sources in GNSS act in radial direction.
- Accurate ellipsoidal heights (at mm-level) require long GNSS positioning (at least three days) and post-processing following the IERS conventions. Otherwise, accuracy in cm- to dm-level.

4.2 Physical height systems

(Primary) vertical coordinate: Level difference between a reference surface W_0 and the equipotential surface passing through $P(\mathbf{X})$ i.e. W_P

$$-\Delta W_P = C_P = W_0 - W_P$$

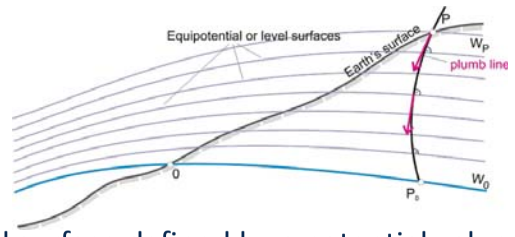

Reference surface: equipotential surface defined by a potential value (called W_0). The **realisation** (geometrical representation) of this equipotential surface with respect to a reference ellipsoid is the so-called ***geoid computation***.

Since the primary observable are level differences, the W_0 value is usually selected arbitrarily. In addition, the W_0 value *per se* does not provide any information about the geometry of the reference surface.

Physical height systems

C_p is called **geopotential number** and it is given in **[m²s⁻²]**. To facilitate its use in practice, C_p is converted in a distance (given in **[m]**) by dividing it by a gravity value $\hat{g}$.

$$H_P = \frac{C_P}{\hat{g}} = \frac{W_0 - W_P}{\hat{g}}$$

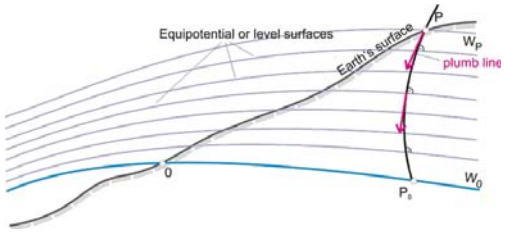

$\hat{g}$ represents the mean gravity value between the reference surface W_0 and the equipotential surface W_P.

The potential difference W_0 - W_P is constant (because they are **equipotential surfaces**) and therefore, the value of H_P depends on the value of $\hat{g}$. As a consequence, we distinguish **dynamic**, **orthometric** and **normal heights**.

Physical heights: some glossary

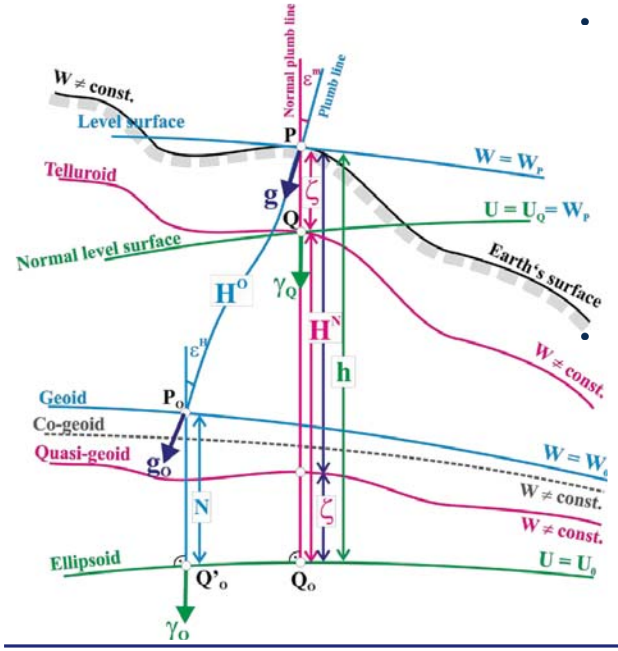

- The **geoid** is the **equipotential surface** that **would coincide** with the mean sea surface if the oceans and atmosphere were in equilibrium; under the influence of Earth's gravitation and rotation alone; without other influences such as winds, tides or gravitational effects of other bodies.
- The **co-geoid** is the estimated geoid, i.e. the real geoid cannot be known, because the actual mass distribution and actual gravity vertical gradient are not known precisely. The assumption of hypotheses about that produces "something similar" to the geoid (the co-geoid), but no the true geoid.

Physical heights: some glossary

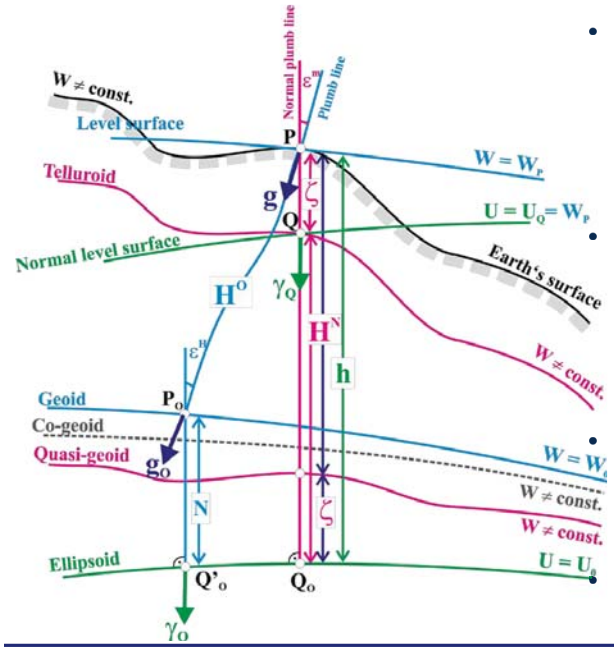

- The **telluroid** is the surface defined by those points Q, whose normal potential U_Q is identical with the actual potential W_P of the points P on the Earth's surface, i.e. $U_Q = W_P$
- The **height anomaly** ζ is the distance, along the normal plumb line, between the Earth's surface and the telluroid. When plotted above the ellipsoid the resulting surface is called the **quasi-geoid**.
- **Telluroid, quasi-geoid and co-geoid are not equipotential surfaces** (the gravity vector is not perpendicular to them).
- **Geoid and quasi-geoid are identical in ocean areas**.

Physical heights: some glossary

$$H_P = \frac{C_P}{\hat{g}} = \frac{W_0 - W_P}{\hat{g}}$$

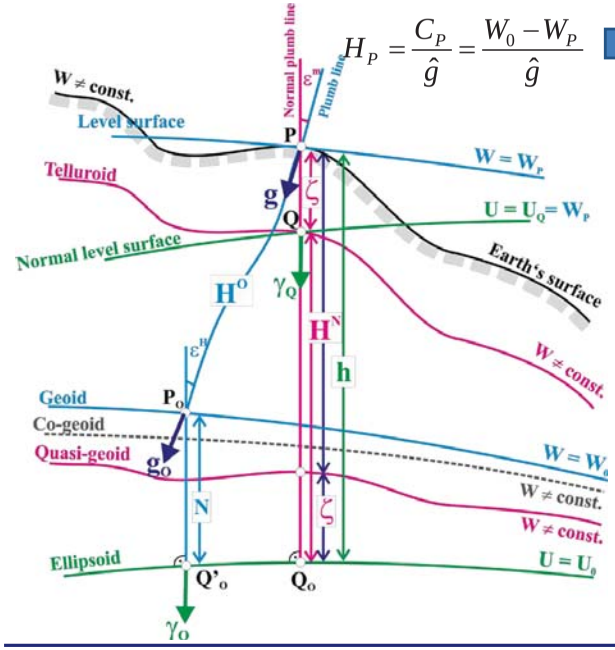

- If $\hat{g}$ is the **mean real gravity value**, along the plumb line, between Earth's surface and geoid, we get **orthometric heights**.
- If $\hat{g}$ is **the mean normal gravity value** between telluroid and ellipsoid (or between Earth's surface and the quasi-geoid), we get **normal heights**.
- If $\hat{g}$ is a **constant normal gravity value**, we get **dynamic heights**.

Geopotential numbers in practice

The derivative of the gravity potential in a given direction is equal to the component of the gravity along this direction. Along the plumb line (perpendicular to the level surfaces), it is:

$$-\frac{dW}{dn} = g \quad ; \quad dW = -g\,dn$$

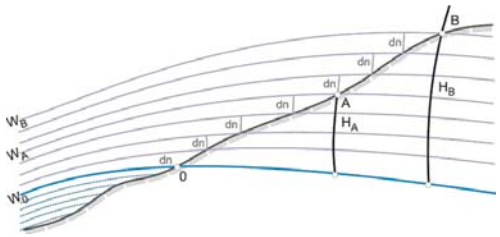

Integrating dn between two points A and B, we have:

$$-\int_A^B dW = \int_A^B g\,\delta n = \hat{g}\left(H_B - H_A\right) = W_A - W_B$$

i.e. the level difference dn between two points (A, B), located on the Earth's surface and on two different equipotential surfaces, corresponds to:

$$dn_{BA} = \left(H_B - H_A\right) = \frac{W_A - W_B}{\hat{g}}$$

$\hat{g}$ is the mean gravity value between the two equipotential surfaces W_A and W_B

Geopotential numbers in practice

If the starting point is *on* the geoid (W_0), we have the geopotential number of B

$$C_B = W_0 - W_B = \int_0^B g\,\delta n \cong \sum_0^B g\,dn$$

g is the average of the gravity along the levelling line connecting 0 and B.

The height value for B is then

$$H_B = \frac{W_0 - W_B}{\hat{g}} = \frac{C_B}{\hat{g}}$$

Note: g and $\hat{g}$ are different values!

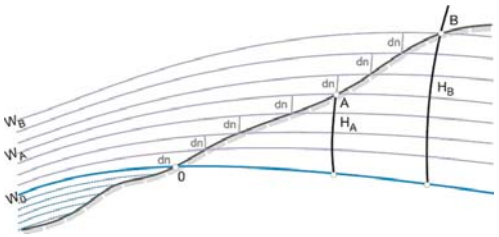

Spirit levelling measures the geometric height difference between two points, without taking care of the effect of the gravity on the level surfaces (non-parallelism), i.e. in a closed levelling loop

$$\oint dn \neq 0$$

which also means

$$\sum_0^B dn \neq H_B$$

Levelled height differences are not the same as physical height differences!!

Geopotential numbers in practice

The levelled height differences must be converted into **potential** differences or into **physical height differences** to satisfy the loop misclosure condition of zero, i.e.

$$\oint dW = 0 \quad \oint (dn + k) = 0$$

Afterwards they are adjusted by the method of condition equations or by the method of parameter variation. k is known as the gravity correction (or reduction) to levelling.

In practice, the potential difference from geometric (spirit) levelling between two bench marks **I** and **II** is given by:

$$\Delta W_{II,I} = (\bar{g}_{IA} \cdot dn_{IA}) + (\bar{g}_{AB} \cdot dn_{AB}) + (\bar{g}_{BC} \cdot dn_{BC}) + \ldots + (\bar{g}_{DII} \cdot dn_{DII})$$

$$\bar{g}_{AB} = \frac{g_A + g_B}{2}$$

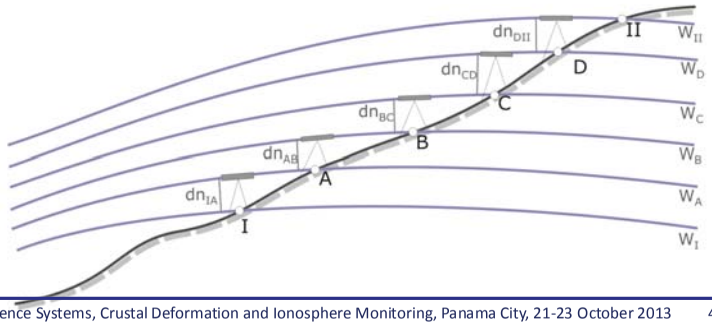

Geopotential numbers in practice

Required input data:

1) **Levelled differences** (dn) with systematic errors reduced (i.e. atmospheric refraction, rod graduation errors, temperature effect on the instrument and rods, etc.). Random errors are compensated by means of the adjustment.

Accuracy standards in levelling:

	Standard deviation of a level difference measured in two directions (back-sight and fore-sigth) :	Standard deviation for a level difference compared with known height differences (junction with existing vertical networks) :
First-order	$s = \pm 2\sqrt{R_{km}}\ mm$	$s = \pm \left(2 + 2\sqrt{R_{km}}\right) mm$
Second-order:	$s = \pm 3\sqrt{R_{km}}\ mm$	$s = \pm \left(2 + 3\sqrt{R_{km}}\right) mm$
Third-order:	$s = \pm 5\sqrt{R_{km}}\ mm$	$s = \pm \left(2 + 5\sqrt{R_{km}}\right) mm$
Fourth-order:		$s = \pm \left(2 + 6\sqrt{R_{km}}\right) mm$

R: length in [km] of the levelling line associated with the measured height difference.

Geopotential numbers in practice

Required input data:

2) **Length of the levelling segments**: the standard deviation of levelling increases inversely proportionally with the distance. The levelling lines shall be adjusted in one block and weighted with the inverse of this standard deviation. For example in South America:

$$s_{dn} = 4mm\sqrt{R_{km}} \quad \rightarrow \quad p_{dn} = \frac{1}{s_{dn}} = \frac{1/16}{R_{km}}$$

Geopotential numbers in practice

Required input data:

3) **Measurement epochs:** to take into account crustal vertical movements

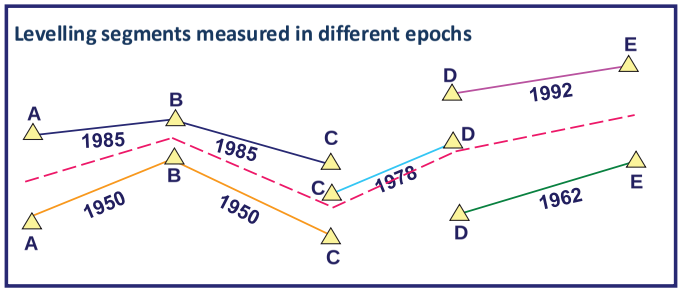

Changes in the levelled height differences are caused by vertical movments? Or are they observation errors?

Geopotential numbers in practice

Required input data:

4) **(Real) gravity values** (observed or interpolated) at levelled points to compute the geopotential numbers.

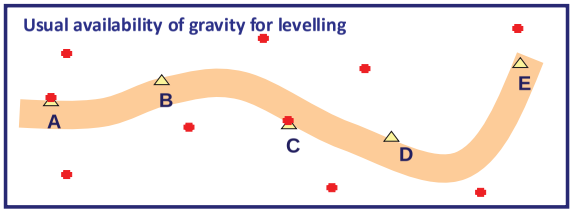

Height [m]	m_g for R = 1 km [10^{-5} m s^{-2}]	m_g for R = 2 km [10^{-5} m s^{-2}]
10	400	566
20	200	283
30	133	189
40	100	141
50	80	113
70	57	81
100	40	57
200	20	28
500	8	11
1000	4	8
2000	2	4
4000	1	2

Minimum accuracy of gravity values for the determination of geopotential numbers

From geopotential numbers to physical heights

Dynamic heights:

From potential differences:

$$H^{DYN} = \frac{C}{\gamma_o^{\varphi}}$$

Using the dynamic correction:

$$\Delta H_{AB}^{DYN} = \Delta n_{AB} + k_{AB}^{DYN}$$

$$k_{AB}^{DYN} = \int_A^B \frac{g-\gamma_o^{45}}{\gamma_o^{45}}\delta n = \sum_A^B \frac{g-\gamma_o^{45}}{\gamma_o^{45}} dn$$

γ_o^{φ} Normal gravity for the surface of the level ellipsoid at certain latitude φ, normally 45°.

Normal heights:

From potential differences:

$$H^N = \frac{C}{\gamma_m} \quad ; \quad \gamma_m = \frac{1}{H^N}\int_0^{H^N} \gamma\, dH^N$$

Using the normal correction:

$$\Delta H_{AB}^{N} = \Delta n_{AB} + k_{AB}^{N}$$

$$k_{AB}^{N} = \int_A^B \frac{g-\gamma_o^{45}}{\gamma_o^{45}}\delta n + \frac{\gamma_m^A-\gamma_o^{45}}{\gamma_o^{45}} H_A^N - \frac{\gamma_m^B-\gamma_o^{45}}{\gamma_o^{45}} H_B^N$$

γ_m Mean normal gravity along the normal plumb line between telluroid and ellipsoid (analytically estimable, iterativ)

$$\gamma_m = \gamma_o + \frac{1}{2}\left(\frac{\partial\gamma}{\partial H}\right)_o H^N + \frac{1}{2!}\left(\frac{\partial^2\gamma}{\partial H^2}\right)_o (H^N)^2 + \ldots = \gamma_o^{\varphi}\left[1-(1+f+m-2f\sin^2\varphi)\frac{H^N}{a}+\frac{(H^N)^2}{a^2}\right] \quad [ms^{-2}]$$

a semi-major axis, f flattening, φ latitude of the point, $m = \frac{\omega^2 a^2 b}{GM}$

From geopotential numbers to physical heights

Dynamic correction in two Colombian levelling lines

Courtesy

Dynamic correction vs. topography (levelling loop length: 1364 km)

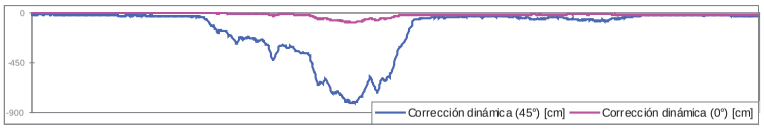

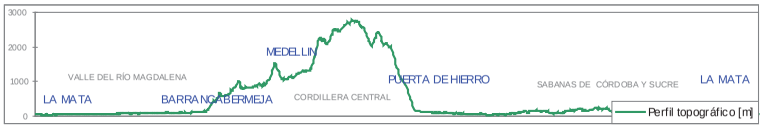

Dynamic correction vs. topography (levelling loop length 1820 km)

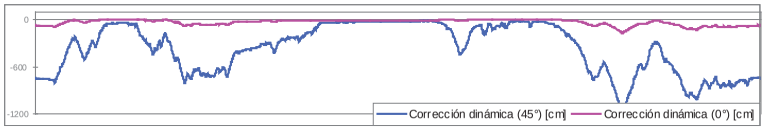

From geopotential numbers to physical heights

Normal correction in two Colombian levelling lines

Courtesy

Normal correction vs. topography (levelling loop length 1640 km)

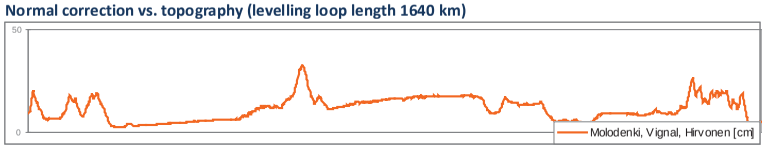

Normal correction vs. topography (levelling loop length 1143 km)

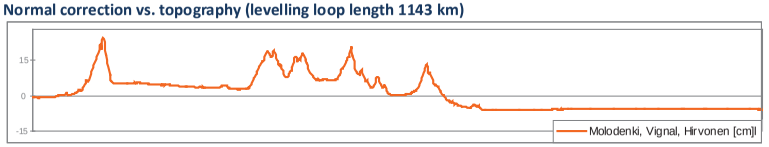

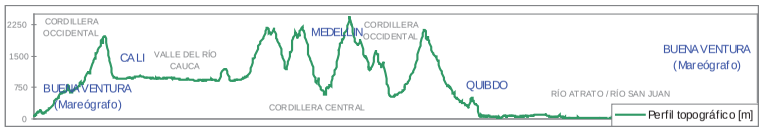

From geopotential numbers to physical heights

Orthometric heights:

From potential differences:

$$H^O = \frac{C}{g_m} \quad ; \quad g_m = \frac{1}{H^O}\int_0^{H^O} g\, dH^O$$

Using the orthometric correction:

$$\Delta H^O_{AB} = \Delta n_{AB} + k^O_{AB}$$

$$k^O_{AB} = \int_A^B \frac{g-\gamma^{45}_o}{\gamma^{45}_o}\delta n + \frac{g^A_m-\gamma^{45}_o}{\gamma^{45}_o}H^O_A - \frac{g^B_m-\gamma^{45}_o}{\gamma^{45}_o}H^O_B$$

g_m Mean real gravity along the plumb line between Earth's surface and geoid. It can only be estimated by means of hypotheses about the (unknown) Earth's internal mass distribution and the (unknown) vertical gravity gradient. **Each different hypothesis produces a different type of orthometric height**.

Some examples of orthometric hypotheses:

Helmert:

$$g_m = g_{H/2} = \frac{1}{2}(g_p + g_0) = g_p + (3{,}086 - 0{,}83818\,\rho_p)10^{-6}\frac{H^O_p}{2}$$

First method of Ramsayer:

$$g_m = \frac{1}{2}(g_p + g_0) - (g_0 - g_0^{AP})\frac{\hat{H}^O}{H^O_p} \quad ; \quad \hat{H}^O = \frac{1}{n}\sum_{i=1}^{n} H^O_i$$

Ledersteger:

$$g_m = \frac{1}{n}\sum_{i=1}^{n}\left(g_i + 3{,}086\,x10^{-6}\,H^O_i\right) - \frac{1}{2}3{,}086\,x10^{-6}\frac{H^O_p}{2}$$

Units: g_p, g_m, $g_{H/2}$, $g_0 \rightarrow$ [m s^{-2}] ; $\rho_p \rightarrow$ [10^{-3} kg m^{-3}] ; $H^O \rightarrow$ [m]

From geopotential numbers to physical heights

Orhometric corrections in two Colombian levelling lines

Courtesy

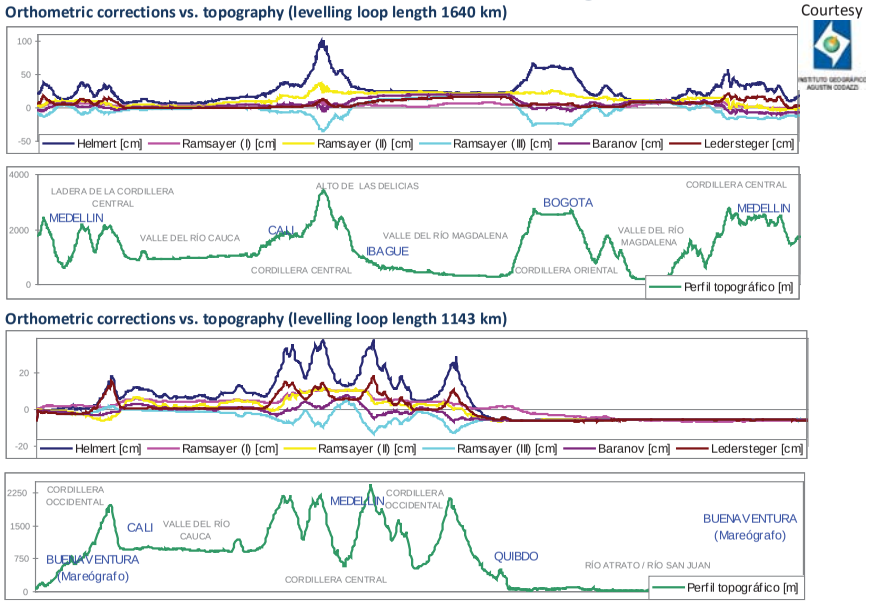

From geopotential numbers to physical heights

Comparison of normal (Molodenskii) and orhometric corrections

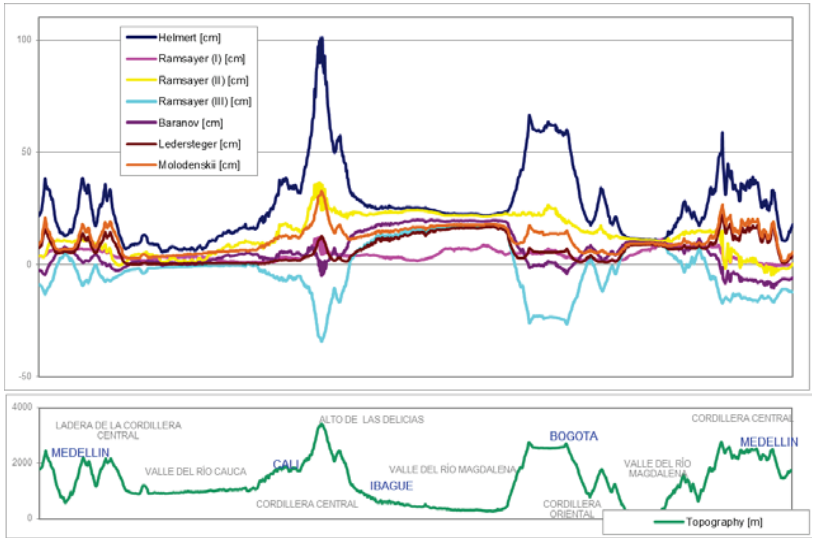

Physical heights summary

	Dynamic heights	Orthometric heights	Nomal heights
Definition of	γ^{φ}_o: constant normal gravity value at an arbitrary latitude φ (usually $\varphi = 45°$).	g_m: Mean real gravity value along the plumb line between the geoid and P.	γ_m: Mean normal gravity value along the normal plumb line between the ellipsoid and the telluroid (or between the quasi-geoid and P).
Description	Simple conversion to height units (scaled geopotential numbers) $H^{DYN} = \frac{C}{\gamma^{\varphi}_o}$	Distance, along the plumb line, between the surface point P and the geoid. $H^O = \frac{C}{g_m} \quad ; \quad g_m = \frac{1}{H^O}\int_0^{H^O} g\, dH^O$	Distance, along the normal plumb line, between the ellipsoid and the telluroid (or between the quasi-geoid and P) $H^N = \frac{C}{\gamma_m} \quad ; \quad \gamma_m = \frac{1}{H^N}\int_0^{H^N} \gamma\, dH^N$
Correction (for levelling)	Magnitude: < 20 m $\Delta H^{DYN}_{AB} = \Delta n_{AB} + k^{DYN}_{AB}$ $k^{DYN}_{AB} = \int_A^B \frac{g-\gamma^{45}_o}{\gamma^{45}_o}\delta n = \sum_A^B \frac{g-\gamma^{45}_o}{\gamma^{45}_o} dn$	Magnitude: mm ... dm $\Delta H^O_{AB} = \Delta n_{AB} + k^O_{AB}$ $k^O_{AB} = \int_A^B \frac{g-\gamma^{45}_o}{\gamma^{45}_o}\delta n + \frac{g^A_m-\gamma^{45}_o}{\gamma^{45}_o}H^O_A - \frac{g^B_m-\gamma^{45}_o}{\gamma^{45}_o}H^O_B$	Magnitude: mm ... dm $\Delta H^N_{AB} = \Delta n_{AB} + k^N_{AB}$ $k^N_{AB} = \int_A^B \frac{g-\gamma^{45}_o}{\gamma^{45}_o}\delta n + \frac{\gamma^A_m-\gamma^{45}_o}{\gamma^{45}_o}H^N_A - \frac{\gamma^B_m-\gamma^{45}_o}{\gamma^{45}_o}H^N_B$
Remarks	• No geometrical meaning • Points on the same level surface have the same height value • Hypotheses are not required	• Reference surface: the geoid $H^O = h - N$ h: ellipsoidal height, N: geoid undulation • Heights of points on the same level surface differ in the same manner as the g_m gravity values • Hypotheses about mass density and distribution as well as about the gravity vertical gradient $(\partial g/\partial H)$ are necessary. The value of H^O depends on the adopted hypotheses. • g_m cannot be estimated univocally, only approximately.	• Reference surface: the quasi-geoid (close to the geoid but not a level surface) $H^N = h - \zeta$ h: ellipsoidal height, ζ: height anomaly • Points on the same level surface and at the same latitude have the same normal heights. In other cases, heights differ in the same manner as γ_m varies with the latitude. • Hypotheses are not required • γ_m is estimable univocally.

Physical heights summary

Characteristics	Height type		
	Dynamic	Orthometric	Normal
Uniqueness Heights values shall be univocally determinable, i.e. they shall not depend on the levelling path.	☺	☺	☺
Zero-height surface with physical meaning and independent of the heights (i.e. the zero-height surface shall not change if heights change).	☹	☹	☹
Geometric meaning Heights shall represent the vertical distance between two points (one on the Earth's surface and one on the reference surface)	☹	☺	☺
Units of length Heights shall be given en units of length (or distance), i.e. in metres.	☺	☺	☺
The same height value on the same equipotential If water does not flow between two points, they shall have the same height value.	☺	☹	☹
Use of hypotheses The use of hypotheses shall be avoided. If hypotheses are improved, the height system must be changed totally.	☺	☹	☺
Connection with geometrical heights Physical heights shall be able to be combined with ellipsoidal heights.	☹	☺	☺
Small gravity corrections To be avoided in practical applications of local extension.	☹	☺	☺

4.3 Sea surface heights

Satellite altimetry, some glossary

Source: http://www.aviso.oceanobs.com

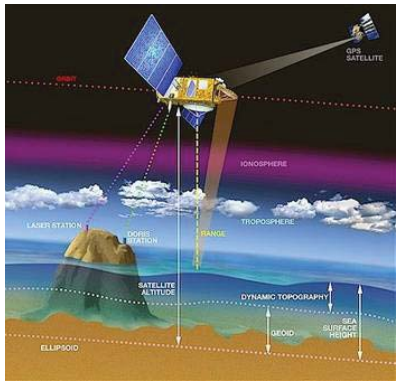

- **Sea surface height** (**SSH**): vertical distance of the sea surface whit respect to the ellipsoid (geometric height)

$$SSH = h_s - r_j$$
$$SSH = N + DT$$

- **Dynamic topography** (**DT**): difference between sea surface and geoid (physical height).

$$DT = h_s - r_j - N$$

It is mainly caused by
- tides
- currents
- winds, Earth rotation, seasons, temperature, salinity, etc.

It is determined using ocean (dynamic) models following the hydrostatic equilibrium laws.

- **Mean sea surface** (**MSS**) : long-term average of sea surface heights.

$$MSS = \frac{1}{y}\sum_{y} MSH$$

Sea surface heights

Satellite altimetry, some glossary

Source: http://www.aviso.oceanobs.com

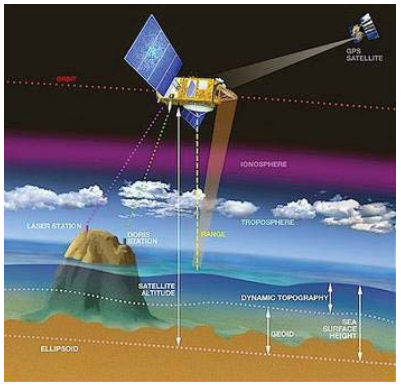

- DT is separated in **mean dynamic topography MDT** (mean over a time period, considered semi-stationary) and **dynamic ocean topography DOT** (time-variable part of DT)

$$DT = MDT + DOT$$

- The **MDT** is the oceanic relief (sea surface topography) corresponding to permanent ocean circulation. It is mainly caused by temperature variations in the ocean (thermal expansion) and permanent currents. It also called **Sea Surface Topography** (**SSTop**):

$$MDT = SSTop = MSS - N$$

- The **DOT** contains contributions from wind and other high frequency effects. Usually depicted as inter-annual, or other short-term, variations from the MDT. It is also called **Sea Level Anomalies (SLA)**.

Sea surface heights

DTU10 Mean Sea Surface Model

Source: http://www.space.dtu.dk/

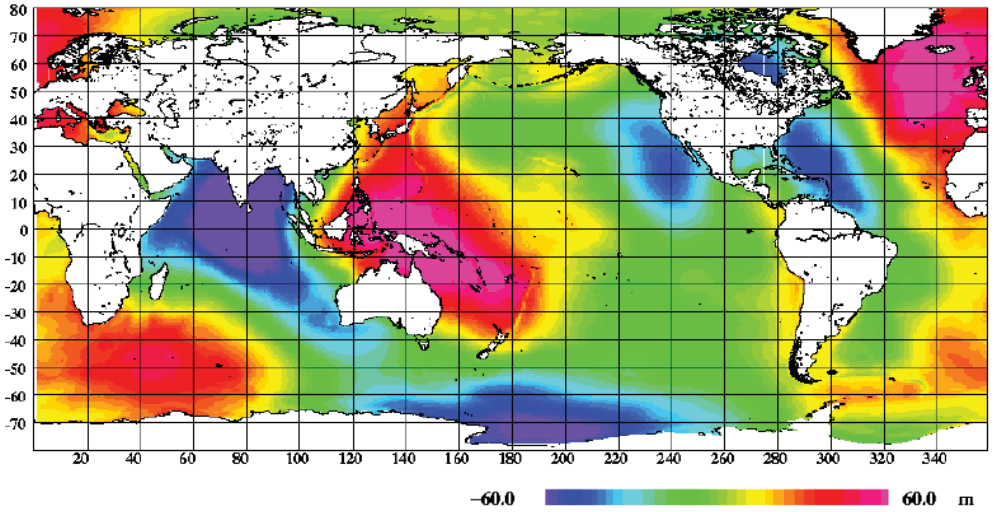

Sea surface heights

CNES/CLS2012 Mean dynamic topography

Source: http://www.aviso.oceanobs.com

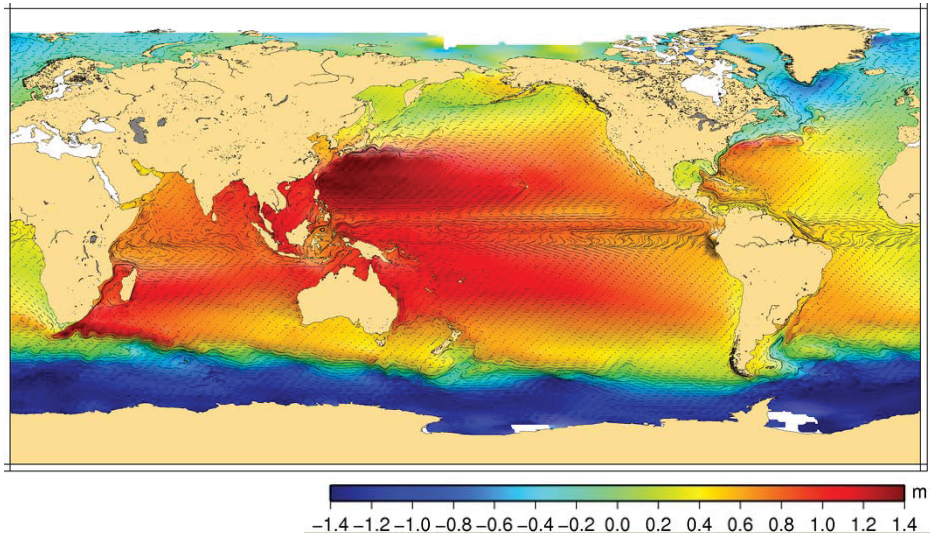

For a sea level anomalies example see movie at www.dgfi.badw.de

Sea surface heights

Sea surface height and mean dynamic topography at tide gauges

$$SSH = h_s = N + MDT = N + H_s$$
$$= h^{GPS} - DH^{lev} - D - R$$
$$MDT = H_s = SSH - N = h_s - N$$
$$= h^{GPS} - DH^{lev} - D - R - N$$

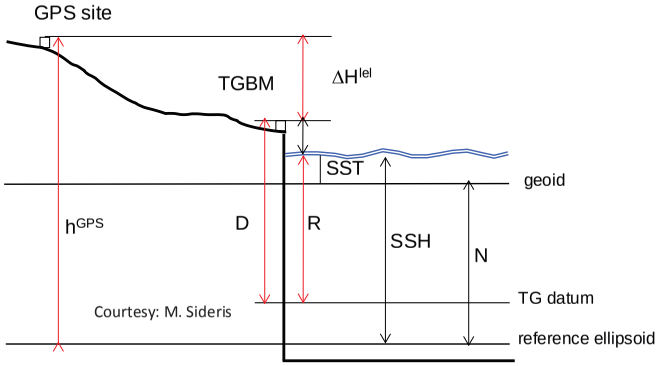

4.4 Physical references surfaces

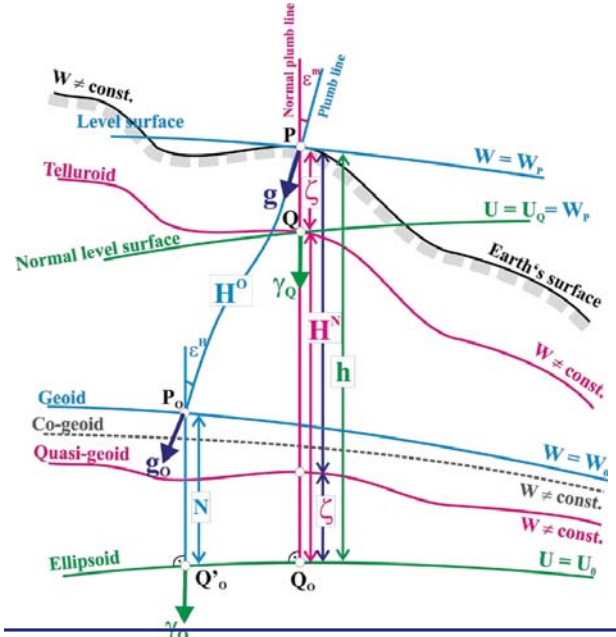

- For orthometric heights**: the geoid**.
- For normal heights: **the quasi-geoid**.

Physical references surfaces

The determination of W is, in general, a nonlinear problem and is further complicated by the fact that W itself is not harmonic

- Both limitations can be overcome by linearization and approximation of the **shape**, **size** and **gravity field of the Earth** by **those of an equipotential ellipsoid of revolution** (*reference ellipsoid*) with the same mass and same rotational velocity as the Earth
- Approximations:
$$W = U + T \quad ; \quad g = \gamma + \delta g \quad ; \quad H = h - N$$
- Since U and its functionals can be computed analytically for a given reference ellipsoid, the problem of estimating W now reduces to determine
$$T = W - U = (V + \Phi) - (u + \Phi) = V - u$$
- T is a harmonic function, i.e. $\nabla^2 T = 0$

Physical references surfaces

- Gravity disturbance:

$$\delta g = g_{P_0} - \gamma_{P_0}$$

- Gravity anomaly:

$$\Delta g = g_{P_0} - \gamma_{Q_0}$$

- The fundamental equation of physical geodesy:

$$\Delta g = \delta g + \frac{1}{\gamma}\frac{\partial \gamma}{\partial h}T = -\frac{\partial T}{\partial h} + \frac{1}{\gamma}\frac{\partial \gamma}{\partial h}T$$

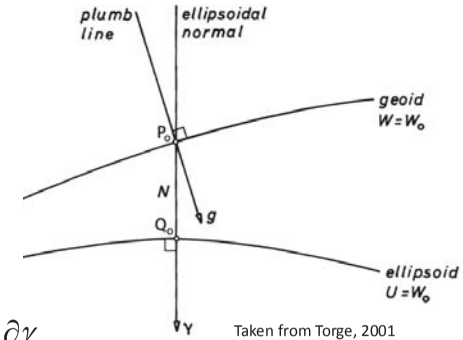

Taken from Torge, 2001

- Brun's equation:

$$N = \frac{T}{\gamma}$$

Physical references surfaces

Theory of Stokes (1849)

Definition: determine T, harmonic outside the geoid, from gravity anomalies on the geoid that satisfy the fundamental equation of physical geodesy.

Boundary surface: the geoid

Approximation surface: the ellipsoid

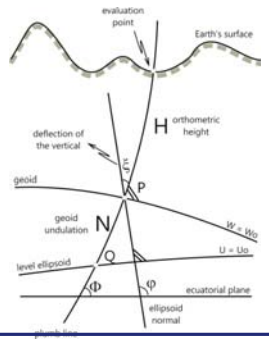

Theory of Molodenskii (1945)

Definition: determine T, harmonic outside the Earth surface, from gravity anomalies on the Earth surface that satisfy the fundamental equation of physical geodesy.

Boundary surface: Earth's surface

Approximation surface: the telluroid

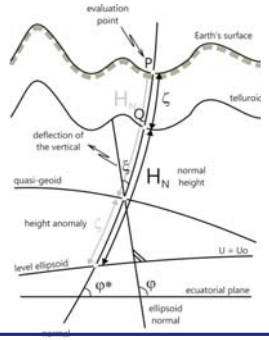

Physical references surfaces

Theory of Stokes (1849)

Gravity anomalies:

$$\Delta g = g_P - \gamma_Q = g_P + R_{FA} + R_B + \ldots$$

$\Rightarrow$ P: on the geoid

$\Rightarrow$ Q: on the ellipsoid

Hypotheses:
The geoid enclosed all masses, gravity reductions for vertical gradient and inhomogeneous mass density are required.

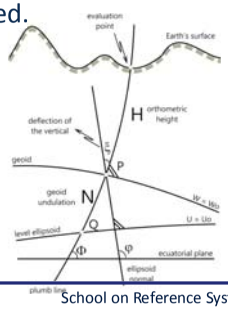

Theory of Molodenskii (1945)

Gravity anomalies:

$$\Delta g = g_P - \gamma_Q$$

$\Rightarrow$ P: on the Earth's surface

$\Rightarrow$ Q: on the telluroid

Hypotheses:
No hypotheses are required.

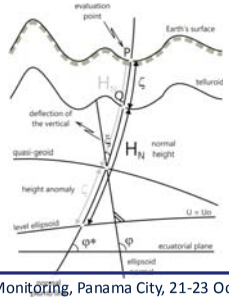

Physical references surfaces

Theory of Stokes (1849)

Disturbing potential:

$$T = \frac{1}{4\pi R}\iint_{Earth} S(\psi)\,\Delta g\, d\sigma$$

$$S(\psi) = \frac{1}{\sin(\psi/2)} - 6\sin\frac{\psi}{2} + 1 - 5\cos\psi - 3\cos\psi\ln\left(\sin\frac{\psi}{2} + \sin^2\frac{\psi}{2}\right)$$

The Stokes solution includes only the first term of the Molodenskii solution.

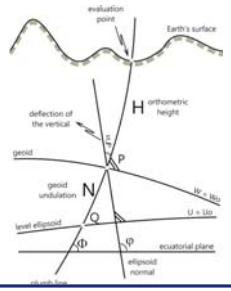

Theory of Molodenskii (1945)

Disturbing potential:

$$T = \sum_0^\infty T_k = \frac{1}{4\pi R}\iint_{Earth} S(\psi)(\Delta g + G_1 + G_2 + \ldots)d\sigma$$

$$S(\psi) = \frac{1}{\sin(\psi/2)} - 6\sin\frac{\psi}{2} + 1 - 5\cos\psi - 3\cos\psi\ln\left(\sin\frac{\psi}{2} + \sin^2\frac{\psi}{2}\right)$$

$$G_1 = \frac{R^2}{2\pi}\iint_\sigma \frac{h - h_p}{l_0^3}\left(\Delta g + \frac{3G}{2R}\zeta_0\right)d\sigma \approx \frac{R^2}{2\pi}\iint_\sigma \frac{h - h_p}{l_0^3}\Delta g\, d\sigma$$

$$l_0 = 2R\sin\frac{\psi}{2}$$

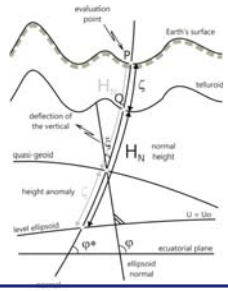

Geoid vs. Quasi-geoid

On ocean areas, geoid and quasi-geoid are the same, i.e. $H^O = H^N = 0$

On land areas, geoid and quasi-geoid differ by: $N - \zeta = \frac{\bar{g} - \bar{\gamma}}{\bar{\gamma}} H^O = H^N - H^O$

$\bar{g}$ mean real gravity value along the plumb line between Earth's surface and geoid.

$\bar{\gamma}$ mean normal gravity value along the normal plumb line between ellipsoid and telluroid (or between Earth's surface and quasi-geoid)

$\bar{g} - \bar{\gamma}$ corresponds, in a very good approximation, to the Bouguer anomaly.

This relationship allows the determination of the geoid from the quasi-geoid (or viceversa). Its hypotheses correspond to the Helmert theory for the determination of orthometric heights.

Geoid vs. Quasi-geoid

Differences between geoid undulations and height anomalies in Colombia.

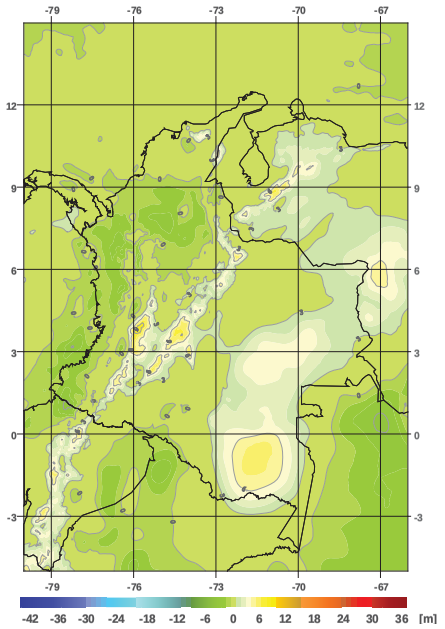

Courtesy

(Sánchez 2003)

http://www.igac.gov.co/

(Quasi-)Geoid computation in practice

The determination of the anomalous potential $T = \sum_0^\infty T_k = \frac{1}{4\pi R} \iint_{Earth} S(\psi)(\Delta g + G_1 + G_2 + \ldots) d\sigma$ at any point requires gravity anomalies all over the Earth.

- The long wavelength contribution N_G is provided by a set of spherical harmonic coefficients (geopotential or global gravity model);
- The middle wavelength contribution N_L is estimated from the local anomalies (terrestrial, marine or aerial gravity in the area of study)
- The short wavelength contribution N_T is computed by using a digital terrain model (topographic heights)

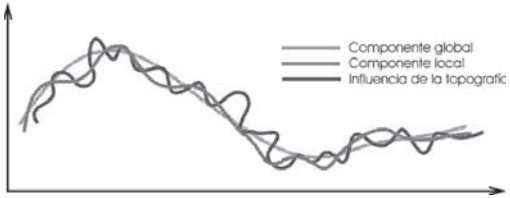

The (quasi-)geoid undulation is given by $N = N_G + N_L + N_T$

Since the gravity anomalies derived from the local terrestrial gravity data contain the contribution of the global gravity model and of the topography, it is necessary to **remove** these two contributions from the local anomalies: $\Delta g = \Delta g_L - \Delta g_G - \Delta g_T$. They are **restored** again, when the (quasi-)geoid undulations are computed.

Courtesy

long wavelength N_G | middle wavelength N_L | short wavelength N_T

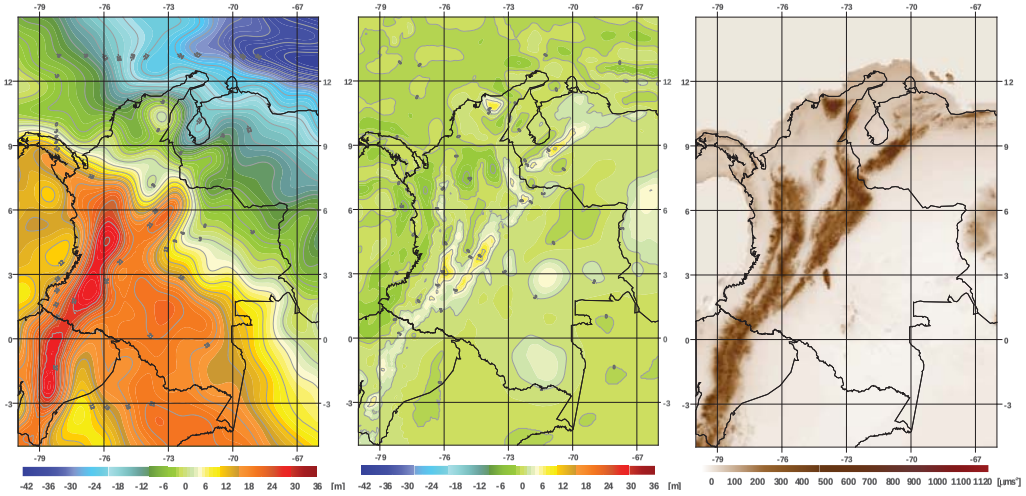

(Sánchez 2003)

http://www.igac.gov.co/

(Quasi-)Geoid computation in practice

Spherical harmonics and the gravity field

$$W_a(r,\lambda,\varphi) = \frac{GM}{R}\sum_{\ell=0}^{\ell_{\max}}\sum_{m=0}^{\ell}\left(\frac{R}{r}\right)^{\ell+1} P_{\ell m}(\sin\varphi)\left(C^W_{\ell m}\cos m\lambda + S^W_{\ell m}\sin m\lambda\right)$$

r, λ, φ	-	spherical geocentric coordinates of computation point (radius, latitude, longitude)
R	-	reference radius
GM	-	product of gravitational constant and mass of the Earth
ℓ, m	-	degree, order of spherical harmonic
$P_{\ell m}$	-	fully normalised Lengendre functions
$C^W_{\ell m}, S^W_{\ell m}$	-	Stokes' coefficients (fully normalised)

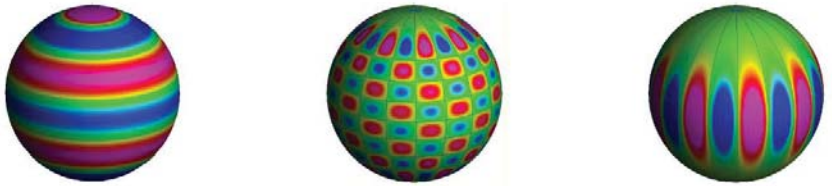

zonal: $\ell = 6,\ m = 0$ tesseral: $\ell = 16,\ m = 9$ sectorial: $\ell = 9,\ m = 9$

Figure 4: Examples for spherical harmonics $P_{\ell m}(\sin\varphi)\cdot\cos m\lambda$ [from −1 (blue) to +1 (violet)]

Taken from GFZ Report 09/02.

(Quasi-)Geoid computation in practice

Spherical harmonic and the gravity field

International Centre for Global Earth Models (ICGEM)
http://icgem.gfz-potsdam.de/ICGEM/

EGM96 coefficients

key	L	M	C	S	sigma C	sigma S
end_of_head			==========	==========	==========	==========
gfc	0	0	1.000000000000E+00	0.000000000000E+00	0.00000000E+00	0.00000000E+00
gfc	2	0	-0.484165371736E-03	0.000000000000E+00	0.35610635E-10	0.00000000E+00
gfc	2	1	-0.186987635955E-09	0.119528012031E-08	0.10000000E-29	0.10000000E-29
gfc	2	2	0.243914352398E-05	-0.140016683654E-05	0.53739154E-10	0.54353269E-10
gfc	3	0	0.957254173792E-06	0.000000000000E+00	0.18094237E-10	0.00000000E+00
gfc	3	1	0.202998882184E-05	0.248513158716E-06	0.13965165E-09	0.13645882E-09
gfc	3	2	0.904627768605E-06	-0.619025944205E-06	0.10962329E-09	0.11182866E-09
gfc	3	3	0.721072657057E-06	0.141435626958E-05	0.95156281E-10	0.93285090E-10

EGM2008 coefficients

key	L	M	C	S	sigma C	sigma S
end_of_head			==========	==========	==========	==========
gfc	0	0	1.0d0	0.0d0	0.0d0	0.0d0
gfc	2	0	-0.484165143790815D-03	0.000000000000000D+00	0.7481239490D-11	0.0000000000D+00
gfc	2	1	-0.206615509074176D-09	0.138441389137979D-08	0.7063781502D-11	0.7348347201D-11
gfc	2	2	0.243938357328313D-05	-0.140027370385934D-05	0.7230231722D-11	0.7425816951D-11
gfc	3	0	0.957161207093473D-06	0.000000000000000D+00	0.5731430751D-11	0.0000000000D+00
gfc	3	1	0.203046201047864D-05	0.248200415856872D-06	0.5726633183D-11	0.5976692146D-11
gfc	3	2	0.904787894809528D-06	-0.619005475177618D-06	0.6374776928D-11	0.6401837794D-11
gfc	3	3	0.721321757121568D-06	0.141434926192941D-05	0.6029131793D-11	0.6028311182D-11

(Quasi-)Geoid computation in practice

Spherical harmonics and the gravity field

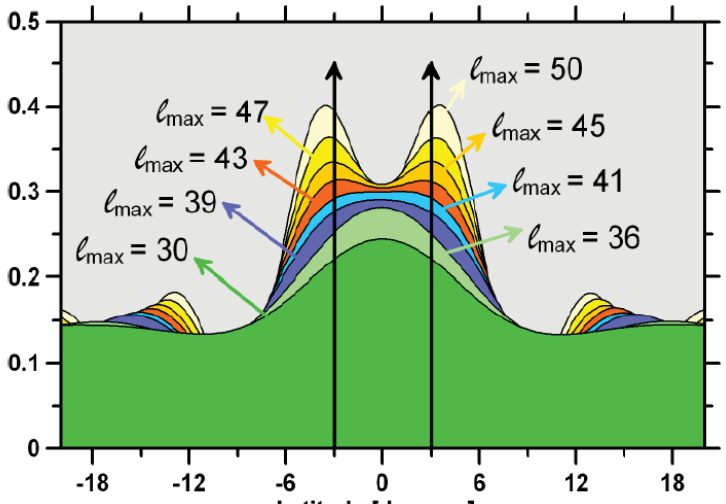

Figure 5: Cross-sections through 2 peaks, which are originally 6° apart, after approximation by spherical harmonics of different maximum degrees ℓ_{max}

Taken from GFZ Report 09/02.

(Quasi-)Geoid computation in practice

Spherical harmonic and the gravity field

Table 1: Examples of spatial resolution of spherical harmonics in terms of the diameter ψ_{min} of the smallest representable shape (bump or hollow) after eqs. (112) and (114)

Maximum Degree	Number of Coefficients	Resolution ψ_{min} eq. (112)		eq. (114)	
ℓ_{max}	N	[degree]	[km]	[degree]	[km]
2	9	90.0	10000.000	77.885	8653.876
5	36	36.0	4000.000	38.376	4264.030
10	121	18.0	2000.000	20.864	2318.182
15	256	12.0	1333.333	14.333	1592.587
30	961	6.0	666.667	7.394	821.587
36	1369	5.0	555.556	6.195	688.321
40	1681	4.5	500.000	5.590	621.154
45	2116	4.0	444.444	4.983	553.626
50	2601	3.6	400.000	4.494	499.342
75	5776	2.4	266.667	3.016	335.073
180	32761	1.0	111.111	1.266	140.690
360	130321	0.5	55.556	0.635	70.540

⇨ Orbit analysis

⇨ Gravity field satellite missions

⇨ Terrestrial and marine gravity anomalies of high-frequency, topography

$$\psi_{min}(\ell_{max}) \approx \frac{\pi R}{\ell_{max}} \quad (112) \qquad \psi_{min}(\ell_{max}) = 4\arcsin\left(\frac{1}{\ell_{max}+1}\right) \quad (114)$$

Taken from GFZ Report 09/02.

(Quasi-)Geoid computation in practice

Orbit analysis

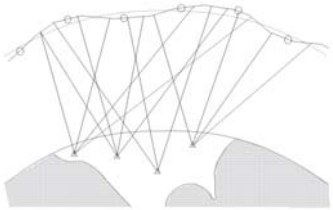

Measurements:

Distances, differences of distance, and directions to satellites (Satellite Laser Ranging - SLR)

Principle:

Comparison of the **non-perturbed orbit** (normal o Keppler orbit) with the **real orbit** described by the satellites. Discrepancies are caused by gravitational effects of anomalous masses (non-homogeneous distribution).

Method:

The variation of the orbit (Keplerian) elements are represented as a function of the anomalous potential. After invertion, this potential is estimated:

$$\frac{de}{dt}=\frac{1-e^2}{na^2e}\frac{\partial R}{\partial M}-\frac{\sqrt{1-e^2}}{na^2e}\frac{\partial T}{\partial \omega}$$

$$\frac{d\omega}{dt}=-\frac{\cos i}{na^2\sqrt{1-e^2}\sin i}\frac{\partial T}{\partial i}+\frac{\sqrt{1-e^2}}{na^2e}\frac{\partial T}{\partial e}$$

$$\frac{di}{dt}=\frac{\cos i}{na^2\sqrt{1-e^2}\sin i}\frac{\partial T}{\partial \omega}-\frac{1}{na^2\sqrt{1-e^2}\sin i}\frac{\partial T}{\partial \Omega}$$

$$\frac{d\Omega}{dt}=\frac{1}{na^2\sqrt{1-e^2}\sin i}\frac{\partial T}{\partial i}$$

$$\frac{da}{dt}=\frac{2}{na}\frac{\partial T}{\partial M}$$

$$\frac{dM}{dt}=n-\frac{1-e^2}{na^2e}\frac{\partial R}{\partial e}-\frac{2}{na}\frac{\partial T}{\partial a}$$

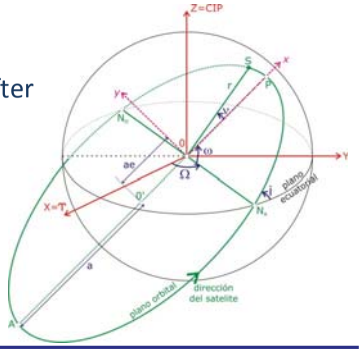

(Quasi-)Geoid computation in practice

Challenging Mini-Satellite Payload for Geophysical Research and Application (CHAMP)

Principle:

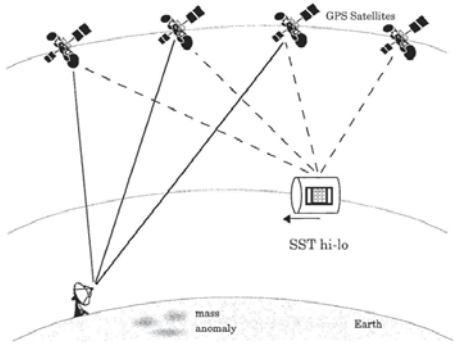

Satellite to satellite tracking: gravity field modelling from variations of the distance between two satellites (CHAMP – GPS).

Design:

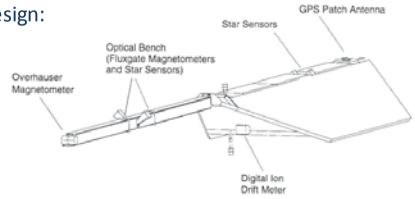

http://www.gfz-potsdam.de/pb1/op/champ/

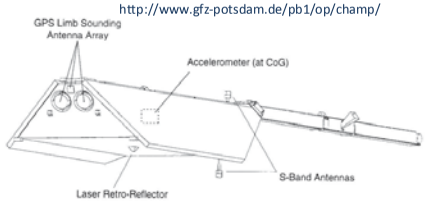

- Modelling of the quasi-stationary and time-dependent components of the gravity field.
- Resolution:
  - 400 km quasi-stationary component
  - 4000 km monthly variations.

(Quasi-)Geoid computation in practice

Gravity Recovery and Climate Experiment (GRACE)

Principle:

Satellite to satellite tracking: distance between two twin satellites (GRACE) and between them and GPS satellites.

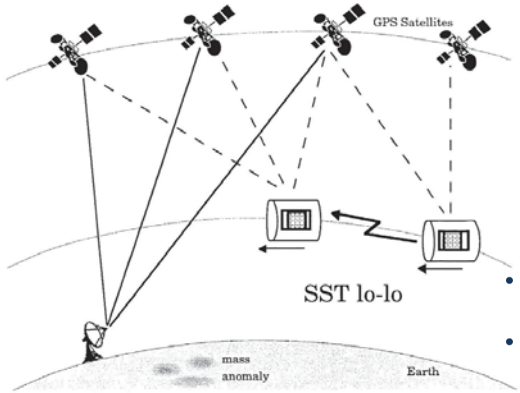

http://www.gfz-potsdam.de/pb1/op/grace/index_GRACE.html

- Modelling of the quasi-stationary and time-dependent components of the gravity field.
- Resolution:
  - 170 km quasi-stationary component
  - 300 km monthly variations.

(Quasi-)Geoid computation in practice

Gravity Field and Steady-State Ocean Circulation Explorer (GOCE)

Principle:

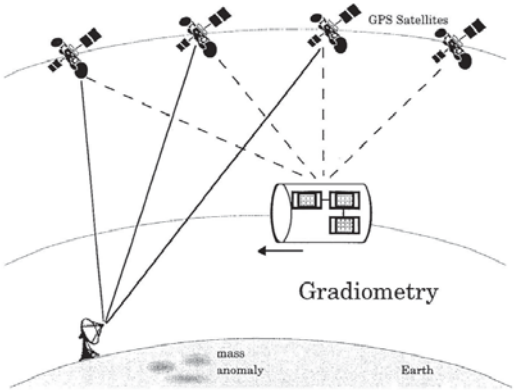

- Modelling of the quasi-stationary gravity field
- Resolution: ~100 km

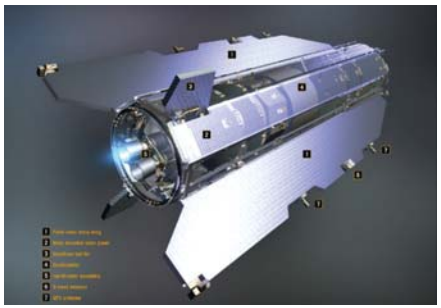

http://www.goce-projektbuero.de/

Satellite gravity gradiometry: measurement of the second derivative of the gravity field (gravitational gradient).

$$V_{ij}=\begin{vmatrix} V_{xx} & V_{xy} & V_{xz} \\ V_{yx} & V_{yy} & V_{yz} \\ V_{zx} & V_{zy} & V_{zz} \end{vmatrix}$$

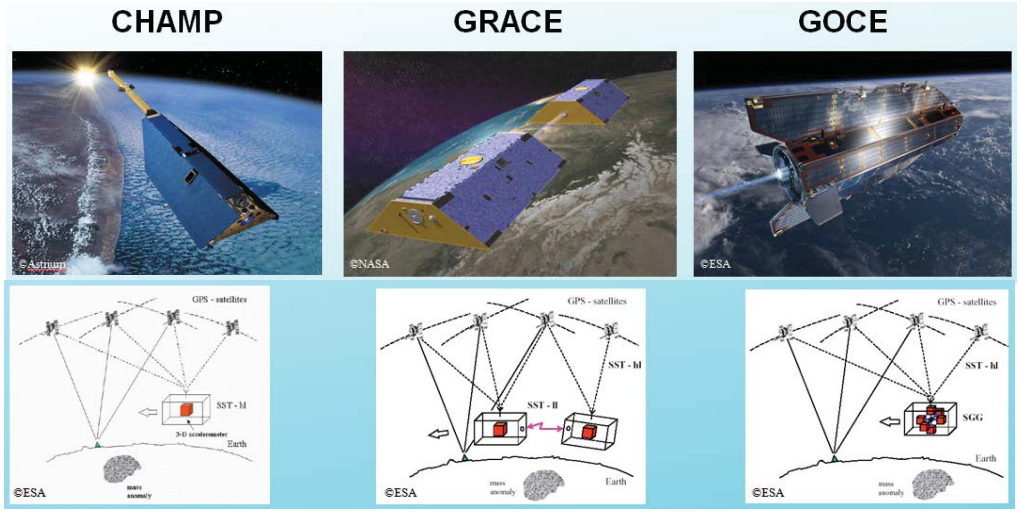

GPS receiver
Accelerometer
Star sensors
15.07.2000 – 19.09.2010
Height: 454 km -> 300 km
Inclination: 87°

GPS receiver
Accelerometer
Star sensors
Distances by microwaves
17.03.2002 - …
Height : 485 km -> 300 km
Inclination: 89°

GPS receiver
Gradiometer
Star sensors
17.03.2009-~27.10.2013
Height : 259 km -> 224 km
Inclination: 96,5°

(Quasi-)Geoid computation in practice

Optimal combination: example model EIGEN6C2 (Förste et al. 2012)

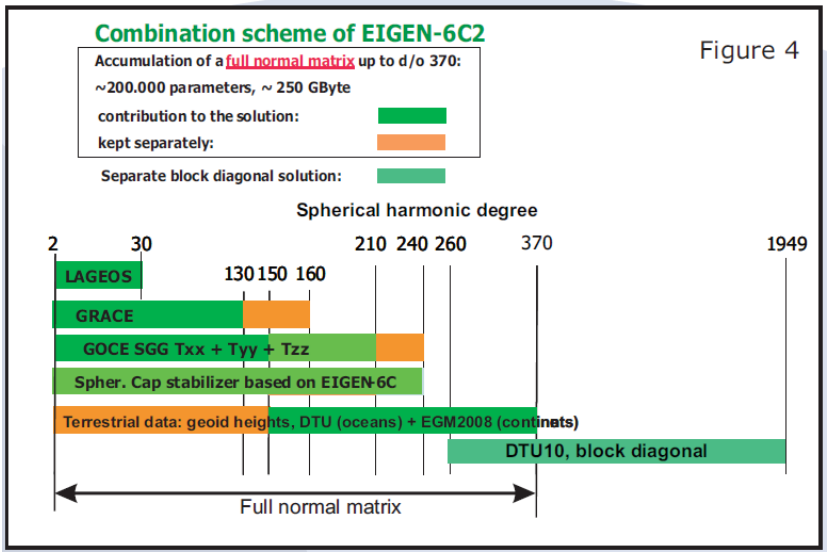

(Quasi-)Geoid computation in practice

Spherical harmonics and the gravity field

Omission error: caused by neglecting degrees larger than l_{max}

Courtesy Ågren 2004)

	Geoid height [m]			Gravity anomaly [mGal]		
l	Tsch/Rapp	Kaula	Jek/Mor	Tsch/Rapp	Kaula	Jek/Mor
180	0.476	0.356	0.667	29.7	40.8	29.7
360	0.228	0.178	0.251	25.3	39.1	18.7
720	0.103	0.089	0.053	20.1	37.4	7.0
1800	0.030	0.035	0.001	12.7	34.9	0.3
3600	0.010	0.018	0.000	7.1	32.9	0.0
10800	0.001	0.006	0.000	1.2	29.6	0.0
21600	0.000	0.003	0.000	0.1	27.2	0.0

The gravity satellite missions provide global gravity models with a resolution of **degree, order 200**. This correspond to a **spatial resolution of about 100 km** and the **omission error** in the derived geoids can reach **up to 50 cm**! The combination of this models with **terrestrial data is absolutely necessary**!

(Quasi-)Geoid computation in practice

Uncertainties in the geoid EGM2008

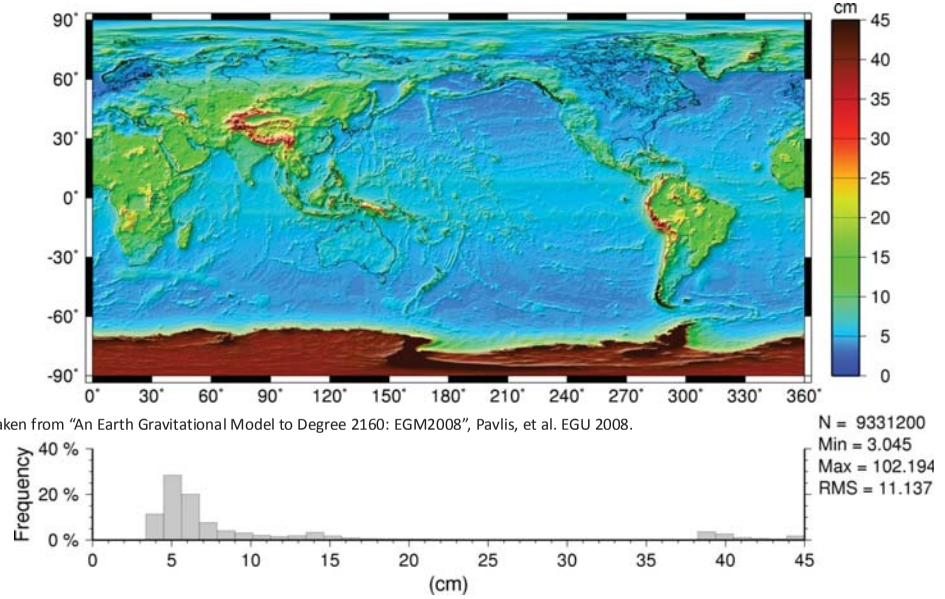

Taken from "An Earth Gravitational Model to Degree 2160: EGM2008", Pavlis, et al. EGU 2008.

(Quasi-)Geoid computation in practice

Uncertainties in the geoid EGM2008

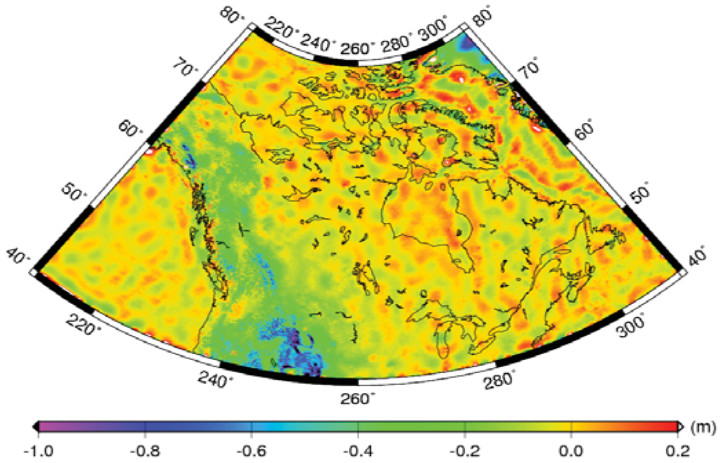

"Differences between the GOCE combined model (TW01 up to degree 210 and terrestrial data) and EGM2008 up to degree 2190" (Cortesy M. Sideris 2011)

(Quasi-)Geoid computation in practice

Other global gravity models

International Centre for Global Earth Models (ICGEM)
http://icgem.gfz-potsdam.de/ICGEM/

Model	Year	Degree	Data	Reference
TUMGOCE02S	2013	230	S(Goce)	Yi et al, 2013
GOGRA02S	2013	230	S(Goce,Grace)	Yi et al, 2013
ULux_CHAMP2013s	2013	120	S(Champ)	Weigelt et al, 2013
ITG-Goce02	2013	240	S(Goce)	Schall et al, 2013
GO_CONS_GCF_2_TIM_R4	2013	250	S(Goce)	Pail et al, 2011
GO_CONS_GCF_2_DIR_R4	2013	260	S(Goce,Grace,Lageos)	Bruinsma et al, 2013
EIGEN-6C2	2012	1949	S(Goce,Grace,Lageos),G,A	Förste et al, 2012
DGM-1S	2012	250	S(Goce,Grace)	Hashemi Farahani, et al. 2012
GOCO03S	2012	250	S(Goce,Grace,...)	Mayer-Gürr, et al. 2012
GO_CONS_GCF_2_DIR_R3	2011	240	S(Goce,Grace,Lageos)	Bruinsma et al, 2010
GO_CONS_GCF_2_TIM_R3	2011	250	S(Goce)	Pail et al, 2011
GIF48	2011	360	S(Grace),G,A	Ries te al, 2011
EIGEN-6C	2011	1420	S(Goce,Grace,Lageos),G,A	Förste et al, 2011
EIGEN-6S	2011	240	S(Goce,Grace,Lageos)	Förste et al, 2011
GOCO02S	2011	250	S(Goce,Grace,...)	Goiginger et al, 2011
AIUB-GRACE03S	2011	160	S(Grace)	Jäggi et al, 2011
GO_CONS_GCF_2_DIR_R2	2011	240	S(Goce)	Bruinsma et al, 2010
GO_CONS_GCF_2_TIM_R2	2011	250	S(Goce)	Pail et al, 2011
GO_CONS_GCF_2_SPW_R2	2011	240	S(Goce)	Migliaccio et al, 2011
GO_CONS_GCF_2_DIR_R1	2010	240	S(Goce)	Bruinsma et al, 2010
GO_CONS_GCF_2_TIM_R1	2010	224	S(Goce)	Pail et al, 2010a

4.5 Heights in the time-dependent Earth's surface and gravity field

The geometry and gravity field of the Earth are under the influence of

Secular effects: like plate tectonics, global isostatic adjustment, polar wandering, subsidence, erosion;

Seasonal effects: like astronomic tides, solid/ocean/atmospheric tides, ocean/atmospheric/hydrologic loading, variation in the longitude of the day, polar motion, mass transports, etc.

Sporadic effects: like earthquakes, landslides, volcano eruptions, etc.

Heights in the time-dependent Earth's surface and gravity field

In general, **plate tectonic movements** are represented by means of **constant station velocities**, and **well-known effects** with magnitudes larger than the precision of the measurements **are usually reduced by using precise models**:

- **Solid Earth tides**: deformation of the solid Earth caused by the gravitational attraction of Sun, Moon, and other celestial bodies;
- **Ocean loading**: elastic response of the Earth's crust to ocean tides;
- **Atmospheric pressure loading**: elastic response of the Earth's crust to the changing atmospheric pressure. Two causes are distinguish: **tidal** (due to the gravitational attraction of Sun and Moon) and **non-tidal** (due to temperature changes, weather conditions, relief, etc.).
- **Rotational deformation** due to polar motion and variations in the angular velocity (longitude of the day) in solid Earth (pole tide) and in ocean areas (ocean pole tide).

Heights in the time-dependent Earth's surface and gravity field

Effect	Geometry on land	Geometry on sea	Terrestrial gravity	Geo-potential numbers	Geoid (extension/ geoid height)
Ocean tides		< 16 m			50 ... 5000 km / 100 ... 150 mm conventional tide free/tide free/zero tide
Earth tides	Conventional tide free	mean tide	mean tide/tide free/zero tide	mean tide/tide free/ zero tide	
Permanent comp.	-0,28 m at pole, +0,14 m at equator (hydrostatic equilibrium, Melchior 1996) -0,12 m at pole, +0,06 m at equator (anelastic response, IERS 2010)		+0,61 mms^{-2} pole -0,30 mms^{-2} equator	Equipotential surfaces move as the geoid, but simultaneously	-0,19 m pole, +0,10 m equator
Periodic comp. (anelastic)	-0,18 m (Moon), -0,08 (Sun) at pole +0,36 m (Moon), +0,16 m (Sun) at equator		-1,1 mms^{-2} ... +0,5 mms^{-2} (Moon) -0,5 mms^{-2} ... +0,3mms^{-2} (Sun)	±0,056 mm/lev km (Moon) ±0,026 mm/lev km (Sun)	As undisturbed sea level - 0,26 m at pole, +0,52 cm at equator
Pole tide (hydrostatic)	±0,0270 m (vert), ±0,0070 m (hz)		> +82 nms^{-2} (Lat = 45°)	±3 cm in 430 days	±0,0270 m
Ocean pole tide (hydrostatic)	±0,0018 m (vert), ±0,0005 m (hz)		?		±0,0018 m
LOD variations (hydrostatic)			0,7 nms^{-2} ... 7 nms^{-2}		
Ocean		Dynamic atmospheric correction: *inverse barometer + barotropic effects* cm ... dm			100 ... 1000 km / 10 mm
tidal loading	+0,10 m		±0,01 mms^{-2} ... ±0,2 mms^{-2}		?
non-tidal loading	?				?
Atmosphere			-3 ... -4 nms^{-2}/hPa ±0,15 mms^{-2} (abs) ±0,03 mms^{-2} (rel)		20 ... 2000 km / 15 mm
tidal loading	±0,0015 m		> 0,003 mms^{-2}		?
non-tidal loading	?		?		?
Hydrology (ground water, snow, ice)			50 nms^{-2} ... 100 nms^{-2}		10 ... 8000 km / 10 ... 12 mm
tidal loading	±0,050 m		?		?
non-tidal loading	?		?		?

Treatment of the permanent tide in heights

In general, the time-depending tidal effects caused by Sun and Moon are reduced from geodetic observations. The treatment of the permanent deformation defines the so called **tide systems**, there are **two concepts for Earth's geometry** (surface, crust or topography) and **three concepts for the Earth's gravity field** (gravity, geoid, physical heights).

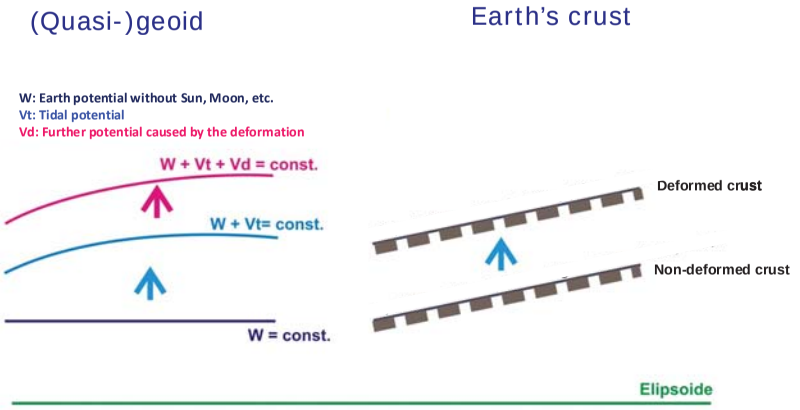

Treatment of the permanent tide in heights

Non-tidal or tide-free system

- The permanent deformation is eliminated from the shape of the Earth.
- From the potential field quantities (gravity, geoid etc) both the tide-generating potential, and the deformation potential of the Earth (the indirect effect) are eliminated.
- This corresponds to physically removing the Sun and the Moon to infinity.
- Typically the permanent deformation is treated using the same Love numbers h and k (and Shida number ℓ) as for the time-dependent tidal effects, not estimates for secular (fluid) Love numbers.
- I.e., conventional tide-free system

EUREF 2008, Brussels,June 17-21, 2008 Jaakko.Makinen@fgi.fi 4

Treatment of the permanent tide in heights

The mean tidal system

- The permanent effect is not removed from the shape of the Earth; the shape therefore corresponds to the long-time average under tidal forcing.
- The potential field retains the potential of this average Earth, and also the time-average of the tide-generating potential (though it is not due to the masses of the Earth).
- Mean-tide potential field describes how water flows and clocks run (general relativity)
- Complications or additional corrections needed in boundary value problems, as the tide-generating masses are outside the Earth

EUREF 2008, Brussels,June 17-21, 2008 Jaakko.Makinen@fgi.fi 5

The zero tidal system

- For the potential field quantities
- A "middle alternative"
- Eliminates the tide-generating potential but retains its indirect effect, i.e., the potential of the permanent deformation of the Earth. Thus its "partner" is the mean system for 3-D shape
- because of this, it is often said that for the 3-D we have zero ≡ mean.
- In this alternative, the gravity field is generated only by the masses of the Earth (plus the centrifugal force).

Schematic representation (I)

Dashed line: crust (topography; 3-D)
mean≡zero crust
conventional tide-free crust at $-hW_2/g$, $h\approx0.6$
fluid tide-free crust at $-hW_2/g$, $h\approx1.93$

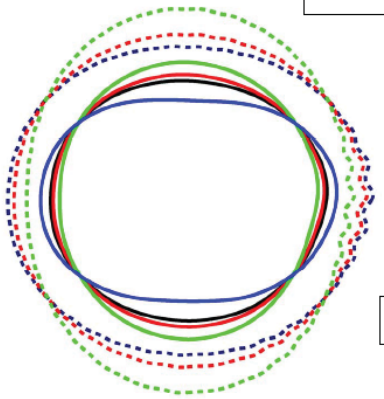

Solid line: geoid
mean at $+W_2/g$
zero
conventional tide-free geoid at $-kW_2/g$, $k\approx0.3$
fluid tide-free geoid at $-kW_2/g$, $k\approx0.93$

$$W_2/g \approx -0.296 \sin^2(\phi)+0.099 \text{ [m]}$$

Schematic representation (II)

Various crusts (topography) above various geoids, using
mean (≡zero) crust above zero geoid as reference:

Geoid \ Crust	Mean	Tide-free
Mean	$-W_2/g$	$(-h+k)W_2/g$
Zero	0	$-hW_2/g$
Tide-free	kW_2/g	$(-h+1)W_2/g$

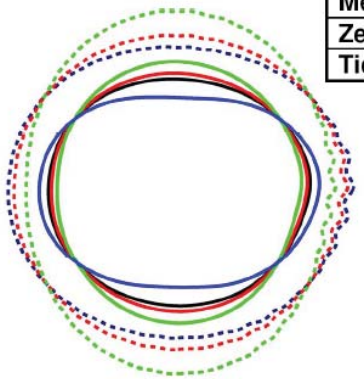

See e.g., Ekman (1989)

$$W_2/g \approx -0.296 \sin^2(\phi)+0.099 \text{ [m]}$$

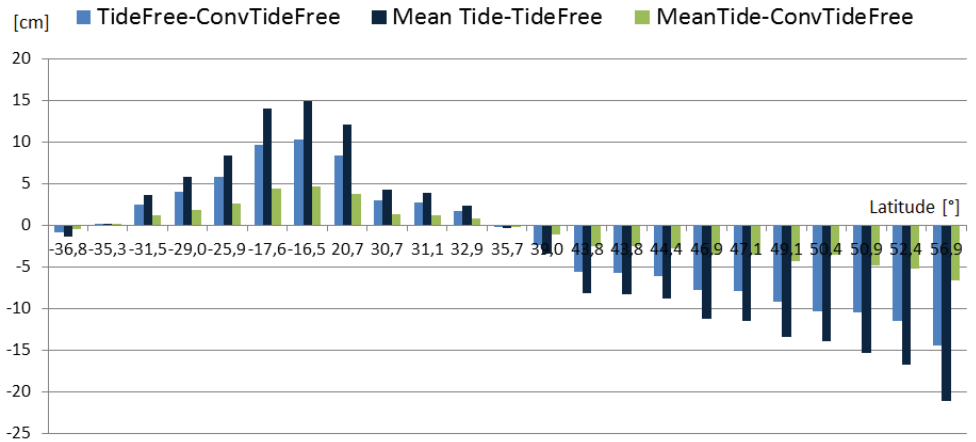

The current resolution (1983) of the **International Association of Geodesy** requires the **zero tide system** for gravity field and related quantities and **zero(=mean) tide system** for geometry (ITRF).

Treatment of the permanent tide in heights

Ellipsoidal heights from conventional tide-free system to zero tide system in [m]:

$$\Delta h_T = 0{,}0602 - 0{,}1790\sin^2\varphi - 0{,}0018\sin^4\varphi$$

Conversion of (quasi-)geoid heights between different tide systems in [m]:

$$N_{mt} - N_{nt} = \delta_t \bar{N} = -0.099(1+k_2)(3\sin^2\theta - 1)$$
$$N_{mt} - N_{zt} = -0.099(3\sin^2\theta - 1)$$
$$N_{zt} - N_{nt} = -0.099k_2(3\sin^2\theta - 1)$$

Treatment of the permanent tide in heights

Conversion of levelling heights between different tide systems in [m]:

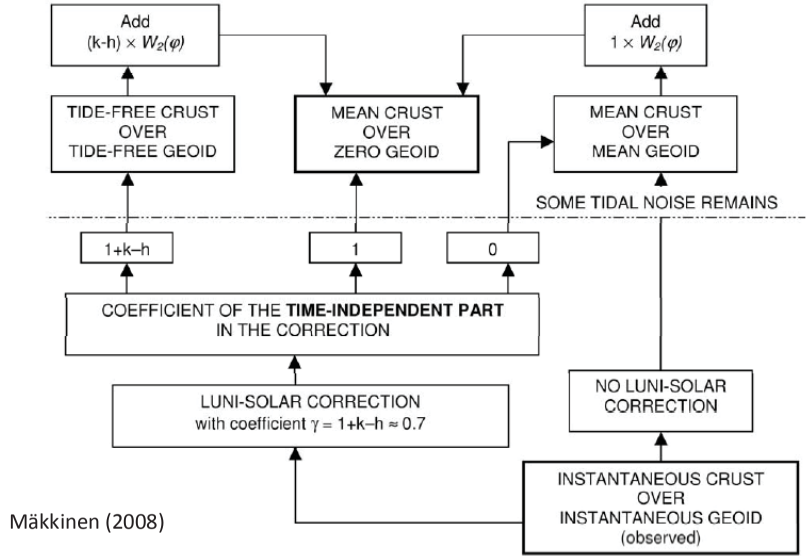

Mäkkinen (2008)

Heights in the time-dependent Earth's surface and gravity field: summary

Direct and indirect permanent tide effects remain the most important issue:

- **Ellipsoidal heights** referred to the IERS/ITRF are in the **conventional tide free system** (nominal Love numbers, anelastic response to semidiurnal frequencies);
- **Sea surface heights** are in **mean tide system** and mean geoids are needed for the computation of DT;
- **Geopotential numbers are in general in mean tide system**. If tide effects are reduced, they can be in tide free (fluid Love numbers) or zero tide (indirect effect restored);
- **Terrestrial gravity** is give in:
  - Mean tide system for IGSN71 values until 1979
  - Tide free system between 1979 and ~ 1988 (International Absolute Gravity Base-station Network - IAGBN)
  - Zero tide system since 1988

Heights in the time-dependent Earth's surface and gravity field: summary

- **Tide system in geoid determination is dominated by the C_{20} coefficient**, i.e. the global gravity model used for the long wavelengths.
- **Transformation between (conventional) tide free system and zero tide system is not homogeneous**:

k_{20} = 0,29 IERS89
k_{20} = 0,30 IERS1992
k_{20} = 0,29525 IERS1992
k_{20} = 0,30190 IERS2003/IERS2010
k_{20} = 0,30 global gravity models

k_s = 0,94 (Lambeck 1980)
k_s = 0,933 (Mathews 1999)

4.6 Classical height systems

Reference surface:
Definition: the geoid
Realisation: mean sea level measured at a tide gauge and averaged over different time periods (ideally 18,6 years).

Vertical coordinate:
Definition: orthometric heights
Realisation: levelling + orthometric correction

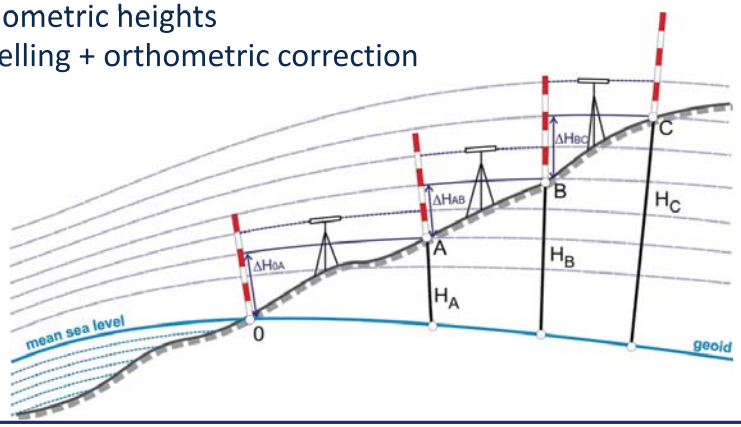

Drawbacks of the classical height systems

Problem 1: the mean sea surface is not an equipotential surface and does not coincide with the geoid.
The dynamic topography varies about ±2m globally.

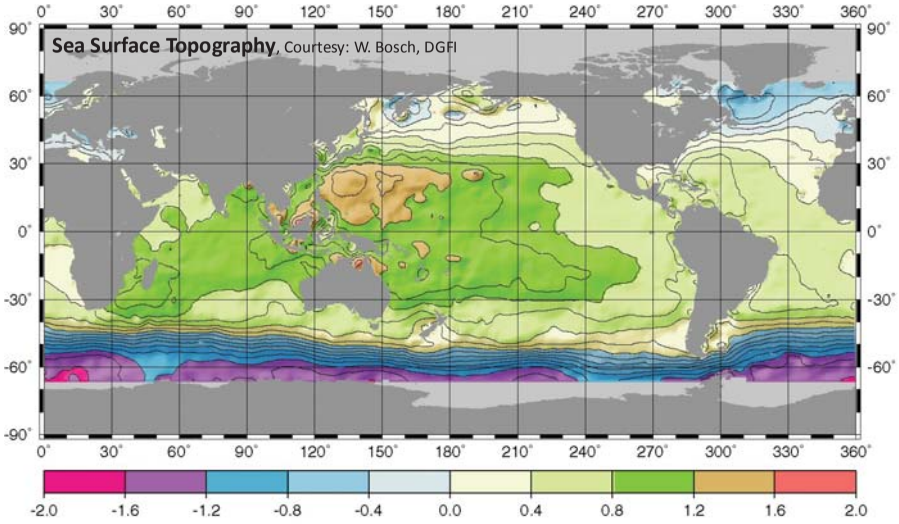

Drawbacks of the classical height systems

Problem 2: sea level changes are not homogeneous globally; tide gauges register different sea level variations depending on the geographical location.

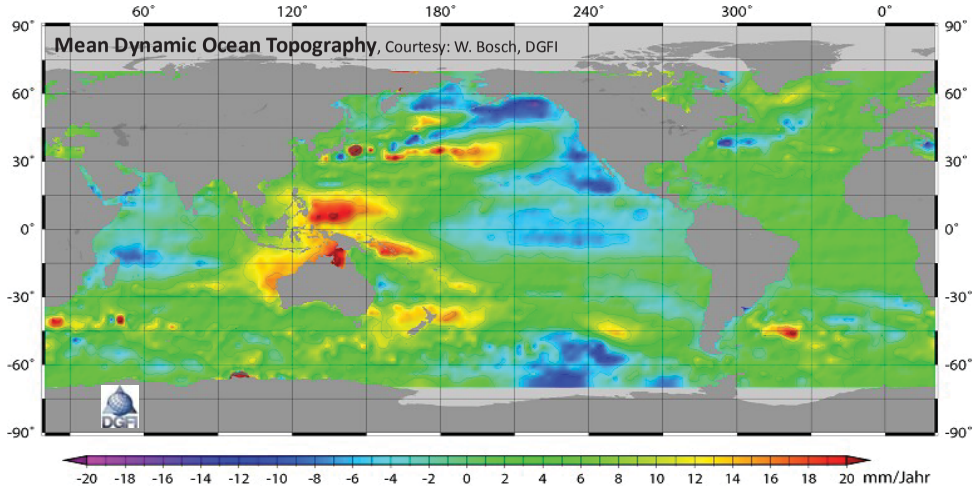

Drawbacks of the classical height systems

Problem 3: secular sea level changes are not taken into account. The reference level depends on the time covered for averaging.

Tide gauge in Mar del Plata (Argentina):

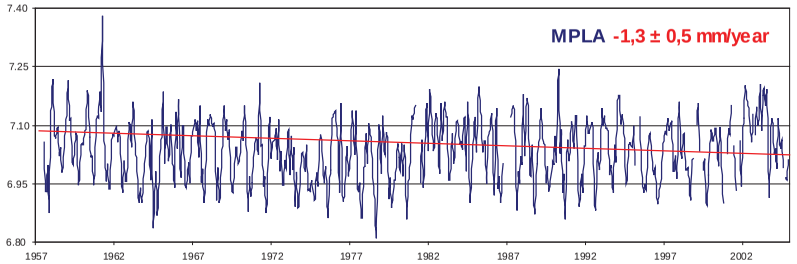

When the vertical datum was established, the mean sea level was 7 cm higher.

Drawbacks of the classical height systems

Problem 4: tide gauge registrations describe vertical crustal movements or sea level changes?

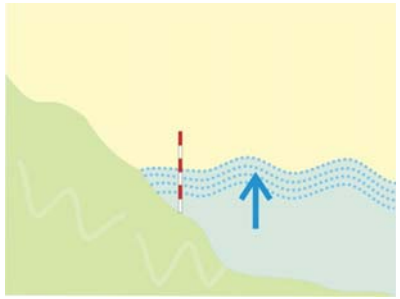

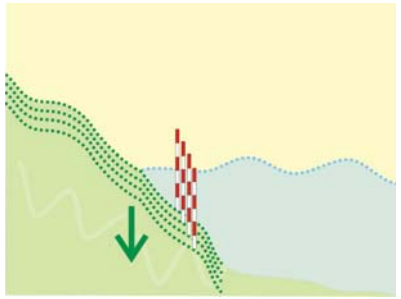

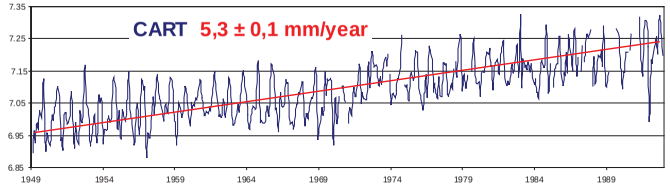

Drawbacks of the classical height systems

Problem 4: tide gauge registrations describe vertical crustal movements or sea level changes?

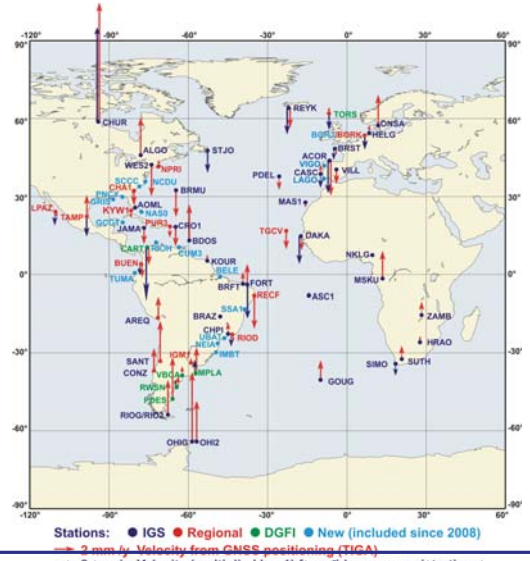

International GNSS Service Working Group
TIGA: GNSS tide gauge benchmark monitoring

Drawbacks of the classical height systems

Problem 5: levelled height differences are corrected using different gravity reductions (orthometric hypotheses, normal, normal orthometric, etc.); sometimes no gravity reductions are applied.

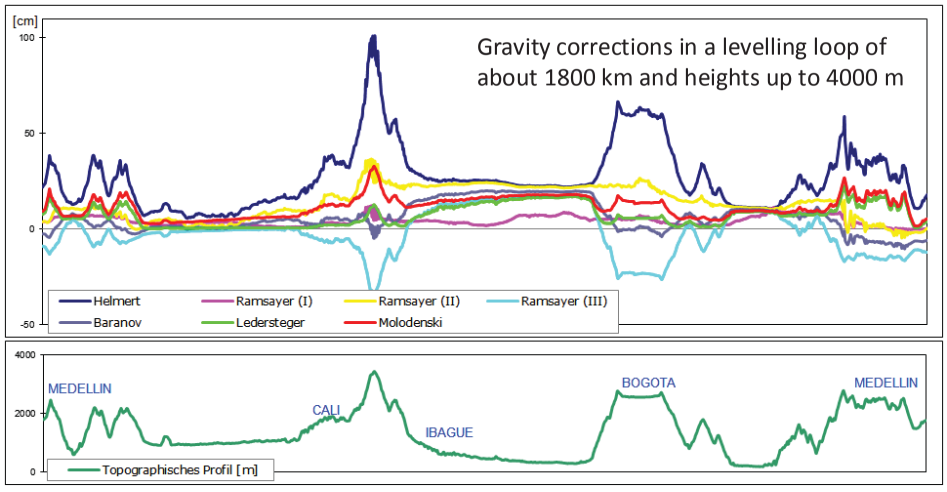

Drawbacks of the classical height systems

Problem 6: (unknown) vertical crustal movements affecting levelling benchmarks were handled as observation errors within the adjustment.

Time series of the GNSS station BOGA (Bogotá, Colombia)

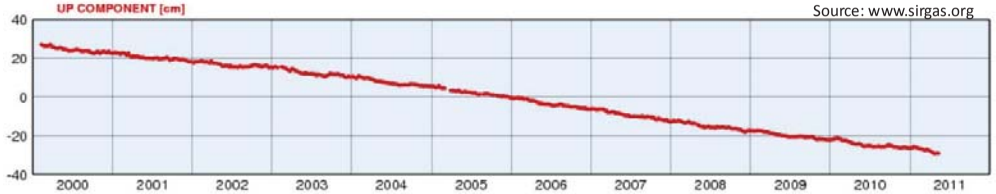

In practice H and N assumed invariant

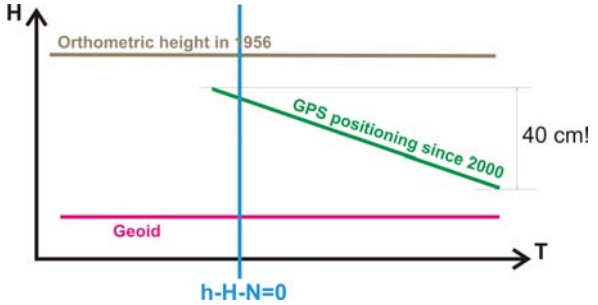

Vertical datum discrepancies in South America

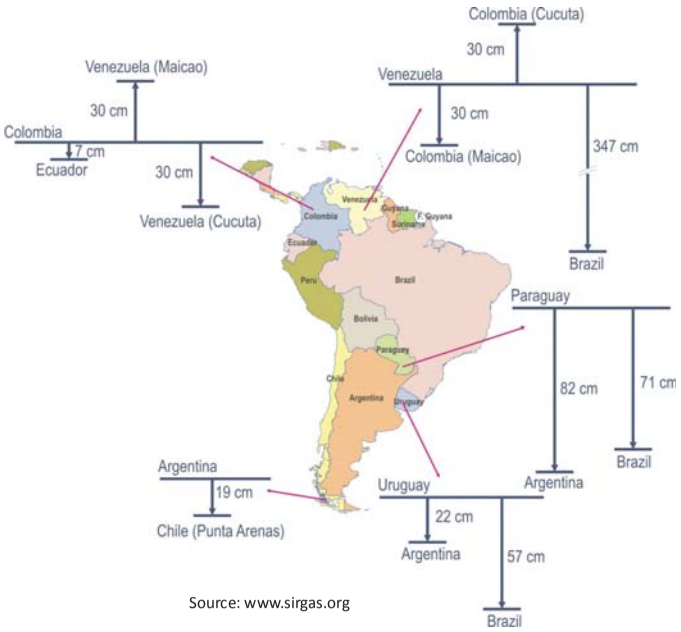

Source: www.sirgas.org

Vertical datum discrepancies in Europe

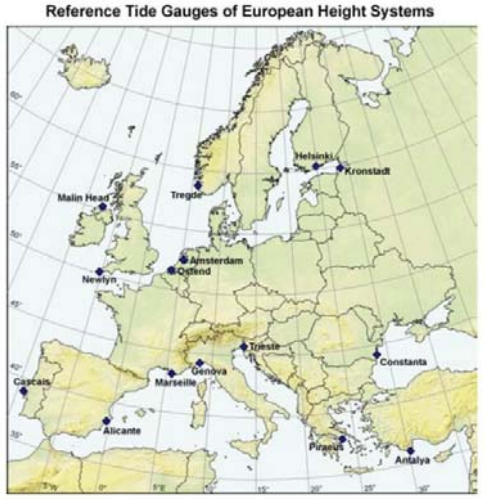

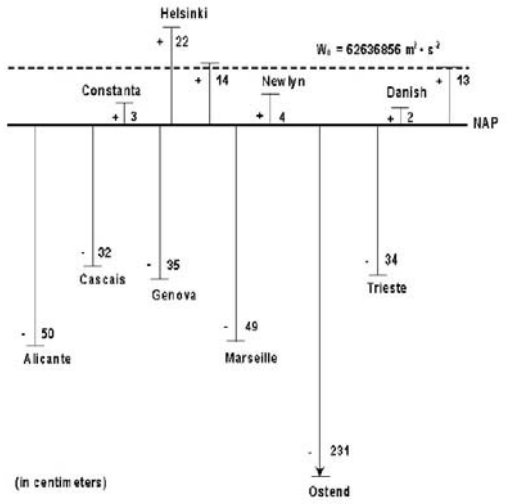

Source: http://www.bkg.bund.de/geodIS/EVRS/

Drawbacks of the classical height systems: Summary

Characteristic	Drawback
The reference level (zero-height surface) is realised by the mean sea level measured at individual tide gauges and averaged during different time periods.	(1) There are as many reference levels (vertical datums) as reference tide gauges and (2) they are related to different reference epochs.
The ocean topography at the local reference tide gauges has not been taken into account.	(1) Equipotential surfaces passing through the different reference tide gauges realise different (local) geoids, which are lying very close to sea surface (< ~2 m) and are practically parallel to each other; but no one coincides with a global geoid. (2) Relationship between local geoids and between them and the global one are unknown.
The vertical control has basically been extended by means of spirit levelling during many years and possible vertical displacements have not been taken into account.	(1) Vertical networks have been adjusted piece-wisely, (2) systematic errors significantly growth with the distance from reference tide gauge, and (3) vertical coordinates refer to different epochs.
Different gravity reductions (sometimes no reduction) have been applied to the measured level differences.	(1) Vertical coordinates realise different physical height types (orthometric, normal, normal-orthometric, etc.) (2) the corresponding reference surfaces do not coincide with a proper geoid or quasi-geoid. (3) These surfaces are height-dependent.
Heights at the border between datum zones present discrepancies at the m-level.	(1) Reference levels and vertical coordinates are usable only in limited geographical areas; (2) their combination at regional or global level is unsuitable.

Classical height systems: Summary

- refer to **different levels** (many [dm] of discrepancy);
- realise **different types of heights** (normal, orthometric, etc.);
- omit (sea and land) **vertical variations** with time,
- do not support the precise combination of **h-H-N**;
- are the base for **vertical data** produced in **the last 150 years**;
- **cannot be replaced** by ellipsoidal heights (these do not describe flow of water);
- Levelling is (much) more precise than the existing geoids and global gravity models.

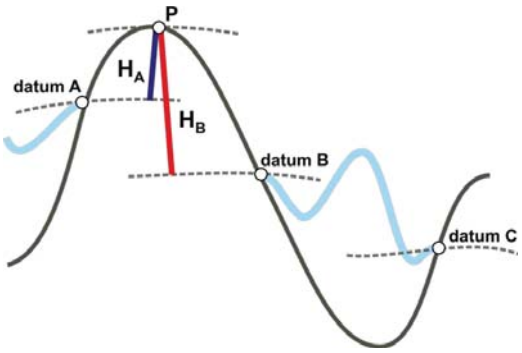

The classical height systems cannot be *thrown away*; they have to be modernised by their integration in a global unified vertical reference system!

4.7 Towards a modern vertical reference system

The ITRS/ITRF provides a highly precise geometrical reference frame (consistent in sub-cm level worldwide);

An equivalent highly precise physical reference frame is missing, it must be given by realising a **unified global vertical reference system**;

Main objectives are:

- to provide a reliable frame for consistent analysis and modelling of global phenomena related to the Earth's gravity field (e.g. sea level variations from local to global scales, redistribution of masses in oceans, continents and the Earth's interior, etc.);
- to allow the reliable combination of physical and geometric heights in order to explode at a maximum the advantages of satellite geodesy (e.g. combination of GNSS with gravity field models for worldwide unified precise height determination).

Towards a modern vertical reference system

Basic idea

1) To satisfy **h-H-N=0** at the **cm-level worldwide**;
   - At present: at the dm- to m-level (too imprecise)
   - Ideal: at the mm-level (still unrealistic)
2) For this combination, the new vertical reference system has to **support geometric and physical heights**;
3) Similar realisation to the ITRF, i.e.
   - a **global network** with known vertical station positions;
   - **regional and national densifications**, i.e. integration (transformation) of the existing local height systems.

Definition and realisation of a modern vertical reference system

Reference for the consistent modelling of geometric and physical parameters, i.e.
$h = H^N + \zeta\ (\approx H + N)$ in a global frame with high accuracy ($> 10^{-9}$)

Geometrical Component	Physical Component
Coordinates: Ellipsoidal heights and their change with time **h (t), dh/dt** Definition: **ITRS + Level ellipsoid ($h_0 = 0$)** a. (**a**, J_2, ω, GM) **or** b. ($\mathbf{W_0}$, J_2, ω, GM) Realisation: 1. Related to the **ITRS** (ITRF) 2. Conventional ellipsoid Conventions: IERS Conventions Ellipsoid constants, W_0, U_0 values, reference tide system have to be aligned to the physical conventions.	Coordinates: Potential differences and their change with time $-\Delta W_P(t) = C_P(t) = W_0 - W_P(t)$; $d\Delta W_0/dt$ Definition: $\mathbf{W_0}$= ***const.*** (as a convention) Realisation: 1. Selection of a global $\mathbf{W_0}$ value 2. Determination of the local reference levels $\mathbf{W_{0,j}}$ 3. Connection of $\mathbf{W_{0,j}}$ with $\mathbf{W_0}$ 4. Geometrical representation of $\mathbf{W_0}$ and $\mathbf{W_{0,j}}$ (i.e. geoid comp.) 5. Potential differences into physical heights (**H** or $\mathbf{H^N}$) **Zero tide system**

84

Definition and realisation of a modern vertical reference system

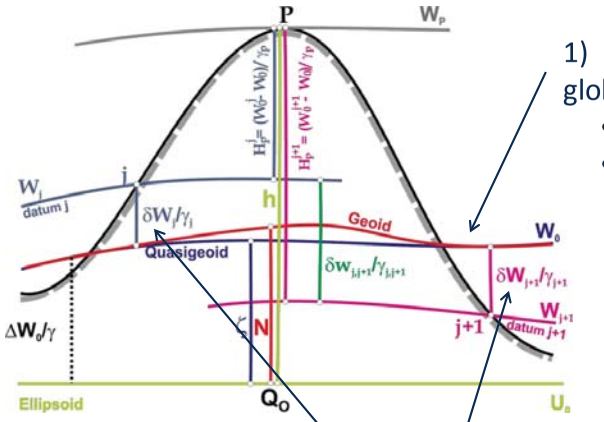

1) Definition and realisation of a global W_0 value
   - W_0 = potential of the geoid
   - Geoid = equipotential surface best fitting the global mean sea (Gauss definition)

2) Connection of the local reference levels with the global W_0

Remarks on the W_0 reference level

- The reference level or potential differences (W_0, $W_{0,j}$) **can arbitrarily be appointed and any W_0 value can be introduced as convention**. However, to get the worldwide consistency desired within a global vertical reference system, the selected W_0 **value must be realisable** with **high-precision at any time and anywhere** around the world.
- Since W_0 represents only one quantity and it is not sufficient to estimate position and geometry of the equipotential surface it is defining; **the main problem to solve here is not the determination of the W_0 value *per se*, but its realisation, i.e. the geoid computation**.
- Therefore, it is necessary to estimate it from **real observations** of the Earth's gravity field and surface.
- The **uniqueness**, **reliability** and **repeatability** of the global reference level W_0 (or global geoid) can only be guaranteed by introducing **specific conventions** (like any other reference system!). On the contrary, there will exist as many height systems as W_0 computations.

W_0 definition

At any tide gauge (TG) 1) $W_0 = W_0^{(i)}$	☹	It cannot realize a global vertical reference level
Mean value of many TGs 2) $W_0 = \frac{1}{N}\sum_{i=1}^{N} W_0^{(i)}$	☹	Its reliability and repeatability depend on the tide gauges included
With a reference ellipsoid 3) $W_0 = U_0$	☹	If the reference ellipsoid changes, the reference level changes, too.
Mean value over ocean areas 4) $\int_{S_O} (W - W_0)^2 \, dS_O = \min$	☹	An equipotential surface averaging the sea surface (DT) in a geometric sense is not determined
Gravity Boundary Value Problem (GVBP) 5) $W_0 = U_0 + \delta W$ $\Delta g = -\frac{\partial T}{\partial h} + \frac{1}{\gamma}\frac{\partial \gamma}{\partial h} T - \frac{1}{\gamma}\frac{\partial \gamma}{\partial h}\delta W$	☺	Required constraints (mainly the vanishing of the gravitational potential V at infinity) are only reliable in the frame of the GBVP

Some examples of a global W_0

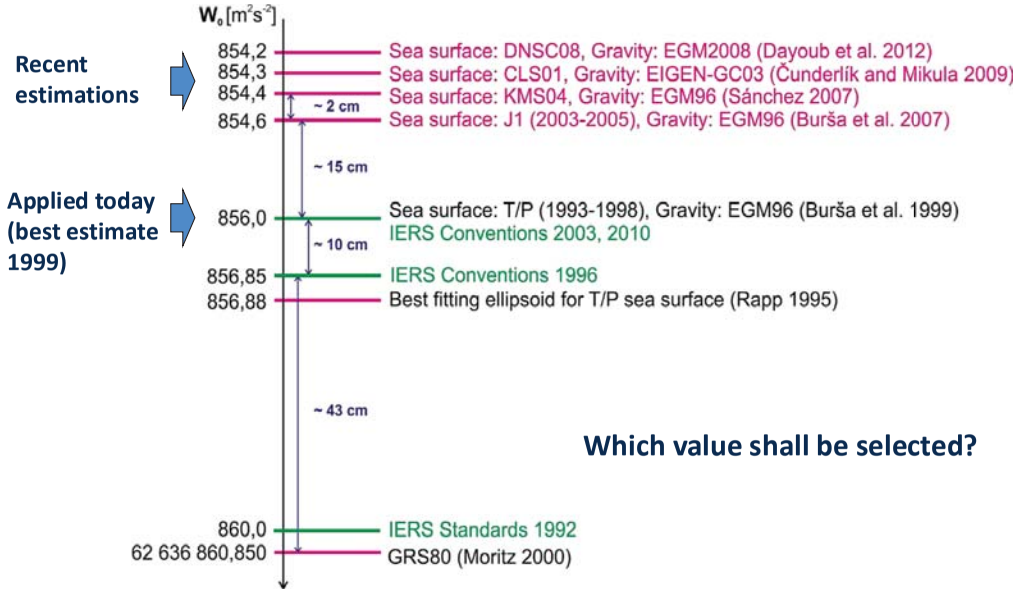

A Unified Height System: a GGOS challenge

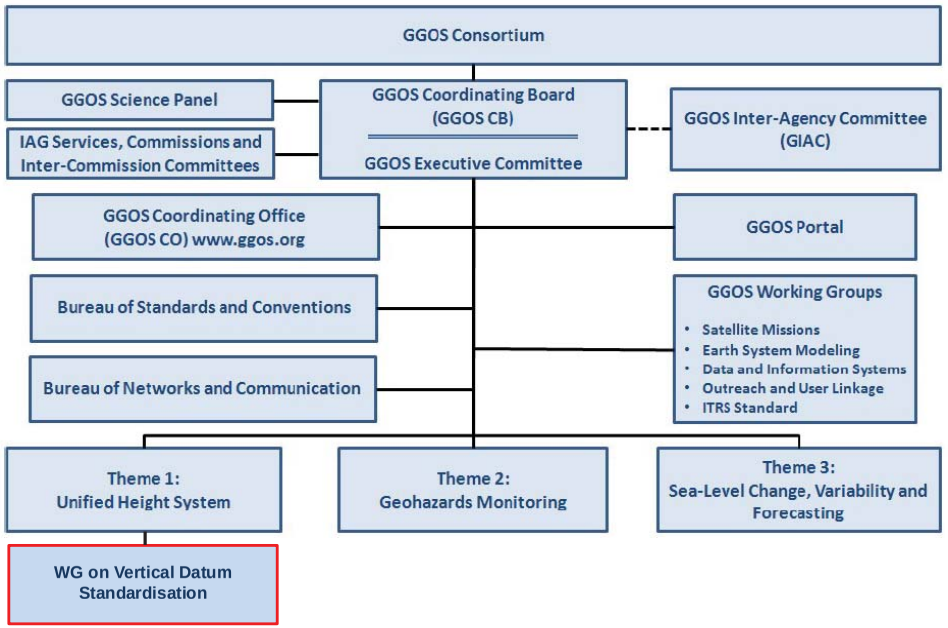

Working Group on Vertical Datum Standardization
http://whs.dgfi.badw.de

- Initiated during the IUGG General Assembly in Melbourne, July 2011
- Approved by the IAG Executive Committee in December 2012
- Term: 2011 – 2015

Objectives

- To bring together all teams working on the computation of W_0 to elaborate an inventory describing individual methodologies, conventions, standards, and models presently applied;
- To implement a new W_0 computation following individual (own) methodologies, but applying the same input geodetic models;
- To make a proposal for a formal IAG/GGOS convention about W_0 supported by a document containing the detailed computation of the recommended value.
- To provide a standard about the usage of W_0 in the vertical datum unification describing a appropriate strategy to connect (unify, transform) any local height system with the global W_0 reference level.

Members and on-going activities

L. Sánchez (Germany), chair	⇨ W_0-computation based on fixed-GBVP, analytical solution
R. Cunderlík (Slovakia) Z. Faskova (Slovakia) K. Mikula (Slovakia)	⇨ W_0-computation based on fixed-GBVP, Boundary Element Method (BEM)
N. Dayoub (Syria) P. Moore (United Kingdom)	⇨ W_0-computation based on averaging W-values from a GGM on points describing the sea surface (MSS) W_0-computation based on a reference ellipsoid ($W_0 = U_0$)
Z. Šima (Czech Republic) V. Vatrt (Czech Republic) M. Vojtiskova (Czech Republic)	⇨ W_0-computation based on averaging W-values from a GGM on points describing the sea surface (MSS)
J. Huang (Canada) D. Roman (USA) Y. Wang (USA) J. Agren (Sweden) C. Tocho (Argentina) J. Mäkinen (Finland) R. Klees (The Netherlands)	⇨ Regional realisation of a global W_0

A new W_0 "best estimate"

Input data:

Mean sea surface models:

- MSS_CNES_CLS11 (Schaeffer et al. 2012)
- DTU10 (Andersen 2010)
- mean yearly models individually computed by
  - Dayoub et al. (2012),
  - Burša et al. (2012),
  - Savcenko and Bosch (2012) - DGFI Altimetry Group.

Global gravity models:

- EGM2008 (Pavlis et al. 2012)
- EIGEN-6C2 (Förste et al. 2012)
- GOCO03S (Mayer-Gürr et al. 2012)
- GO_CONS_GCF_2_DIR_R4 (Bruinsma et al. 2013)

Dependence of the W_0-estimate on the spectral resolution of the gravity model (n,m)

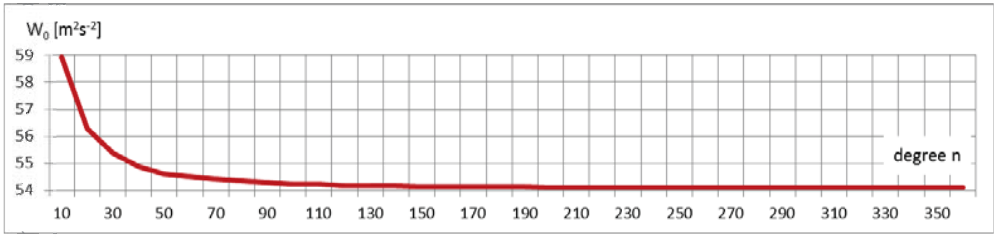

The use of a satellite-only gravity model is suitable.
After n,m = 200 the largest differences are **0,001 m^2s^{-2}**, which are totally negligible.

Note: Computations carried out in zero tide system, the MSS-CNES-CLS11 sea surface model and the EIGEN-6C2 gravity model.

Dependence of the W_0-estimate on the choice of the gravity model

EGM2008 n/m = 2159	ITG-GRACE03S 5-min mean free air anomalies (terrestrial, altimetry, aerial data, topography)	62 636 854,26
GOCO03S n/m = 250	GOCE 1 year CHAMP 8 years GRACE 7 years LAGEOS 5 years	**54,18**
EIGEN-6C2 n/m = 1949	GOCE 350 days GRACE 7,8 years LAGEOS 25 years DTU10 gravity anomalies and ocean geoid EGM2008 continental geoid	**54,12**
GO_CONS_GCF_2_ DIR_R4 n/m = 260	GOCE 837 days GRACE 9 years LAGEOS 25 years	**54,12**

Models including GRACE, GOCE and Satellite Laser Ranging data are preferred. Recent models deliver maximal differences of **0,06 m^2s^{-2}** (~ 6 mm vertical distance).

Note: Computations carried out in zero tide system and the MSS-CNES-CLS11 sea surface model.

Dependence of the W_0-estimate on the choice of the sea surface model

MSS_CNES_CLS11	16 years altimetry data (T/P, T/P TDM, J1, ERS1 ERM+GM, ERS2 ERM, ENVISAT, GFO) Reference period: 1993 – 1999 Coverage: 80°S – 84°N Mean tide system	62 636 854,12
DTU10	17 years altimetry data (T/P, T/P TDM, J1, ERS1 ERM+GM, ERS2 ERM, ENVISAT, GEOSAT GM, ICESAT, GFO) Reference period: 1993 – 2009 Coverage: 84°S – 90°N Mean tide system	**53,81**

There is a difference of **0,31 m^2s^{-2}**, which reflects the mean discrepancy of ~ 3 cm between both models. Possible causes:
- Different strategies to process the altimetry data;
- Different reductions taken into account in each model;
- Different periods (inter-annual ocean variability).

Note: Computations carried out in zero tide system and the EIGEN-6C2 gravity model

Dependence of the W_0-estimate on the choice of the sea surface model

Computation of yearly mean sea surface models to refer the sea surface heights to a univocal reference epoch:

1) Dayoub et al. (2012): 1992 - 2009 (T/P and Jason 1)
2) Burša et al. (2012): 2003 - 2011 (Jason 1)
3) Savcenko and Bosch (2012): 1992 – 2011 (T/P, T/P-EM, ERS2, Jason 1, Jason 2, Envisat)

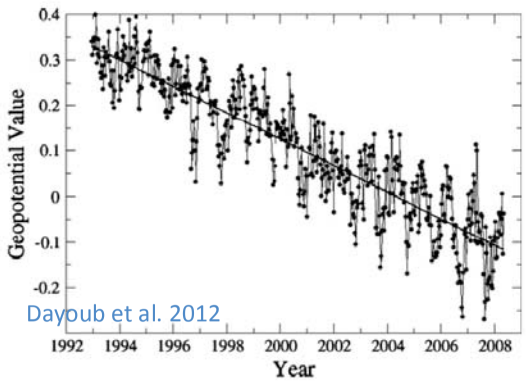

Dependence of the W_0-estimate on the choice of the mean sea surface model

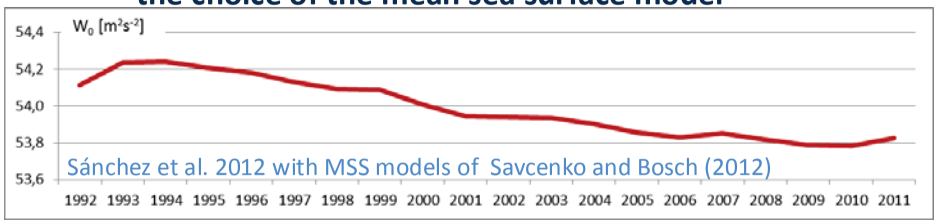

- The W_0 estimates reflect (with opposite sign) the sea level rise measured by satellite altimetry;
- The extreme values occurred in 1993 (maximum) and 2010 (minimum), difference **0,46 m^2s^{-2}**; mean value for the 20 years: **62 636 853,99 m^2s^{-2}**
- These differences shall not be understood as a change in W_0, but in the sea level; e.g. the geoid is not growing/decreasing with the mean sea level!
- This only means that the mean sea level coincides with a different equipotential surface depending on the period utilized for the average of the sea surface heights.

Dependence of the W_0-estimate on the latitudinal extension of the mean sea surface model

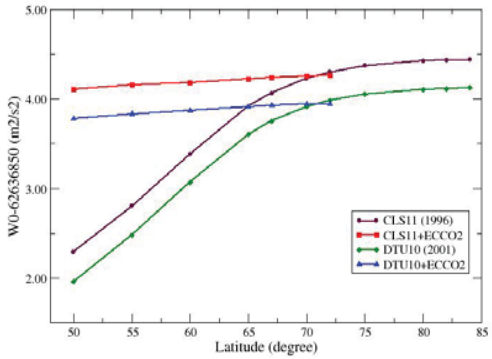

- The lower the considered latitude the lower the W_0 value;
- This dependence decreases if the mean sea surface heights are reduced by a oceanographic mean dynamic topography model, in this case the ECCO2 model (Menemenlis et al. 2008);
- It should considered the maximal latitudinal extension available.

Recommendation on W_0

- The four teams working on the empirical estimation of W_0 agree on recommending as a **best estimate** the value

$$W_0 = 62\,636\,854{,}0 \pm 0{,}2 \ \ m^2s^{-2}$$

Value used at present: $62\,636\,8\underline{56{,}0 \pm 0{,}5}\ m^2s^{-2}$

(**level difference of about 20 cm!**).

- This new W_0 value should be used for
  - the definition of **the constant L_G** (necessary for the transformation between Terrestrial Time and Geocentric Coordinate);
  - as a **defining parameter for a new reference ellipsoid**;
  - as **defining reference level** for the global vertical reference system.

Present activities regarding W_0 (status Oct. 2013)

- To support this recommendation, the WG on Vertical Datum Standardisation is
  - preparing a **position document** describing all the computations and error analysis;
  - working together with the **GGOS Bureau for Standards and Conventions** to outline the computation of a **new reference ellipsoid**;
  - defining **adequate strategies** for the realisation of this reference level **in global, regional and local frames**.
- **Please keep in mind**: The equipotential surface appointed as the zero-height level
  - is **defined by** a certain geopotential value called **W_0**;
  - shall be **realised by a global geoid model**; i.e. geometric representation of the zero-height surface with respect to a reference ellipsoid.

Definition and realisation of a modern vertical reference system

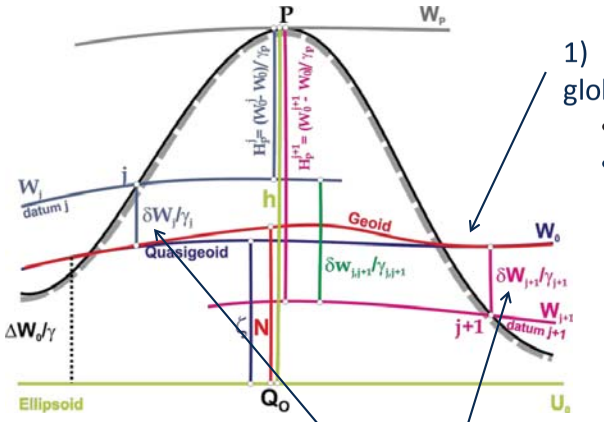

1) Definition and realisation of a global W_0 value
   - W_0 = potential of the geoid
   - Geoid = equipotential surface best fitting the global mean sea (Gauss definition)

2) Connection of the local reference levels with the global W_0

Realization of W_0 ($W_{0,j}$) by the GBVP

	Ocean areas	Land areas
	Fixed gravimetric GBVP provides the global reference level (W_0)	Scalar-free GBVP provides the local reference levels (W_j)
Formulation	$\nabla^2 T = 0$ *outside boundary surface* ; $T = W - U$	
	$-\frac{\partial T}{\partial r} = \delta g$	$-\frac{\partial T}{\partial r} - \frac{2}{r} T = g_j - \frac{2}{r}\Delta W_j$ $\Delta W_j = W_0^j - U_0$
Constraints	$T = 0$ *at* ∞ ; $\int_{sea} T\,d\sigma = k_i$; $\int_{land} T\,d\sigma = k_j$; $\int k_i + \int k_j = 0 \Rightarrow T_{00} \equiv \int T\,d\sigma = 0$	
Solution	$T = \frac{\Delta GM}{R} + \frac{R}{4\pi}\iint_\sigma B_j\, S(\psi)\,d\sigma + \sum_{n=1}^{\infty}\frac{R}{4\pi}\iint_\sigma G_n\, S(\psi)\,d\sigma$	
	$j = 1$; $B_1 = \delta g$ (gravity disturbances) $S(\psi) = S'(\psi)$	$j = 1 \ldots J$; $B_j = g_j - \frac{2}{r}\Delta W_j$ $g_1 = \Delta g$; $g_2 = \Delta C$; etc.

vertical datum unification strategies

Empirical estimation of W_0

Solution of the fixed geodetic boundary value problem in ocean areas

on sea

$$T = f_i + \Delta W_i \xrightarrow[\text{sat. gravimetry}]{\text{sat. altimetry}} T = f + \Delta W_0$$

provides the global reference level (W_0)

on land

$$-\frac{\partial T}{\partial r} - \frac{2}{r} T = g_j - \frac{2}{r}\Delta W_j$$

provides the local reference levels (W_j)

vertical datum unification strategies

- Since in the oceans geoid and quasi-geoid are identical, it is advantageous to estimate W_o with data on S_S only. To avoid multiple datum effects, satellite altimetry data and satellite-only GGM shall be applied.
- The **known** boundary surface S_S is given by a **mean sea surface model** derived from satellite altimetry and the **boundary condition** corresponds to the **gravity disturbances**
$$-\frac{\partial T}{\partial r} = \delta g$$
- δg can be obtained from a global gravity model in combination with the gravity field of a reference ellipsoid.

103

Vertical datum unification in practice

W_0 in the frame of the geodetic boundary value problem (GBVP)

on sea

$$T = f_i + \Delta W_i \xrightarrow[\text{sat. gravimetry}]{\text{sat. altimetry}} T = f + \Delta W_0$$

provides the global reference level (W_0)

on land

$$-\frac{\partial T}{\partial r} - \frac{2}{r} T = g_j - \frac{2}{r}\Delta W_j$$

provides the local reference levels (W_j)

vertical datum unification strategies

- GBVP is solved following the Molodenskii theory, without orthometric hypotheses to avoid misrepresentations in ΔW caused by inconsistencies between different assumptions.
- The quasi-geoid is not an equipotential surface, but it coincides with the geoid on marine and coastal areas. Therefore, it can define the local reference levels.
- All datum zones ($j = 1 \ldots J$) shall apply the same global gravity model (GGM) by solving the mixed GVBP. This GGM should be a satellite-only model.
- All datum zones shall apply the same reference surface and normal gravity (and potential) field for the linearization of the GBVP. It should correspond to the conventional ellipsoid of the geometrical reference system (e.g. GRS80).
- All observations shall refer to the ITRF and to the same epoch to avoid misrepresentations caused by horizontal local datums or temporal changes.

104

Vertical datum unification in practice

1) Establishment of a vertical frame including: reference tide gauges, main levelling points (nodes), ITRF (SIRGAS, EPN, …) stations;
2) Connection of the levelling networks between neighbouring countries (or vertical datum zones): $\Delta W_{ij} = C_i - C_j$;
3) Computation of T_j (GBVP solution) and comparison with the geometric reference system (γh) and geopotential numbers C_j in three approaches:

Oceanic approach	Coastal approach	Terrestrial approach
(DT around gauges)	(reference tide gauges)	(geometric reference stations)
• h from satellite altimetry combined with tide gauge registrations; • C_i = oceanic geopotential numbers ($=\gamma DT$); • T_i from satellite-only GGM.	• h from GNSS positioning at tide gauge benchmarks; • C_i = 0 (or close to 0 for non-reference tide gauges); • T_i from satellite-only GGM + terrestrial gravity.	• h from GNSS positioning at ITRF stations and levelling nodes (including points with border connections), • C_i geopotential numbers from levelling, • T_i from satellite-only GGM + terrestrial gravity.

4) Least squares adjustment of (2) and (3).

Definition and realisation of a modern vertical reference system: Summary

A global vertical reference system

- To solve the **discrepancies** between the **existing height systems** and
- To support the **different** techniques for **height determination**.

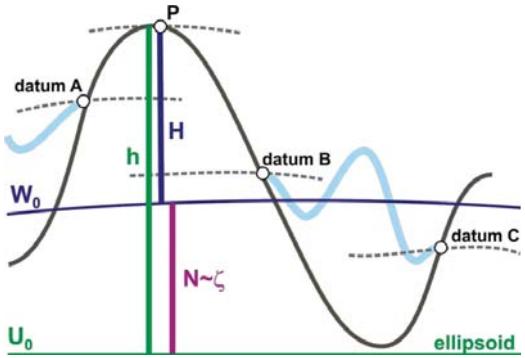

Implicit characteristics:

- One reference level (W_0 or geoid) to be used globally;
- All existing geopotential numbers (physical heights) referring to one and the same global level;
- Precise combination with geometric heights and geoid models of high resolution, i.e. h-H-N=0.

Definition and realisation of a modern vertical reference system: Summary

Definition
type of coordinates, reference surfaces, consistency between geometric and physical heights

→ **Realisation**

- Conventions to realize the definition (W_0, tide system, reference epoch, etc.)
- Establisment of a global reference frame (similar to ITRF)
- Determination of (vertical) coordinates for the reference frame according to the definition and conventions
- Unification of the existing local height systems into the global one
  - SSTop at and around reference tide gauges
  - Connection of the local levels to the ITRS/ITRF
  - Connection of neighbouring local height systems
  - Connection parameters at epoch of local level definitions
    - Time variations of sea level at the reference tide gauges
    - Separation of crustal movements from sea level changes
    - Vertical movements of height benchmarks
- Re-calculation of the height related observables and iteration of the realization procedure until getting a mm-level accuracy

4.8 Physical height systems in South America

	Definition	Realization
Reference surface	geoid	mean sea level at local tide gauges
Station positions	orthometric heights	spirit levelling with gravity reductions (by definition, but not in practice)

Physical height systems in South America

Mean sea level determined

- ❑ at different tide gauges
- ❑ at different definition periods (most of them unknown)
- ❑ Omission of vertical movements (of the Earth crust and sea level)

Physical height systems in South America

- Different levelling epochs assuming dH/dt = 0
- Omission (in general) of gravity reductions or usage of different (orthometric) hypotheses
- Unreliable levelling connections in the Amazonas jungle and Andean region (> 6000 m)
- Vertical networks individually adjusted
- Unclear reference tide system

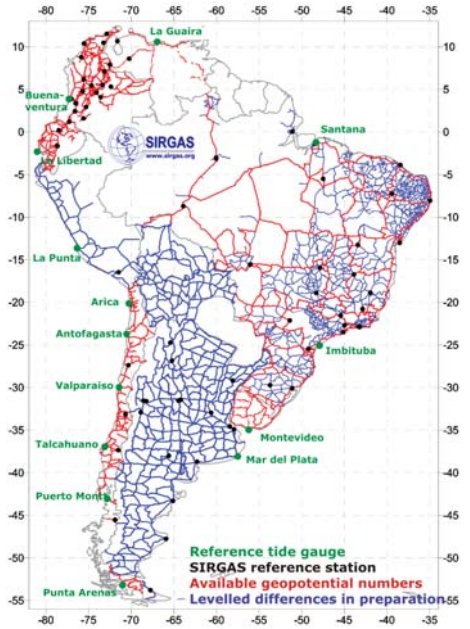

Physical height systems in South America

Height discrepancies at the borders, include

- (local and temporal) discrepancies between local reference levels
- systematic levelling errors
- discrepancies between different gravity reductions
- vertical movement effects

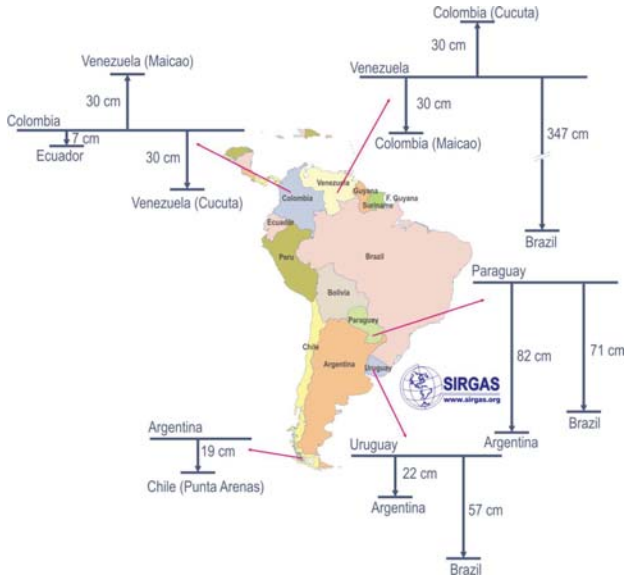

Physical height systems in South America

- There are as many height systems as reference tide gauges (and applied orthometric reductions);
- Relationship between the local reference surfaces and a global geoid is unknown;
- Combination of levelled heights with GNSS positioning and gravity geoid models is unrealistic (at meter-level);
- Relative precision is high, absolute precision is too unreliable for understanding global change phenomena/effects.

Motivation for a new vertical reference system in South America

- To provide a highly precise physical reference frame (consistent at sub-cm level beyond national borders) equivalent to the geometrical one, i.e. SIRGAS (densification of ITRF);
- To satisfy h-H-N=0 at the cm-level in a global frame;
- To support determination and combination of geometric and physical heights;
- To establish a similar realization to ITRF/SIRGAS, i.e.
  - a global network with known vertical coordinates;
  - regional and national densifications, i.e. integration (transformation) of the existing local height systems.

Definition of the new vertical reference system for South America

Geometrical Component	Physical Component
Coordinates: Ellipsoidal heights **h (t), dh/dt** Definition: **ITRS + Level ellipsoid ($h_0 = 0$)** a. (**a**, J_2, ω, GM) **or** b. (**W_0**, J_2, ω, GM) Realization: 1. Related to the **ITRS** (SIRGAS/ITRF) 2. Conventional ellipsoid Conventions: IERS Conventions Ellipsoid constants, W_0, U_0 values, reference tide system have to be aligned to the physical conventions.	Coordinates: Potential differences **$-\Delta W_P(t) = W_0(t) - W_P(t)$; $d\Delta W_0/dt$** Definition: **W_0= *const.*** (as a convention) Realization: 1. Selection of a **W_0** reference value 2. Determination of the local reference levels **$W_{0,j}$** 3. Connection of **$W_{0,j}$** with **W_0** 4. Geometrical representation of **W_0** and **$W_{0,j}$** (i.e. geoid comp.) 5. Potential differences into physical heights (**H** or **H^N**) **Zero tide system**

Vertical datum standardisation in practice

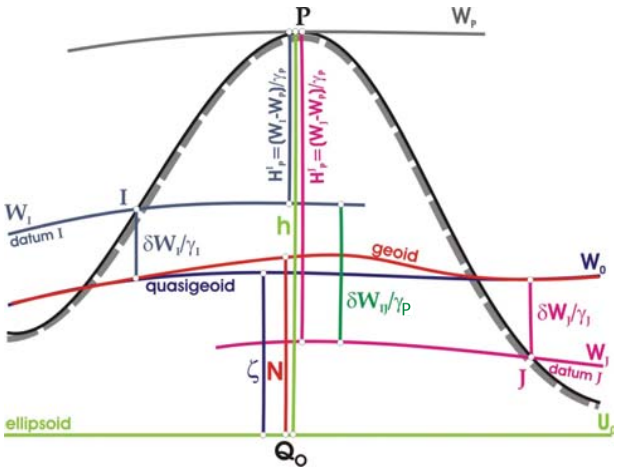

Determination of: $\delta W_i = W_0 - W_i$, $\delta W_{ij} = W_j - W_i$

Vertical datum standardisation in practice

1) Establishment of a vertical frame including: reference tide gauges, main levelling points (nodes), ITRF (SIRGAS, EPN, …) stations;
2) Connection of the levelling networks between neighbouring countries (or vertical datum zones): $\Delta W_{ij} = C_i - C_j$;
3) Computation of T_j (GBVP solution) and comparison with the geometric reference system (γh) and geopotential numbers C_j in three approaches:

Oceanic approach
(DT around gauges)
- **h** from satellite altimetry combined with tide gauge registrations;
- **C_i** = oceanic geopotential numbers ($=\gamma DT$);
- **T_i** from satellite-only GGM.

Coastal approach
(reference tide gauges)
- **h** from GNSS positioning at tide gauge benchmarks;
- **C_i** = 0 (or close to 0 for non-reference tide gauges);
- **T_i** from satellite-only GGM + terrestrial gravity.

Terrestrial approach
(geometric reference stations)
- **h** from GNSS positioning at ITRF stations and levelling nodes (including points with border connections),
- **C_i** geopotential numbers from levelling,
- **T_i** from satellite-only GGM + terrestrial gravity.

4) Least squares adjustment of (2) and (3).

Example: South America

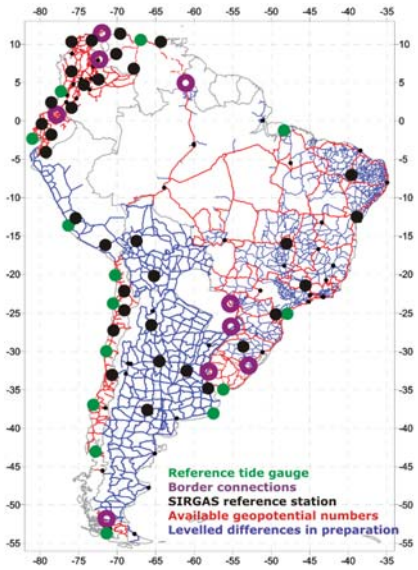

1. **14 reference tide gauges**

$$\delta W_i = \gamma\, h_{Sat.Alt+TG} - T_{GGM}$$

$$\delta W_i^{TG} = \gamma\, h_{SIRGAS} - T_{GGM+Terr.Data}$$

2. **37 SIRGAS reference stations**

$$\delta W_i^{SIRGAS\ stations} = \gamma\, h_{SIRGAS} - C_i - T_{GGM+Terr.Data}$$

3. **8 connections between neighbouring countries**

$$\delta W_{ij} = C_j - C_i$$

Unknowns: 15 vertical datums (14 tide gauges + Paraguay)

Observation equations: 73

Adjusted values: $\delta W_i^* = \left[A^T P A\right]^{-1}\left[A^T P\, \delta W_i\right]$

Example: South America

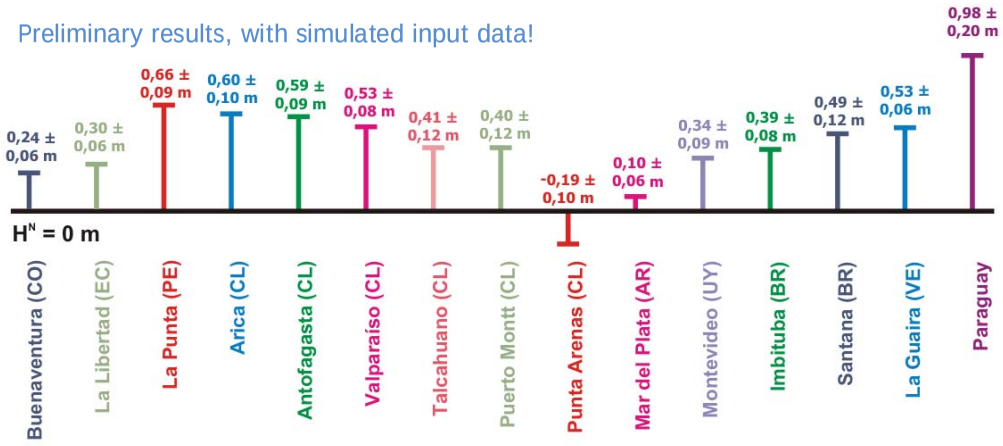

- The accuracy of estimated datum discrepancies is at the dm-level;
- Paraguay presents the largest uncertainty: no tide gauge, no SIRGAS reference station.

Major open issues

- Continental adjustment (free normal equations) of the levelling networks in South America. Present related tasks are:
  - Identification of levelling gaps (especially between neighbouring countries)
  - Standardization of gravity values for computation of geopotential numbers
  - GNSS positioning at tide gauges
- Treatment of time-dependent components (parameters), i.e. a reference epoch and dh/dt, dC/dt, dN/dt;
- Identification (correction) of uncertainties in δW_j due to systematic errors (in levelling networks, GNSS at tide gauges, etc.);
- Reliable combination of satellite-only GGMs and terrestrial gravity data.

4.9 Closing remarks

1) The availability of GNSS techniques motivates the combination of ellipsoidal heights and (quasi-) geoid models to obtain physical heights related, as far as possible, to the local vertical datums.
2) Levelling is expensive, laborious and time-consuming. In addition, it is difficult in remote and mountainous areas and the inherent systematic errors grow very quickly over large distances.
3) On the contrary, h from GNSS can be obtained quickly and inexpensively and N is usually available from the international geodetic community or from mapping agencies.
4) The relationship $h = H + N$ is widely used for
   - evaluating or refining global gravity models;
   - estimating deformations in the vertical networks;
   - determining local reference levels (local W_0 values);
   - vertical datum unification;
   - GNSS levelling, etc.

Closing remarks

5) In general, the input data in $h = H + N$ are taken as they are. There are nor further considerations about
   - random errors in the combined/obtained heights h, H, and N
   - datum inconsistencies inherent among the height types
   - systematic effects and distortions (long-wavelength geoid errors, poorly modelled GNSS errors and over-constrained levelling network adjustments)
   - assumptions/theoretical approximations made in processing observed data (e.g., atmospheric delay in GNSS, neglecting sea surface topography or river discharge corrections at tide gauges)
   - omission or approximate gravity height reductions
   - instability of reference station monuments over time (geodynamic effects, land uplift/subsidence).

Using a *corrector surface*
More details in: G. Fotopoulos (2003)

- Problem formulation: Use of a *corrector surface* to model the datum discrepancies and systematic effects when combining GNSS, geoid and orthometric heights
  - 1D network adjustment of co-located h, H and N data
  - Observations $l_i = h_i - H_i - N_i \neq 0$
  - Stochastic model $\mathbf{C}_l = \sigma_h^2 \mathbf{Q}_h + \sigma_H^2 \mathbf{Q}_H + \sigma_N^2 \mathbf{Q}_N$
  - Parametric model $h_i - H_i - N_i - \mathbf{a}_i^T \mathbf{x} = 0$
  - Observation equation $l_i = h_i - H_i - N_i = \mathbf{a}_i^T \mathbf{x} + v_i$
  - Unknowns $\mathbf{x}$, $\boldsymbol{\sigma} = (\ \sigma_h^2 \quad \sigma_H^2 \quad \sigma_N^2\ )^T$
  - NOTE: residuals v can further be modeled by, e.g., LSC

Taken from Sideris 2010.

Using a *corrector surface*
More details in: G. Fotopoulos (2003)

- Semi-automated Parametric Model Testing Procedure

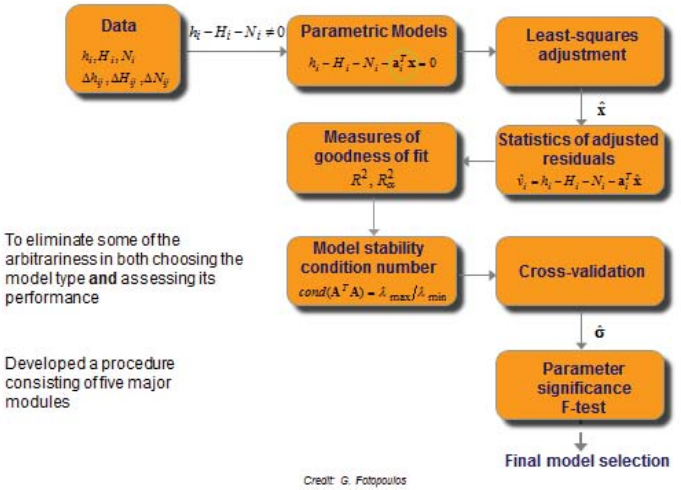

Taken from Sideris 2010.

Using a *corrector surface*
More details in: G. Fotopoulos (2003)

- Example of type/order of parametric model in Canada

1 dφ dλ dφdλ dφ² dλ² dφ²dλ dφdλ² dφ³ dλ³ dφ²dλ² dφ³dλ dφdλ³ dφ⁴ dλ⁴

Standard 4-parameter model: $\boldsymbol{a}^T\boldsymbol{x} = a_0 + a_1\cos\varphi\cos\lambda + a_2\cos\varphi\sin\lambda + a_3\sin\varphi$

Estimated Variance Components (Canadian test network)

parametric model	$\hat{\sigma}_h^2$	$\hat{\sigma}_H^2$	$\hat{\sigma}_N^2$
constant bias	7.16	16.59	0.12
4-parameter	7.20	3.97	0.28
1st order poly.	6.92	4.72	0.26
2nd order poly.	7.85	3.58	0.28
3rd order poly.	divergence, negative estimates		
4th order poly.	divergence, negative estimates		

inadequate parametric model, over-parame-terization

Taken from Sideris 2010.

Using a *corrector surface*
More details in: G. Fotopoulos (2003)

- Use of Corrector Surface to Get New H or ΔH
- Orthometric height H of new point P

$$H_p = \underbrace{h_p - N_p}_{\text{known}} - \mathbf{a}_p^T \hat{\mathbf{x}}$$

corrector surface

known height data from GNSS measurement and geoid model

- ΔH of new GNSS-levelling baseline

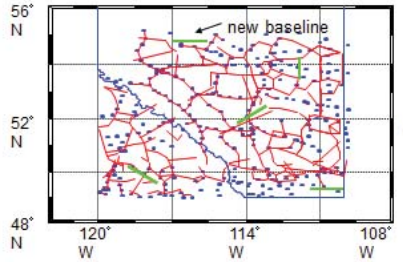

$$\Delta H_{kl} = \Delta h_{kl} - \Delta N_{kl} - (\mathbf{a}_l^T - \mathbf{a}_k^T)\hat{\mathbf{x}}$$

$$\sigma^2_{\Delta H_{kl}} = \sigma^2_{\Delta h_{kl}} + \sigma^2_{\Delta N_{kl}} + (\mathbf{a}_l^T - \mathbf{a}_k^T)\mathbf{C}_{\hat{\mathbf{x}}}(\mathbf{a}_l - \mathbf{a}_k)$$

'3rd term': accuracy contribution of corrector surface

Taken from Sideris 2010.

Using a *corrector surface*

1) The basic approach is based on the comparison of heights, i.e. $\Delta H = \Delta h - \Delta N$, absolute heights $H = h - N$ are not adequate.
2) The applicability of the *corrector surface* depends on the number and quality of the included points with co-located data (h, H, N);
3) The more points the better the *corrector surface*;
4) The better the geographic distribution of co-located data the better the *corrector surface*;
5) GNSS points and levelling points of low order should not be included;
6) The predicted data are the height uncertainties; the original data are not improved;
7) This method is useful for applications requiring a accuracy in dm-level.

High expectation for improvement: gravity field dedicated satellite missions

1) The new satellite-borne gravity field missions, together with the high accuracy of the geometrical reference system and the improved geometrical representation of the sea surface through satellite altimetry, shall allow the application in practice of different theoretical approaches that were not realistic before for the precise height determination.
2) In particular, the combination of the gravity data provided by CHAMP, GRACE and GOCE present as main advantages:
   - global consistency;
   - non-dependence of the local vertical datums (like terrestrial gravity anomalies)
   - accuracy of about 3 cm in geoid height with a spatial resolution up to degree and order 200 (when expressed in terms of spherical harmonic expansion); this corresponds to ~ 100 km.

High expectation for improvement: gravity field dedicated satellite missions

3) However, the gravity satellite missions provide global gravity models with a resolution of **degree, order 200**. This correspond to a **spatial resolution of about 100 km** and the **omission error** in the derived geoids can reach **up to 50 cm**! The combination of this models with **terrestrial data is absolutely necessary**!
4) The present tendency is to compute global gravity models based on the gravity satellite mission and **to refine them including the high-frequencies of EGM2008**. In this case, it shall take into account the uncertainty of this model and to follow **a rigorous error propagation analysis**.

Local geoid-model-based vertical datums

1) **Objective**: to define the vertical reference surface by a geoid model.
2) **Strategy**: to compute the *best possible* geoid by solving the geodetic boundary value problem.
3) **Advantages**:
   - No more levelling (money and time savings, avoiding large systematic errors);
   - Accessibility to the reference surface by means of GNSS positioning.
4) **Disadvantages**:
   - Low reliability in areas with poor gravity data coverage;
   - Lower relative accuracy in height differences over short areas in comparison with levelling;
   - Minimisation of vertical errors in GNSS positioning (long occupation sessions, high-precise post-processing);
   - How to access the vertical datum without GNSS equipment?
   - Vertical datums continue being local; a global vertical datum cannot be realised.

Local geoid-model-based vertical datums

Open questions:

- The geoid computation is not a unified/standardised procedure. Shall it be given as many vertical datums as geoid computations?
- In a similar way, GNSS positioning under different conditions or processed with different strategies produces different heights. Shall it be given as many H values as GNSS occupations at the same point?
- If new gravity data and new analysis strategies are available, it is usual to compute improved geoid models. How frequently shall the vertical datum be updated? Is it convenient for the users to change height values regularly?
- The sate-of-the-art allows the computation of geoid models with a maximum accuracy in dm-level. This could satisfy some practical applications, but what about measuring, understanding and modelling global change effects?
- The relationship $h = H + N$ is applied today to estimate the reliability of the different heights derived from independent methods. If H from levelling does not exist anymore, how can we verify the reliability of H=h-N ?

Closing remarks

- The present geodetic techniques provide **measurements with high-precision**. Processing and analysing those measurements must be also high-precise. **Geodesist and non-geodesist shall update their "know-how" accordingly**.
- Thanks to the present geodetic techniques and the Internet, **a huge amount of geodetic data** is available for everyone. However, before working with these data, **geodesist and non-geodesist should be sure what kind of data they are, how they were processed, which reductions they contain, which are their drawbacks.**
- At present, not only **a huge amount of geodetic data** is available but also **a huge amount of dedicated literature**. Before handling with the geodetic data, **geodesist and non-geodesist shall have an impression about works developed by other specialists in the specified topics. It is not necessary to discover *fire* again**.

Closing remarks

- Geodesists from over the world cooperate through the **International Association of Geodesy (IAG)** for advancing Geodesy. Under the umbrella of the IAG, achievements, on-going activities, and new challenges are discussed. So, in geodetic matters, **we shall look in the same direction as the IAG; in particular, we shall follow the direction outlined by the Global Geodetic Observing System (GGOS)**;
- The establishment of a global unified vertical reference system of high-precision is only possible in the frame of the IAG, GGOS and its services.

5. Reference system and frame for the Americas (SIRGAS)

Objective

To provide a **reliable reference frame** for:

1) **Earth System research**;
2) **Scientific and practical applications based on high-precise positioning**.

This implies a reference system realisation with

1) A significantly **higher accuracy than the magnitude of the phenomena we want to study**;
2) Homogeneous reliability and global consistency (**the same accuracy everywhere**);
3) Long-term stability (**the same accuracy at any time**).

5.1 SIRGAS components

SIRGAS comprises:

1) A regional densification of the ITRF (the realisation of the ITRS), as continental reference frame;
2) National densifications of the continental reference frame;
3) A unified vertical reference system.

To guarantee:

- Accessibility to the global reference system at regional, national, and local levels.
- Full consistency with the reference system of the (GNSS) satellite orbits.
- Standardisation of the gravity field-related heights.
- Precise combination of physical and geometrical parameters.

5.2 SIRGAS structure

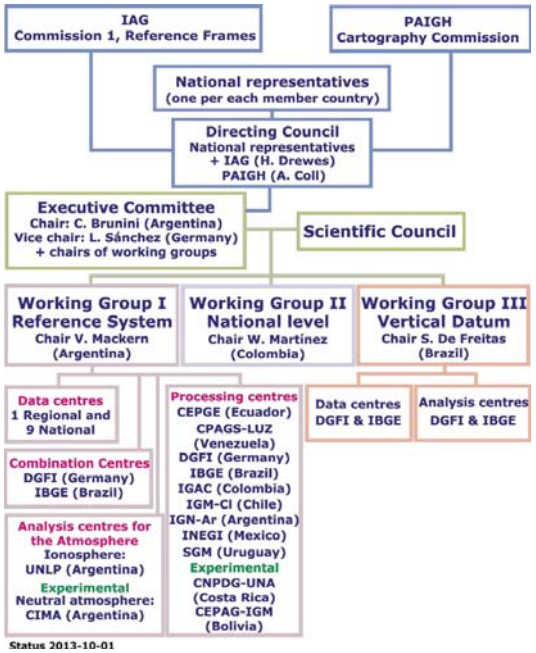

Members	
Argentina	Guatemala
Bolivia	Honduras
Brazil	México
Chile	Nicaragua
Colombia	Panamá
Costa Rica	Paraguay
Ecuador	Peru
El Salvador	Uruguay
Guyana	Venezuela
French Guyana	

SIRGAS is the ***Sub-commission 1.3b*** *(Regional Reference Frame for South- and Central America)* *of the* ***Commission 1*** *(Reference Frames)* of the **Internatiónal Association of Geodesy** (IAG).

SIRGAS is a Working Group of the **Cartography Commission** of the **Pan-American Institute for Geography and History** (PAIGH).

5.3 SIRGAS definition and realisation

SIRGAS as **geometrical reference system** is defined to be **identical with the ITRS (International Terrestrial Reference Frame).**

SIRGAS as **reference frame** is a regional densification (**continental network**) of the global **ITRF** (International Terrestrial Reference Frame).

At present, there are **three SIRGAS** realisations:

- by means of GPS campaigns:
  1) SIRGAS95 (ITRF94, 1995.4)
  (58 stations over South America)
  2) SIRGAS2000 (ITRF2000, 2000.4)
  (184 stations over North, Central, and South America)
- by means of continuously operating stations:
  3) SIRGAS-CON

First SIRGAS realisation: SIRGAS95

- Obs.: **1995-05-26 ... 1995-06-04**;
- **58 stations** in South America;
- **Processing**:
  - DGFI (Bernese V. 3.4)
  - NIMA (GIPSY/OASIS II)
- Discrepancies between the two solutions: max. **3,5 cm with RMS ±1,0 cm in X, ±1,4 cm in Y and ±0,7 cm in Z**;
- Causes: different satellite orbits and non-dependence of the phase centre variations on the vertical angle in the NIMA solution;
- Final combined solution: **SIRGAS95: ITRF94, epoch 1995.4.**

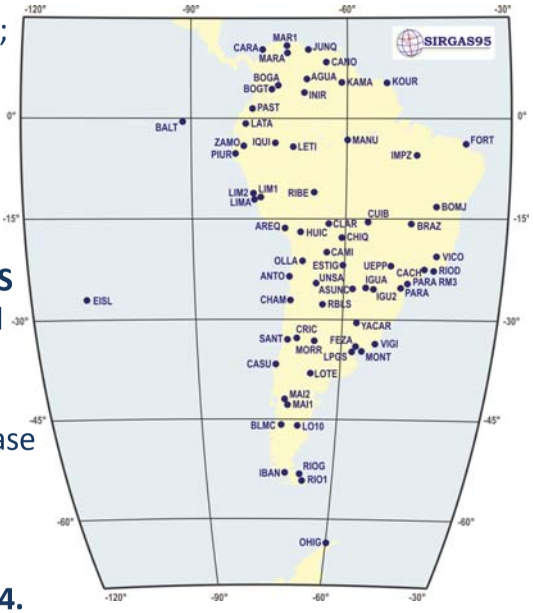

Second SIRGAS realisation: SIRGAS2000

- **Re-measuring campaign** to
  - Estimate constant **velocities for SIRGAS95**
  - First approach for a **SIRGAS vertical reference frame**;
- **Obs.: 2000-05-10/19**;
- **184 stations** in North, Central and South America;
- **Processing**:
  - DGFI (Bernese, v. 4.0)
  - IBGE (Bernese, v. 4.0)
  - BEK (GIPSY/OASIS II);
- Final solution: combination of the individual normal equations. **SIRGAS2000: ITRF2000, época 2000.4**
- **Precision: ±3 … ±6 mm**.

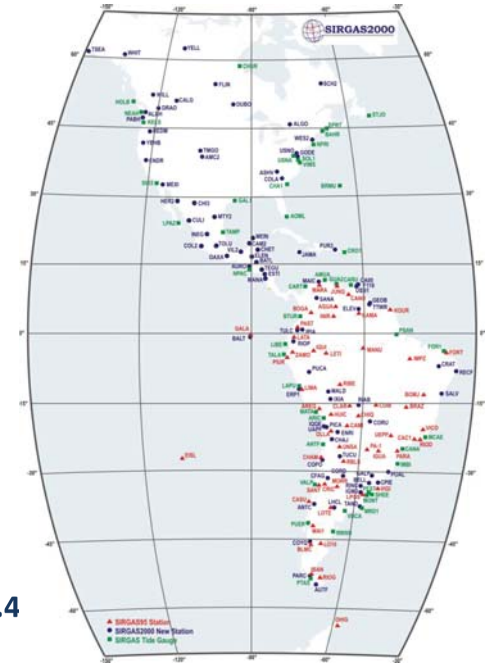

From South America to the Americas

- The **SIRGAS2000** station positions were transformed to the ITRF94 to be compared with the **SIRGAS95** positions and **to determine constant velocities**.
- The **United Nations Organization**, through its **7th Cartographic Conference for The Americas** (New York, January 22 – 27, 2001), **recommend to adopt SIRGAS as official reference system in all American countries**;
- The original acronym of SIRGAS (**Geocentric Reference System for South America**) was changed in 2001 to **Geocentric Reference System for the Americas**.

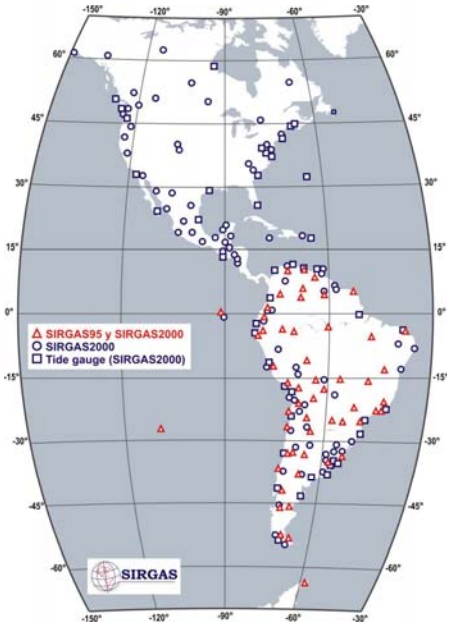

Third SIRGAS realisation: SIRGAS continuously operating network SIRGAS-CON

- One core network (SIRGAS-C) as the primary densification of ITRF in Latin America;
- National reference networks (SIRGAS-N) improving the densification of the core network and providing accessibility to the reference frame at national and local levels.
- The core network and the national networks satisfy the same characteristics and quality; and each station is processed by three analysis centres.

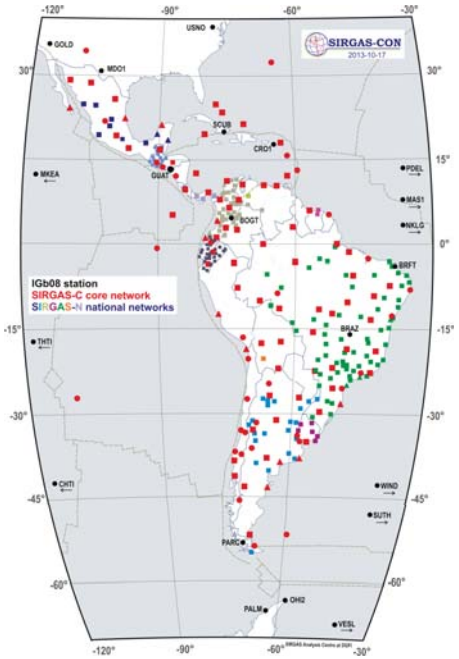

Third SIRGAS realisation: SIRGAS continuously operating network SIRGAS-CON

- 319 stations;
- 75 common stations with the IGS (to be included in the next ITRF solution);
- 181 stations with GLONASS;
- 7 stations with GALILEO;
- 69 station with capability for data transmission in real time;
- Weekly processing.

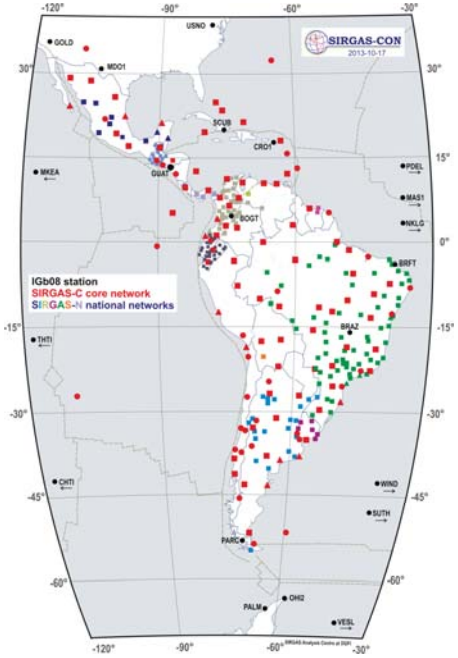

Third SIRGAS realisation: SIRGAS continuously operating network SIRGAS-CON

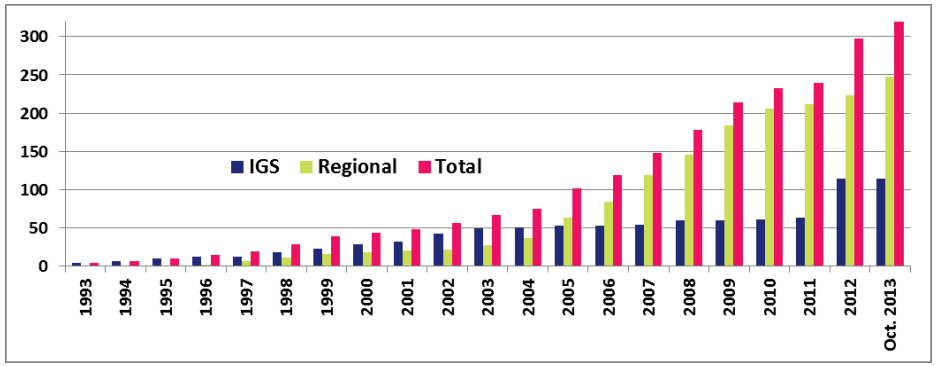

- In the early years of SIRGAS the CON stations were installed mostly by the IGS.
- By 2003 the national organizations committed to a policy aimed at improving the geodetic infrastructure of the Americas and the number of stations began to grow quickly.
- The national reference stations are integrated into the continental reference frame (SIRGAS-CON) for common processing and to guarantee consistency with the ITRF.

5.4 SIRGAS National Reference Networks

County	Densification SIRGAS/ITRF	No. stations pillars/CON
Argentina	ITRF2005, 2006.6	178 / 38
Bolivia	SIRGAS95, 1995.4	125 / 10
Brasil	SIRGAS2000, 2000.4	1903 / 95
Chile	SIRGAS2000, 2002.0	269 / 12
Colombia	SIRGAS95, 1995.4	70 / 45
Costa Rica	ITRF2000, 2005.8	34 / 9
Ecuador	SIRGAS95, 1995.4	135 / 11
El Salvador	IGS05, 2007.8	34 / 1
F. Guiana	ITRF93, 1995.0	7 / 1
Guatemala	ITRF2005, 2009,6	160 / 16
Mexico	ITRF92, 1988.0	0 / 19
Panama	ITRF2000, 2000.0	20 / 4
Peru	SIRGAS95, 1995.4	47 / 3
Uruguay	SIRGAS95, 1995.4	17 / 7
Venezuela	SIRGAS95, 1995.4	156 / 5

5.5 SIRGAS contribution to the International GNSS Service (IGS)

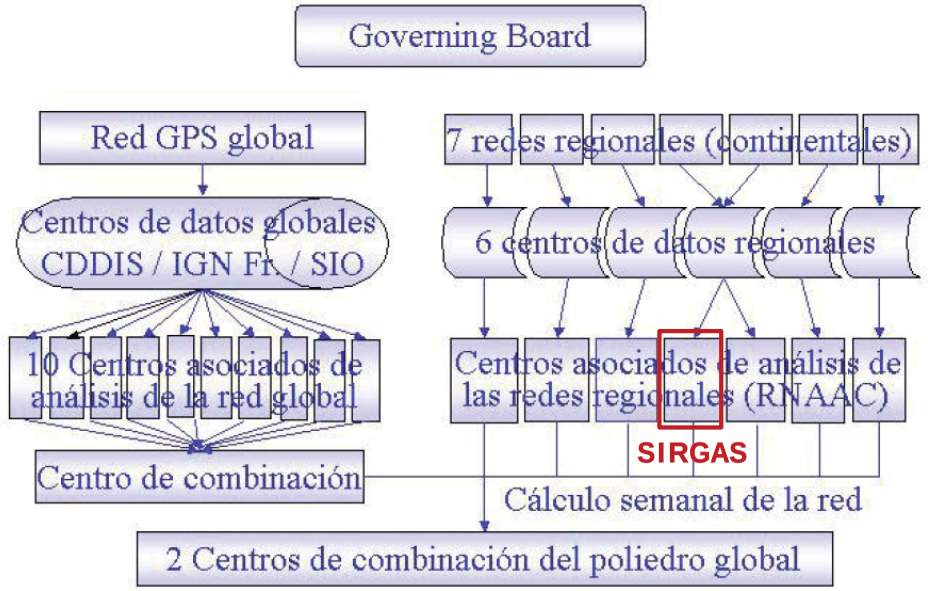

IGS Regional Network Associate Anaylsis Centre for SIRGAS IGS RNAAC SIR

- It is under the responsibility of DGFI since June 1996, when it was created;
- It has to deliver loosely constrained weekly solutions of the SIRGAS-CON network to the IGS. These solutions are combined together with those generated by the other IGS Global and Regional Analysis Centres to form the IGS polyhedron.
- The processing of the SIRGAS-CON network in the frame of the IGS RNAAC SIR also includes the computation (since 2001) of weekly coordinate solutions aligned to the ITRF and cumulative (multi-year) position and velocity solutions for estimating the kinematics of the network.
- Until 31 August 2008 (GPS week 1495), DGFI processed the entire SIRGAS-CON network in one block. Now, with the participation of Latin American entities processing SIRGAS stations, DGFI is responsible for processing the SIRGAS-C core network, for the weekly combination of the individual solutions, and for the computation of the multi-year solutions.

SIRGAS contribution to the International GNSS Service (IGS)

IGS tracking network

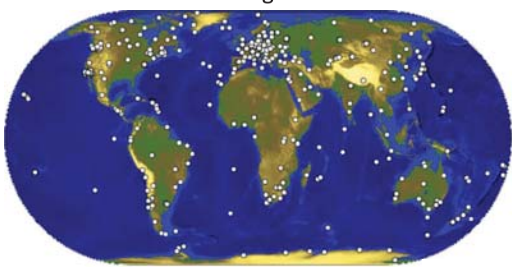

IGS polyhedron

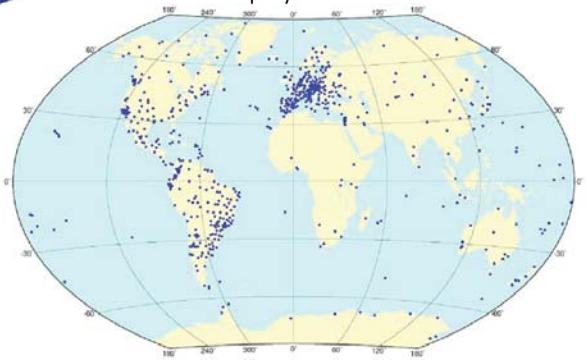

5.6 Weekly processing of the SIRGAS Reference Frame

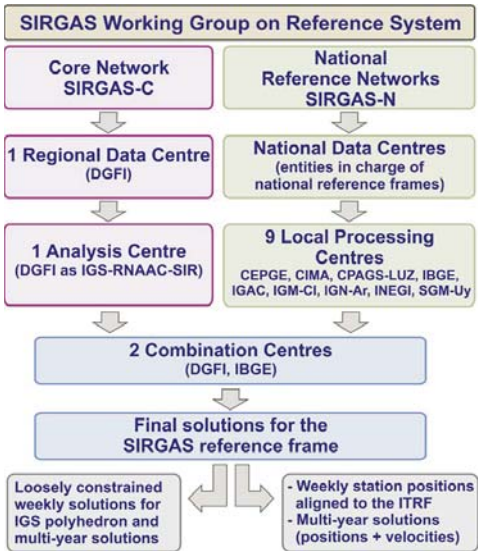

- 9 processing centres;
- 2 experimental processing centres;
- 2 combination centres;
- Each station is included in three individual solutions;
- Unified processing standards following IGS and IERS conventions.

CEPGE-Ec INEGI-Mx CPAGS-Ve IGM-CI

IBGE-Br IGAC-Co SGM-Uy IGN-Ar

Experimental

DGFI-De CNPDG-Cr CEPAG-Bo

Weekly processing of the SIRGAS Reference Frame

- Elevation mask and data sampling rate: 3° and 30 s, respectively.
- IGS absolute calibration values for the antenna phase centre corrections (http://igscb.jpl.nasa.gov/igscb/station/general/pcv_archive/).
- Satellite orbits, satellite clock offsets, and Earth orientation parameters are fixed to the combined IGS weekly solutions (Dow et al. 2009, http://igscb.jpl.nasa.gov/igscb/ product/);
- Solution of phase ambiguities for L1 and L2 as far as possible;
- Modelling of periodic site movements due to ocean tide loading according to the FES2004 ocean tide model (Letellier 2004). The corresponding values are provided by M.S. Bos and H.-G. Scherneck at http://holt.oso.chalmers.se/loading/.
- The Niell (1996) dry mapping function is applied to map the a priori zenith delay (~ dry part), which is modelled using the Saastamoinen model (1973). The wet part of the zenith delay is estimated at a 2 hours interval within the network adjustment and it is mapped using the Niell wet mapping function. Standard changed in July 2012! Now: the Vienna Mapping Function must be applied!

Weekly processing of the SIRGAS Reference Frame

- Processing centres compute daily free normal equations that are be combined for providing a loosely constrained weekly solution for station positions (all station coordinates are loosely constrained to ±1 m).
- Stations with large residuals in the weekly combination (more than ±20 mm in the N-E component, and more than ±30 mm in the height component) are reduced from the normal equations.
- The individual loosely constrained solutions are made available to be combined with the corresponding solutions delivered by the other SIRGAS Processing Centres.

Combination of the individual solutions in a unified solution for the entire network

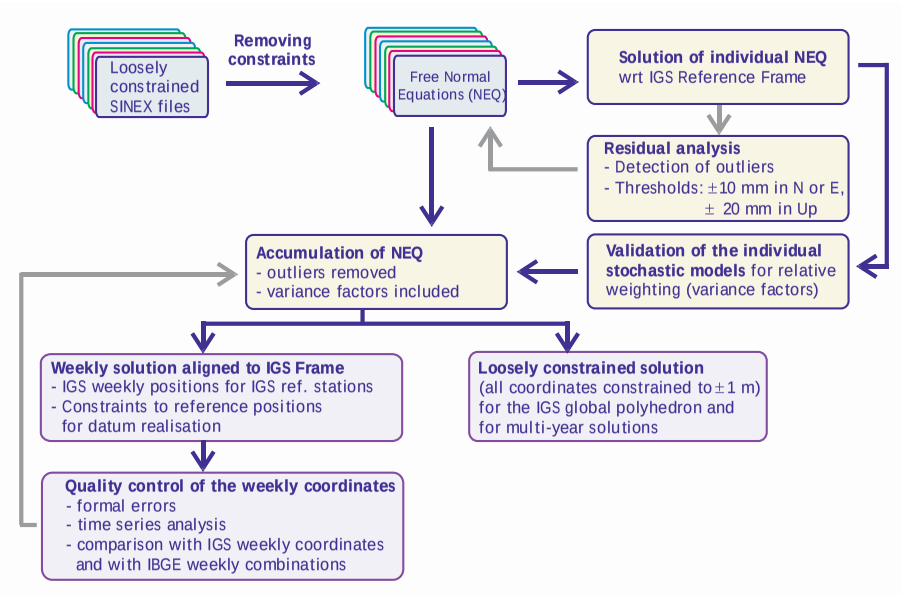

Quality control of the individual solutions

Objective: Determination of variance factors for relative weighting of the individual solutions to compensate possible differences in the stochastic models.

Criteria:

- Mean standard deviations of coordinates based on minimum datum conditions (NNR and NNT) with respect to IGS Reference Frame (formal errors of the individual solutions);
- Weekly repeatability of station coordinates for each Processing Centre (individual precision of the weekly coordinate solutions);
- Comparison with the IGS weekly coordinates for common stations (reliability of the individual solutions).

Quality control of the individual solutions

(mean values GPS weeks 1700 – 1758)

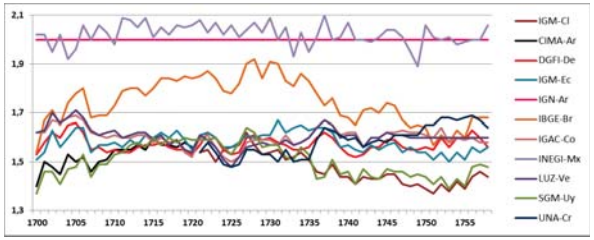

Formal errors in [mm] of the individual solutions.

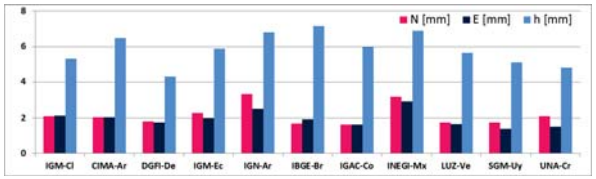

Consistency of the weekly station positions in the individual solutions.

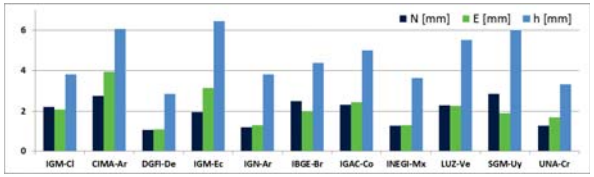

Reliability of the individual solutions (comparison with IGS).

Quality control of the final weekly station positions

Objective: to ascertain the accuracy and reliability of the weekly solutions for the entire SIRGAS-CON network (combination of the core network with the national reference networks).

Criteria:

- Mean standard deviation for station positions after aligning the network to the IGS reference frame (formal error of the final combination);
- Residual analysis after combining the individual solutions (internal consistency of the combined network);
- Time series analysis for station coordinates (compatibility of the combined solutions from week to week);
- Comparison with the weekly IGS coordinates (consistency with the IGS global network);
- Comparison with the IBGE weekly combination (required redundancy to generate the final SIRGAS products).

Quality control of the final weekly station positions

(mean values GPS weeks 1700 – 1758)

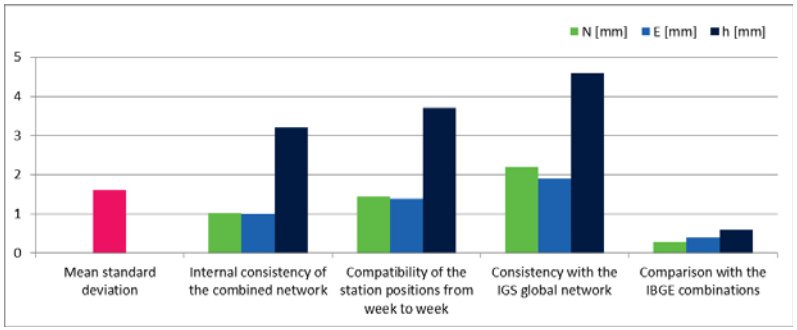

- The mean standard deviation of the combined solutions agrees quite well with those computed for the individual contributions, i.e. **the quality of the individual solutions is maintained and their combination does not deform or damage the internal accuracy of the entire SIRGAS network**.
- **Internal consistency: ~±1,0 mm in N-E and ~±3,6 mm in h.**
- **Reliability: ~±2,0 mm in N-E and ±4,5 mm in h.**
- The differences between **both processing centres** are within the expected level (**less than 1,0 mm**).

5.7 Multi-year (cumulative) solutions

Objective: to know the kinematics of the reference frames (station positions in a certain epoch + constant velocities).

These solutions include those models, standards, and strategies widely applied at the time in which they were computed and cover different time spans depending on the availability of the weekly solutions:

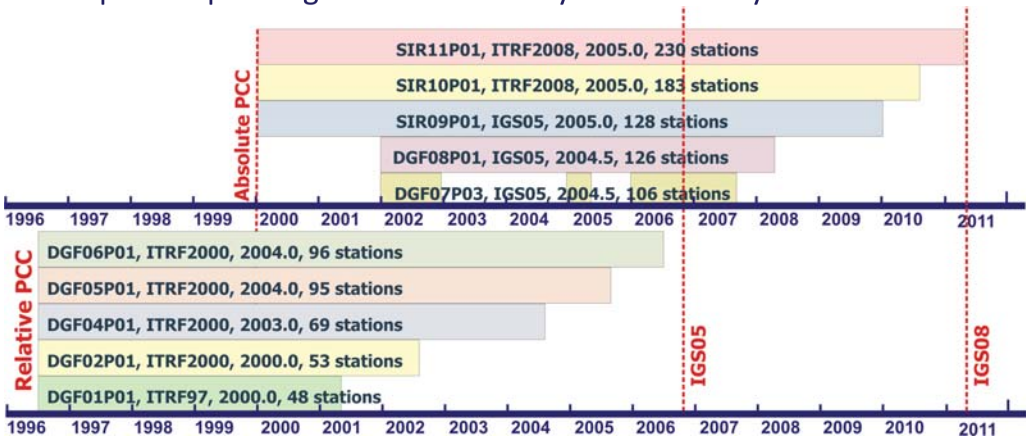

Comparison of the different SIRGAS-CON multi-year solutions with the ITRF2008

Solution	Common stations with ITRF2008	Comparison with the ITRF2008					
		Position deviations: Offsets ± RMS			Velocity deviations: Offsets ± RMS		
		N[mm]	E[mm]	h[mm]	VN[mm/a]	VE[mm/a]	Vh[mm/a]
DGF01P01	27	-16,3 ± 8,0	7,2 ± 19,5	27,9 ± 16,2	-0,4 ± 2,6	3,1 ± 4,7	1,3 ± 4,5
DGF02P01	24	-2,4 ± 3,7	-2,5 ± 5,8	4,0 ± 13,9	1,1 ± 1,6	1,4 ± 2,1	-3,7 ± 6,7
DGF04P01	35	-0,4 ± 4,3	-3,4 ± 5,0	1,3 ± 14,9	1,9 ± 2,3	1,3 ± 2,1	0,1 ± 3,6
DGF05P01	34	0,2 ± 3,8	-2,0 ± 5,0	0,1 ± 13,1	1,8 ± 2,1	1,1 ± 2,1	1,2 ± 3,6
DGF06P01	32	0,0 ± 3,9	-1,7 ± 4,9	1,1 ± 12,3	2,0 ± 2,2	1,0 ± 1,9	0,8 ± 3,0
DGF07P03	22	-1,3 ± 5,1	0,9 ± 6,2	-4,4 ± 19,5	0,5 ± 1,3	-0,4 ± 1,3	0,5 ± 2,7
DGF08P01	28	-3,2 ± 5,1	1,1 ± 8,9	-8,0 ± 10,0	0,5 ± 1,3	-0,5 ± 1,6	1,0 ± 2,3
SIR09P01	34	0,3 ± 4,0	-0,6 ± 6,7	-5,1 ± 12,0	0,3 ± 1,0	0,0 ± 1,1	-0,2 ± 1,9
SIR10P01	74	0,8 ± 5,0	0,3 ± 3,6	-4,9 ± 8,6	-0,1 ± 1,1	-0,1 ± 1,1	0,0 ± 2,2
SIR11P01	82	-0,3 ± 5,0	-0,1 ± 5,1	0,1 ± 7,5	-0,4 ± 1,9	0,1 ± 2,0	0,1 ± 1,4

Multi-year (cumulative) solutions: computation

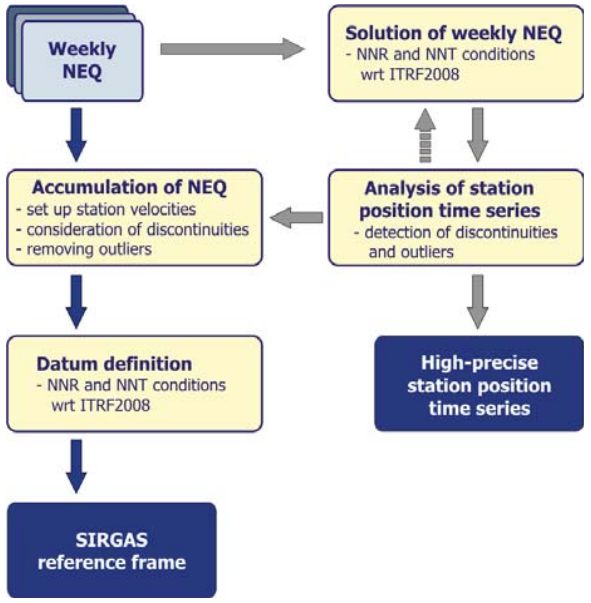

Multi-year (cumulative) solutions: time series analysis

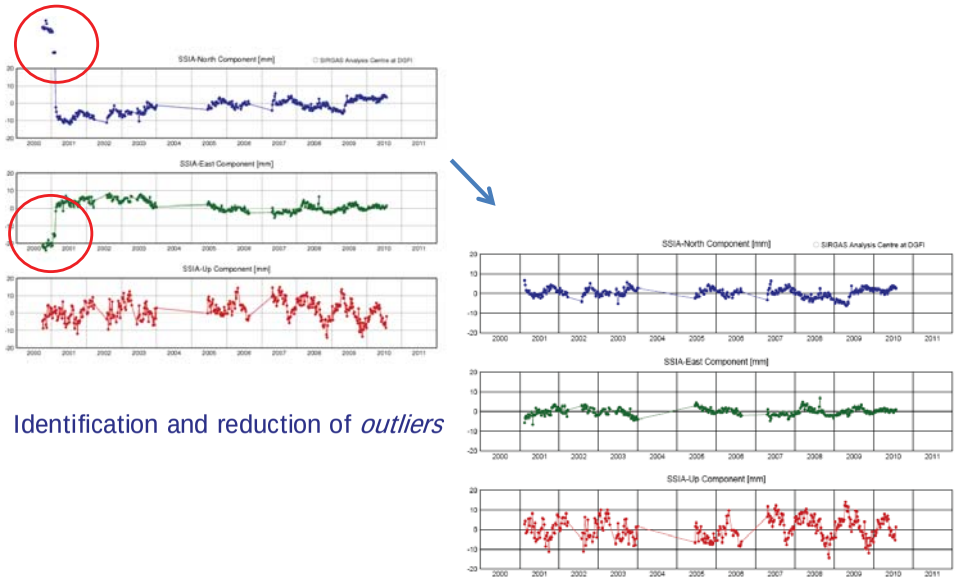

Identification and reduction of *outliers*

Multi-year (cumulative) solutions: time series analysis

Identification of jumps

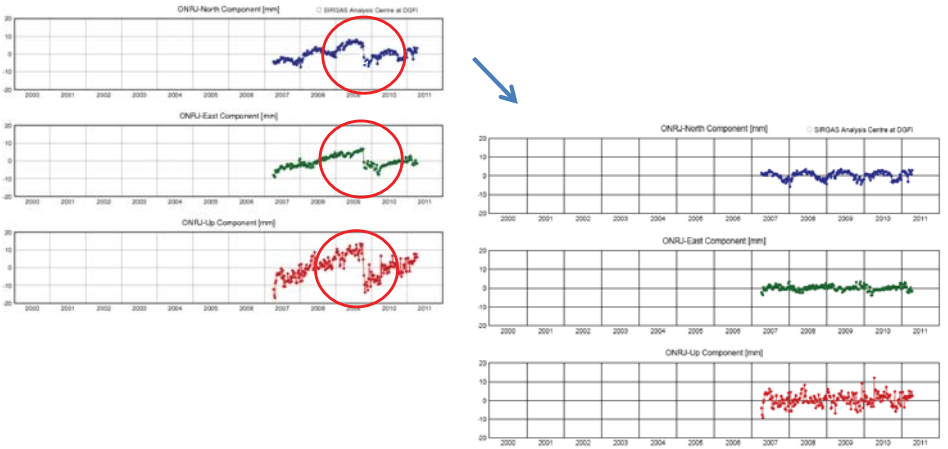

Multi-year (cumulative) solutions: time series analysis

Identification of trend changes.

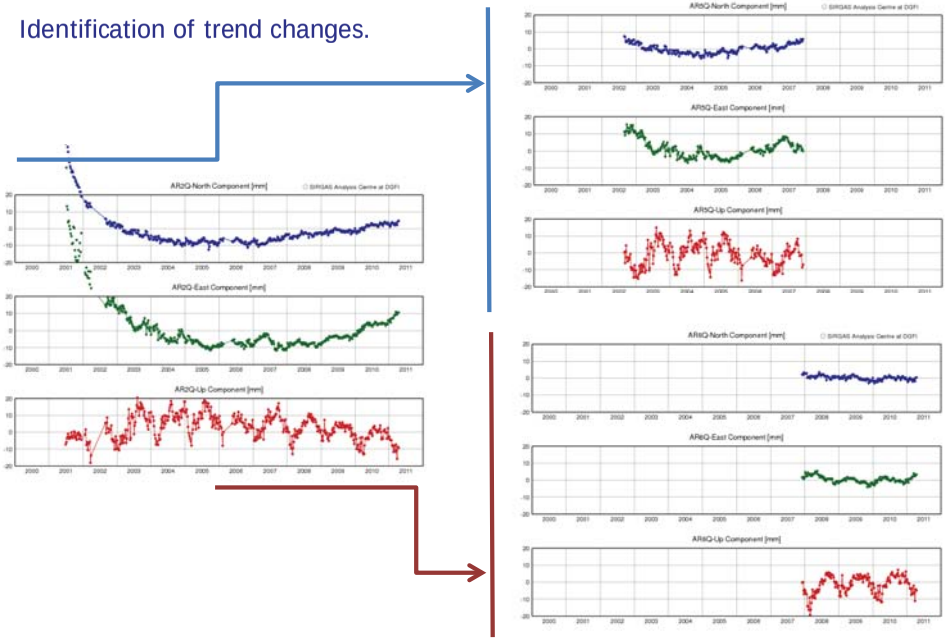

Setting up discontinuities

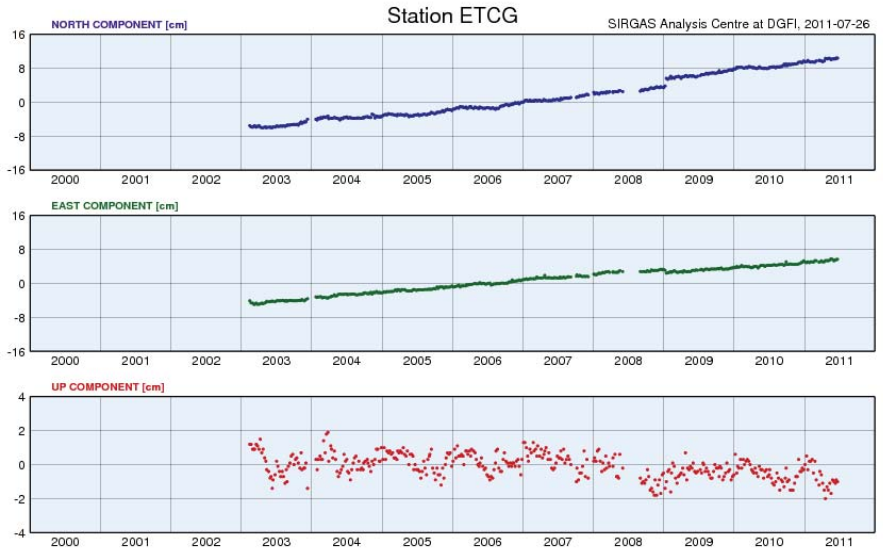

Setting up discontinuities

Station: ETCG 40602M001
Location: Heredia, Costa Rica
Status: active

Coordinates and velocities:

Time series for this station presents discontinuities or trend changes.
Therefore, coordinates and velocities are classified in different periods

Solution:	**SIR11P01**	Solution:	**SIR11P01**
Epoch:	**2005.0**	Epoch:	**2005.0**
Period:	**2009-01-11 – 2011-04-16**	Period:	**2003-02-11 – 2009-01-09**
Geocentric values		**Geocentric values**	
X:	645208.2328 ± 0.0007 m	X:	645208.2376 ± 0.0004 m
Y:	-6249842.1907 ± 0.0031 m	Y:	-6249842.1967 ± 0.0008 m
Z:	1100399.4501 ± 0.0008 m	Z:	1100399.4368 ± 0.0003 m
Vx:	0.0119 ± 0.0003 m/a	Vx:	0.0129 ± 0.0003 m/a
Vy:	0.0049 ± 0.0003 m/a	Vy:	0.0061 ± 0.0003 m/a
Vz:	0.0176 ± 0.0003 m/a	Vz:	0.0155 ± 0.0003 m/a
Ellipsoidal values		**Ellipsoidal values**	
Height:	1193.6232 ± 0.0037 m	Height:	1193.6272 ± 0.0014 m
Latitude:	09° 59' 58.137413'' ± 0.0010	Latitude:	09° 59' 58.136951'' ± 0.0004
Longitude:	-84° 06' 21.229897'' ± 0.0013	Longitude:	-84° 06' 21.229760'' ± 0.0006
V-North:	0.0180 ± 0.0013 m/a	V-North:	0.0161 ± 0.0007 m/a
V-East:	0.0124 ± 0.0013 m/a	V-East:	0.0134 ± 0.0006 m/a
V-Up:	-0.0005 ± 0.0021 m/a	V-Up:	-0.0019 ± 0.0017 m/a

Latest multi-year solution SIR11P01

- Computed by the DGFI as IGS RNAAC for SIRGAS
- Absolute PCV corrections
- Satellite orbits and EOPs wrt IGS05
- Minimum constrained solution (NNR+NNT conditions wrt ITRF)
- Time period:
  02-01-2000 – 16-04-2011;
- Stations:
  229 (296 occupations);
- Reference frame:
  ITF2008, epoch 2005.0;
- Precision of positions at reference epoch:
  ± 0,5 mm (hor), ± 0,9 mm (up);
- Precision of constant velocities:
  ± 0,4 mm/a

VEMOS: Velocity model for SIRGAS

- Reliable station velocities can be computed after two years (at least).
- Applications requiring time-dependent coordinates and relying on stations with less than two years of operation may use a model representing the annual mean station position changes.

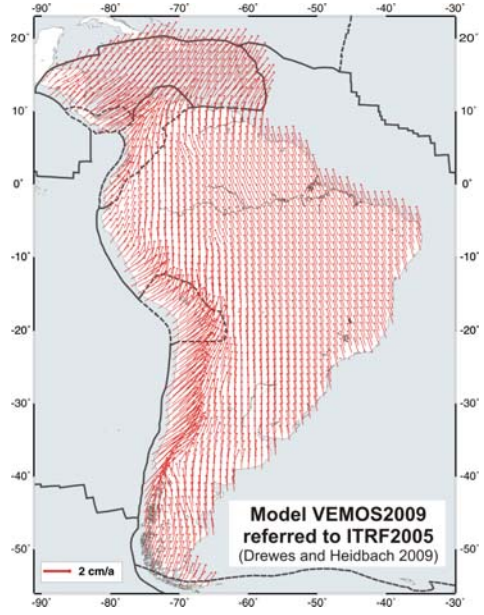

From IGS05 to IGS08: changes in the horizontal position

"*the scale difference between IGS05 and IGS08 (due to the ITRF2005 to ITRF2008 datum shift) will cause a mean decrease of station heights by ~6 mm. The Z translation will accentuate this effect in the Southern hemisphere and attenuate it in the Northern hemisphere. The Z translation will also cause positive North shifts, especially at low latitudes*" (see [IGSMAIL-6354]).

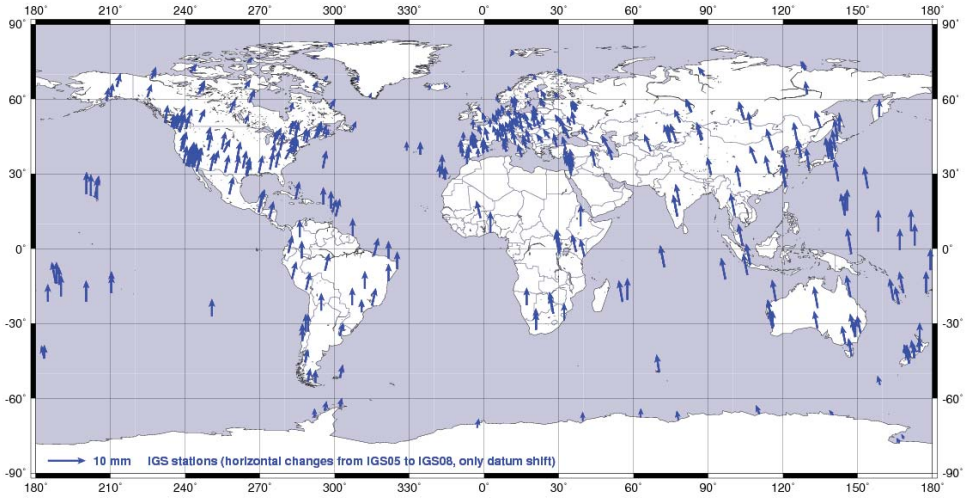

From IGS05 to IGS08: changes in the vertical position

"*the scale difference between IGS05 and IGS08 (due to the ITRF2005 to ITRF2008 datum shift) will cause a mean decrease of station heights by ~6 mm. The Z translation will accentuate this effect in the Southern hemisphere and attenuate it in the Northern hemisphere. The Z translation will also cause positive North shifts, especially at low latitudes*" (see [IGSMAIL-6354]).

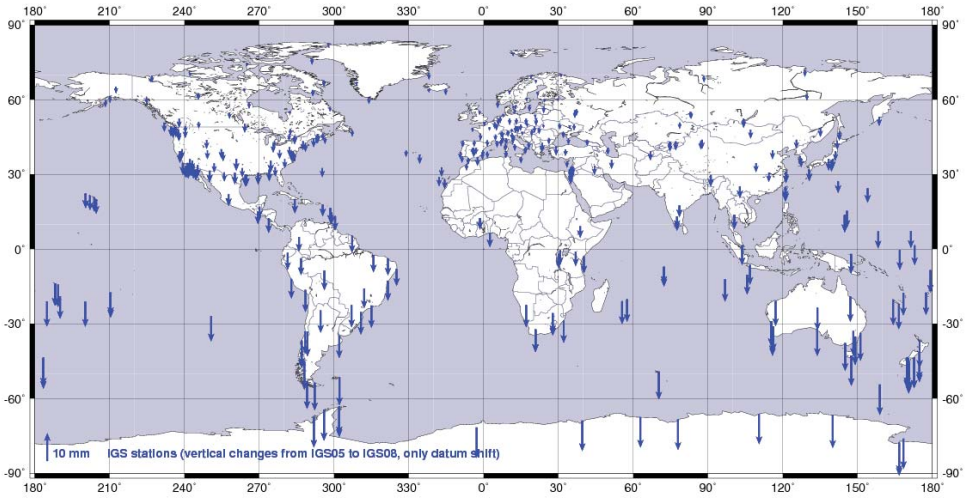

From IGS05 to IGS08

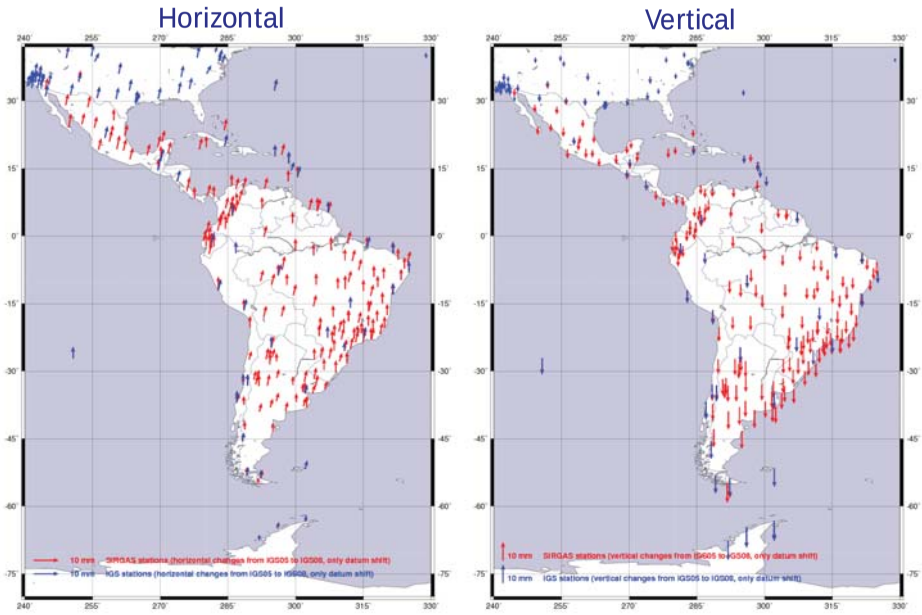

From IGS05 to IGS08

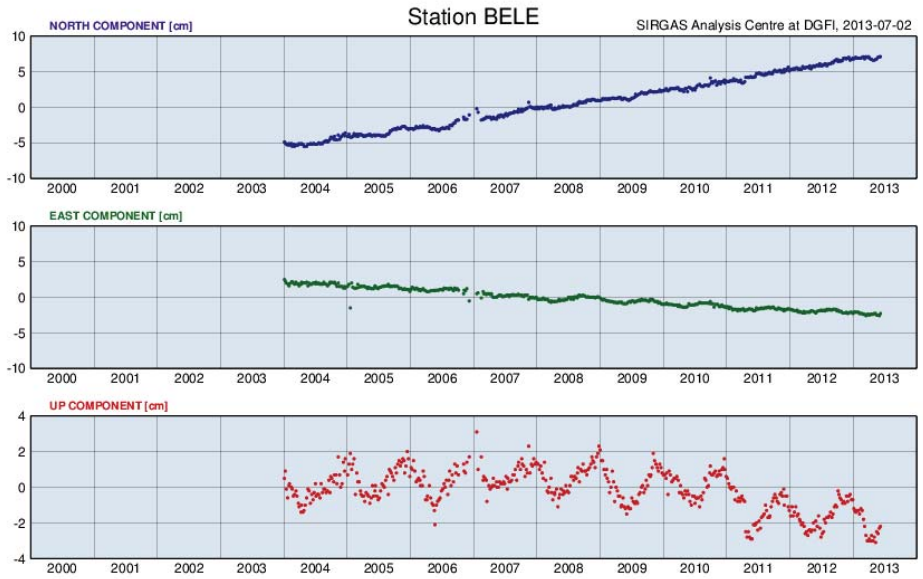

From IGS05 to IGS08

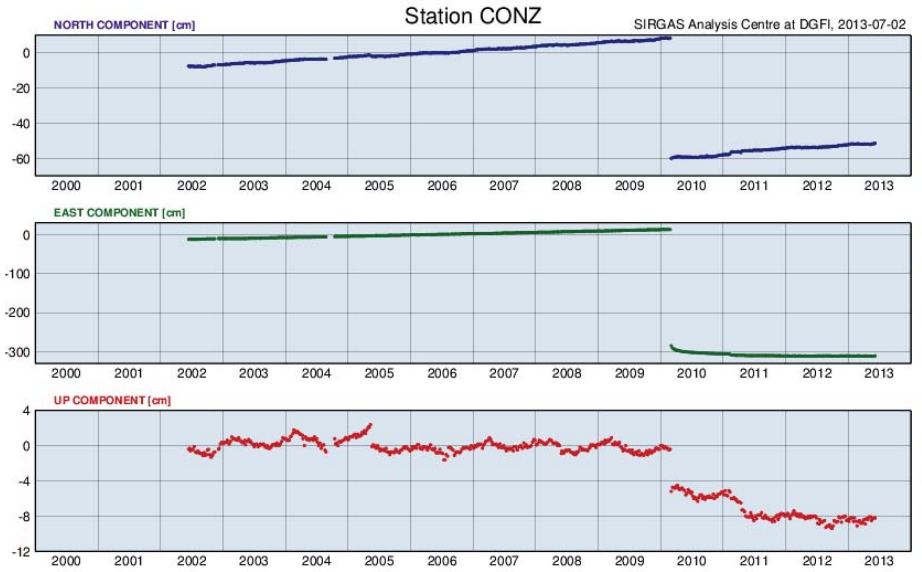

From IGS05 to IGS08

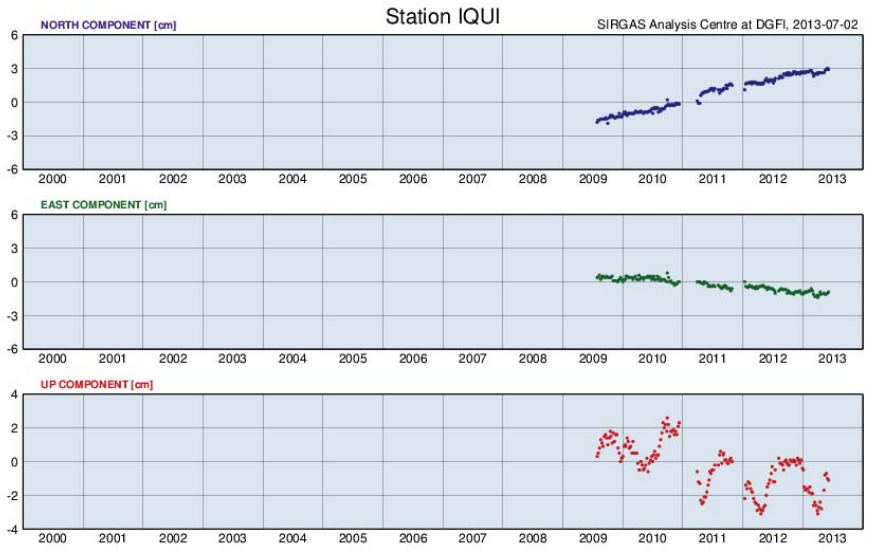

From IGS05 to IGS08

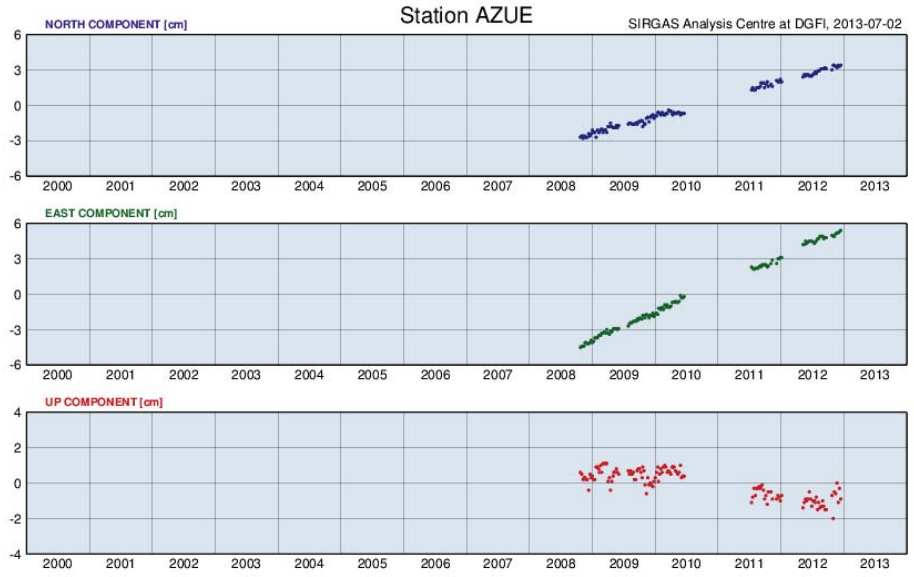

From IGS05 to IGS08

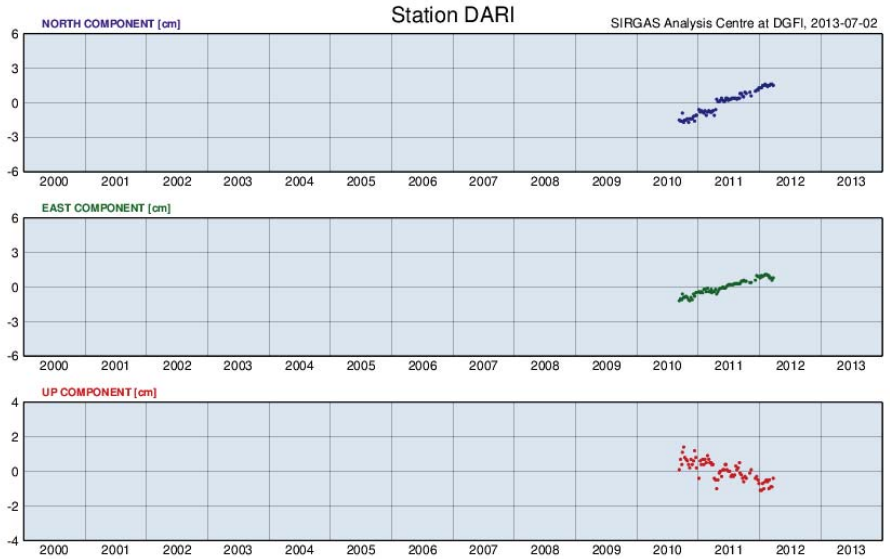

From IGS05 to IGS08

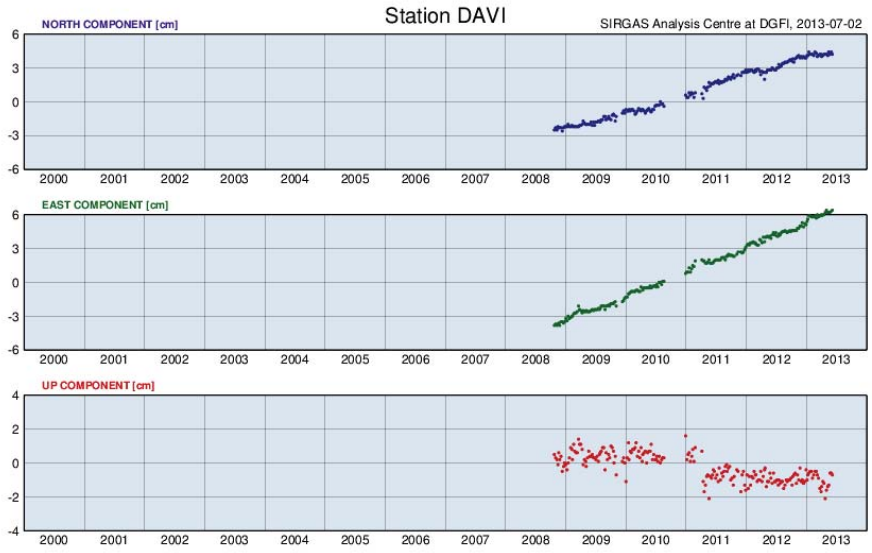

From IGS05 to IGS08

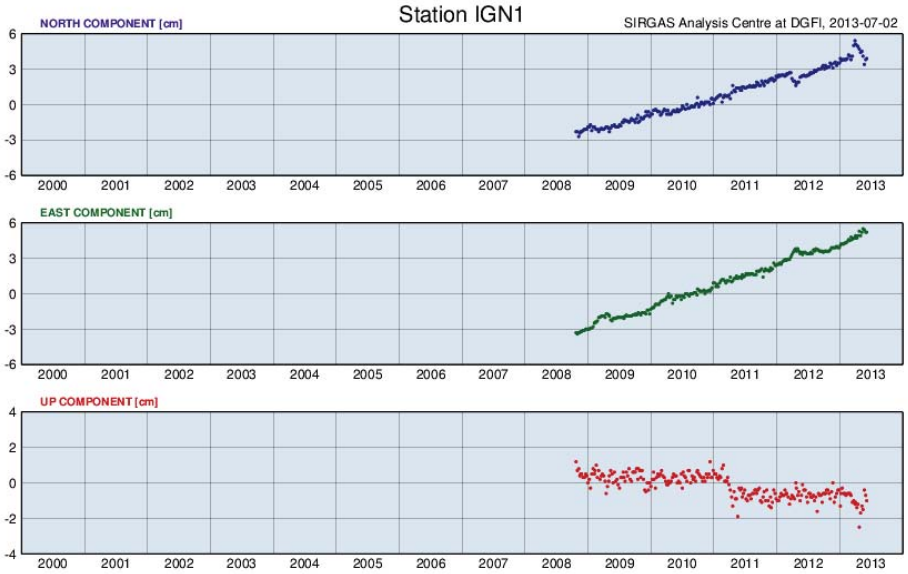

From IGS05 to IGS08

Since the switch to IGS08 reference frame causes a discontinuity of some millimetres in the station position time series, the SIR11P01 solution is the last one that can be computed with the available data. A new multi-year solution of the SIRGAS reference frame **demands the re-processing of all previous weekly solutions using the IGS08 frame**.

Horizontal

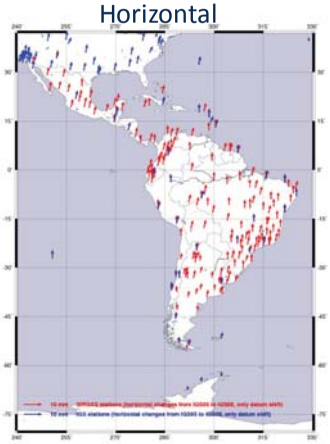

Vertical

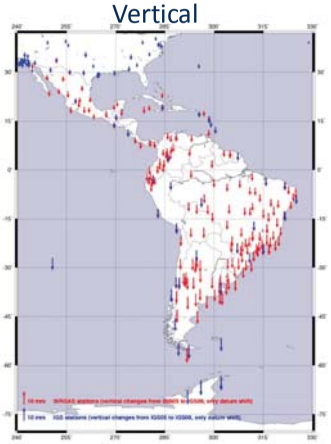

Present challenges: Constant velocities are highly dependent on the considered time period

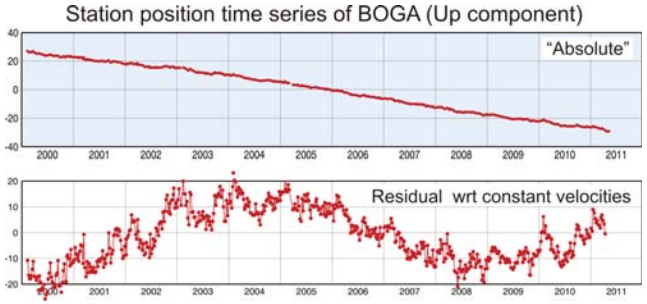

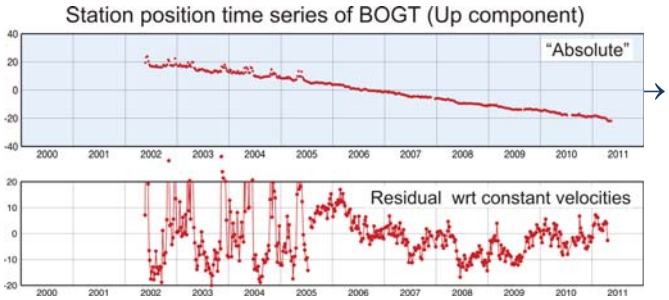

Estimates for vertical velocity of BOGA:

Feb 2000 to Jun 2004
-0,0419 ± 0,0001 m/y

Jun 2004 to Dec 2008
-0,0612 ± 0,0002 m/y

Feb 2000 to Apr 2011
-0,0503 ± 0,0001 m/y

→ **<u>Requirement</u>: Longer time series to increase the reliability of position variation estimates.**

Present challenges: omission of seasonal position variations

Most of the SIRGAS-CON stations present significant seasonal position variations (mainly in the Up component). These variations are ignored when constant velocities (linear position changes) are computed.

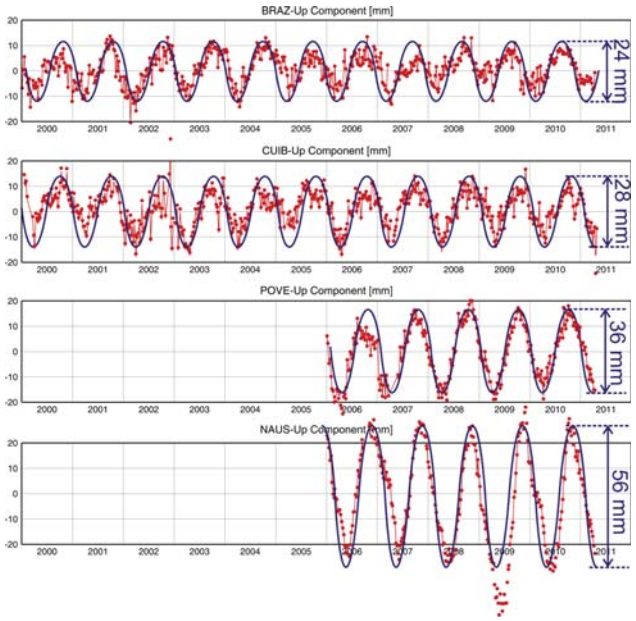

Amplitude (cm) of seasonal variations in the height component of the SIRGAS-CON stations

SIRGAS stations with seasonal movements with amplitude larger than 2 cm

→ **Requirement: analysis and modelling of seasonal station positions variations within the reference frame computation.**

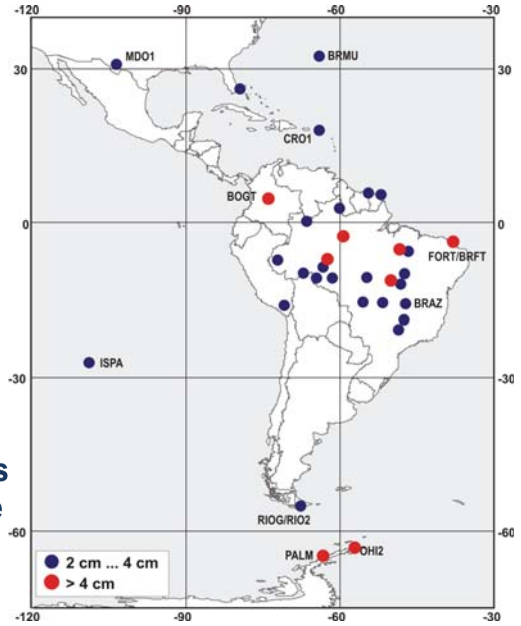

Present challenges: modelling reference frame deformations due to seismic events

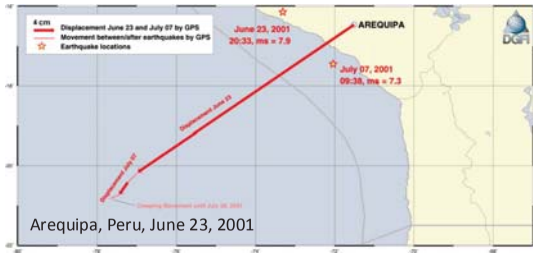

Arequipa, Peru, June 23, 2001

Guatemala, November 7, 2012

Baja California, Mexico, April 4, 2010

El Maule, Chile, Mexico, February 27, 2010

Present challenges: modelling reference frame deformations due to seismic events

SIRGAS stations strongly affected by earthquakes since 2001

Location	Date	Mw	Coordinate change	Affected stations
Concepción, Chile	2011-02-12	6,1	2 cm	CONZ
Mexicali, Mexico	2010-04-04	7,2	23 cm	MEXI
Chile	2010-02-27	8,8	1 to 305 cm	23 stations
Costa Rica	2008-01-08	6,1	2 cm	ETCG
Martinique	2007-11-29	7,4	1 cm	BDOS, GTK0
Copiapo, Chile	2006-04-30	5,3	2 cm	COPO
Tarapaca, Chile	2005-06-13	7,9	6 cm	IQQE
Managua, Nicaragua	2004-10-09	6,9	1 cm	MANA
Arequipa, Peru	2001-06-23	8,4	52 cm	AREQ
El Salvador	2001-02-13	7,8	4 cm	SSIA

Present challenges: not only co-seismic jumps, but also changes in the "normal" movement

Usual approximation: many short time intervals Δt_i combined with a sequence of constant velocities V_i

→ $\Delta X = \Sigma(V_i * \Delta t_i)$

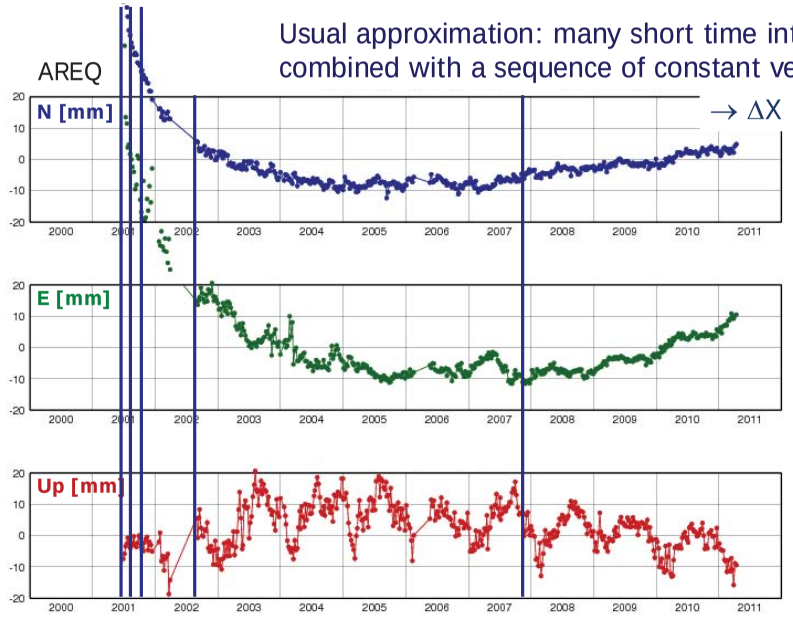

Comparison of pre-seismic and post-seismic (constant) velocities (the first year after)

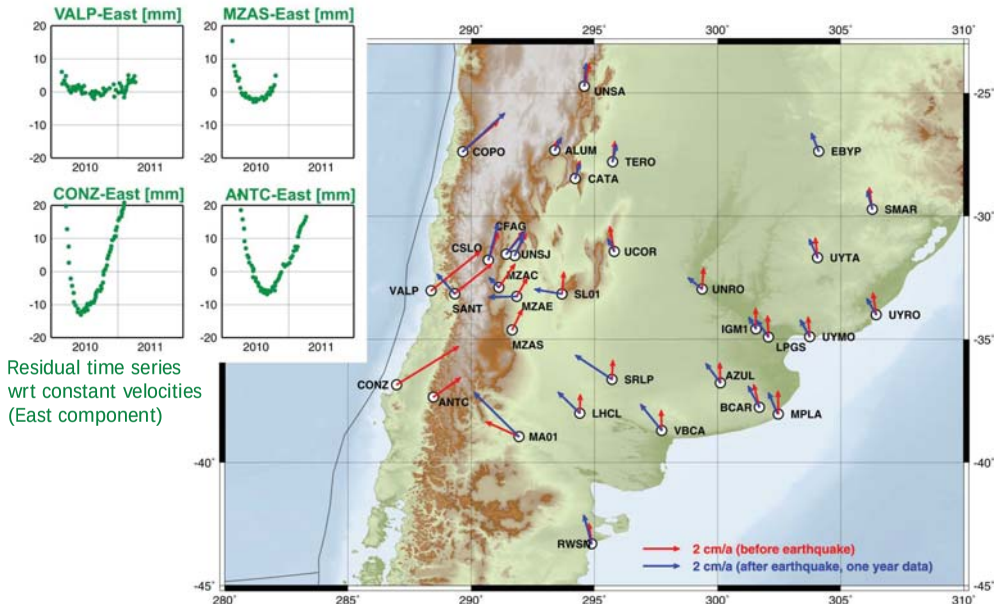

On-going activities to keep undated the SIRGAS reference frame

1) Second reprocessing of the entire SIRGAS reference frame:
   - New computation of daily normal equations between January 1, 1997 until December 31, 2012
   - Including the new geodetic standards outlined by the IERS (International Earth Rotation and Reference Systems Service) and the IGS (International GNSS Service);
   - Inclusion of GLONASS measurements;
2) Modelling of seasonal movements at the combination level of the weekly solutions;
3) Computation of deformation models derived from discrete (weekly) station positions to incorporate seismic discontinuities in the computation of the reference frame.

Final comments

- SIRGAS is the regional densification of the ITRF in Latin America and the Caribbean.
- SIRGAS is the backbone for all projects based on the generation and use of geo-referenced data in a national as well in an international level.
- Besides to provide the reference coordinates for the development of practical applications such as engineering projects, digital administration of geographical data, geospatial data infrastructures, global navigation, etc., SIRGAS is also the platform for a wide range of scientific researches related to global change and geodynamics.
- SIRGAS is also a capacity building platform in the Latin American and Caribbean region.

6. Crustal deformation: Observation and Modelling
6.1 Earth structure and geodynamic processes

The Earth's structure
(radial stratification)

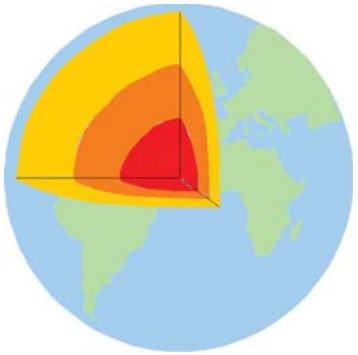

Important geophysical parameters:

- Mass density ρ as a function of depth (surface: 2.6 g/cm^3, average: 5.5 g/cm^3)
- Gravity **g**(r) as a function of the density distribution within the Earth
- Pressure p(r) as a function of density and gravity distribution within the Earth
- Elasticity parameters as a function of depth (e.g. Lamé parameters λ and μ)
- Temperature T as a function of depth

Disciplines: seismology, gravimetry, thermodynamics, palaeomagnetism

Principle of seismology

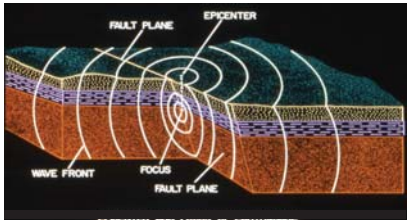

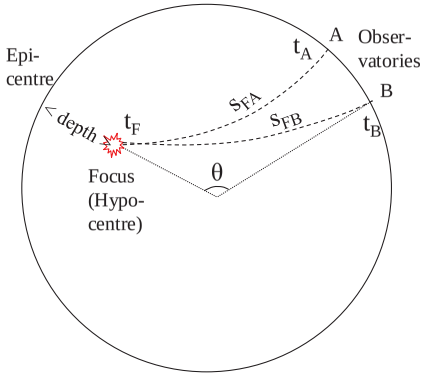

Origination of earthquakes

Earthquakes are caused by the release of accumulated stress along faults.

The released energies propagate as elastic waves in the solid Earth.

Observations: wave arrival times t_O at the observatories

To be adjusted:
- travel time $t_O - t_F$,
- relative positions θ_F,
- event time t_F,
- travel path $s_{F\text{-}O}$,
- wave velocities v along the path $s_{F\text{-}O}$ (a function of depth)

Seismic waves

P-waves **S-waves**

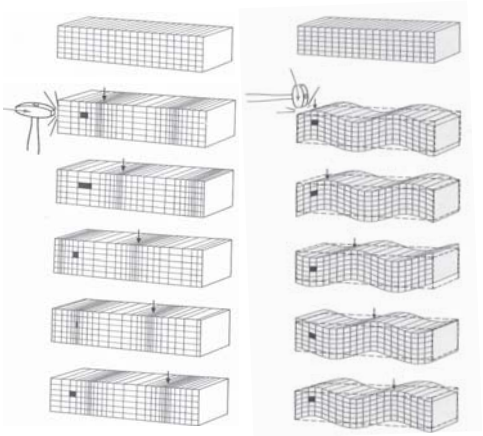

$$v_P = \sqrt{\frac{\lambda + 2\mu}{\rho}} \qquad v_S = \sqrt{\frac{\mu}{\rho}}$$

(Lamé parameters λ and μ)

Example elasticity parameters

Material	λ [10^9 Nm^{-2}]	μ [10^9 Nm^{-2}]
Steel	80	80
Crustal rocks	18	25
- Lime rock		
- Granite	< 0.1	20
- Gabbro	37	44
- Peridotite	50	60
Gum	1.3	0.3
Water	2	0

Examples ($\rho_{Peridotite}$ = 3.2 g/cm^3)

Peridotite: v_P = 7.3 km/s, v_S = 4.3 km/s

Water: v_P = 1.4 km/s, v_S = 0.0 km/s

Magnitude and statistics of earthquakes

Magnitude (Richter 1935):
Local magnitude M_L is the base-10 logarithm of the amplitude of a short-period seismometer of amplification 2800 in a distance of 100 km.

Moment magnitude scale (Hanks & Kanamori 1979):

$M_W = {}^2/_3 \log_{10} \cdot M_0 - 10.7$
(subscript w = mechanical work, M_0 = seismic moment [N·m])

Both scales are similar, they are identical for M = 5.0)

Magnitude	Events/year	Energy
≥ 8.0	1	50 %
7.0 … 7.9	18	35 %
6.0 … 6.9	120	10 %
5.0 … 5.9	800	3 %
4.0 … 4.9	6200	1 %
3.0 … 3.9	49000	< 1 %
2.0 … 2.9	300000	<< 1 %

Depth	No.	Energy
0 … 70 km	30 %	85 %
70 … 300 km	45%	12 %
300 … 720 km	25%	3%

Geographical distribution of earthquakes

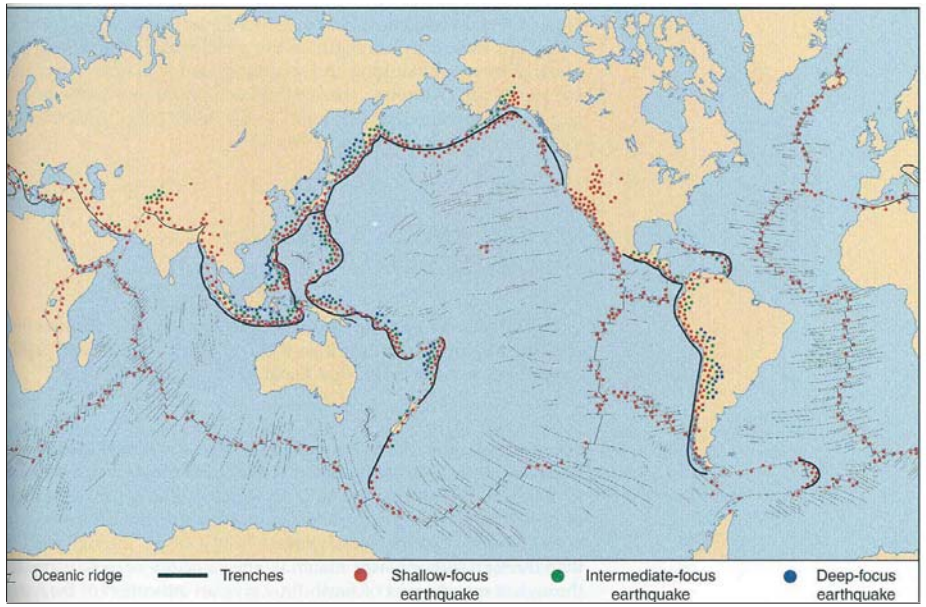

Seismic wave propagation

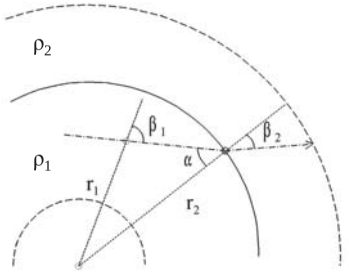

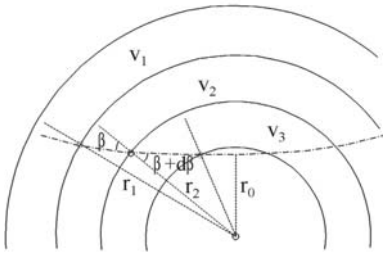

Refraction at spherical boundary surfaces

$$\frac{r_1}{r_2} = \frac{\sin\alpha}{\sin(180° - \beta_1)} = \frac{\sin\alpha}{\sin\beta_1}$$

$$\frac{\sin\alpha}{\sin\beta_2} = \frac{v_1}{v_2}; \quad \frac{r_1 \sin\beta_1}{r_2 \sin\beta_2} = \frac{v_1}{v_2}$$

The propagation equation fixes the geometry of the wave path assuming velocities as a function of the radius

$$\frac{r \sin\beta}{v(r)} = const.$$

Fundamental equation of seismology: The wave path is circular in a radially stratified Earth.

Propagation of waves

Nomenclature according to propagation path

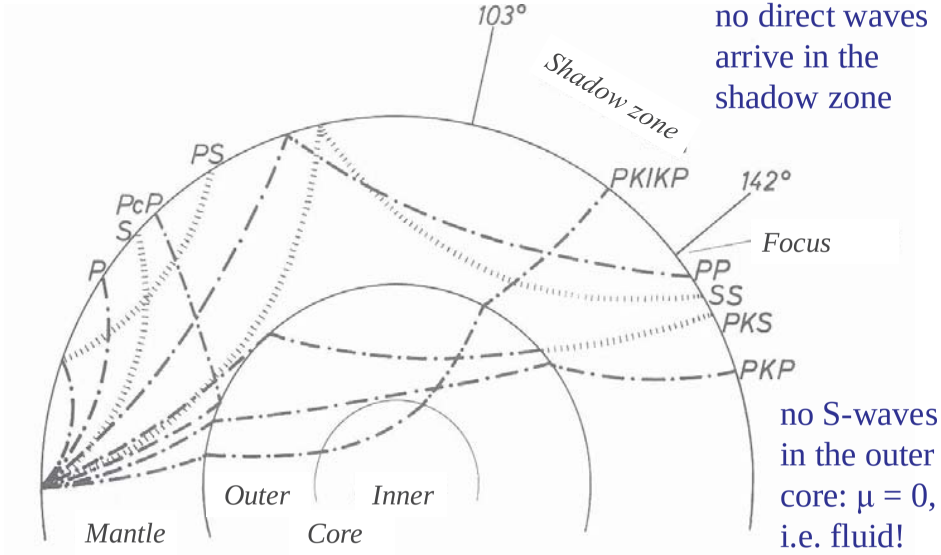

no direct waves arrive in the shadow zone

no S-waves in the outer core: μ = 0, i.e. fluid!

Classical Earth stratification from seismology

Jeffreys 1939, Gutenberg 1958

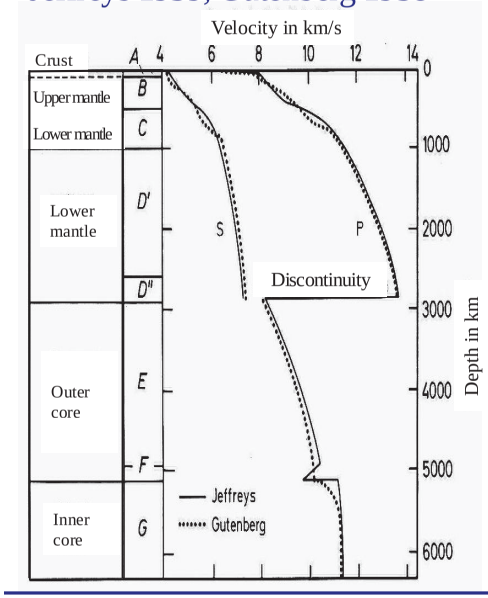

Derived parameters

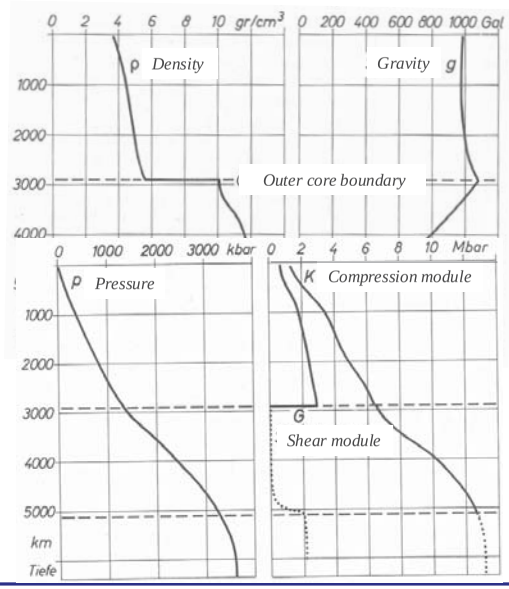

Preliminary Earth Reference Model (PREM)

(Dziewonski/Anderson 1981: Earth mass density from seismology)

Denomination	Radius	Density [g/cm³]
Inner Core	0 ... 1222	13,09 ... 12,76
Outer Core	1222 ... 3480	12,17 ... 9,90
Lower Mantle	3480 ... 5701	5,57 ... 4,38
Transition Zone	5701 ... 6151	3,99 ... 3,44
LVZ (LID)	6151 ... 6347	3,36 ... 3,38
Lower Crust	6347 ... 6356	2,90
Upper Crust	6356 ... 6368	2,60
Oceans	6368 ... 6371	1,02

Principle of gravimetry / Earth gravity field

The Earth gravity field is nowadays determined by a combination of satellite gravity field missions GRACE (Gravity Recovery and Climate Experiment) and GOCE (Gravity Field and Steady-State Ocean Circulation Experiment) with airborne / terrestrial gravimetry results.

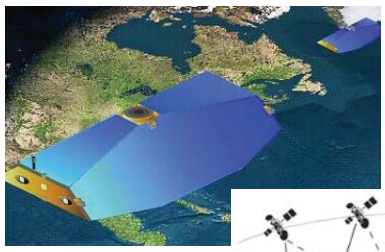

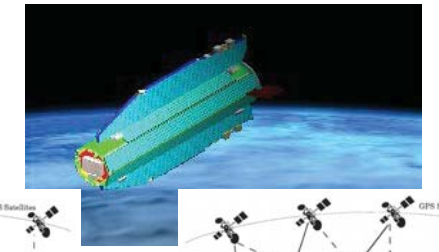

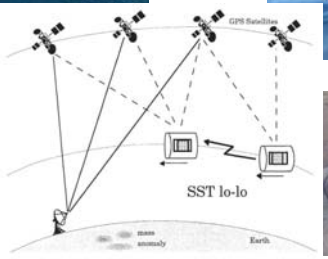

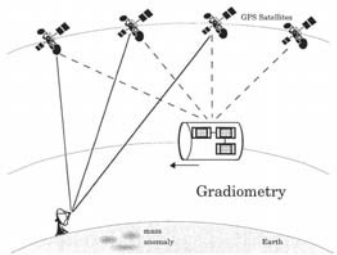

Representation of the gravity field by the geoid

e.g. Gravity field models EIGEN (GFZ Potsdam, Foerste et al.)

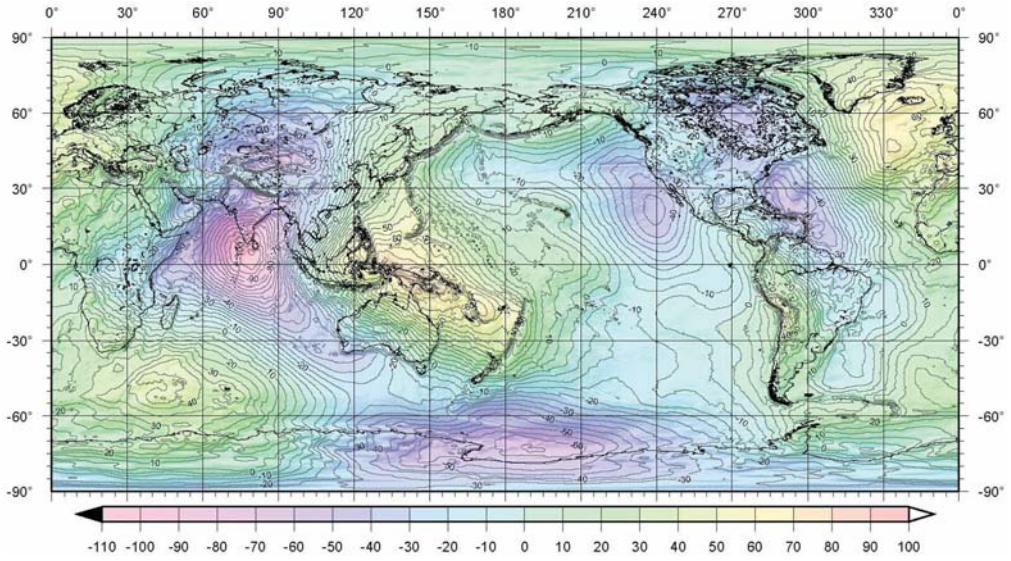

Inversion of the gravity field into mass structures

The in version of the gravity field into the mass distribution inside the Earth is not possible without constraints (improperly posed problem).

Introducing the structure from seismology (PREM) as constraints, we may estimate the mass irregularities at the layer boundaries.

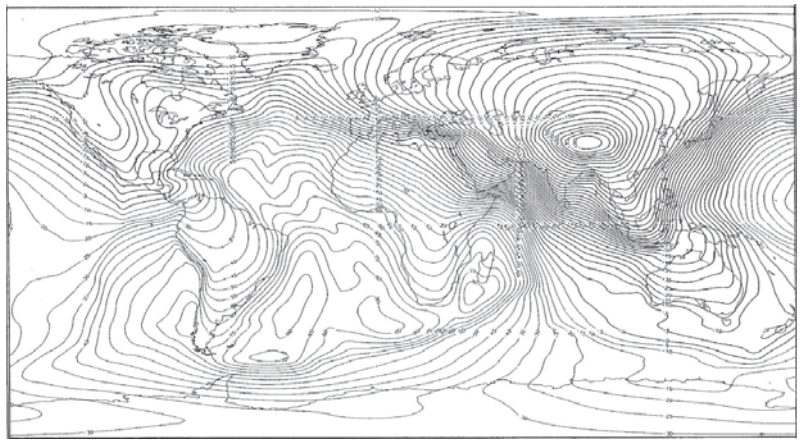

Lithosphere part of the geoid from an inversion into 4 layers of the Earth

Inversion of the gravity field into Earth structure

Earth's mantle part of the geoid from an inversion into a four layers model of the Earth

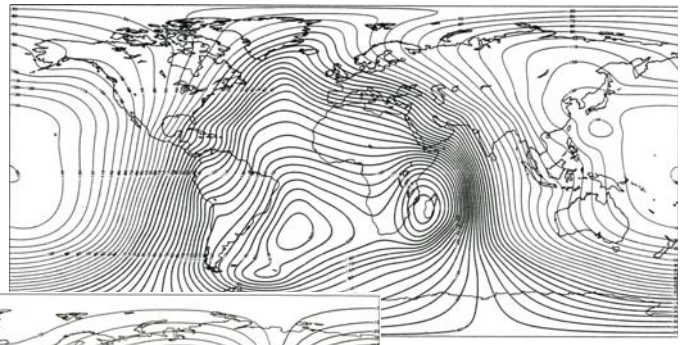

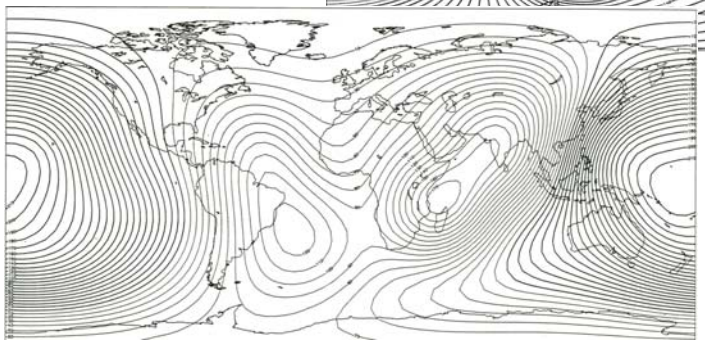

Earth's core part of the geoid from an inversion into a 4-layers model of the Earth

Principle of thermodynamics (Heat flow)

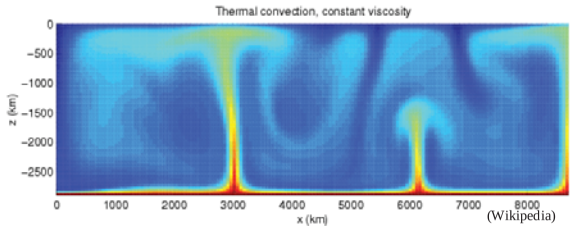

Heat flow:

$Q = -\lambda \; grad \; T$

λ [J m^{-1}s^{-1}K^{-1}] = heat conductivity

$div \; Q = c \cdot \rho \cdot dT/dt$

c [J g^{-1} K^{-1}] = specific heat

Thermal conduction equation:

$$\frac{dT}{dt} = \frac{\lambda}{(c \cdot \rho)} div \; grad \; T = \frac{\lambda}{(c \cdot \rho)} \Delta T = \kappa \, \Delta T$$

Δ = Laplace operator

κ = thermal diffusivity

Material	ρ [10^6 g m^{-3}]	Λ [J s^{-1} m^{-1} K^{-1}]	c [J m^{-1} K^{-1}]	κ [10^6 m^2 s^{-1}]
Water	1	0.6	4.2	0.14
Glas	2.5	1.1	0.8	0.55
Rocks	2.2 … 3.2	2 … 4	0.8 … 1.2	0.8 … 1.8
Silver	10.5	410	0.23	170

Measurement of heat flow

Field measurements: grad T = (T_{below} – T_{above}) / (h_{below} – h_{above})

In the laboratory: λ (experimentally at drill core samples)

Spherical harmonics development (degree 12) of measurements

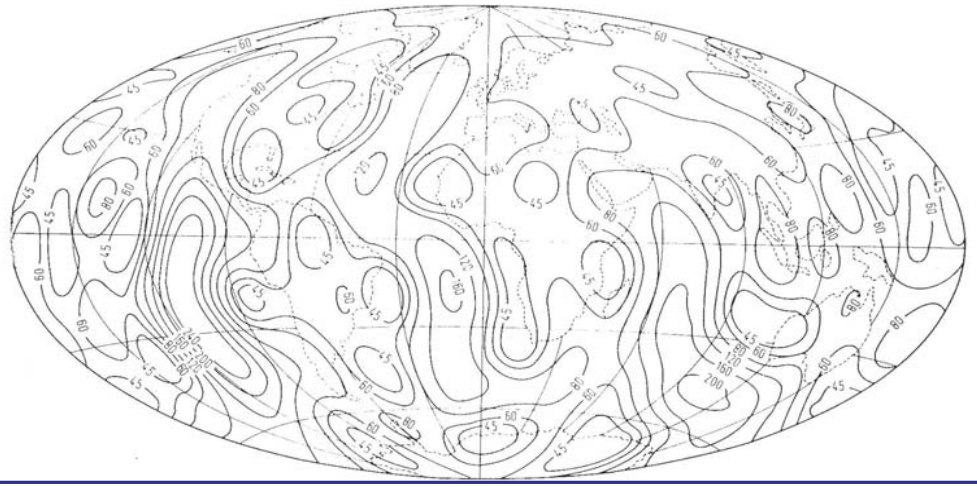

Thermal definition of the lithosphere

The lithosphere (Greek *lithos* = rocky) is the solid layer of the upper Earth. The lower boundary is defined by the melting point of rocks.

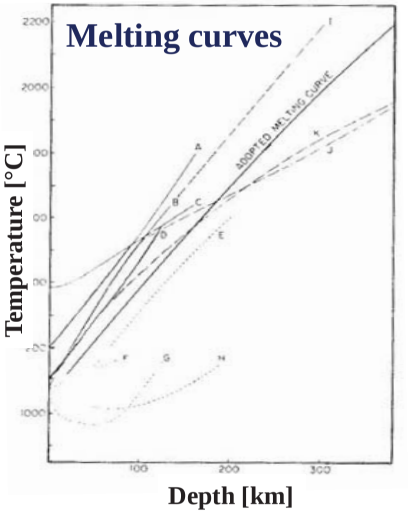

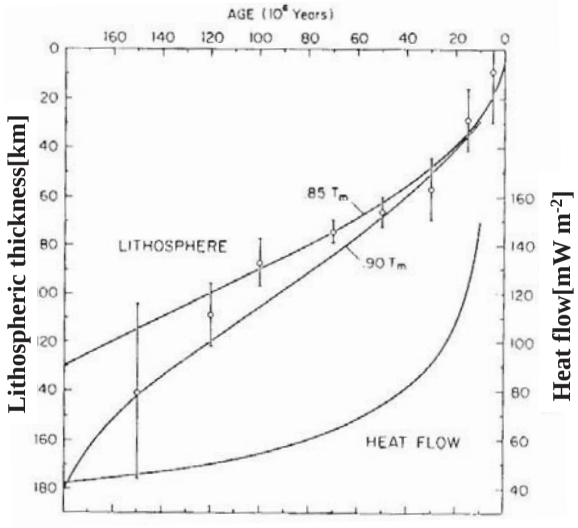

Thickness of the lithosphere

Result from heat flow measurements and conversion via melting rock temperature into depth

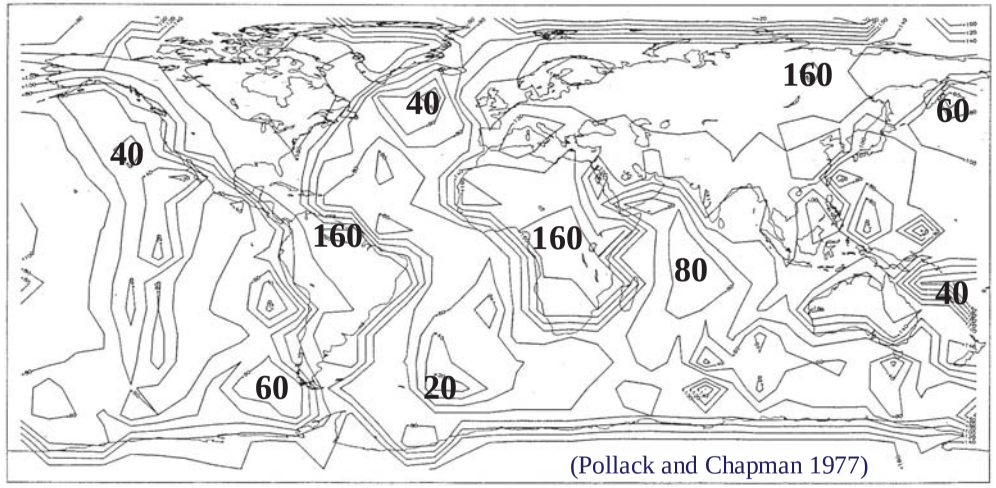

(Pollack and Chapman 1977)

Principle of palaeomagnetism

The magnetic dipole field

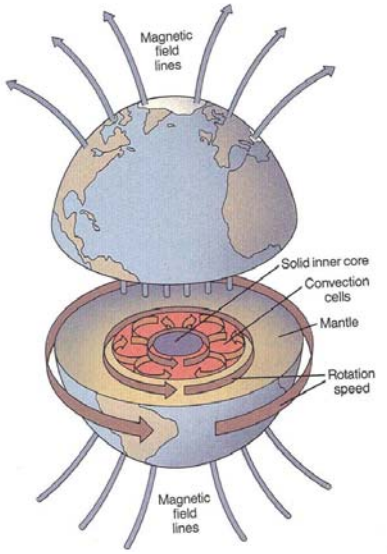

The Earth's magnetic field extends from the inner core to where it meets the solar wind. It is approximately a magnetic dipole field tilted at an angle of 10° with respect to the rotation axis.

Magnetism of rocks

Rocks can be permanently magnetised by the Earth's magnetic field.

The **Curie point** is where a magnetic mineral crystal melts enough to loose the polarity of its magnetism,

e.g. magnetite (Fe_3O_4) at 580°C,

ferric trioxide (Fe_2O_3) at 680°C.

Geomagnetic reversals

The Earth's magnetic field inverts occasionally its polarisation.

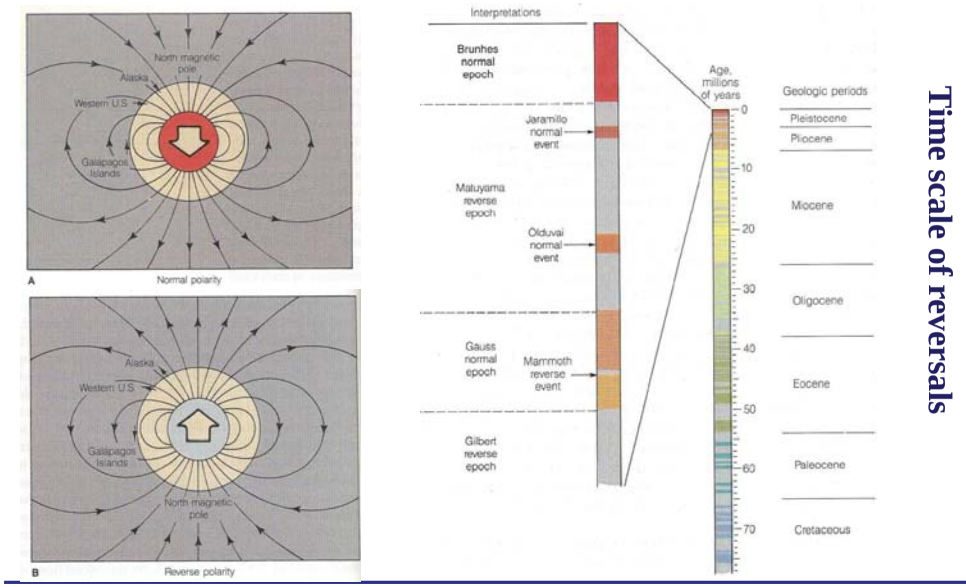

Magnetisation of magmatic rocks

Rising Magma takes the effective polarisation of the Earth's magnetic field when cooling down to the Curie point.

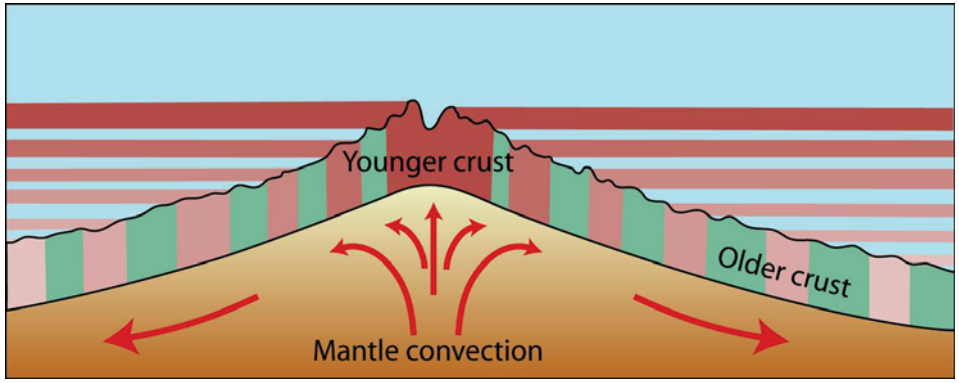

"Normal" and "inverse" polarised rocks are situated side by side. This happens along all the spreading ridges of the Earth.

Magnetisation of magmatic rocks

Pattern of polarised magnetic rocks in oceanic ridges

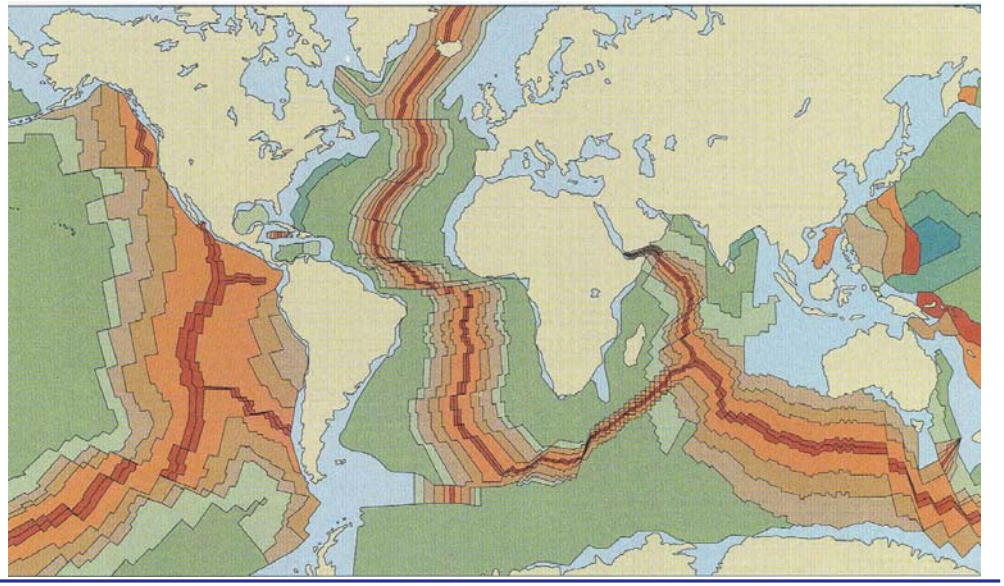

Summary of the Earth's structure

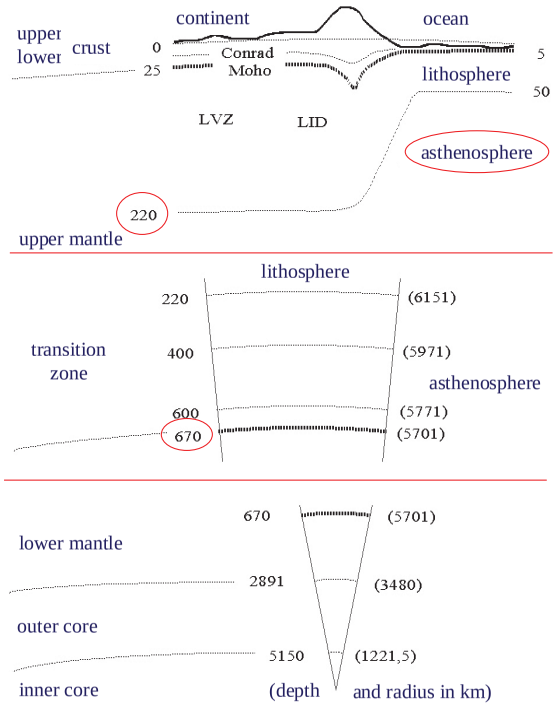

The nomenclature of the stratification has changed due to the modern studies of composition, dynamics and physical properties.

The lithosphere includes the crust and parts of the upper mantle.

The asthenosphere includes the rest of the lower mantle.

Geodynamic processes

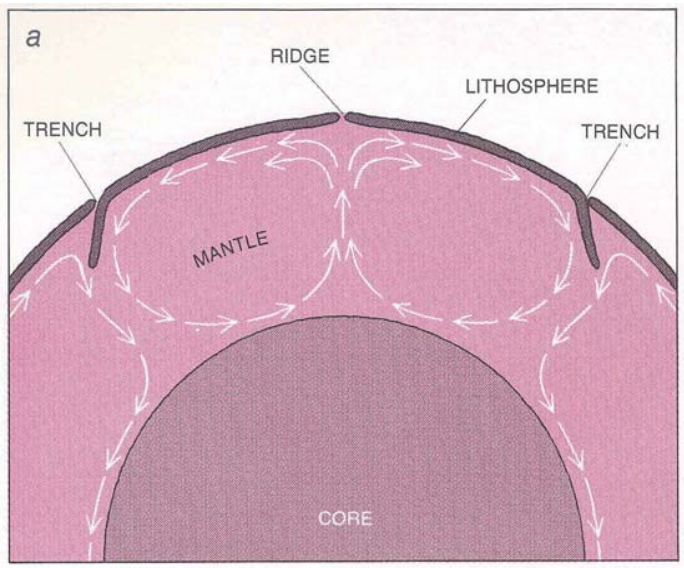

A principal dynamic process in the Earth is the convection in the viscous mantle.

Masses heated by the Earth's core are rising in the mantle and spreading aside when cooled beneath the lithosphere. The streams separate the lithosphere forming diverging ridges.

The lithosphere subducts into the asthenosphere forming trenches.

Geodynamic process in the Atlantic

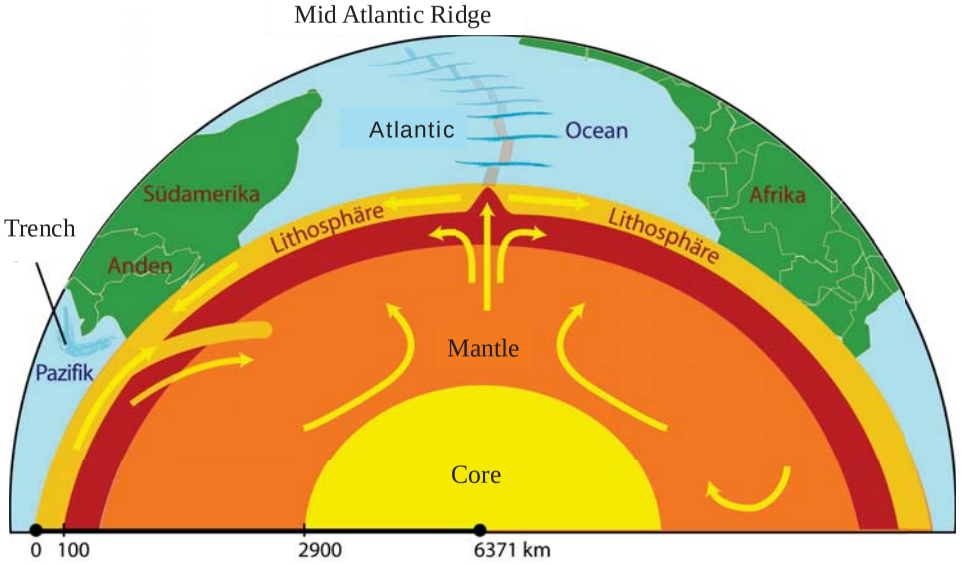

The Mid Atlantic Ridge is a spreading zone between America and Africa

6.2 Plate tectonics and plate kinematics

Structure of the lithosphere

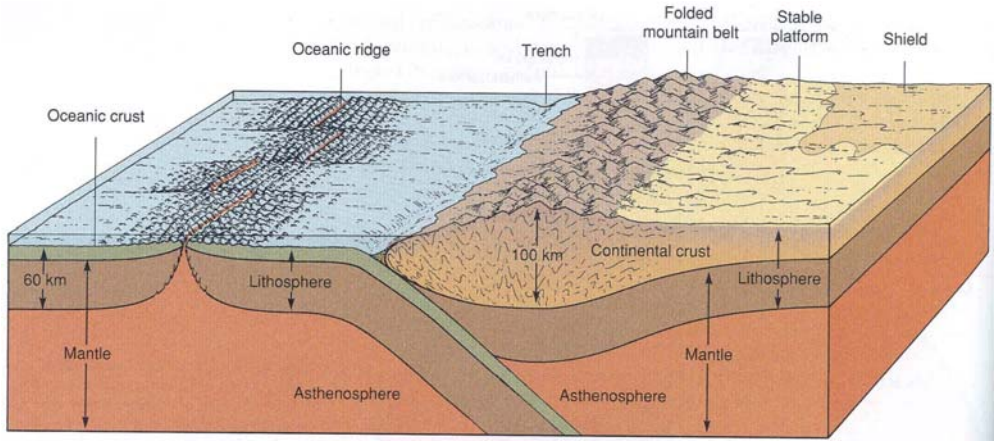

Dynamics: Oceanic ridge spreading, lithosphere subduction, collison

Driving forces of plate tectonics

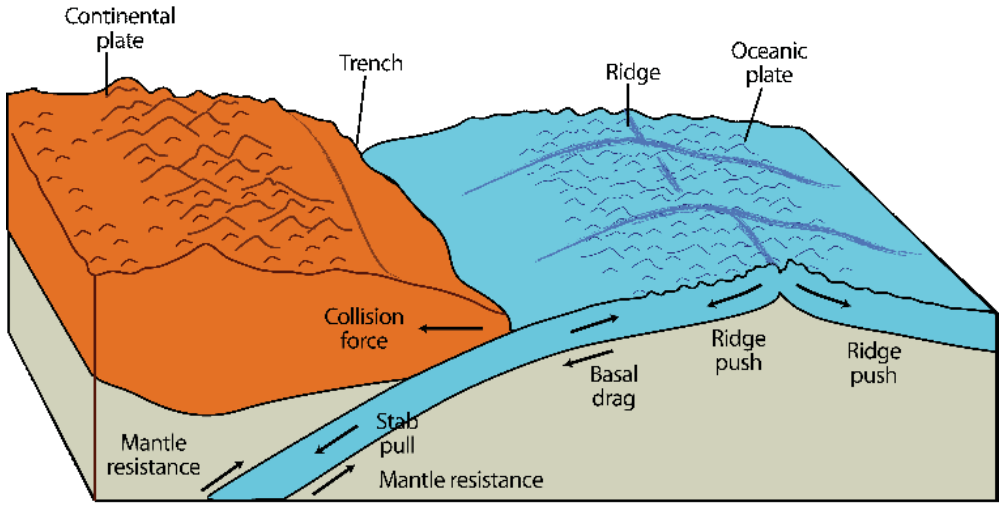

+ Slab pull − Resistence − Collision + Drag + Ridge push

Modelling plate kinematics

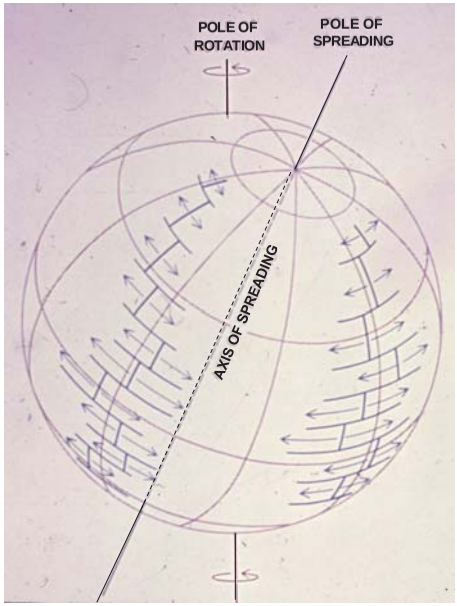

Theorem of Euler: A straight motion on a sphere can be described as a rotation around a geocentric axis.

To determine the rotation axis and the rotational velocity we have three geophysical observation types:

- Spreading rates at oceanic ridges
- Azimuths of spreading ridges
- Azimuths of seismic faults

and four geodetic observation types:

- Very Long Baseline Interferometry
- Global navigation satellite systems
- Satellite laser ranging
- Doppler satellite radio-positioning

Spreading velocities at oceanic ridges

Method of spreading rates (velocities) from magnetic reversals

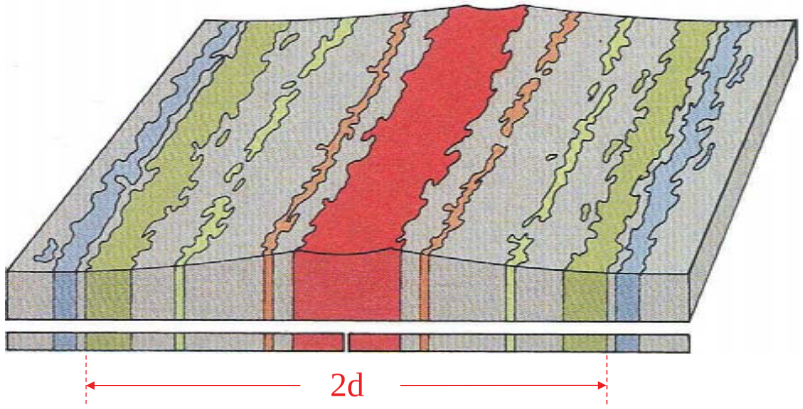

One determines the age of the magnetic stripes (normal or inverse), measures the distance between those of the same age and computes the velocity v = d/t.

Azimuths of oceanic ridge spreading

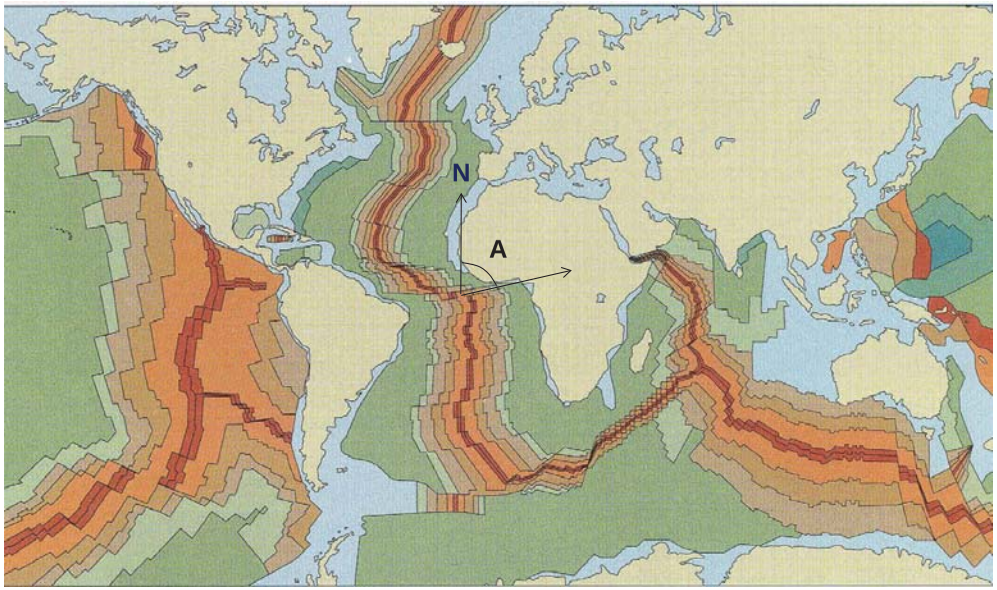

Azimuths of seismic faults: Fault plane solution

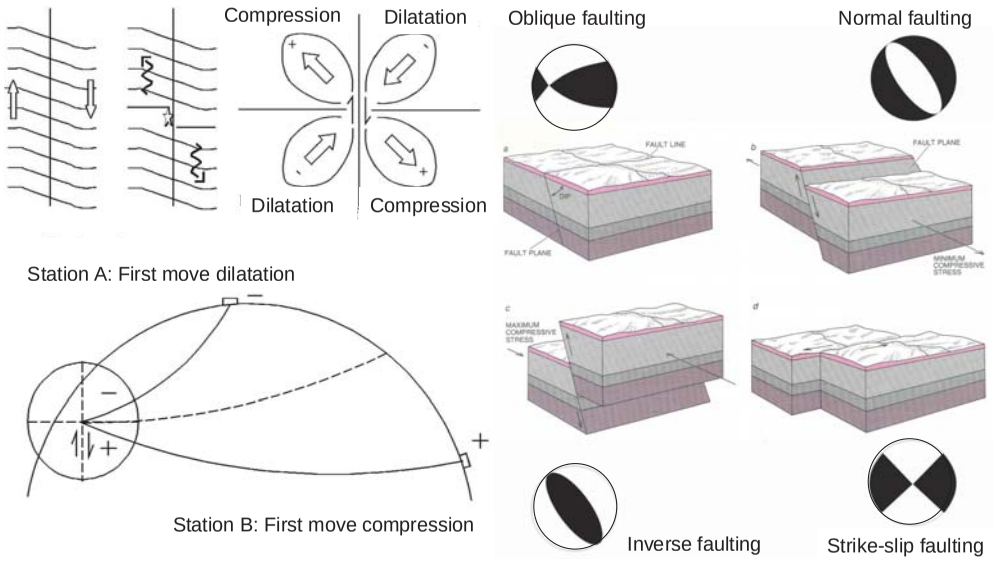

The first move of the seismograph indicates the direction of motion

Fault plane solutions: Example Mediterranean

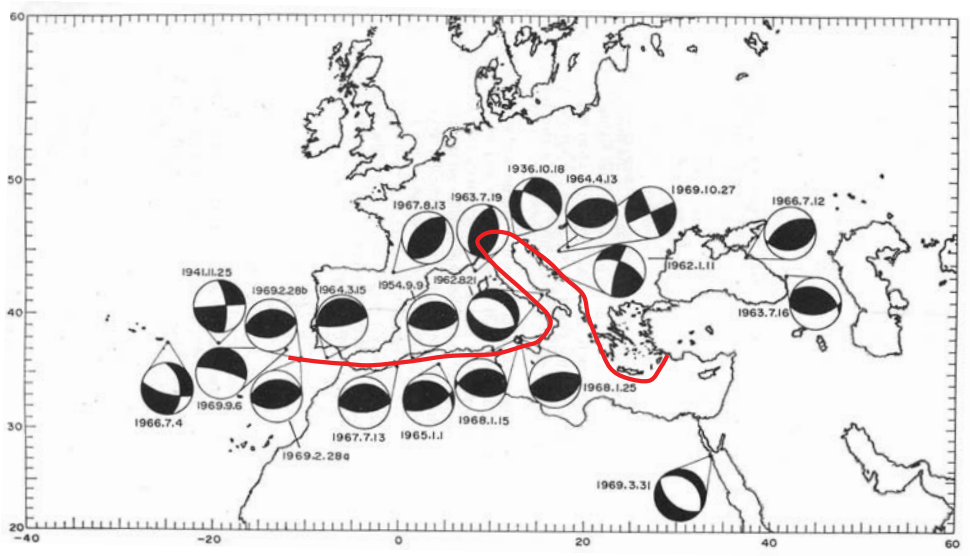

Inverse faulting along the Eurasian – African plate boundary

Modelling of plate kinematics

Theorem of Euler: each differential motion of an entire spherical cap can be described mathematicaly by one centric rotation:

$$\mathbf{dX}/dt = \Omega \times \mathbf{X}$$

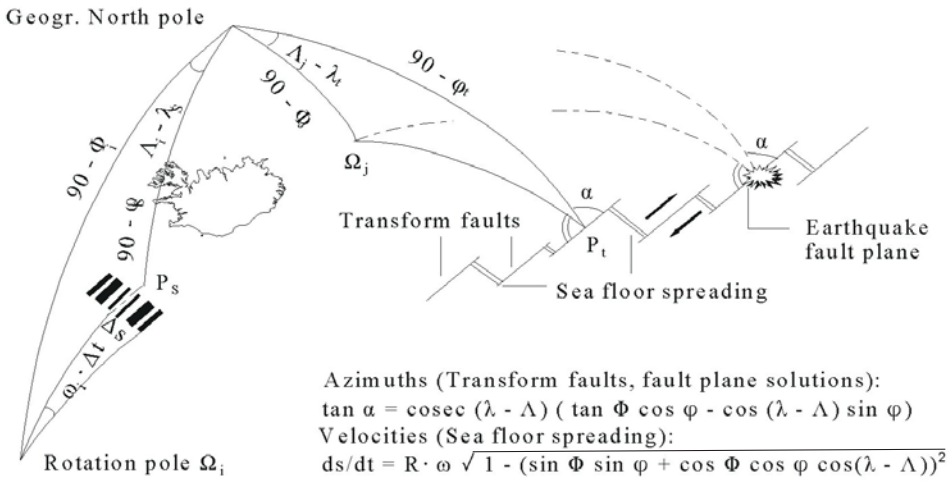

Azimuths (Transform faults, fault plane solutions):

$$\tan \alpha = \operatorname{cosec}(\lambda - \Lambda)\,(\tan \Phi \cos \varphi - \cos(\lambda - \Lambda) \sin \varphi)$$

Velocities (Sea floor spreading):

$$ds/dt = R \cdot \omega \sqrt{1 - (\sin \Phi \sin \varphi + \cos \Phi \cos \varphi \cos(\lambda - \Lambda))^2}$$

Geologic-geophysical plate model NNR NUVEL-1A

Observations of the plate model NUVEL-1A (De Mets et al. 1990)

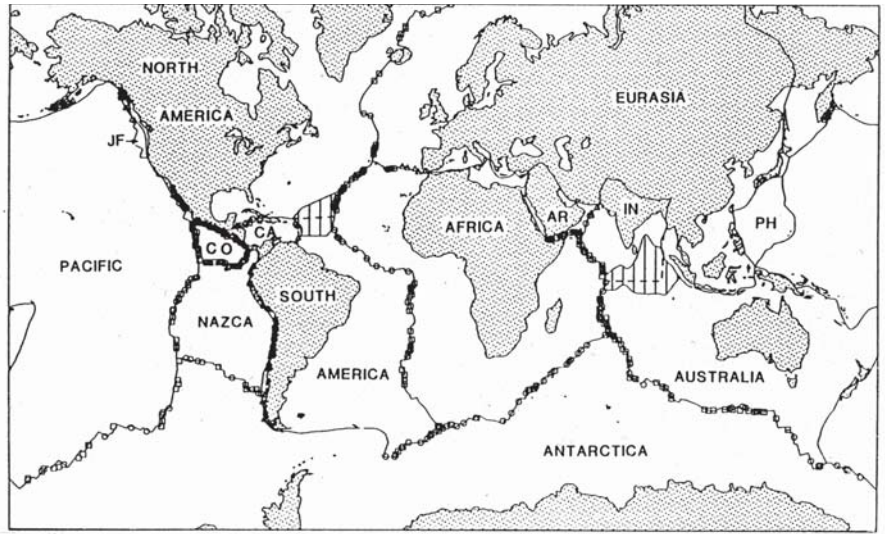

277 extensions, 121 fault azimutes, 724 spreading rates = 1122 in total

Geologic-geophysical plate model NNR NUVEL-1A

Plate name	Φ [°]	Λ[°]	ω[°/ Ma]
Africa	50.5740	286.0407	0.2909
Antartica	62.9943	244.2353	0.2383
Arabia	45.2329	355.5436	0.5455
Australia	33.8532	33.1708	0.6461
Caribbean	25.0052	266.9898	0.2143
Cocos	24.4856	244.2414	1.5103
Eurasia	50.6195	247.7258	0.2337
India	45.5102	0.3436	0.5453
N. America	-2.4280	274.1002	0.2069
Nazca	47.8005	259.8728	0.7432
Pacific	-63.0451	107.3271	0.6409
S. America	-25.3483	235.5830	0.1164

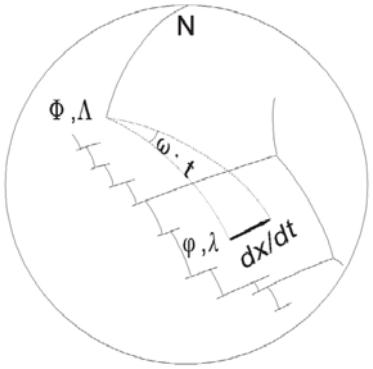

With rotation pole (Φ, Λ) and velocity (ω) you can compute velocities (d**x**/dt) of any point on the Earth.

Geologic-geophysical plate model NNR NUVEL-1A

General motion and plate rotation poles in the SIRGAS region (ω is positive in clockwise rotation).

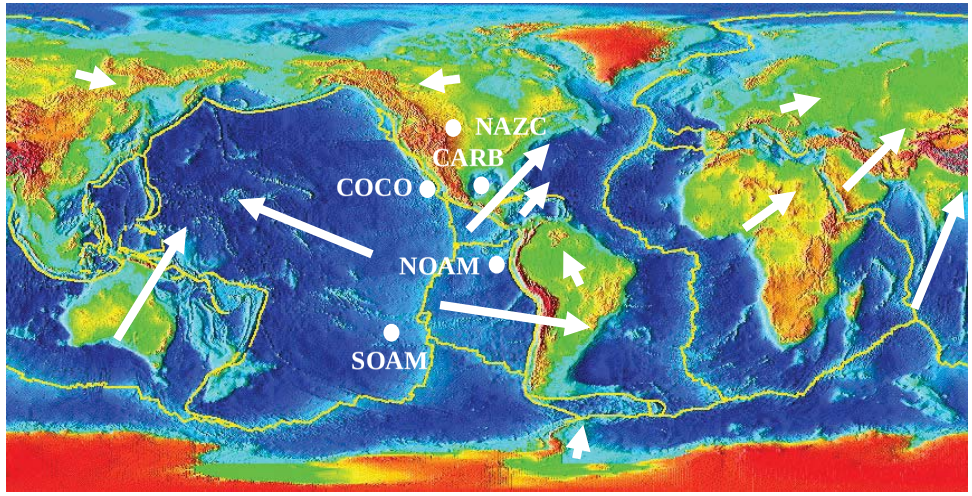

Problem of the NUVEL-1A velocities for geodesy

Global rotation with respect to the Earth crust ("no net rotation")

The ITRF refers to the geologic-geophysical model NNR NUVEL-1A.

The integration (interpolation) of the ITRF velocities over the entire Earth crust yields a global rotation (1 mas = 31 mm at the equator):

ω_X = -0,04 mas/a, ω_Y = 0,03 mas/a, ω_Z = -0,03 mas/a (~ 2 mm/a)

This is due to the NNR NUVEL-1A model, which does **not** provide the present rotation, but the average over ~3 Million years. In addition it does **not** include plate (crustal) deformations.

It's possible to compute a kinematic plate model including crustal deformations from geodetically observed velocities (e.g. ITRF2008) fulfilling the NNR condition and providing consistency with the EOP.

The input data are all the observed station velocities of the ITRF.

Geodetic modelling of a no net rotation plate model

Modelling of plate rotation vectors from geodetic point velocities:

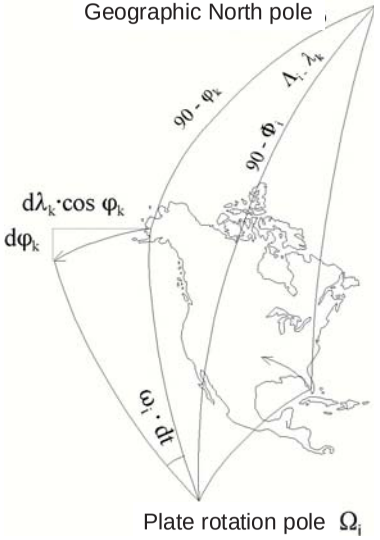

$(d\varphi/dt)_k = \omega_i * \cos \Phi_i * \text{sen}(\lambda_k - \Lambda_i)$

$(d\lambda/dt)_k = \omega_i * (\text{sen } \Phi_i - \cos(\lambda_k - \Lambda_i) * \tan \varphi_k * \cos \Phi_i)$

Modelling of deformations of the Earth crust (non rigid plates):

$(d\mathbf{v}/dt)_{pred} = c^T C^{-1} (d\mathbf{v}/dt)_{obs}$

v = vector of velocities (φ, λ)

obs = observed

pred = predicted

Integration: $\Sigma \Sigma \mathbf{v}_{1°\times1°} \rightarrow \mathbf{0}$

"no net rotation" compatible with EOP

Geophysical plate model PB2002 (Bird 2003)

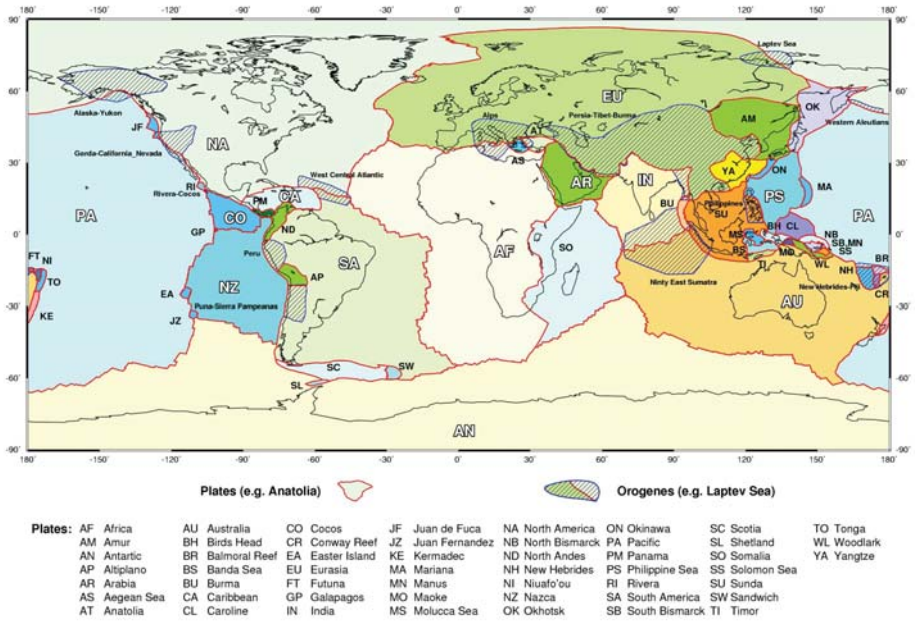

Actual Plate Kinematik Model (APKIM)

Plate (PB2002)	APKIM ITRF2008 NNR			PB2002		
	Latitude	Longitude	Velocity	Latitude	Longitude	Velocity
AF Africa	48.80 ± 0.16	-77.11 ± 0.53	0.2808 ± 0.0010	50.5643	-73.9481	0.2909
AM Amur	60.59 ± 8.21	-104.91 ± 16.9	0.2851 ± 0.0240	44.3353	-98.3803	0.3079
AN Antarctic	59.51 ± 0.24	-120.15 ± 0.46	0.2293 ± 0.0027	62.9970	-115.7365	0.2384
AR Arabia	49.42 ± 0.41	2.94 ± 1.74	0.5880 ± 0.0145	46.6691	-6.1940	0.5929
AT Anatolia	40.14 ± 0.12	28.11 ± 0.22	2.0153 ± 0.0790	40.9338	27.2489	1.2102
AU Australia	32.89 ± 0.09	35.86 ± 0.18	0.6381 ± 0.0007	33.8554	33.1689	0.6462
CA Caribbean	31.11 ± 1.92	-107.81 ± 5.12	0.1968 ± 0.0206	34.0376	-87.5775	0.2912
EU Eurasia	54.74 ± 0.22	-94.40 ± 0.36	0.2674 ± 0.0009	50.6311	-112.2750	0.2337
IN India	49.84 ± 0.93	9.87 ± 6.77	0.5599 ± 0.0203	45.5120	0.3448	0.5454
MA Mariana	12.32 ± 0.49	144.12 ± 0.27	3.6205 ± 1.2470	15.1572	139.5455	1.1971
NA N.America	-4.39 ± 0.55	-84.11 ± 0.13	0.1951 ± 0.0010	-2.4098	-85.8946	0.2069
NZ Nazca	45.07 ± 0.55	-100.95 ± 0.24	0.6519 ± 0.0041	47.8041	-100.1303	0.7432
ON Okinawa	39.17 ± 1.34	138.00 ± 1.59	1.7743 ± 0.3439	31.8492	-97.7137	0.2359
PA Pacific	-63.27 ± 0.06	110.79 ± 0.32	0.6705 ± 0.0008	-63.0448	107.3246	0.6408
SA S. America	-15.33 ± 0.64	-122.22 ± 1.72	0.1185 ± 0.0011	-25.3247	-124.4300	0.1164
SO Somalia	50.16 ± 0.69	-88.42 ± 1.52	0.3212 ± 0.0056	49.7622	-93.2661	0.3478
SU Sumatra	33.35 ± 3.65	-79.98 ± 1.29	0.5001 ± 0.0578	45.1695	-73.1976	0.4755
YA Yangtze	56.80 ± 6.02	-99.58 ± 8.49	0.3164 ± 0.0043	66.8484	-150.4806	0.3928

Geophysical and geodetic plate kinematic models

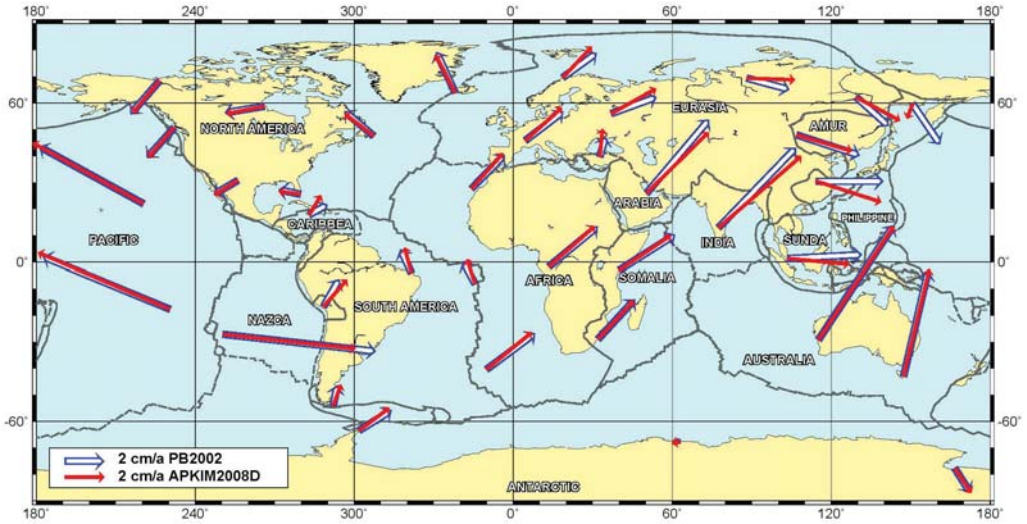

(The model PB2002 is identical to NNR NUVEL-1A in the mayor plates)

6.3 Intra-plate and inter-plate crustal deformation

Crustal deformations mostly are generated by colliding/diverging plates

Three types:

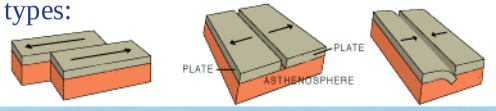

- Conservative (transverse faults)
- Constructive (spreading ridges)
- Destructive (subduction, collision)

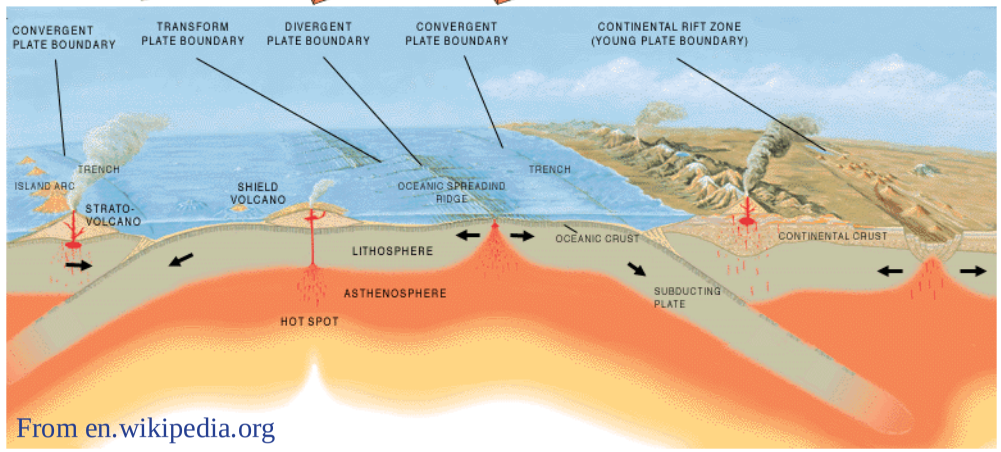

From en.wikipedia.org

Plate motions and deformation types

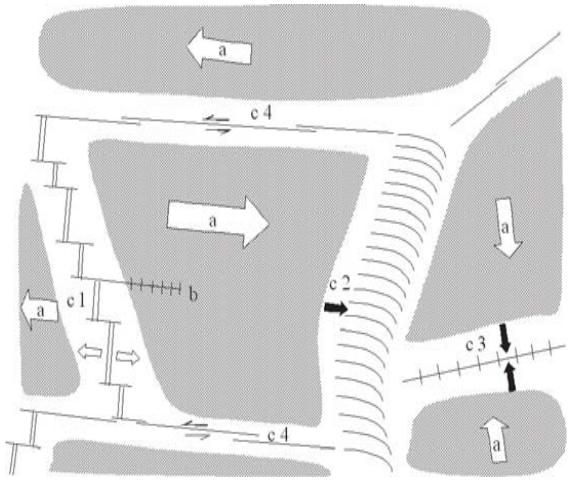

Long-term deformations

(a) Plate rotations

(b) Intra-plate deformation

(c) Inter-plate deformation

(c1) Sea floor spreading

(c2) Ocean plate subduction

(c3) Continents collision

(c4) Shear strain (strike-slip)

(d) Other deformations

(d1) Isostatic adjustment

(d2) Sediment basins

There are other short-term (periodic, seasonal, episodic) deformations, e.g. from environmental loading, seismic events, which are not treated

Deformation zones (Argus and Gordon 1996)

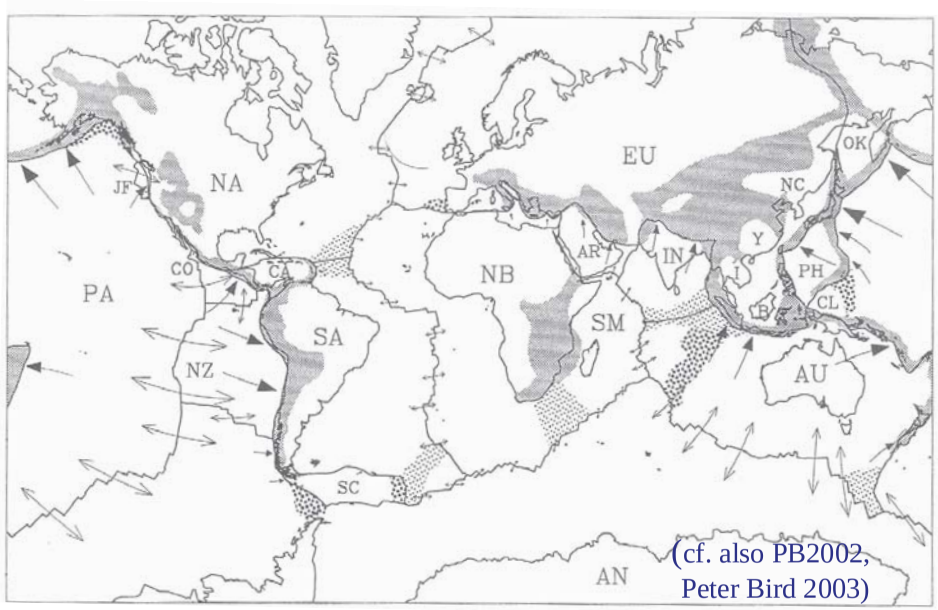

(cf. also PB2002, Peter Bird 2003)

How to model crustal deformations?

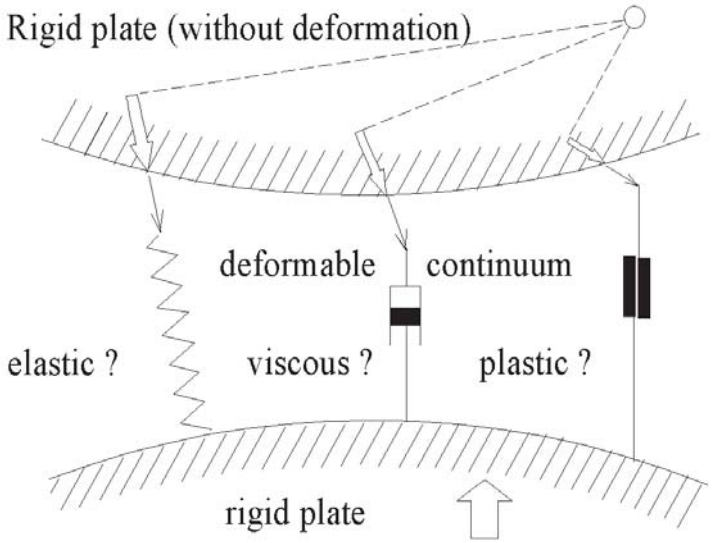

Modelling as a deformable continuum

Defining the used material property is the most important prerequisite for an adequate approximation of reality.

Rock rheology

Basic physical materials

De-nomination	Mechanical analogon	Diagram σ-ε or ε-t	Relative strain at σ = const.	Examples for geo-dyn. applications
rigid (Euklid material)	σ	ε, σ	ε = 0 for all σ	models of rigid plates (e.g. NUVEL)
elastic (Hook material)	ε, σ	ε, σ	ε = σ/E	plates flexure under loading
viscous (Newton material)	ε, σ	ε, t	ε = (σ/η)· t	Mantle convection, long-term deforma-tion of lithosphere
plastic (St. Venant-Material)	σ	ε, σ_0, σ	ε = 0 for σ<σ_0 ε = indefinite for σ >σ_0	processes in the fault plane during seismic events

Rock rheology

Combined model materials

De-nomination	Mechanical analogon	Diagram σ-ε or ε-t	Relative strain at σ = const.	Examples for geo-dyn. applications
visco-elastic (Kelvin-Voigt material)	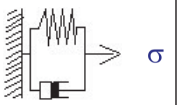	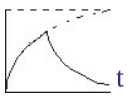	$\varepsilon = \sigma / E \cdot (1 - e^{-t/t_1})$ where $t_1 = \eta / E_1$	Earth tides, Chandler wobble of polar motion
elasto-viscous (Maxwell-material)		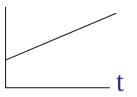	$\varepsilon = \sigma/E + (\sigma/\eta) \cdot t$	general lithosphere (incl. mantle)
elasto-plastic (Prandtl-material)	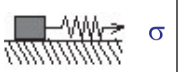	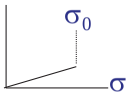	$\varepsilon = \sigma/E$ for $\sigma < \sigma_0$ ε = indefinite for $\sigma > \sigma_0$	flexure of plates in subduction zones
elasto-visco-plastic (Bingham-mat.)	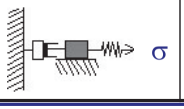		$\varepsilon = \sigma/E$ for $\sigma < \sigma_0$ $\varepsilon = (\sigma - \sigma_0) \cdot t/\eta + \sigma/E$ for $\sigma > \sigma_0$	processes of mountain building

Elastic deformations: elasticity parameters

Linear deformation:

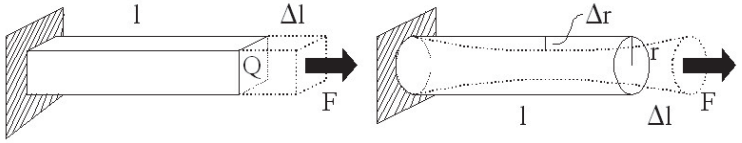

$$\frac{\Delta l}{l} = \frac{1}{E}\frac{F}{Q}; \quad \varepsilon = \frac{1}{E} \cdot p \qquad \sigma = \frac{\Delta r}{r} : \frac{\Delta l}{l} \quad (0 \le \sigma \le 0{,}5)$$

E = elasticity module (Young's-modulus) σ = Poisson's ratio (number)

Volume deformation:

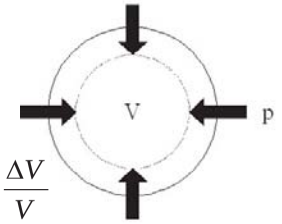

$$p = K \frac{\Delta V}{V}$$

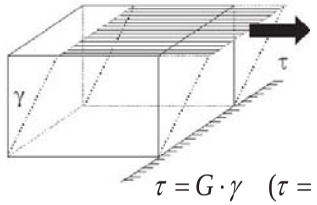

$$\tau = G \cdot \gamma \quad (\tau = F/Q)$$

K = compressive modulus G = shear modulus

Interrelation of elasticity parameters

(in any case only two are independent of each other)

$$K = \frac{E}{3\,(1-2\sigma)} \qquad G = \frac{E}{2\,(1+\sigma)} = \mu$$

$$E = \frac{3\,K \cdot G}{K + 1/3\,G} \qquad \sigma = \frac{1/2\,K - 1/3\,G}{K + 1/3\,G}$$

$$\lambda = \frac{E \cdot \sigma}{(1+\sigma)\cdot(1-2\sigma)} = K - \frac{2}{3}G \qquad \mu = \frac{E}{2\,(1+\sigma)} = G$$

λ, μ = Lamé parameters (mainly used in seismology)

Modelling of an elastic continuum

Hooke's law for isotropic elastic material:

$$p_{ij} = \lambda\, \delta_{ij}\, \varepsilon_{kk} + 2\,\mu\, \varepsilon_{ij}$$

(p = stress-, ε = deformation tensor, λ, μ = Lamé elasticity parameters, δ = Kronecker delta, i, j, k = 1 ... 3)

Equation of motion of the elastic deformation:

$$\rho \cdot \frac{\partial^2 \underline{u}}{\partial t^2} = \mu \cdot \Delta \underline{u} + (\lambda + \mu)\, grad\ div\ \underline{u} + \underline{f}$$

ρ = rock density, Δ = Laplace operator

Solution of the differential equation by integration with finite elements

$$\underline{u} = \underline{S}^{-1} \cdot \underline{f}$$

$\underline{u}$ = point velocity
$\underline{f}$ = force function
$\underline{S}$ = stiffness matrix
$\underline{S} = \underline{S}(x, \lambda, \mu)$

Solution of the modelling

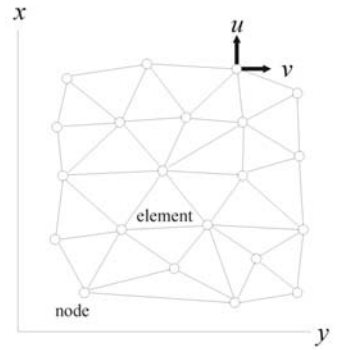

Result of the modelling using the finite element method

Strain-Tensor $\underline{e} = \underline{\varepsilon} + \underline{\gamma}$

Example for three-dimensional models:

$$Extension: \quad \varepsilon = \begin{vmatrix} \frac{\partial u}{\partial x} & 0 & 0 \\ 0 & \frac{\partial v}{\partial y} & 0 \\ 0 & 0 & \frac{\partial w}{\partial z} \end{vmatrix}$$

$$Shear: \quad \gamma = \begin{vmatrix} 0 & \frac{1}{2}\left(\frac{\partial u}{\partial y}+\frac{\partial v}{\partial x}\right) & \frac{1}{2}\left(\frac{\partial u}{\partial z}+\frac{\partial w}{\partial x}\right) \\ \frac{1}{2}\left(\frac{\partial u}{\partial y}+\frac{\partial v}{\partial x}\right) & 0 & \frac{1}{2}\left(\frac{\partial v}{\partial z}+\frac{\partial w}{\partial y}\right) \\ \frac{1}{2}\left(\frac{\partial u}{\partial z}+\frac{\partial w}{\partial x}\right) & \frac{1}{2}\left(\frac{\partial v}{\partial z}+\frac{\partial w}{\partial y}\right) & 0 \end{vmatrix}$$

Example for South America

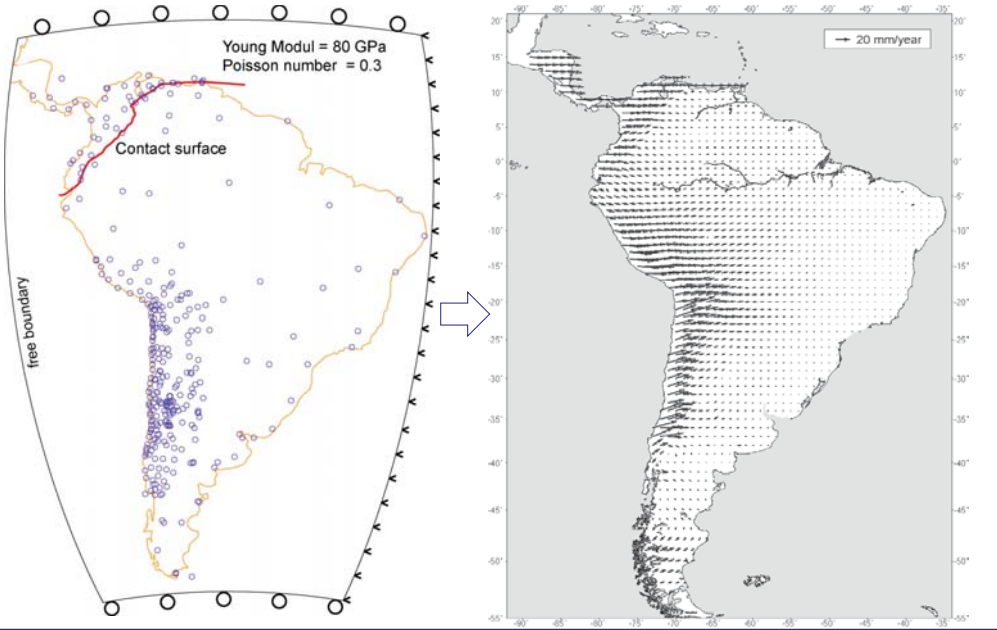

Global modelling of deformation zones

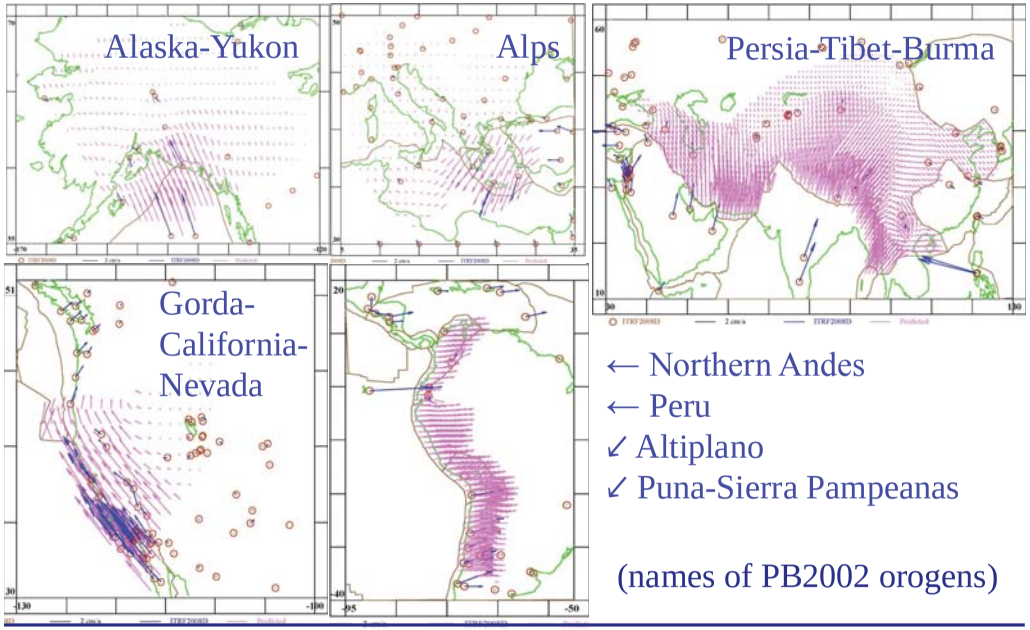

← Northern Andes
← Peru
↙ Altiplano
↙ Puna-Sierra Pampeanas

(names of PB2002 orogens)

6.4 Monitoring seismic deformations by GNSS

Besides long-term plate tectonic motions and intra-plate deformations there are episodic deformations, mainly generated by earthquakes.

10 largest earthquakes since 1900

Probability M > 8 is one per year

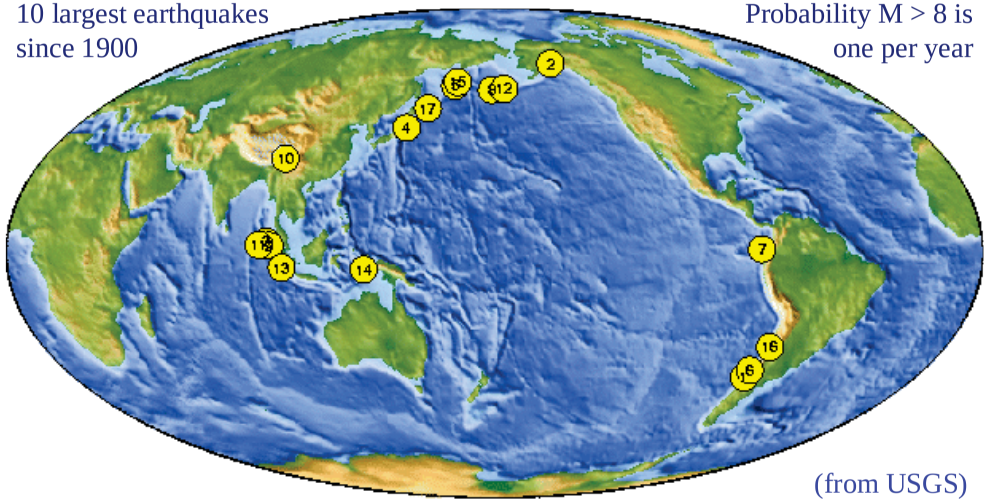

(from USGS)

Earthquakes M ≥ 8 from 2008 to 2012

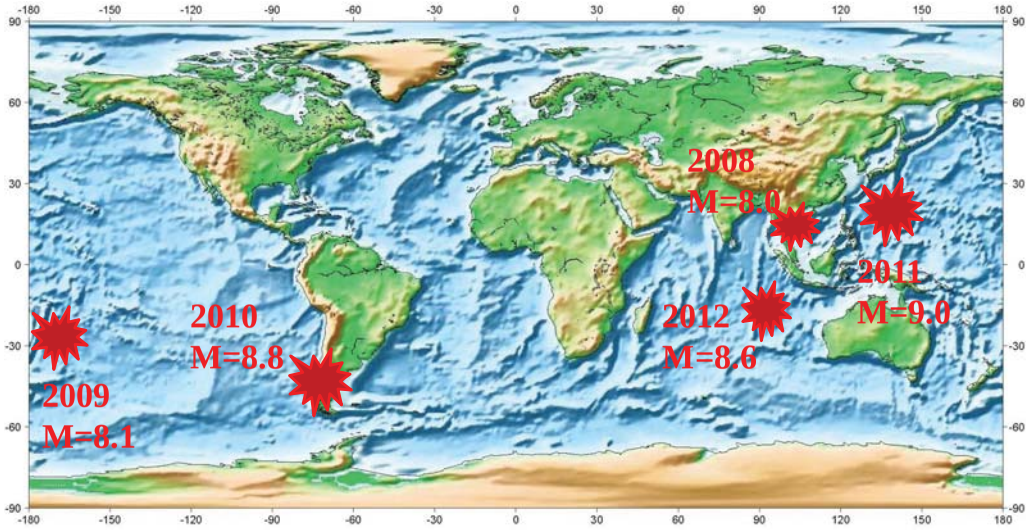

The seismic deformations cannot be modelled like plate motions and inter-plate deformations. They must be observed by geodetic methods.

Deformations of the Tōhoku earthquake 2011

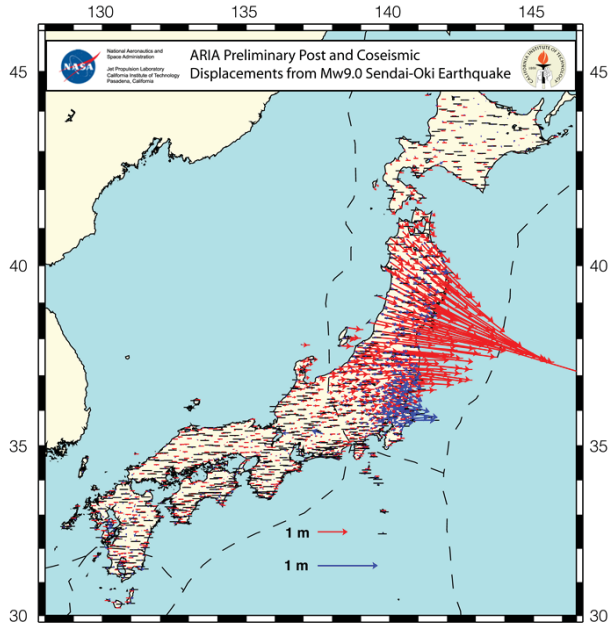

Displacements observed by the GPS GEONET of the Geospatial Information Authority (GSI) of Japan before and after the M=9.0 earthquake, 2011-03-11.

There are more than 1000 continuously observing GPS sites in a spacing of about 25 km.

Data are processed and interpreted in nearly real-time in order to allow a prognostic alert.

Campaign observations of the Cariaco earthquake

The M=7.0 earthquake in Cariaco, Venezuela, 9 July 1997 was one of the first large earthquakes monitored by GPS (CASA) in Latin-America.

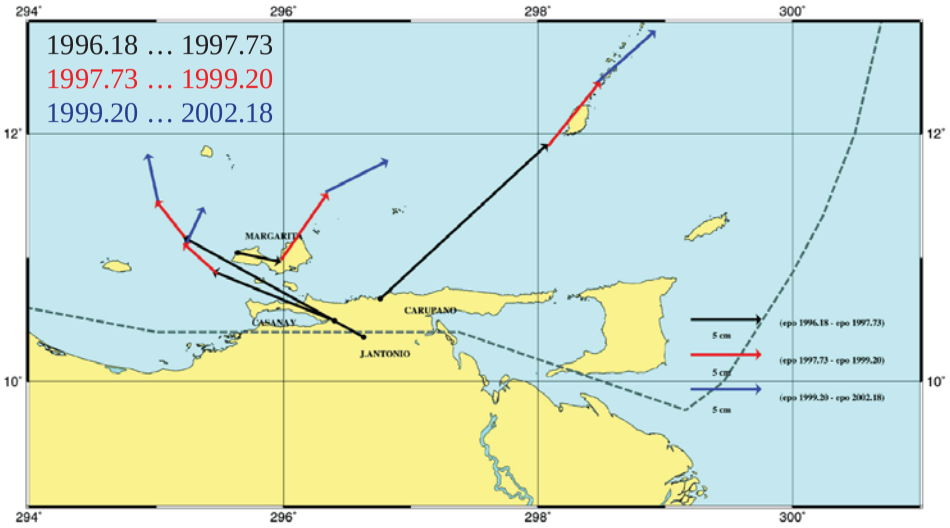

Continuous observations in Arequipa

The M=8.4 earthquake in Arequipa, Peru, 23 June 2001 was the first large earthquake monitored by SIRGAS continuously observing stations.

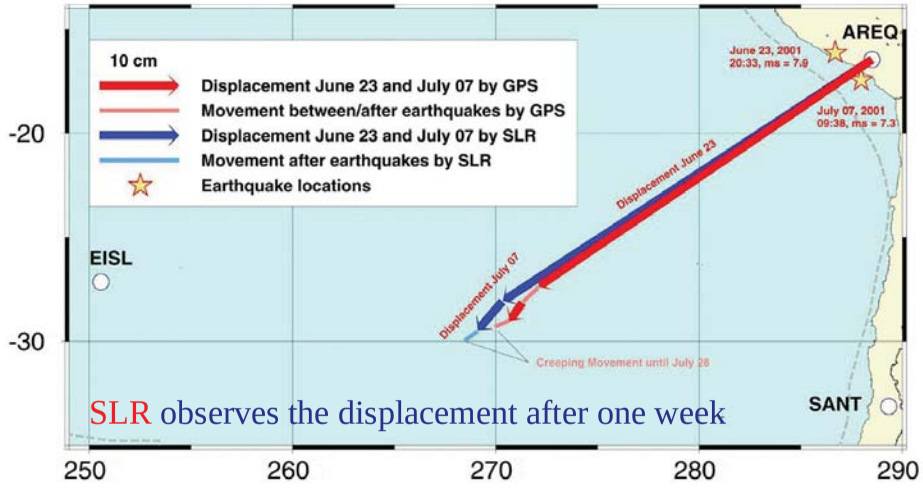

SLR observes the displacement after one week

GPS weekly time series in Arequipa

SIRGAS provides the continuous time series showing clearly the jump.

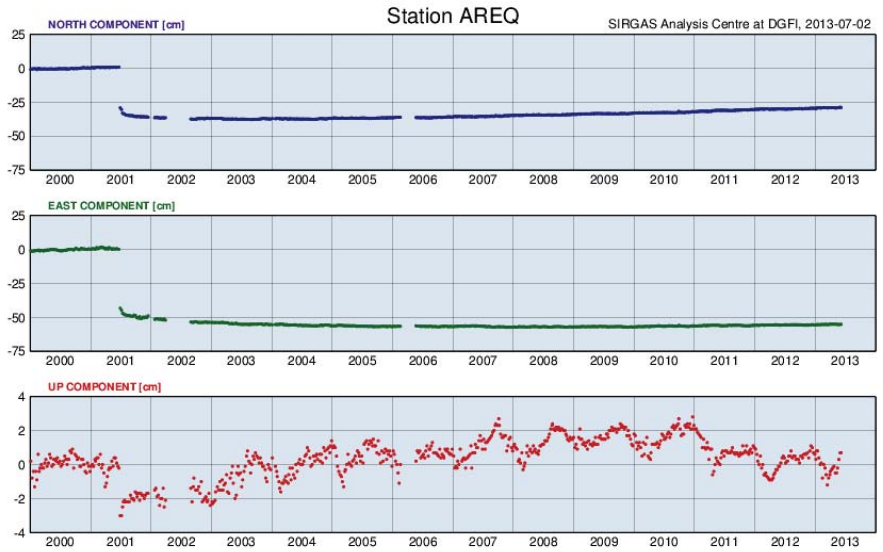

Irregular station velocity after the earthquake

Non-linear station velocity more than five years after the earthquake

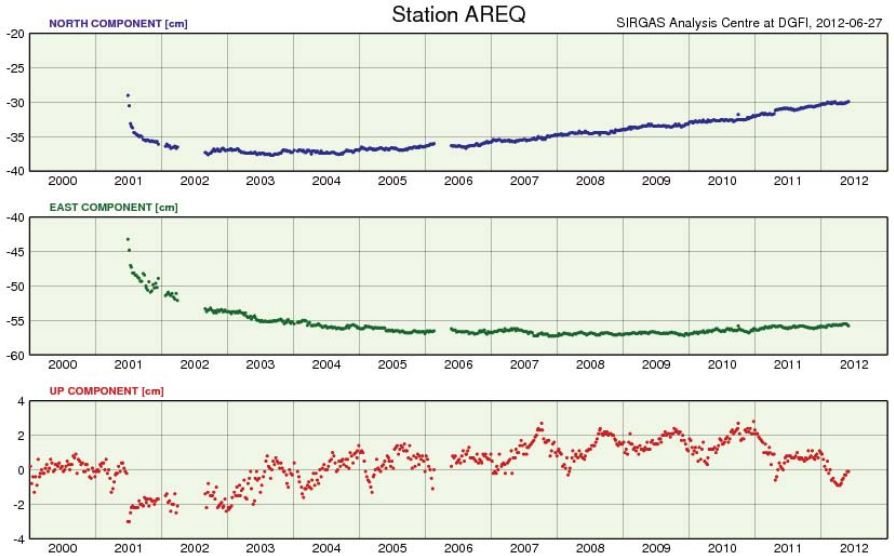

El Salvador M=7.7 earthquake 2001

Main shock (15 Jan.) and aftershock (13 Feb.) clearly identified

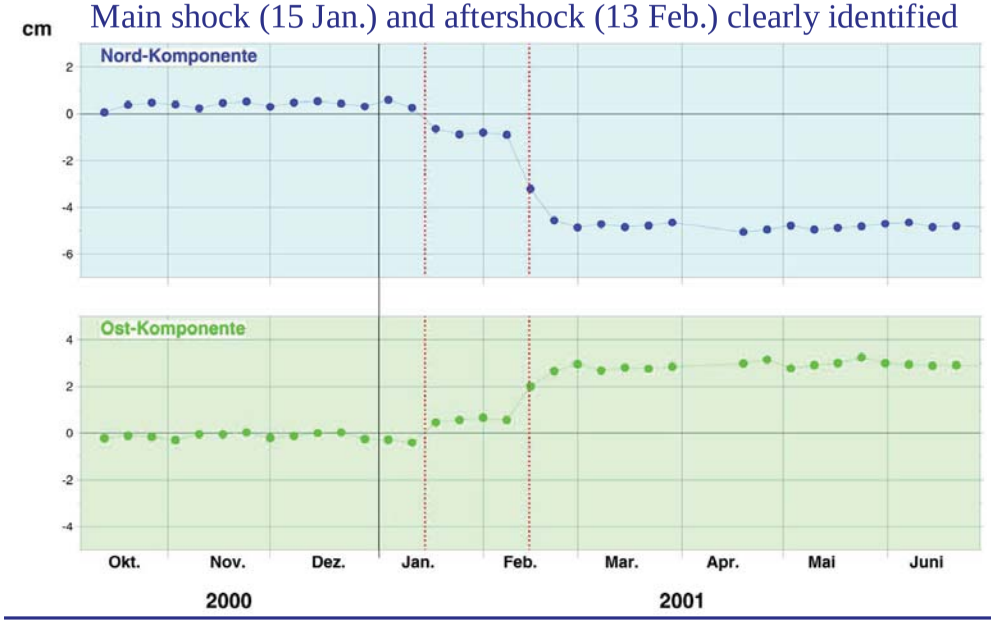

Mexicali M=7.2 earthquake 4 April 2010

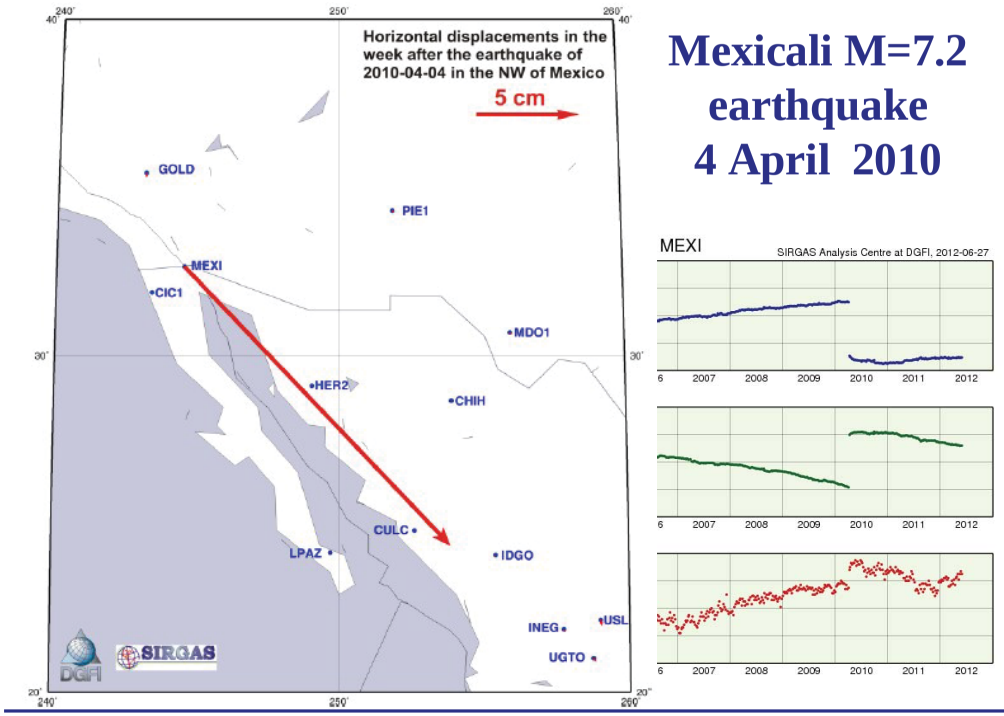

Maule M=8.8 earthquake, 27 February 2010

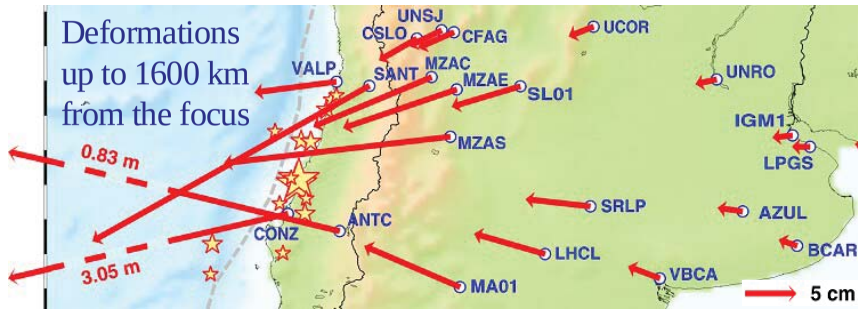

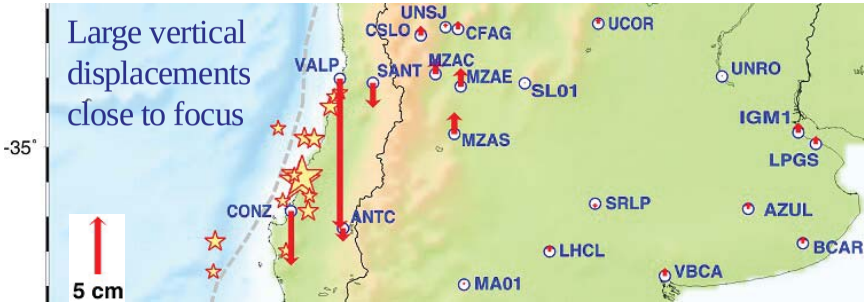

Time series of deformations in Concepción

Velocities have not yet recovered to the normal status

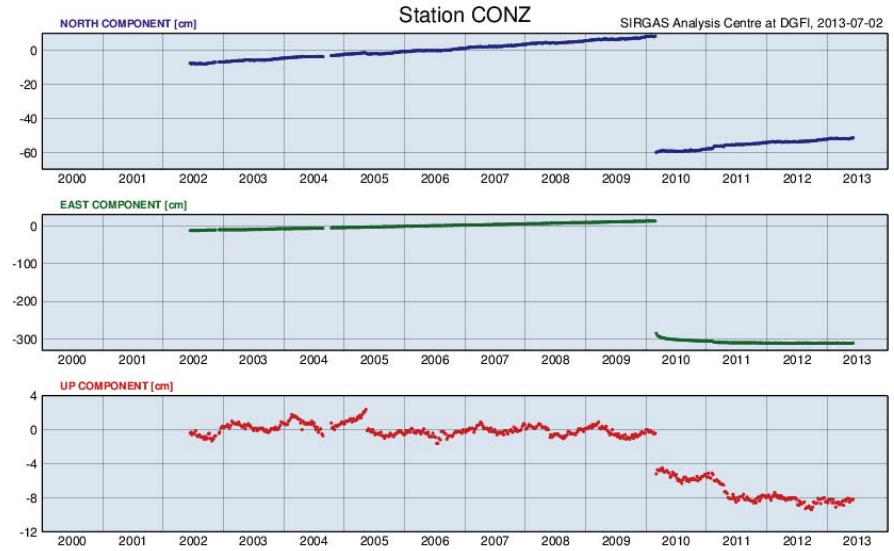

No earthquake in Manzanillo, Mexico, 2002-11-15

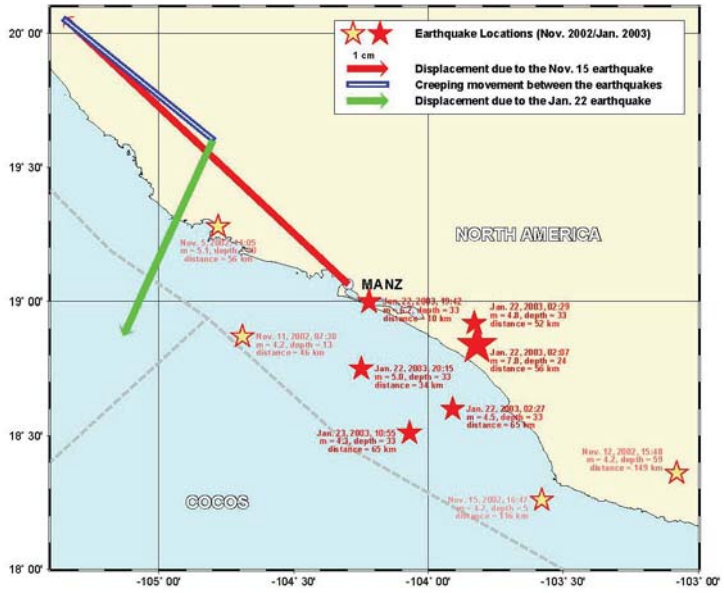

In Manzanillo there was **no** earthquake on 15 Nov. 2002, but a collision of a ship with the pier where the GPS antenna was installed.

There were some earthquakes on 22 Jan. 2003!

Caution with interpretations!

7. Ionospheric modelling and analysis

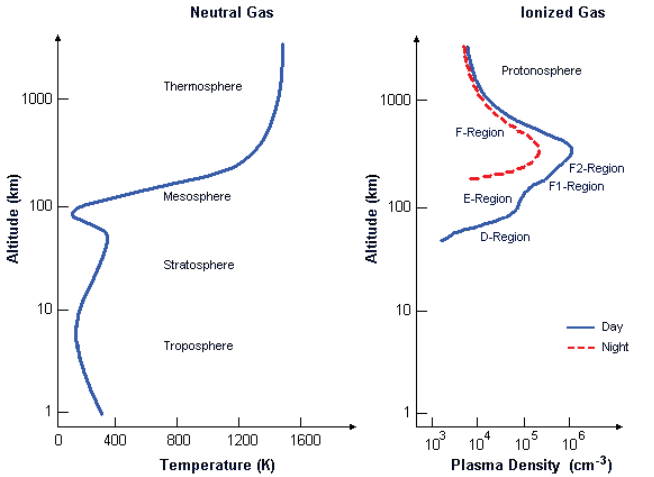

The Earth's ionosphere

The ionosphere is defined as the region of the high altitude atmosphere where free electrons exist in sufficient amount to disturb the propagation of electromagnetic waves.

Free electrons are produced mostly by the UV and X radiation of the Sun, which causes the photo-ionization of the atmosphere's gases.

The inverse process is called 'recombination': free electrons are re-captured by positive ions.

Discovery of the ionosphere

The ionosphere can carry electrical currents, which influence the magnetic field measured on the Earth; it allowed the German scientist Carl Friedrich Gauss, in 1839, speculating about the existence of electrically charged layers on the upper atmosphere.

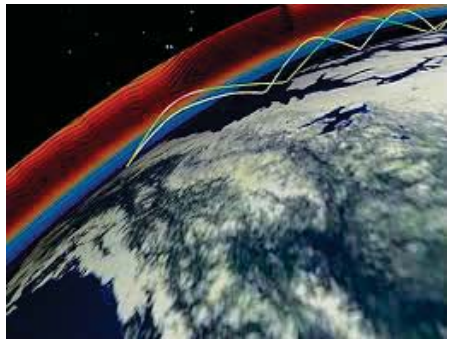

The ionosphere can reflect, deflect, and scatter radio waves; it allowed the Italian scientist Guillelmo Marconi, in 1901, performing the first radio-communication between Europe and USA.

Why study the ionosphere?

Form the scientific point of view, the ionosphere is a extraordinary 'plasma-physics laboratory'.

From the technological point of view, the ionosphere affects a variety of devices that are powered by radio waves that must pass through the ionosphere, or use it as a natural reflector to make the wave returns to earth:

- *terrestrial communications systems for medium, long and very long distances,*
- *satellite communications systems;*
- *satellite-based global navigation;*
- *satellite-base Earth observing systems;*
- *over the horizon radars.*

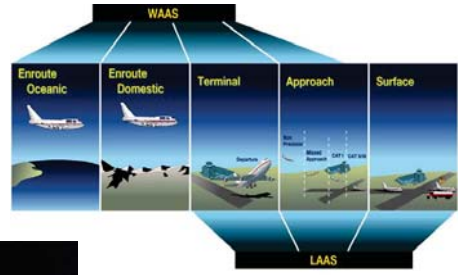

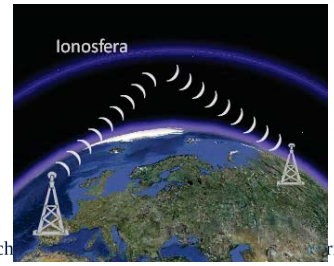

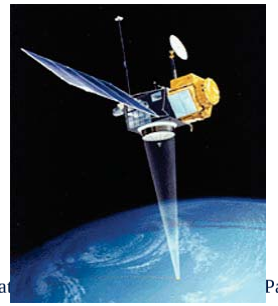

Chemical composition of the ionosphere

The ionosphere contains less than 0.1% of the atmosphere's mass, and less than 1% of that mass becomes ionised.

In spite of that, the charged particles make the gas electrically conducting, which completely changes its characteristics.

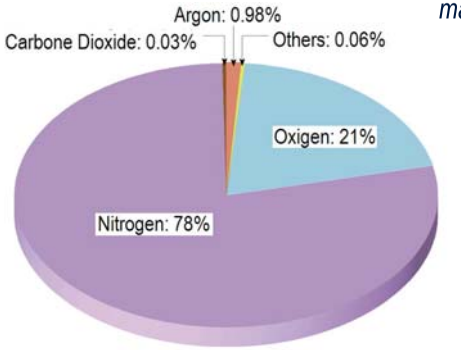

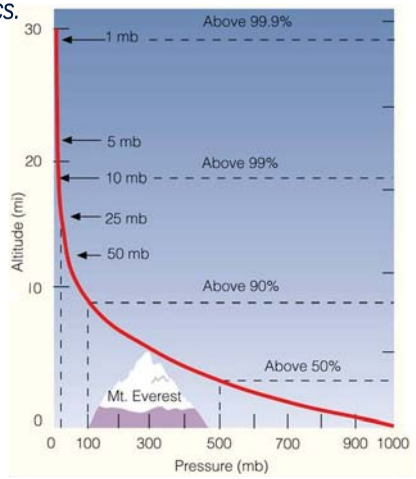

The most abundant gas molecules in the ionosphere are:

- *below 200 km: molecular oxygen (O_2) and nitrogen (N_2);*
- *Between 200 and 600 km: atomic oxygen (O);*
- *above 600 km: hydrogen (H) and Helium (He).*

The geomagnetic field

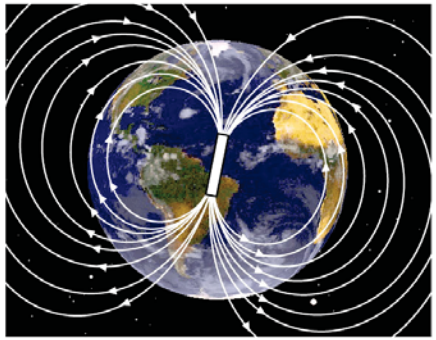

As a first approximation the geomagnetic field is approximately the field of a magnetic dipole, tilted at an angle of 11° with respect to the rotational axis (as if there were a bar magnet placed at that angle at the center of the Earth).

The differences between the actual geomagnetic field and the dipole approximation are called 'geomagnetic anomalies'; the most noticeable of them is the South Atlantic Magnetic Anomaly (SAMA), which is characterized by a depletion of the field intensity.

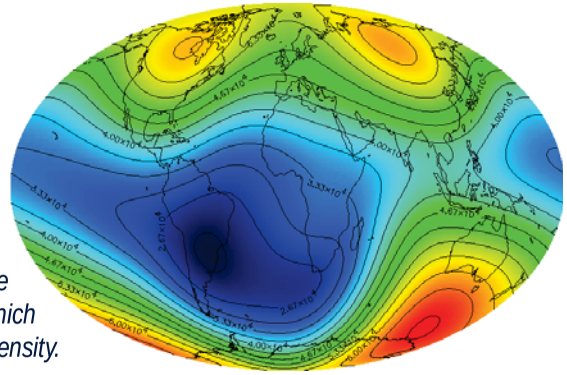

The ionospheric dynamo

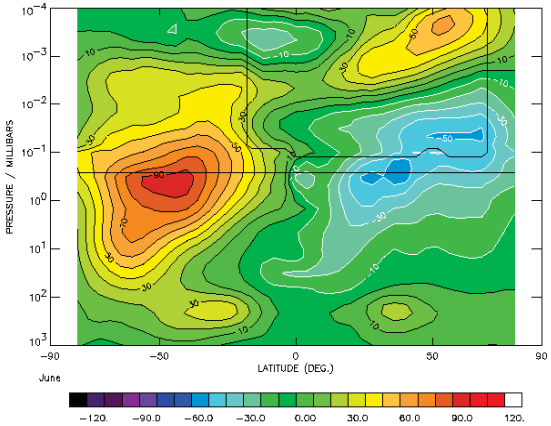

Global pattern of zonal winds in June
red -> East to West; blue -> West to East

The mix of positively and negatively charged ions, negative electrons and neutral gas is called 'plasma', which is the most common state of the universe.

Atmospheric tidal winds due to differential solar heating or gravitational lunar forcing move the plasma against the geomagnetic field lines, thus generating currents and electric fields perpendicular to the magnetic lines, just like a dynamo loop moving against magnetic field lines.

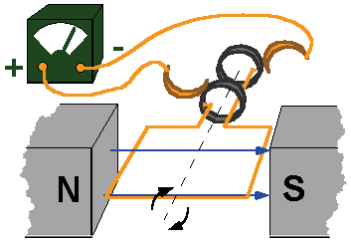

The solar-terrestrial environment

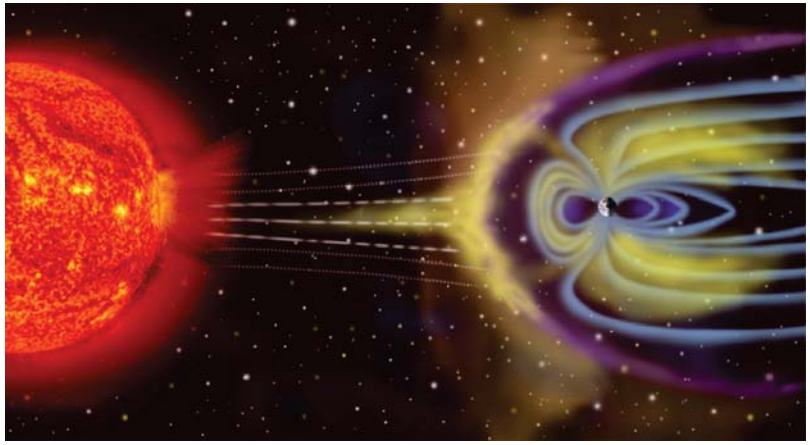

Sun, solar corona,
radiation, flares,
solar wind, coronal mass ejection,
interplanetary magnetic field

Earth, gravity field,
atmosphere, upper atmosphere winds, electric fields,
magnetic field, magnetosphere

Solar radiation

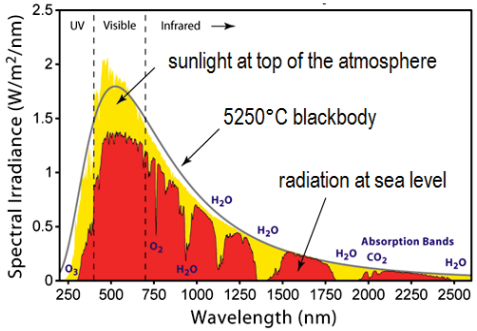

The X and UV radiation of the sun penetrates the upper atmosphere up to height of the Ozone layer.

That portion of the spectra produces photo ionization and photodissociation of different molecular species.

The Sun emits EM radiation across most of the electromagnetic spectrum, ie: X, UV, visible and infrared.

The ionizing X and UV radiation is generated by the solar corona; it encompasses a small fraction of the power output by the sun.

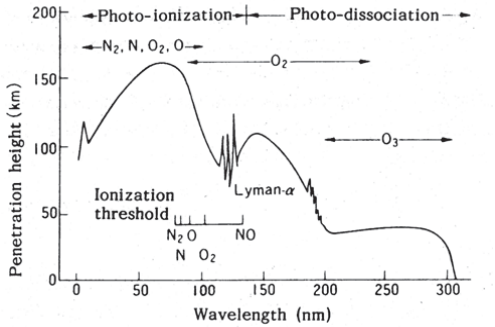

Solar wind and interplanetary magnetic field

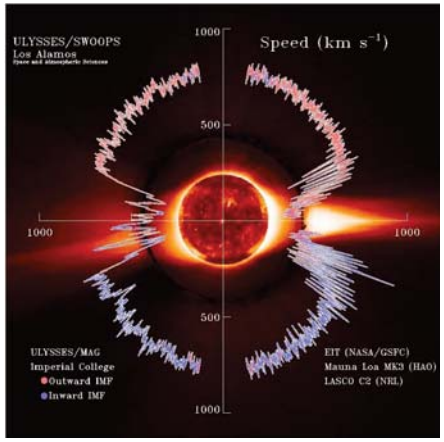

The solar corona ejects to space a stream of charged particles (mostly electrons and α-particles) named the solar wind.

Although no uniformly, the solar wind flows readily from the Sun in all directions with speeds from 400 to 800 km/s.

This high conductive plasma carries the magnetic field of the Sun thorough the solar system thus creating the interplanetary magnetic field (IMF).

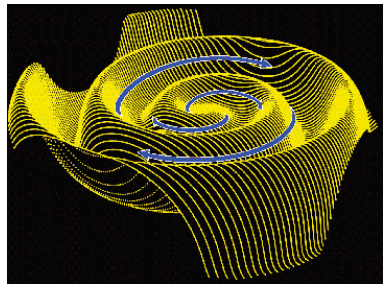

Due to the combination of the radial flow and the Sun's rotation, the solar wind and the imbedded IMF creates an undulated spiral with a 'ballerina skirt' shape.

Solar cycle

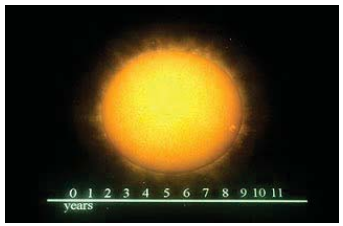

The activity of the Sun (magnetic field, ejection of solar material, radiation intensity) changes with a period of approximately 11 years.

These changes are highly correlated with the number of dark regions in the solar corona (sunspot) that have been observed for several centuries.

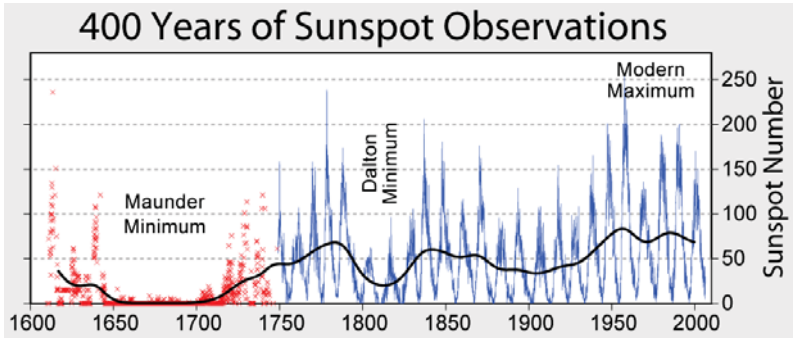

The magnetosphere

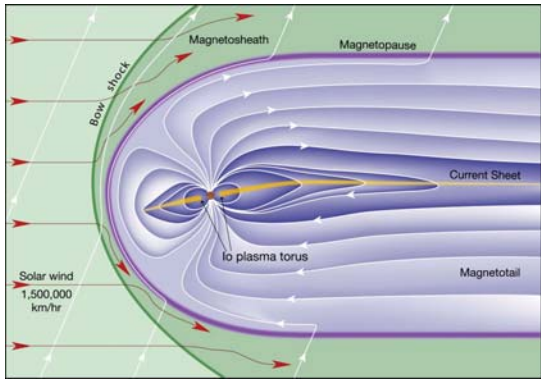

The space surrounding the Earth where its magnetic field is stronger than the interplanetary magnetic field is called the magnetosphere.

It forms a barrier to the solar wind.

Without the solar wind, the magnetic field lines of the Earth would be symmetric and similar to those of a bar magnet.

However, the solar wind pressure strongly compresses the magnetosphere on the dayside and draws it out into an extremely long tail on the night side of the Earth.

Since the charged particles of the solar wind cannot cross the Earth's magnetic field lines, they flow around the magnetosphere similar to water around a rock in a river.

his forms a standing shock wave in space upstream of the Earth, called the bow shock, much like the boom of an aircraft breaking the sound barrier

Magnetosphere – Solar Wind interaction

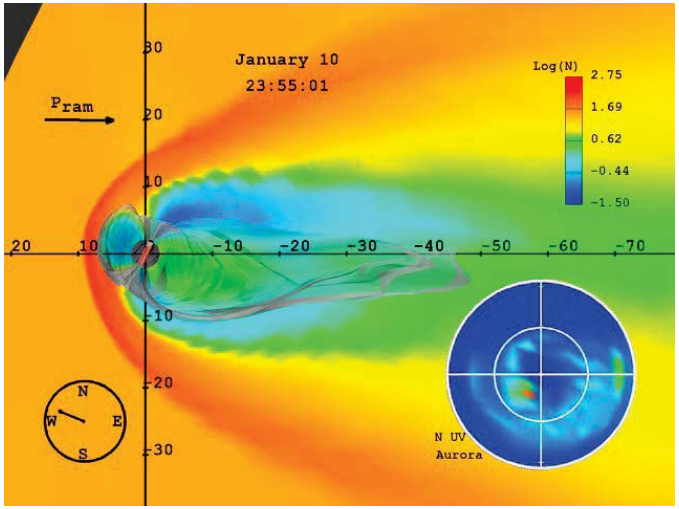

The magnetospheric tail flaps in space much like a flag in the wind.

Magnetic and ionspheric storms

Massive explosions in the sun's corona (specially during high solar activity periods) result in Coronal Mass Ejections (CME).

If the ejected mass is directed toward the Earth, tit reaches the magnetosphere (in 1-2 days) and produces a great distortion of the whole magnetic field, thus creating a 'magnetic storm'.

In most cases, magnetic storms are associated to great perturbations in the ionosphere, which are known as 'ionospheric storms'.

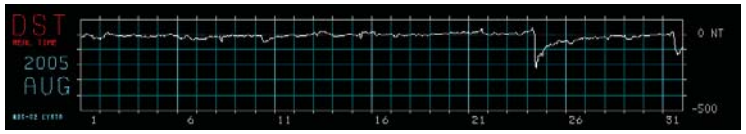

Physical process in the ionosphere

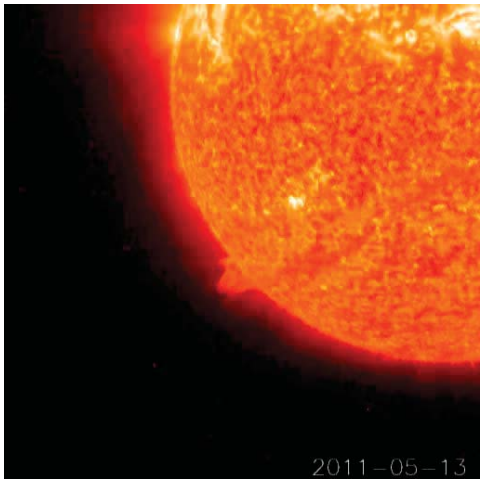

Solar flares are sudden brightening observed over the Sun's atmosphere associated to energetic emission of X and UV radiation.

They are mainly followed by a coronal mass ejection.

Both together –radiation and mass ejection– can severely disturb the onosphere and disrupt radio communications, radars, GNSS and other devices.

Vertical structure of the ionosphere

The ionosphere is stratified in different layers according to the chemical and physical processes that dominate at different heights.

Edward Appleton named the E (electrical) layer in 1927 after Guglielmo Marconi showed, during communication experiments in 1901, that radio waves between Europe and America had to be bouncing off an electrically conducting layer at around 100 – 150 km altitude.

Subsequently, other layers were discovered which simply received the names D- and F-layers.

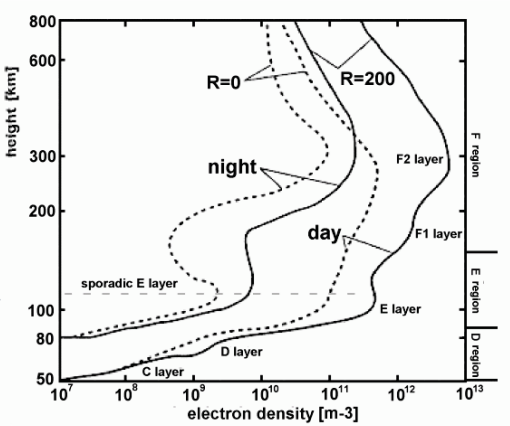

The D-layer is particularly complicated with more than 50 chemical reactions present.

The E layer is the main responsible of the ionospheric dynamo.

The F-layer presents the maximum electron density.

The electron density distribution undergoes a strong daily variation, especially at sunrise and sunset, as well as annual and solar cycle fluctuations.

Parameters used to characterize the ionosphere

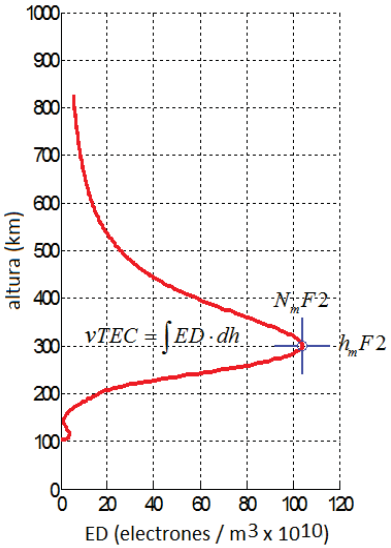

Electron density (ED)

Height of the F2 peak (h_mF2)

Electron density of the F2 peak (N_mF2)

Total Electron Content (TEC)

The global vertical TEC distribution

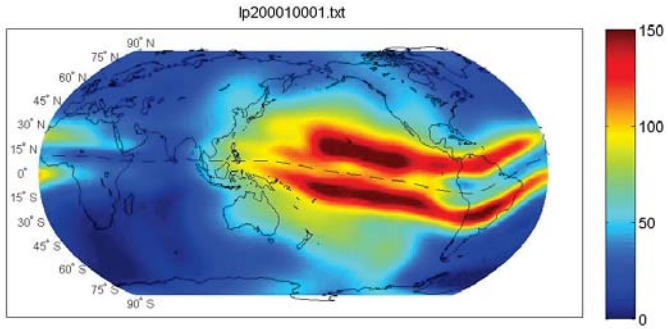

The Equatorial Anomaly

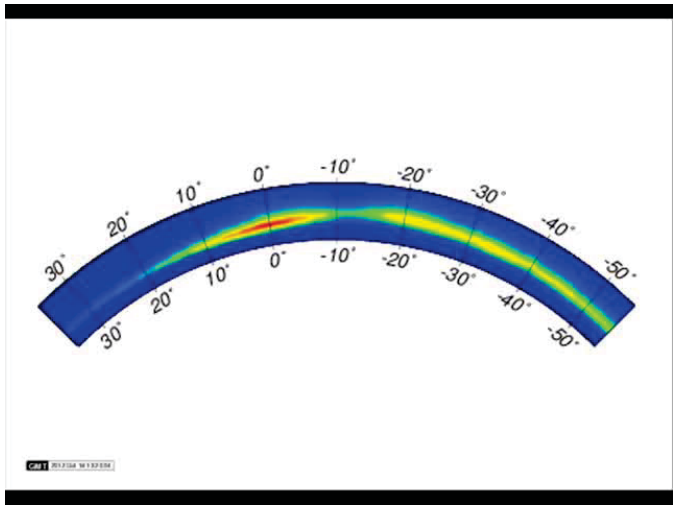

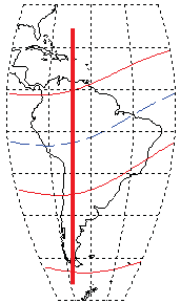

Physical process behind the Equatorial Anomaly

During daytime, the eastward dynamo electric field from the E region maps along the magnetic field to F-region heights above the magnetic equator. The plasma moves upward due to ExB drift and then diffuses along the magnetic field to form two crests with maximum ionization density near ±15º magnetic latitude and minimum ionization at the magnetic equator.

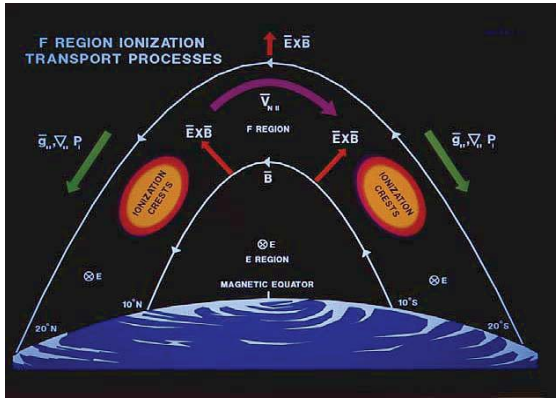

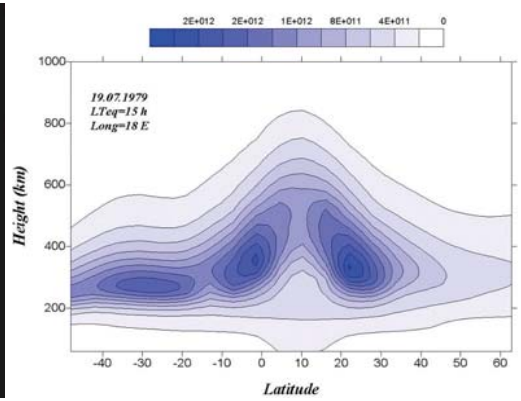

Solar cycle and seasonal variations

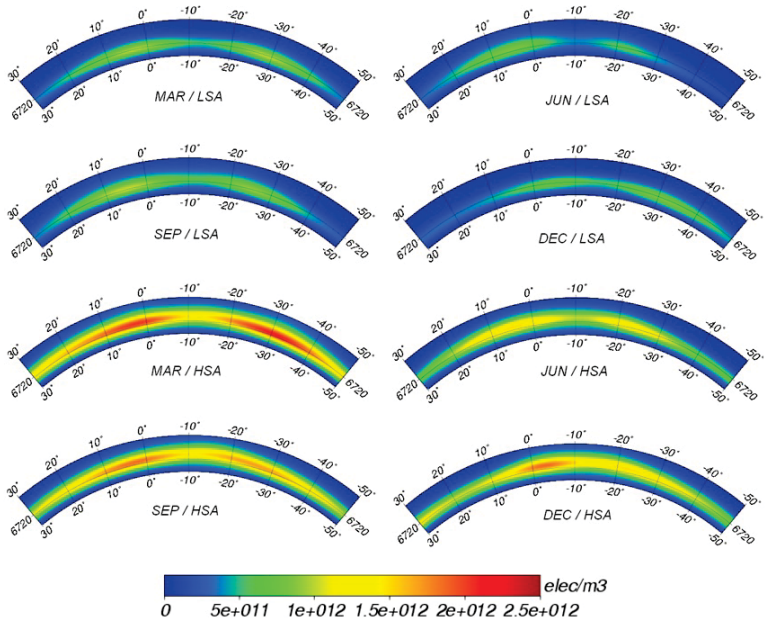

Quiet ionosphere

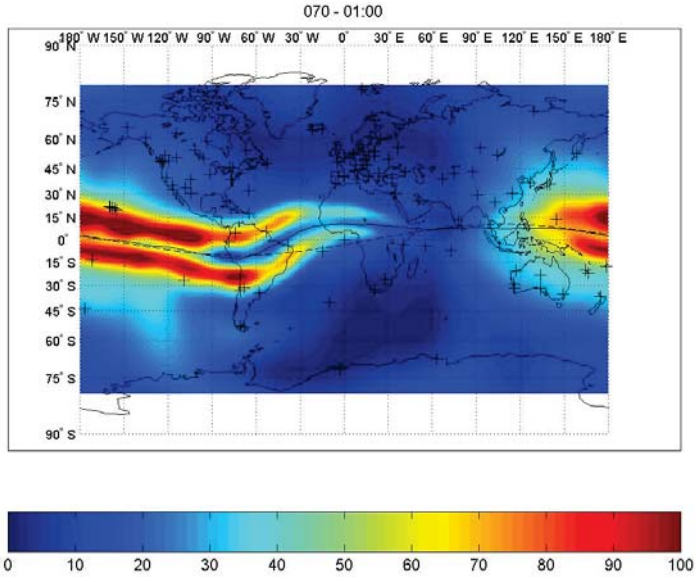

Disturbed ionosphere

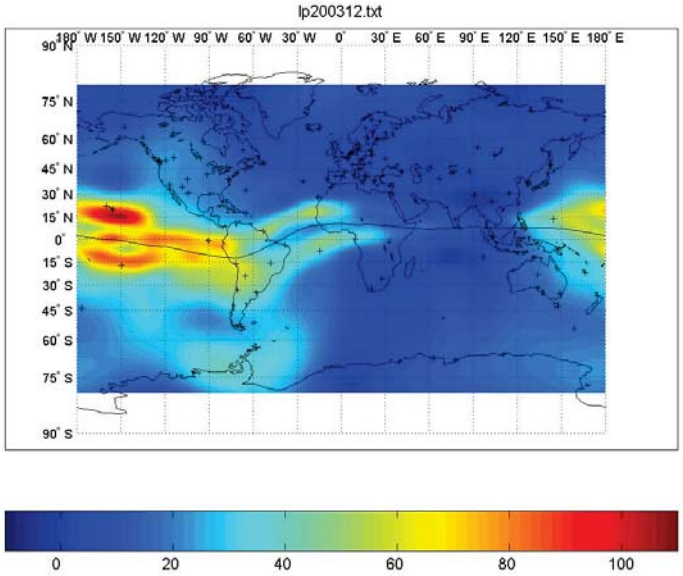

Observation of the ionosphere

The classical instrument is the ionozonde, which is a radar that emits an electromagnetic signal vertical upward and receives the echo produced by different ionospheric stratus; the frequency of the signals varies from 1 to 14 MHz.

Since the electron density of the stratus that produces the echo is proportional to the squared frequency, the instrument allows measuring the electron density and the height (based on the travelling time) in the different layers.

The major limitation of these instruments is the impossibility of sounding the ionosphere region above the F2 peak (the ionosphere topside).

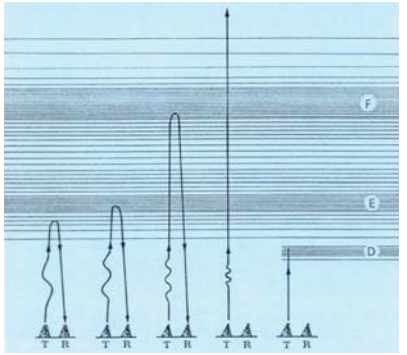

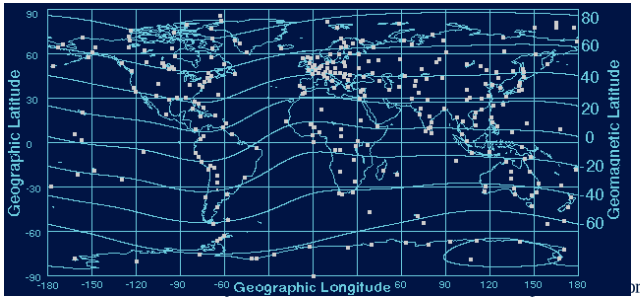

Global network of 100-200 ionozondes in operation since late 50s.

Observation of the ionosphere

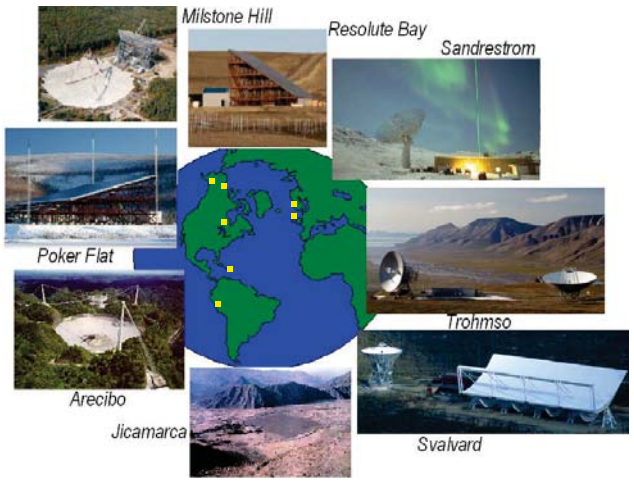

Exploring the topside requires much powerful, complex, and expensive radar named 'Incoherent backscatter radars'.

Around 10 of these instruments are presently in operation around the world.

Observation of the ionosphere

In 1957 the spatial era began allowing the exploration of the ionosphere using the satellites as dual frequency beacons (e.g.: TRANSIT system).

Presently, more than 60 satellites beacons are available including GPS, GLONASS and Galileo.

Large networks of continuously operational receivers (such as SIRGAS and IGS) collect high quality measurements, which are useful for ionospheric studies.

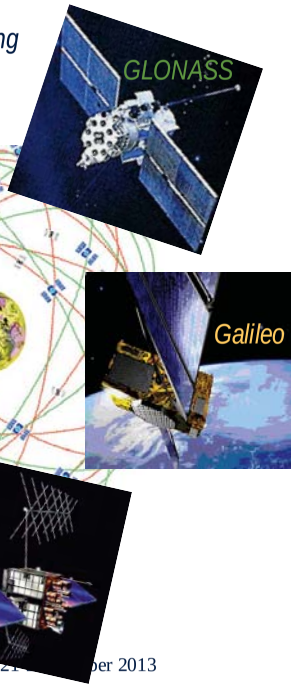

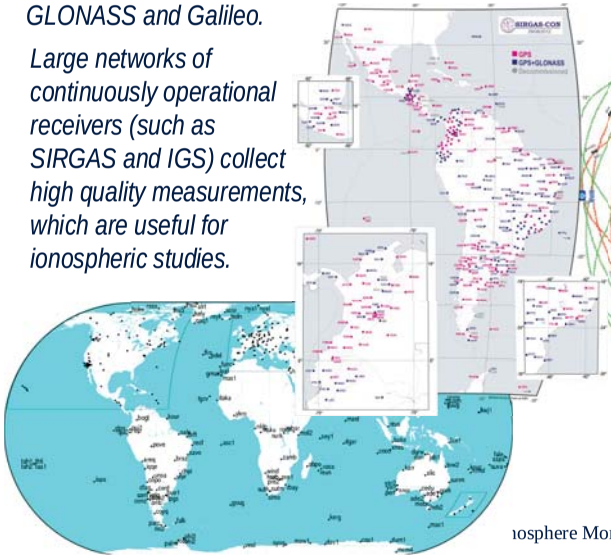

Observation of the ionosphere

Several dual frequency GPS receivers are flying onboard low Earth orbiter (LEO) satellites at 600–800 km above the Earth surface.

These receivers provide ~2500 radio ocultations per day, during which the LEO 'sees' the GPS satellite set or rise behind the Earth's limb, while the signal line-of-sight slices almost horizontally through the Earth's atmosphere.

GPS receivers onboard LEOs provide dual frequency observations distributed almost uniformly around the globe, describing the TEC distribution at different heights.

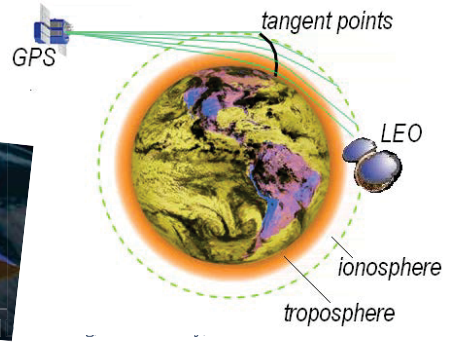

Ionospheric models

Can be classified in two major groups:

Theoretical

Consider the balance between production, loss, and transport of ionospheric electrons and ions, and obtain the electron density by solving a coupled system of differential equations.

Empirical

Are based largely on experimental data, and use empirically established mathematical functions to represent the characteristic variation patterns seen in long data records;

Empirical models have often been favored in an operational setting.

Large efforts for developing ionospheric models were done during the second world war to improve radio communication between commanders and troops.

Reestablished the peace, the 'International Telecommunications Union' (ITU), the 'International Union of Radio Sciences' (URSI), and the Committee on Space Research (COSPAR) led the development of models.

A well known examples is the 'International Reference Ionosphere' (IRI), developed by a cooperative efforts supported by COSPAR and the ITU; it is based mostly on ionosonde measurements;

Chapman model

A vertical electron density distribution is predicted by the simplified Chapman theory, which assumes monochromatic radiation, photoionization of a single specie neutral gas, and recombiantion of that specie; and neglects transport processes.

$$N_e(h) = N_m \cdot e^{k\cdot\left(1-z-e^{-z}\right)} \qquad z = \frac{h-h_m}{H}$$

where N_m is the electron density at layer peak, h_m is the height of the layer peak, H is the scale height of the layer, and k is constant that depends on the recombination process..

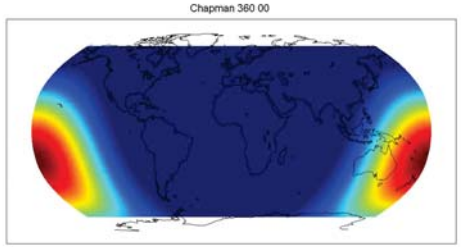

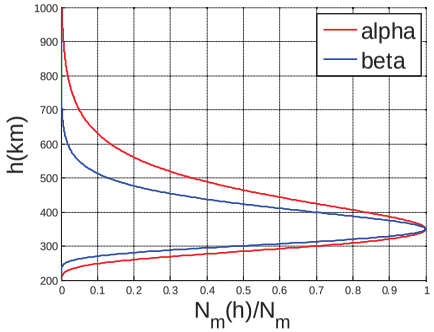

GNSS-based ionospheric observable

Dual frequency GNSS measurements (either ground- or space-bases) provide information on the total electron content (TEC), which defined as the number of free electrons within an imaginary cylinder of one square meter cross section whose longitudinal axis is the signal ray path.

$$TEC = 10^{-16} \cdot \int_S N_e \cdot ds$$

TEC is usually measured in TEC unities (TECu)

1 TECU = 10^{16} electrons per square meter.

According to the Appleton-Hartree theory (which provides the refraction index for the ionospheric plasma), the ionosphere range delay (in meters) is proportional to the TEC (in TECu) and inversely proportional to the square of the radio-signal frequency (in Hz).

$$\Delta R_{iono,f} = \frac{40.3\times10^{16}\cdot TEC}{f^2}$$

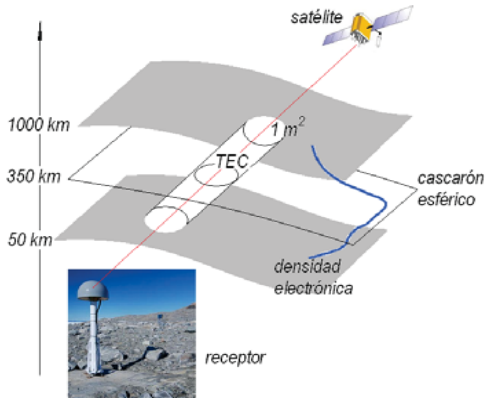

GNSS-based ionospheric observable

The equation of observation for P codes reads

$$P_i = R - \Delta R_{Rclk} + \Delta R^{Sclk} - \Delta R_{RPi} + \Delta R^{SPi} - \Delta R_{iono,i} - \Delta R_{trop} + \upsilon_{Pi} \qquad \sigma_{Pi} \approx 0.3\ m$$

$$\Delta R_{iono,i} = \frac{40.3\times10^{16}\cdot TEC}{f_i^2} \qquad TEC = 10^{-16}\cdot\int_S N_e \cdot ds$$

where the subindex $i=1$ or 2 indicates the carrier frequency; P is the observation (in linear units); R, the satellite-to-receiver range; ΔR_{Rclk} and ΔR^{Sclk} are the receiver and satellite clock errors; ΔR_{RPi} and ΔR^{SPi} are hardware delays produced in the receiver and the satellite; $\Delta R_{ion,i}$ and ΔR_{trop} are the ionospheric and tropospheric delays; and υ_{Pi} is the measurement error including multipath.

For the carriers

$$L_i = R - \Delta R_{Rclk} + \Delta R^{Sclk} - \Delta R_{RLi} + \Delta R^{SLi} + \Delta R_{iono,i} - \Delta R_{trop} + n_i\cdot\lambda_i + \upsilon_{Li} \qquad \sigma_{Li} \approx 0.002\ m$$

where L is the carrier observation (in linear units); the other symbols are similar to P code observations; λ is the wavelength of the carrier and n is the (integer number) ambiguity.

GNSS-based ionospheric observable

Subtracting dual frequency observations cancels the satellite-receiver geometrical range and all the frequency-independent terms but retains the TEC information:

✓ Ionospheric signal from code observations

$$\tilde{TEC}_P = P_1 - P_2 = \underbrace{40.3\times10^{16}\cdot\left(\frac{f_1^2 - f_2^2}{f_1^2\cdot f_2^2}\right)}_{\kappa=0.105\ m/TECu}\cdot TEC - \beta_{RP} + \beta^{SP} + \upsilon_{TEC,P}$$

where $\beta_{RP} = -\Delta R_{RP1} + \Delta R_{RP2}$ and $\beta^{SP} = \Delta R^{SP1} - \Delta R^{SP2}$ are the differential hardware delays for P code.

✓ Ionospheric signal from carrier observations

$$\tilde{TEC}_L = L_2 - L_1 = \underbrace{40.3\times10^{16}\cdot\left(\frac{f_1^2 - f_2^2}{f_1^2\cdot f_2^2}\right)}_{\kappa=0.105\ m/TECu}\cdot TEC - \beta_{RL} + \beta^{SL} + \beta_R^S + \upsilon_{TEC,L}$$

where the symbols are similar to the code equation and $\beta_R^S = n_2.\lambda_2 - n_1.\lambda_1$ is the combination of the carrier ambiguities.

Code observations provide low precision ($\sim\pm3\ TECu$) and un-calibrated, but unambiguous TEC information; carrier observations provide high precision ($\sim\pm0.03\ TECu$), un-calibrated and ambiguous TEC information.

GNSS-based ionospheric observable

In order to estimate the ambiguity term, β_R^S, the average of the differences between carrier and code ionospheric signals is computed for every continuous arc

$$\left\langle \tilde{TEC}_L - \tilde{TEC}_P \right\rangle = -\beta_{RP} + \beta^{SP} + \beta_{RL} - \beta^{SL} - \beta_R^S + \underbrace{\left\langle \upsilon_{TEC,P} - \upsilon_{TEC,L} \right\rangle}_{\approx\left\langle \upsilon_{TEC,P} \right\rangle}$$

and then subtracted from the carrier observations

$$\hat{TEC} = \tilde{TEC}_L - \left\langle \tilde{TEC}_L - \tilde{TEC}_P \right\rangle = \kappa\cdot TEC - \beta_{RP} + \beta^{SP} + \left\langle \upsilon_{TEC,P} \right\rangle + \upsilon_{TEC,L}$$

ionospheric signal (in TECu)
red: code / blue: carrier

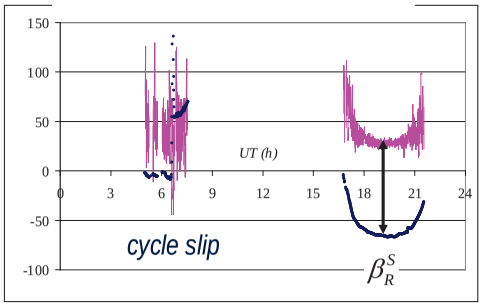

$\hat{TEC}_L$ is the carrier-to-code "levelled" ionospheric observable.

It is free from the carrier ambiguities but still affected by the P code differential hardware delays in both, the GPS receiver and satellite; both together may easily reach 50 TECu!

The observational noise of this observable is very small ($\sim\pm0.03\ TECu$), but it might be affected by a systematic bias due to the presence of the $\left\langle \upsilon_{TEC,P} \right\rangle$ term, which may reach several TECu due to P code multipath.

SIRGAS ionospheric model

It is based on the 'La Plata Ionospherc Model' (LPIM) developed at the GESA laboratory of the La Plata University; its development started in 1994 and the first operational version was released on 1998.

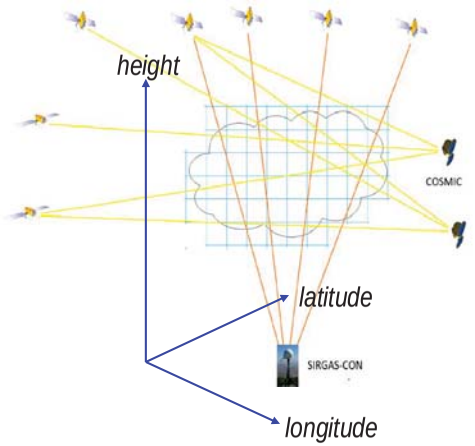

Presently, the SIRGAS model is capable of describing the 4-D (latitude, longitude, height, and time) distribution of the electron density based on the assimilation of ground- and space-based GNSS measurements.

Combination of ground-based and space-based GNSS measurements allows a tomography reconstruction of the electron distribution in the ionosphere (like the technique used in medicine to study the human brain).

SIRGAS TEC model

$$TEC = 10^{-16} \cdot \int_S N_e \cdot ds$$

S is the emitter to receiver ray path (from the GNSS satellites to either, the ground-based or the space-based receivers).

LPIM models the vertical profile of electron density by means of a superposition of 4 alpha-Chapman layers which represent the E, F1, F2 and topside.

Each layer is characterized by 3 parameters:

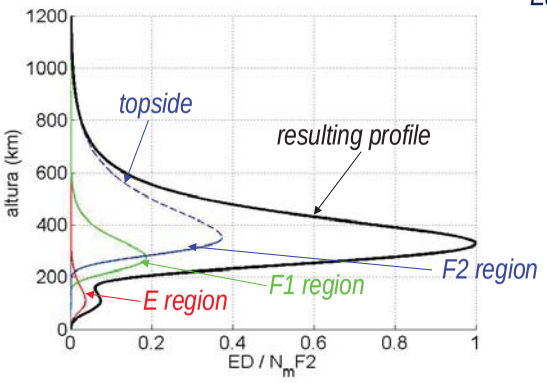

$$N_e(h) = N_{e,max} \cdot e^{\frac{1}{2}\left(1 - z - e^{-z}\right)}$$

maximum electron density of the layer

height of the layer peak

$$z = \frac{h - h_{max}}{H}$$

Scale eight of the layer

SIRGAS model for the F2 layer parameters

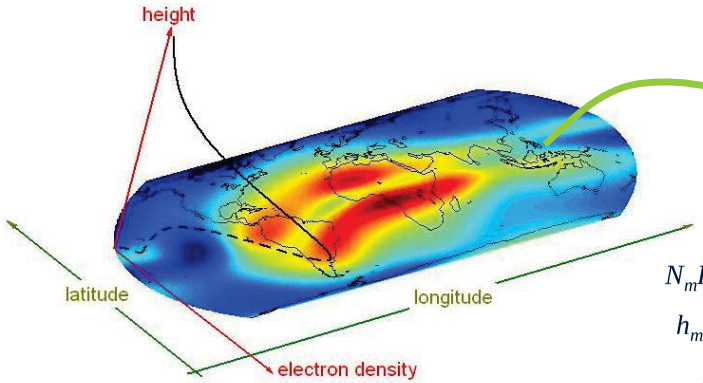

The F2 peak parameters:

N_mF2 (maximum electron density);

h_mF2 (height of the F2 peak); and

HF2 (scale height of the layer),

are separately modeled with spherical harmonics expansions dependent on the modip latitude and the geographic longitude, and time dependent coefficients that are the main parameters to be estimated by the Kalman filter:

$$\Omega(\mu,\lambda,t) = a_0(t) + \sum_{l=1}^{L}\sum_{m=1}^{l}\left[a_{lm}(t)\cdot\cos\left(m\cdot\frac{2\pi}{24}\cdot\lambda\right) + b_{lm}(t)\cdot\cos\left(m\cdot\frac{2\pi}{24}\cdot\lambda\right)\right]\cdot P_{lm}(\sin\mu)$$

SIRGAS model for the vertical profile

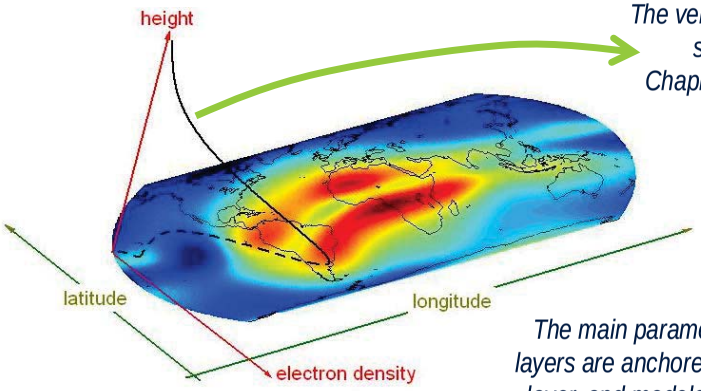

The vertical profile is modeled as a superposition of three alpha-Chapman layers for the E, F1, F2 and topside layers

The main parameters of the E, F1 and topside layers are anchored to the parameters of the F2 layer, and modeled in accordance to the ITU-R recommendations.

Data assimilation scheme

Quasi-real-time data from different sources (ground- and space-based GNSS, and satellite altimetry)

robust and adaptive Kalman filter

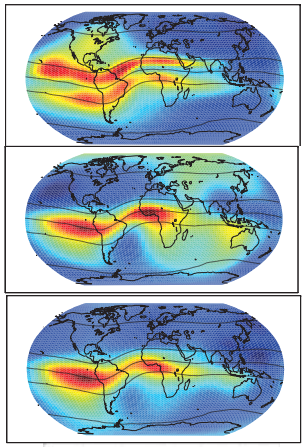

Global maps of N_mF2, h_mF2 and $HF2$ and electron density profiles

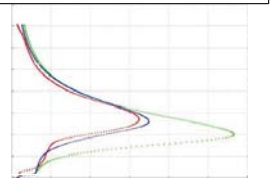

Some results

Profiles and residuals for December 2011, 15 LT

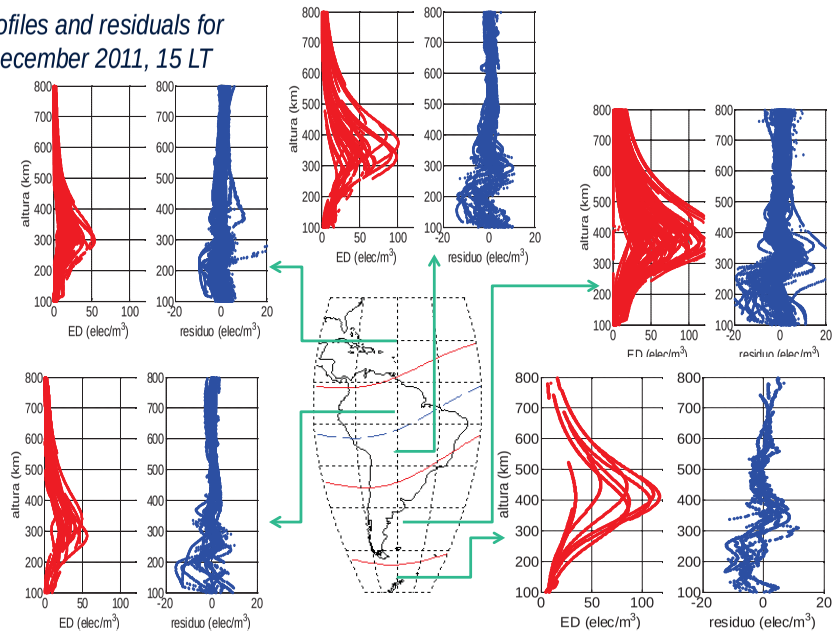

Some results

hmF2 for Diciembre, 2011, 19 LT

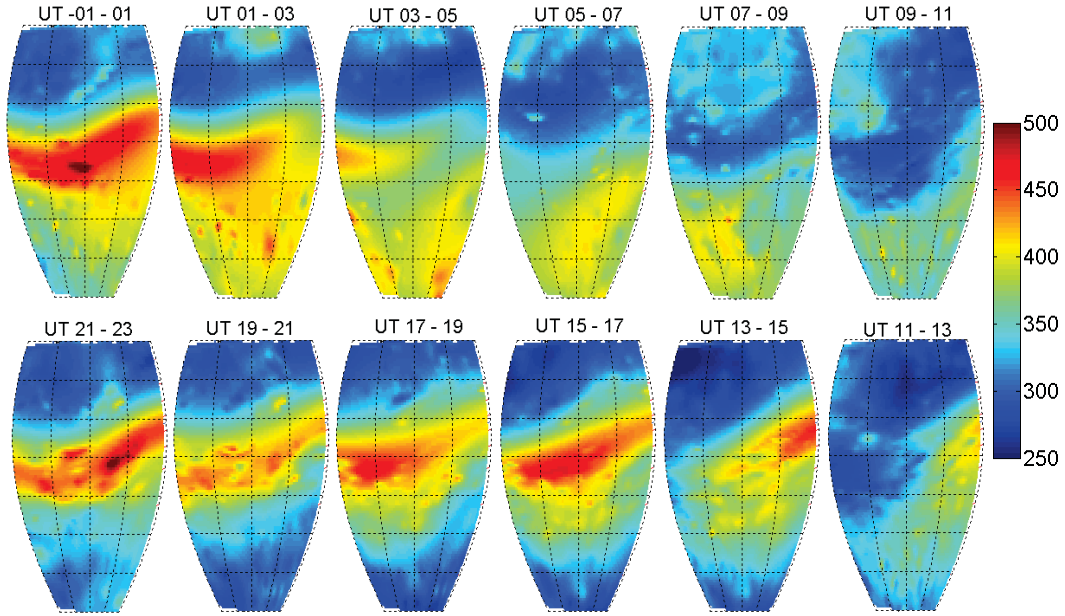

Some results

NmF2 for Diciembre, 2011, 19 LT

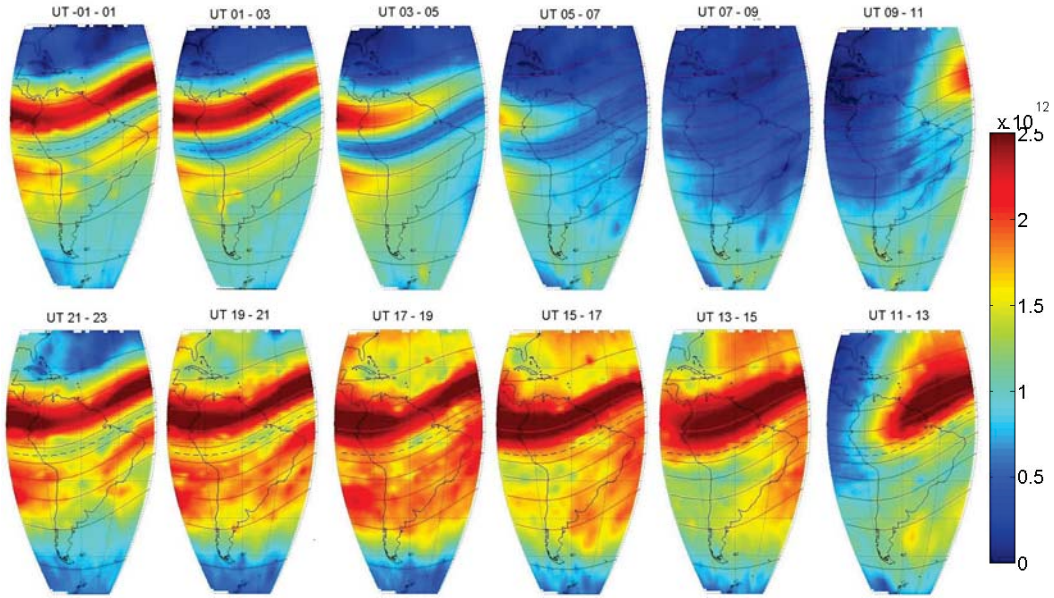

Some results

Vertical TEC for Diciembre, 2011, 19 LT